Ion Pairing LC-MS/MS Method for Analysis of Intracellular Phosphorylated Metabolites

Wahyu Utami

Thesis submitted to the University of Nottingham for the degree of Doctor of Philosophy

July, 2015

DECLARATION

Except where acknowledged in the text, I declare that this dissertation is my own work and is based on research that was undertaken by me in the School of Pharmacy, University of Nottingham.

ABSTRACT

Nucleoside analogues have been extensively used in medication. The nucleoside analogue cordycepin is the principal bioactive compound found in the caterpillar fungi (*Cordyceps* and *Ophiocordyceps*). It has been shown to have biological activity, including anti-inflammatory, immunomodulatory and anti-proliferative activity in many kinds of malignant cells. Intracellular drug interactions at the nucleotide level can be explained by understanding the intracellular metabolism of nucleoside analogues as well as their plasma metabolism since their efficacy of therapy or toxicity does not associate with the plasma level of nucleoside. Therefore, investigation of the metabolism of nucleoside analogues is required for a full understanding of their pharmacological activity and toxicity. For that reason, here an ion pairing LC-MS/MS method has been developed for quantitative analysis of the nucleoside analogue cordycepin and the metabolites and its application to cell culture, using *in vitro* and *in vivo* studies.

Several HPLC parameters and extraction techniques have been optimised, followed by optimisation of the mass spectrometry method by examining the fragmentation of nucleotides. The method was then validated and applied to study the metabolism of cordycepin *in vitro* and *in vivo*, to investigate the effect of the cordycepin treatment with or without pentostatin on the intracellular level of endogenous nucleotides, and to examine the intracellular metabolism of nucleoside analogue 4-thiouridine and the effect of its metabolite on the metabolic balance of adenine and uridine nucleotides.

The study on the intracellular metabolism of cordycepin in MCF7 and HeLa cells shows that cordycepin was rapidly metabolized into the deaminated form by

adenosine deaminase (ADA) in culture medium as well as in cancer cells; therefore combination with pentostatin, an ADA inhibitor, resulting in the highly accumulated phosphorylated metabolite intracellularly. In contrast, cordycepin in *C. militaris* extracts showed much lower degradation in non-heat-treated serum compared with pure cordycepin that indicates a strong evidence of the presence of a deaminase inhibitor in the extract of *Cordyceps*. Moreover, the determination of concentrations of cordycepin and the metabolites in the plasma and liver of rats dosed with cordycepin proves that the half-life of cordycepin and its metabolites are very short in the plasma; nevertheless they are accumulated in the liver with repeated administration. Treatment using cordycepin initially caused an increase in the intracellular concentrations of nucleoside triphosphate, but in the long term, the active metabolite of cordycepin likely induced a long term change in the cell resulting in a drop in nucleotide levels. Pentostatin on its own reduced nucleoside triphosphates levels in the long term and combination with cordycepin increased the effect of cordycepin on nucleotide concentrations. High levels of the accumulated cordycepin triphosphate led to a massive decline in nucleotide levels.

A study on the intracellular metabolism of nucleoside analogue 4-thiouridine has shown that generally the uptake of 4-thiouridine into NIH 3T3 cells was fast and the phosphorylated metabolite rapidly was developed only after two min labelling. However, it was also shown that its phosphorylation was not very efficient, but the level of the phosphorylated metabolite increased in serum-stimulated cells likely because the enzyme was upregulated in the presence of growth factor. Moreover, the present study provides additional evidence that 4-thiouridine and its metabolite have no adverse effect on the metabolic balance of adenine and uridine nucleotides.

This study confirms that pharmacological activity of nucleosides analogues and their cytotoxicity highly rely on the accumulation of their phosphorylated metabolites. Consequently, the activity and the level of the enzymes involved in their metabolism are highly influential on their pharmacological action as well as their toxicity.

ACKNOWLEDGEMENTS

First and foremost, all praise and thanks are due to Allah, the Most Gracious, and the Most Merciful for all his blessings and for making me able to through this PhD journey and produce this thesis.

I would like to thank to my supervisors, Prof Dr. David A. Barrett and Dr. Cornelia De Moor for their patience, encouragement, guidance and support throughout this work. The writing of this thesis has been one of the most significant academic challenges I have ever had to face. Without their support, patience and guidance, this study would not have been completed. It is to them that I owe my deepest gratitude. I would also like to thank to IDB, Islamic Development Bank and the University of Nottingham for the funding throughout my postgraduate study.

I wish to thank to Dr. Catherine Ortori and Paul Cooling for all the technical help in the lab. I also thank to the members of RNA group, Hannah Parker, Asma Khurshid, Richa Singhania, and Barbara who help me in the cell culture lab and Dr James Burston for help with the rat plasma and liver samples.

I am grateful to all my friends, in particular Lina, Zakky, and Denny. Your supports have taught me so much what friends are for. I must thank to Anita and Erin who help me to settle in my first years of being PhD student, and also to my friends "Arabian girls", Lina, Maysaa, Laila, Neven, Nesma, and Azzah for the lovely company to get away from the stressful time. I thank to all members of PeDLN society as my family in Nottingham and also to IDB scholars community.

I would like to thank to Valerie Watson who gives me a support and encouragement during the tough times. I also thanks to my colleges at Universitas Muhammadiyah Surakarta who always give their support and help during my PhD.

TABLE OF CONTENT

LIST OF FIGURES

LIST OF TABLES

LIST OF ABBREVIATIONS

ACN	acetonitrile
ADA	adenosine deaminase
ADP	adenosine-5'-diphosphate
ADK	adenylate kinase
AK	adenosine kinase
AMP	adenosine-5'-monophosphate
ATP	adenosine-5'-triphosphate
cAMP	3'-5'-cyclic adenosine monophosphate
APCI	atmospheric pressure chemical ionization
CE	capillary electrophoresis
CF	coformycin
CHO	Chinese Hamster ovary
CMP	cytidine-5'-monophosphate
CDP	cytidine-5'-diphosphate
CTP	cytidine-5'-triphosphate
dCF	deoxycoformycin
DMHA	N, N-dimethylhexylamine
DMEM	Dulbecco's modified Eagle medium
DMSO	dimethyl sulfoxide
DNA	deoxyribonucleic acid
dATP	2’-deoxyadenosine-5'-triphosphate
dCTP	2’-deoxycytidine-5'-triphosphate
dGTP	2’-deoxyguanosine-5'-triphosphate
dTTP	2’-deoxytymidine-5'-triphosphate
dCK	deoxycytidine kinase
dGK	deoxyguanosine kinase
dNK	deoxyribonucleoside kinase
EC	energy charge
EDTA	ethylenediaminetetraacetic acid
EI	electron impact
ESI	electrospray ionization
FAB	fast atom bombardment
FAD	flavin adenine dinucleotide
FBS	foetal bovine serum

GMP	guanosine-5'-monophosphate
GDP	guanosine-5'-diphosphate
GTP	guanosine-5'-triphosphate
HPLC	high-performance liquid chromatography
IMP	inosine monophosphate
IP	ion pairing
LC	liquid chromatography
LOD	limit of detection
LOQ	limit of quantification
MALDI	matrix assisted laser desorption ionization
MIA	monosodium iodoacetate
MS	mass spectrometry
MM	multiple myeloma
MRM	multi reaction monitoring
mRNA	messenger ribonucleic acid
Na2-EDTA	ethylenediaminetetraacetic acid calcium disodium salt
5’-NT	5’-nucleotidase
NAD	nicotinamide adenine dinucleotide
NADP	nicotinamide adenine dinucleotide phosphate
NMDK	nucleoside diphosphate kinase
NMPK	nucleoside monophosphate kinase
NP	nucleoside phosphorylase
NTPs	nucleotide triphosphates
NTRI	nucleoside reverse transcriptase inhibitors
PAP	poly(A) polymerase
PARP	poly(ADP-ribose) polymerase
PBMC	peripheral blood mononuclear cell
PCA	perchloric acid
PDGF	platelet-derived growth factor
PNP	purine nucleoside phosphorylase
PPP	platelet-poor plasma
PRPP	phosphoribosyl pyrophosphate
PRT	phosphoribosyl transferase
RIA	radio immunological assay
rNK	ribonucleoside kinase
RR	ribonucleotide reductase

RP	reversed phase
RNA	ribonucleic acid
SAX	strong anion-exchange
SD	standard deviation
SEM	standard error of the mean
SPE	solid-phase extraction
UCK	uridine-cytidine kinase
UMP	uridine-5'-monophosphate
UDP	uridine-5'-diphosphate
UTP	uridine-5'-triphosphate
TAN	total adenine nucleotide
TBAH	tetrabutylammonium hydroxide
TCA	trichloroacetic acid
TEA	triethylamine
TK	thymidine kinase
TLC	thin layer chromatography
tR	retention time
tRNA	transfer ribonucleic acid
UV/Vis	ultraviolet/visible
WAX	weak anion-exchange
ZDV	zidovudine

CHAPTER 1
GENERAL INTRODUCTION

GENERAL INTRODUCTION

1.1. Nucleoside and nucleotides and their biological activities

Nucleosides and nucleotides are endogenous compounds that play essential roles in several cellular processes. Deoxyribonucleotides are the building units of DNA and ribonucleotides are the constituent units of RNA. Both of them are constructed by a nitrogen ring-structured base (purine or pyrimidine), pentose sugar (deoxyribose or ribose), and a phosphate group. DNA polymerase catalyses a replication of DNA by synthesizing the complementary strand from deoxyribonucleoside triphosphates (dATP, dCTP, dGTP, and dTTP) using single-stranded DNA as template. DNA chains are extended in the 5' ---> 3' direction by adding the nucleotides to the free 3'-OH groups of the base-paired polynucleotide (Figure 1.1).

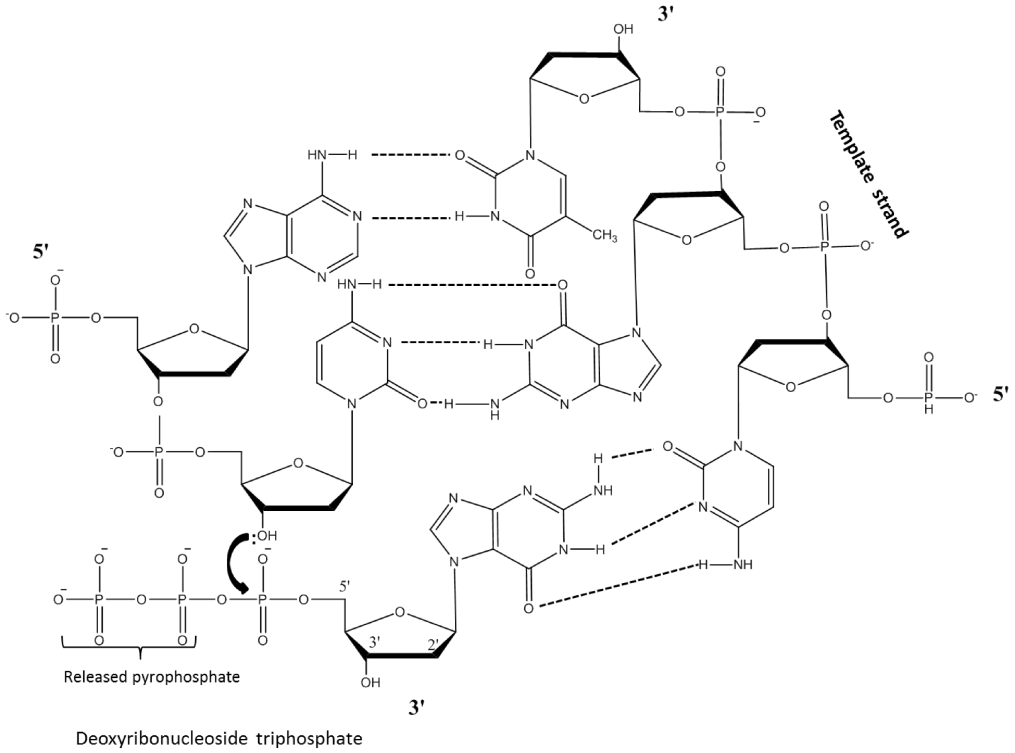

Figure 1.1. Deoxyribonucleoside triphosphates are the substrates of DNA polymerase catalysed replication of DNA. DNA chains are extended in the 5' ---> 3' direction by adding the nucleotides to the free 3'-OH groups of the base-paired polynucleotide. The dotted lines are hydrogen bonds between complementary nucleic acids.

In addition to their functions as the activated precursors of DNA and RNA synthesis, they have a range of other roles in every cell such as metabolic regulation, cell signalling, and involvement in many biosynthesis as activated intermediates. Nucleoside triphosphates, especially ATP and GTP are usually used as a source of energy in biological systems; meanwhile adenine monophosphates are parts of the structure of coenzymes, such as nicotinamide adenine dinucleotide (NAD^+) and $NADP^+$, coenzyme A, and flavin adenine dinucleotide (FAD). Moreover, cAMP is one of the intracellular second messengers which are connected with the inner face of the plasma membrane (1). Other nucleoside triphosphates also have an important role in metabolic systems. CTP has a role in lipid synthesis, GTP in protein synthesis and intracellular signal transduction, and UTP in polysaccharide synthesis (2). Since nucleotides are crucial for biochemical processes, interference in nucleotide metabolism would have several important physiological effects (3).

The adenine nucleotide pool is vital for basic metabolic reactions including synthesis of nucleic acid and energy transfer reactions (4). The intracellular level of ATP depends on the adenylate pool and on the energy charge. Energy charge of the cells control many reactions in metabolism. This energy is proportional to the mole fractions of ATP and half the mole fractions of ADP (4).

$$\text{Energy charge} = \frac{\text{ATP}+0.5\ \text{ADP}}{\text{ATP}+\text{ADP}+\text{AMP}}$$

In normal physiological environments, the value of EC is from 0.7 to 1.0. While EC is equal to 1, intracellular adenylate will be predominantly present in the form of ATP; whereas the value is 0, all adenylates be present in the form of AMP. When the metabolism is more vigorous, the cells have a higher EC value (5). Intracellular

adenylate pool is a sum of concentrations of ATP, ADP, and AMP. The reactants at their equilibrium concentrations are maintained by the fast reaction of adenylate kinase:

$2[ADP] \leftrightarrow [ATP] + [AMP]$

According to the equation above, the cell stabilizes its energy charge. The intracellular adenylate pool is expected to follow the changes in the energy charge.

1.2. Nucleotide Metabolism

There are two pathways for synthesis of intracellular nucleotides, the salvage pathway and the de novo pathway (Figure 1.2). Through the de novo pathway, ribonucleotides are synthesized from small molecules (ribose-5'-phosphate, amino acid, and CO_2) to ribonucleoside monophosphates and then further phosphorylated into their corresponding triphosphates (6); meanwhile, 2'-deoxyribonucleoside diphosphates are produced from ribonucleoside diphosphates by an irreversible reduction reaction catalysed by ribonucleotide reductase (RR) and then further metabolized into their triphosphates forms (7). Moreover, ribonucleotides are synthesized through salvage pathways from phosphorylation of free bases by sugar phosphate transfer reaction catalysed by phosphoribosyl transferase (PRT) or from phosphorylation of ribonucleoside to their nucleotides by ribonucleoside kinases (rNKs), nucleoside monophosphate kinases (NMPKs), and nucleoside diphosphate kinases (NMDKs). Deoxyribonucleotides are synthesized through this pathway from deoxyribonucleoside catalysed by deoxyribonucleoside kinases (dNKs) and further phosphorylated by NMPKs and NMDKs (6, 7). Deoxyribonucleotide synthesis by de novo pathway is the primary source for DNA replication (8), while the salvage pathway is supposed to be essential for DNA repair (9). Nucleosides are transported

into the cells by facilitated diffusion or active transport via nucleoside transporters (10) and phosphorylated into their nucleoside monophosphates catalysed by dNKs and rNKs through irreversible reactions. Then, through reversible reactions, the nucleoside monophosphates are further phosphorylated into their triphosphates forms by NMPKs and NDPKs (6).

Moreover, nucleotides are further metabolized in order to maintain their levels in intracellular and extracellular cells. There are four types of enzymatic reactions which contribute in catabolism of purine nucleotides: de-phosphorylation, deamination, cleavage of glycosidic bonds, and oxidation. The catabolism of pyrimidine nucleotides are through the same reaction as purine nucleotides: phosphorylation, deamination, and cleavage of glycosidic bonds. Nonetheless, the pyrimidine bases are most generally exposed to reduction instead of oxidation (1).

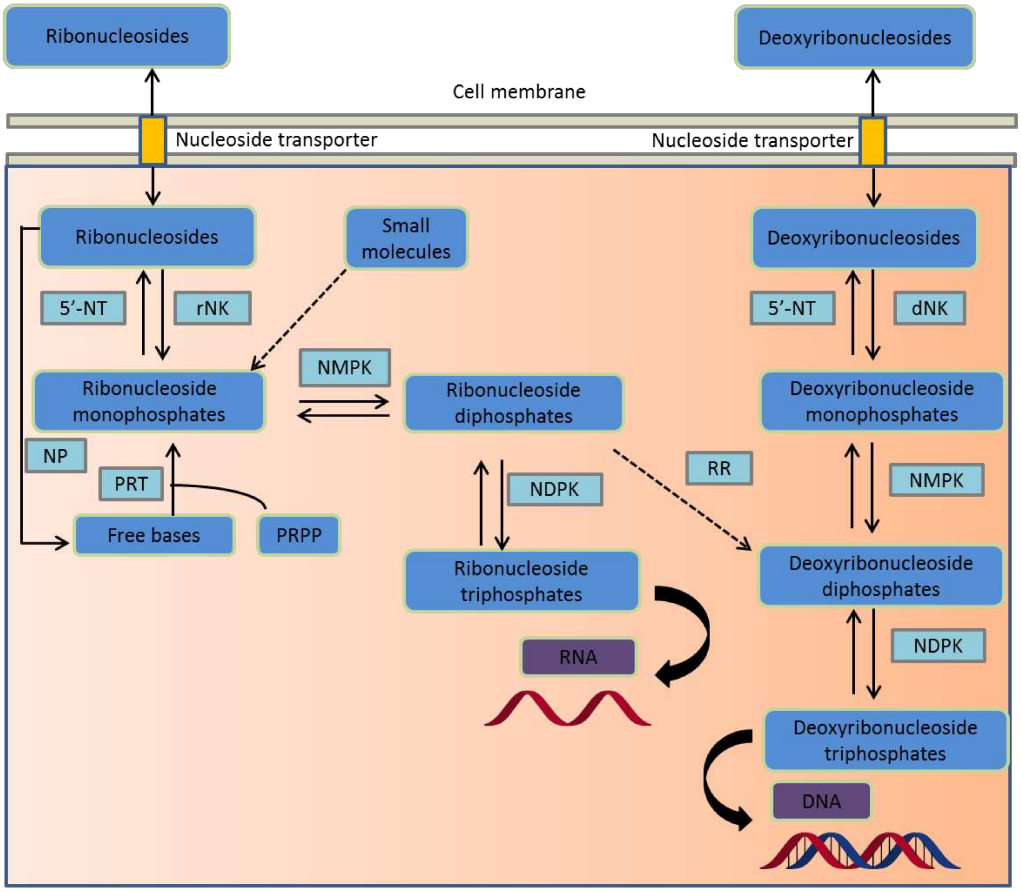

Figure 1.2. De novo and salvage pathways of ribonucleotides and deoxyribonucleotides synthesis

Via de novo pathway, ribonucleotides are synthesized from small molecules to ribonucleoside monophosphates and then further phosphorylated into their corresponding triphosphates; 2'-deoxyribonucleoside diphosphates are produced by reduction ribonucleoside diphosphates and then further metabolized into their triphosphates forms.

Ribonucleotides are synthesized through salvage pathways from phosphorylation of free bases or from phosphorylation of ribonucleoside to their nucleotides. Deoxyribonucleotides are synthesized through this pathway from deoxyribonucleoside and then further phosphorylated.

5'-NT: 5'-nucleotidase; rNK: ribonucleoside kinases; dNK: deoxyribonucleoside kinase; NMPK: nucleoside monophosphate kinase; NDPK: nucleoside diphosphate kinase; RR: ribonucleotide reductase; NP: nucleoside phosphorylase; PRT: phosphoribosyl transferase; PRPP: phosphoribosyl pyrophosphate

Nucleotides monophosphates could be dephosphorylated to their nucleosides by 5'-nucleotidase (5'-NT). Furthermore, the nucleoside products could inhibit, to some extent, the activity of the enzyme. Deamination is irreversible reaction and most of

the reactions are catalysed by specific deaminases. Adenylate deaminases catalyse the deamination of adenine into hypoxanthine and AMP into IMP; while adenosine, deoxyadenosine and their analogues are substrates for adenosine deaminase (ADA). Guanine is metabolized into xanthine by guanine deaminase; whereas guanylate reductase, which catalyses a reductive deamination instead of a hydrolytic deamination, converts GMP into IMP. Cytidine, deoxycytidine, and their halogen derivatives are deaminated by cytidine deaminase into uridine or its analogues. Cleavage of glycosidic bonds of a nucleoside is a reversible reaction and catalysed by purine nucleoside phosphorylase (PNP). Most of this reaction in biological systems is through the phosphorolytic cleavage of nucleosides. Hypoxanthine and xanthine could be further metabolized by oxidation into uric acid by xanthine oxidase, while pyrimidine bases are further metabolized by reduction of the double bound of the pyrimidine ring (1).

Extensive studies have been done on the activities of enzymes which catalyse synthesis and catabolize adenosine in human tissues and the functional consequences of metabolism of purine nucleotides (11). Four enzymes are directly involved in conversion or synthesis of adenosine: adenosine kinase (AK), ecto 5'-NT, e-Ns 5'-NT, and ADA; whereas three enzymes, c-N-II 5'-NT, PNP, and adenylate kinase (ADK), contribute to nucleotide catabolism or regulation of the energy charge of the cell. Adenosine is generally formed by de-phosphorylation of AMP by 5'-NT; it is re-phosphorylated to AMP by AK and then AMP could be metabolized to ADP and ATP by ADK. Adenosine is converted into inosine through deamination by ADA. Inosine is further catabolised into hypoxanthine by PNP. An overview of adenosine metabolism pathways is shown in Figure 1.3.

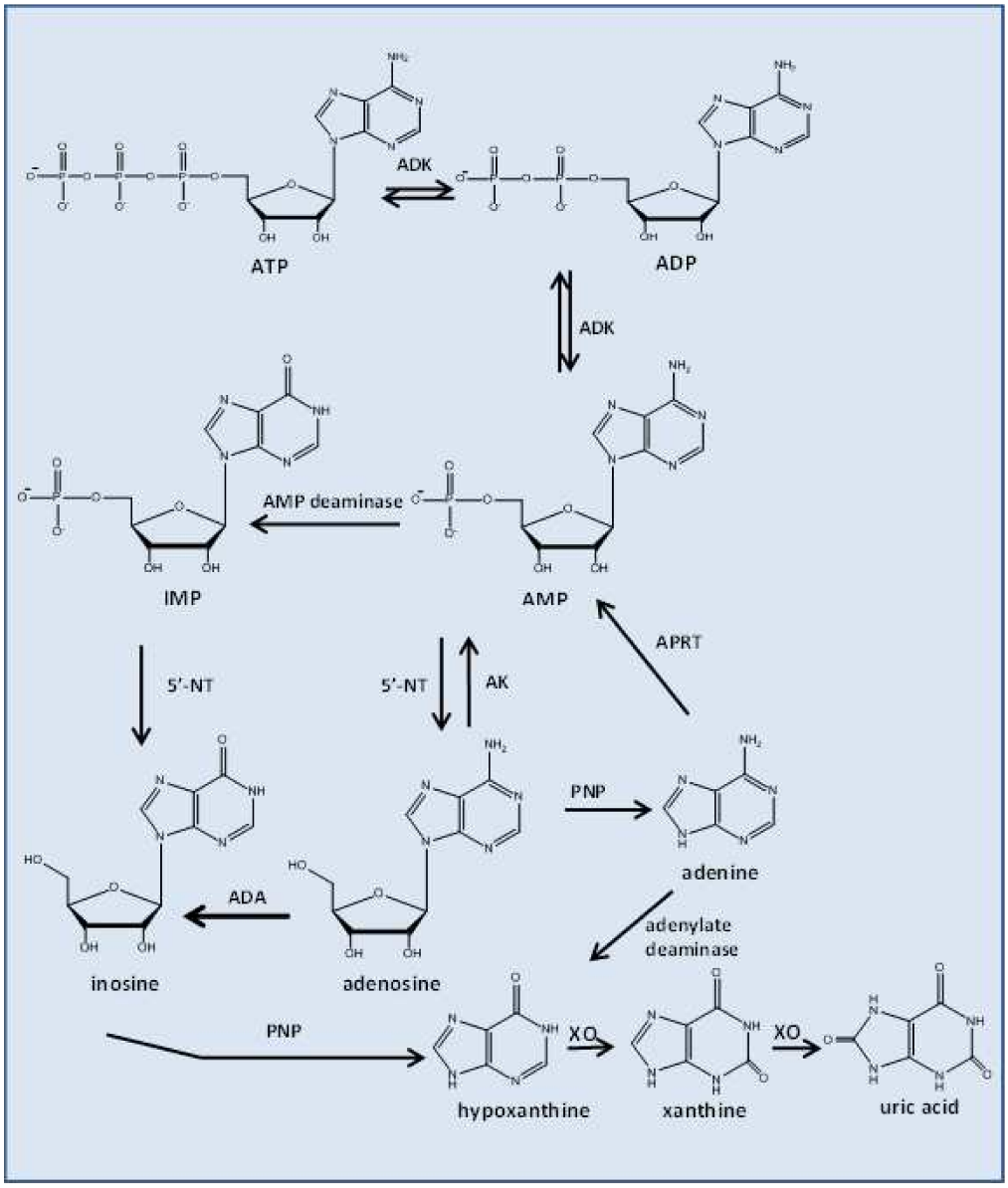

Figure 1.3. Adenosine metabolism pathways

ADK: adenylate kinase; 5'-NT: 5'-nucleotidase; AK: adenosine kinase; ADA: adenosine deaminase; APRT: adenine phosphoribosyl transferase; PNP: purine nucleoside phosphorylase; XO: xanthine oxidase

Since AK catalyses phosphorylation of adenosine into AMP, it has a key role in maintaining both intracellular and extracellular levels of adenosine. It is widespread in most tissues and animal species. High levels of adenosine could inhibit activity of

AK; and concentration of Mg^{2+} ions affects the affinity of substrate to enzyme (12). 5'-NT is considered as a vital enzyme in purine catabolism. There are seven forms of 5'-NT including the two soluble 5'-NT (e-Ns and c-N-II) and ecto 5'-NT which is a glycoprotein on the external plasma membrane. The function of c-N-II 5'-NT is regulating intracellular monophosphate nucleoside levels and it is IMP-dependent, meanwhile e-Ns 5'-NT is AMP-dependent (13). The main role of ecto 5'-NT is to hydrolyse extracellular AMP to adenosine (14).

ADA also has a role in the regulation of intracellular and extracellular adenosine levels by catalysing the degradation of adenosine into inosine. This reaction is the rate limiting step in adenosine degradation due to the irreversibility of the reaction. It exists in all mammalian tissues and its activity varies according to the location (15). The enzyme has a major role in the human immune system and deficiency of the enzyme is linked with severe combined immunodeficiency (11).

PNP also plays a role in the adenine nucleotides catabolism. In the presence of inorganic phosphate, PNP catalyses a reversible reaction which degrades inosine to hypoxanthine and ribose 1-phosphate (16). ADK is involved in the balance of adenine nucleotide composition in cells. It is universal enzyme and present as five isoforms. The enzyme is particularly abundant in cells with high rates of ATP synthesis and utilization, for example skeletal muscle (17).

Regardless of the physiological role of the purine and pyrimidine kinases, the enzymes have a vital role in clinical therapy with nucleoside analogues.

Phosphorylation of nucleoside analogues into their nucleotides is compulsory for the pharmacological activity of most of these compounds. Furthermore, the enzymes are responsible for degradation of the nucleosides and their nucleotides; therefore, play a significant contribution to their pharmacological activity as well as the toxicity.

1.3. Nucleotide signalling

A release of nucleotides from their intracellular compartments into the extracellular space occurs during inflammation, mechanical injury, necrosis, or apoptosis activation. ATP is released from intracellular into extracellular locations in some cells in certain conditions, such as ischaemia or inflammation (18). Adenosine and ATP are essential endogenous signalling molecules in inflammation and immunity (19). Other nucleotides such as UTP, UDP and UDP-glucose have also been observed to be released during cystic fibrosis (20) from injured cells or produced by non-lytic mechanisms and might be responsible for an significant mechanism involved in the activation of leukocytes and platelets (21).

Beside its function as a universal energy source, extracellular ATP has a different role. Extracellular nucleotides have a role as signalling molecules through the activation of nucleotide receptors which are known as purinergic P2 receptors. ATP and other nucleotides stimulate P2 receptors, meanwhile P1 receptors are activated by adenosine, the ATP metabolite. Based on the signalling properties, P2 receptors are subdivided into metabotropic P2Y receptors (P2YRs) that are G-protein-coupled, and ionotropic P2X receptors (P2XRs) that are nucleotide-gated ion channels (22).

P2YRs became a pharmacological target for the action of anti-inflammatory or anti-infection agents since they have important roles in regulating immune responses (22). A recent study showed that P2Y2R agonists have an ability to stimulate production of mucin and induce secretion of chloride (23). Moreover, the agonists play a role in the promoting wound healing by facilitating the differentiation and proliferation of structural cells and are involved with the activation of leukocytes to the site of injured tissue (24), and also contribute to the resolution of inflammation by stimulating phagocytic clearance (25).

UDP can activate $P2Y_6R$ which has been shown has a role in native immune reactions against infection (26). Stimulation of the receptor generates chemokine release from monocytes, dendritic cells, eosinophils and endothelial cells, therefore supporting recruitment of inflammatory cells to the location of infection (26-28). Meanwhile, in endothelial (29) or epithelial (30) inflammations, $P2Y_6R$ signalling is destructive. Likewise, $P2Y_{12}R$ signalling has been involved in controlling inflammatory reactions (31). It is highly expressed on platelets and plays a significant part in platelet activation and aggregation through stimulation of the activity of phosphatidylinositol-3 kinase and inhibition of adenylyl cyclase activity. These activities cause the stimulation of the fibrinogen receptor which is critical for platelet aggregation (18). $P2Y_{12}R$ antagonists have been used effectively in clinical practice as a antithrombotic agent (18).

Extracellular ATP also directly stimulates P2XRs which are plasma membrane channels selective for monovalent and divalent cations such as Na^+, K^+, and Ca^{2+} (32). Binding of three molecules of ATP to P2X results in opening of the channel, therefore

allow the flux of ions such as Na^+, Ca^{2+}, and K^+ across the membrane. This flux causes depolarization of the membrane and stimulation of Ca^{2+} signalling flows, such as p38 mitogen-activated protein kinases (MAPK) or phospholipase A2 (33). $P2X_7R$ signalling plays a substantial part in facilitating proper immunological and inflammatory responses against pathogens or cancer cells. However, it might contribute to chronic inflammatory syndrome when activated inappropriately such as asthma and chronic lung disease (22).

Nucleotide and nucleoside signalling is terminated when the compounds are metabolized by their related enzymes. Ectonucleotidases which are highly expressed in many tissues have a functional role in the termination of P2R signalling through catalysis of the conversion of extracellular ATP/ADP to adenosine (34-36). ATP or ADP is converted to AMP by ectonucleoside triphosphate diphosphohydrolase (CD39) which is subsequently converted to adenosine through ecto-59-nucleotidase (CD73). These conversions cause termination of ATP signalling and result in the production of extracellular adenosine.

Extracellular AMP from phosphohydrolysis of ATP or ADP has no evidently characterized signalling function. Nevertheless, it provides the substrate for the formation extracellular adenosine (18). This extracellular adenosine activates four different P1 receptors: $AdoRA_1$, $AdoRA_{2A}$, $AdoRA_{2B}$ or $AdoRA_3$. Adenosine provoked P1 receptor signalling reduces acute inflammation and tissue injury (37), thus opposing inflammatory functions of P2Rs (38). Compared to normal or unstressed cells, high concentrations of adenosine are present in cells stressed or inflammatory states. Additionally, genetic changes which arise throughout cancer development

increase the level of adenosine in the cell (39). High levels of extracellular adenosine stimulate adenosine receptors resulting in the activation of cell signalling cascades and the induction of anti-inflammatory and immune responses. Also, activation of adenosine receptors can lead to increase proliferation, apoptosis and metastasis of cancer cells (40, 41). This signalling is ended through uptake of adenosine from the extracellular into the intracellular part via equilibrative nucleoside transporters and is converted to inosine by adenosine deaminase (42) or to AMP by adenosine kinase (43).

1.4. Nucleoside and nucleotide analogues

Nucleoside and nucleotide analogues have been extensively used in medication. They are chemically modified compounds that have been developed to mimic their natural nucleosides or nucleotides and generally used as anticancer and antiviral agents (44-46). One of the cellular targets of nucleoside and nucleotide analogues is nucleotide metabolism. The general structure of nucleosides is contained of a nucleobase (a purine or pyrimidine derivative) and a sugar moiety (ribose or deoxyribose). Meanwhile, nucleoside analogues are modified at the base moiety or sugar moiety (Figure 1.4) (46). Structures of nucleotide or nucleoside analogues shown such as fludarabine, cytarabine, and gemcitabine (Figure 1.5), or nucleobases such as, thioguanine and 6-mercaptopurine are associated to physiological compounds which involved in the nucleotide metabolic pathway (47, 48).

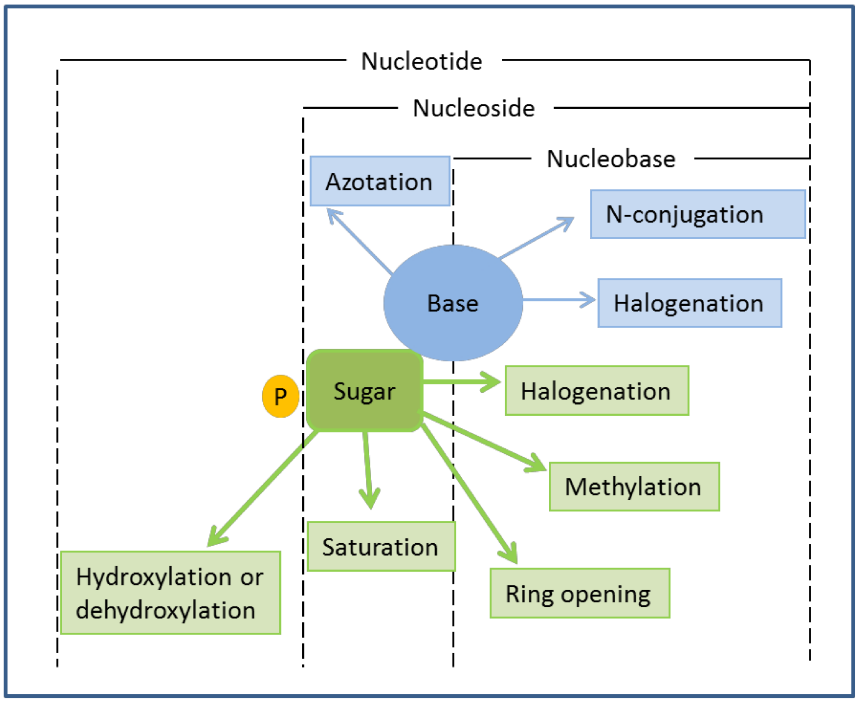

Figure 1.4. General structural and chemical modifications of nucleoside and nucleotide analogues

Nucleoside consist of a nucleobase (a purine or pyrimidine derivative) connected to a sugar moiety. The analogues are modified at the base moiety or sugar moiety by modifications such as shown in this figure (46).

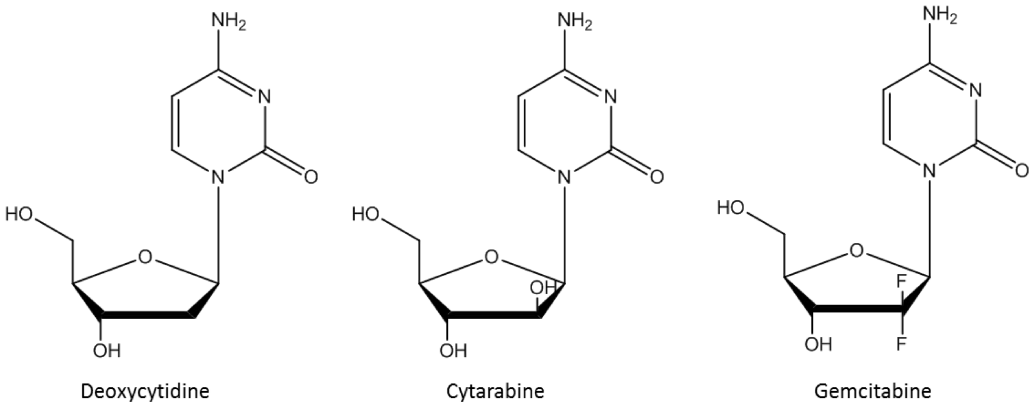

Figure 1.5. Structure of nucleoside analogues cytarabine and gemcitabine are similar enough to the native nucleoside deoxycytidine to be incorporated into DNA.

The metabolism and mechanism of action of nucleotide and nucleoside analogues are based on the interaction with membrane transporters, kinases and intracellular enzymes (Figure 1.6). They are metabolized through the similar pathways as their endogenous nucleosides, but they also inhibit these pathways (49). Since they are relatively hydrophilic, they enter cells through specific nucleoside transporters (10, 50) and then are subsequently phosphorylated to their nucleoside monophosphates through nucleotide salvage pathway by dNKs or rNKs and further metabolized into their analogous triphosphate form by NMPKs and NDPKs (6). The main active metabolite typically is the triphosphate form which is incorporated into nucleic acid or inhibits essential enzymes such as DNA or RNA polymerases, kinases, and ribonucleotide reductase (46). The rate limiting step in the production of nucleoside triphosphate analogues is mostly the first phosphorylation reaction by dNKs or rNKs. In human cells, there are three kinds of rNKs: adenosine kinase (AK), uridine-cytidine kinase 1 (UCK1) and UCK2; and four kinds of dNKs, thymidine kinase 1 (TK1), TK2, deoxycytidine kinase (dCK), and deoxyguanosine kinase (dGK) (6).

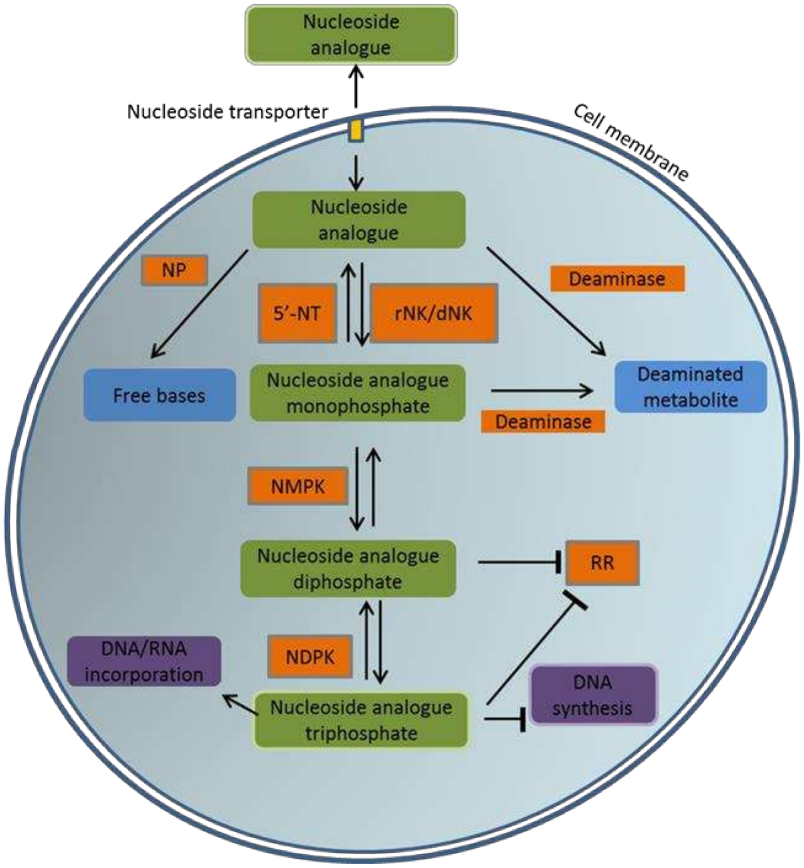

Figure 1.6. Mechanism of action of nucleoside analogues

Nucleoside analogues require intracellular phosphorylation for their activity. They are imported into the cells and metabolized by rNK or dNK to their nucleoside monophosphate which further phosphorylated into their corresponding triphosphate form by NMPK and NDPK. The nucleoside triphosphates could be incorporated in nucleic acids or inhibit nucleic acid synthesis; meanwhile the di- or triphosphates metabolite could also inhibit RR. Deamination by deaminase or dephosphorylation by 5'NT may decrease the quantity of the active metabolites (46).

5'-NT: 5'-nucleotidase; rNK: ribonucleoside kinase; dNK: deoxyribonucleoside kinase; NMPK: nucleoside monophosphate kinase; NDPK: nucleoside diphosphate kinase; RR: ribonucleotide reductase; NP: nucleoside phosphorylase

The effects of the nucleotides on cellular activity are ended when the active compound is further metabolized by its relevant enzyme into its inactive metabolite. Nucleoside or nucleotide analogues could be metabolized into their inactive deaminated metabolites catalysed by deaminase. Moreover, nucleotide analogues are typically enzymatically degraded to their nucleosides by 5'-NT. Nucleosides are further metabolized through phosphorolytic cleavage by nucleoside phosphorylases

(NP) into their free bases and ribose 1-phosphate (Figure 1.6). Ribose 1-phosphate is isomerized by phosphoribomutase to form ribose 5-phosphate which is a substrate of phosphoribosyl pyrophosphate (PRPP) synthesis. Some of the bases are reused for nucleotide synthesis through salvage pathways (Figure 1.2). Other bases are converted to compounds that are excreted (3). Several studies on the mechanisms of resistance to some nucleoside analogues proposed that a deficiency of intracellular nucleoside kinases and an increased activity of ribonucleotide reductase or activity of 5'−NT, are all related to a reduced toxicity of nucleoside analogues in cell and clinical samples (51-54). Furthermore, the competition between the endogenous nucleotides and the analogues indicates that the pools of the natural nucleotides and the relative concentration of the analogue might effect on the cellular activity of the analogues (55).

In addition of synthetic nucleoside analogues which chemically modified from their natural counterparts, there are also several naturally occurring modified nucleosides. Such examples of these compounds are cordycepin and pentostatin that have potential therapeutic benefits as anticancer agents, and 4-thiouridine which has been widely used as a photoactivatable agent.

1.5. Nucleoside analogue pentostatin

Pentostatin or deoxycoformycin (dCF) is an antibiotic which was isolated for the first time in 1974 from the fermentation medium of a strain of *S*. *antibioticus* (56). The nucleobase of this compound is similar to coformycin (CF) with the sugar moiety is deoxyribose instead of ribose (Figure 1.7). Both compounds are potent inhibitors of adenosine deaminase (ADA) (57). The structure of the nucleobase of these

compounds is a derivative of imidazodiazepin with a hydroxyl group attached to a seven membered ring; they are different from the natural purine base. These minor structural changes, however, result in a significant increase in the affinity of the molecules to the catalytic site of ADA (56).

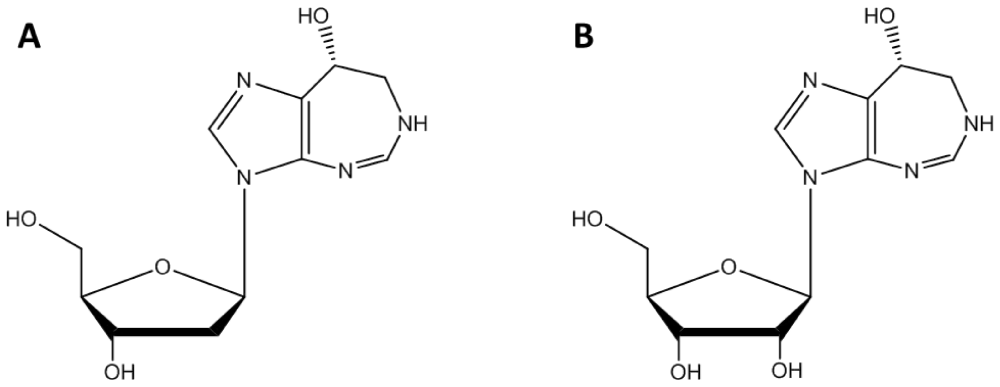

Figure 1.7. Chemical structure of deoxycoformycin or pentostatin (A) and coformycin (B)

Pentostatin inhibits the enzyme adenosine deaminase (ADA), therefore induces accumulation of deoxyadenosine (56, 57) which subsequently phosphorylated into deoxy-ATP by deoxycytidine kinase and adenylate kinase (58). High levels of deoxy-ATP would inhibit ribonucleotide reductase (59) and induce an imbalance in the cellular levels of deoxy nucleoside triphosphates leading to inhibition of DNA synthesis.

1.6. Nucleoside analogue cordycepin

The nucleoside analogue cordycepin is the principal bioactive compound found in the caterpillar fungi (*Cordyceps* and *Ophiocordyceps*). It was first isolated in 1950 from *C. militaris* (60) and its chemical structure was confirmed as 3'-deoxyadenosine (61). *Cordyceps* fungi and extracts derived from these are well-known traditional Chinese medicines, which are referred to caterpillar fungus because they are a complex of the fungus which grows on the caterpillar (Figure 1.8). *Cordyceps* species, including *Cordyceps sinensis*, *Cordyceps militaris*, *Cordyceps pruinosa* and *Cordyceps ophioglossoides*, are valued traditional medicines (62). These fungi exhibit anti-inflammatory, anti-bacterial, antifungal, and anticancer effects (63-65). There is scientific evidence that shows significant pharmacological activity of extracts of *Cordyceps* which have been investigated (Table 1.1).

Figure 1.8. (A) *Cordyceps militaris* (B) *Cordyceps ophioglossoides* (Wikipedia common)

Table 1.1. Pharmacological activity of extracts of *Cordyceps*

	Pharmacological Activity
C. sinensis	*in vitro* (66) and *in vivo* antioxidant activity (67)
	immunomodulator (68-71)
	cytotoxic activities to L-929, A375, and HeLa cells (72)
	protection of chronic renal (73)
C. militaris	anti-inflammatory (74, 75)
	immunomodulator (76)
	anti-allergic (77)
	anticancer (75)
C. pruinosa	induce apoptosis of HeLa cells (78)

Many low molecular weight compounds in *Cordyceps* have been isolated and elucidated, with a range of biochemicals identified including nucleosides and their related compounds (79, 80), saccharides (71, 73, 81-83), peptides (72), sterol, fatty acid (84), crude protein and metal elements (85). Nucleosides are found in relatively high concentrations in *Cordyceps*. More than 15 nucleosides and their transformation products have been investigated for bioactivity in natural and cultured *Cordyceps* including adenosine, cytosine, cordycepin, guanosine, hypoxanthine, uracil, and 2'-deoxyuridine (79, 80). Some reports found a very low content of cordycepin in natural and cultured *C. sinensis*, whereas it was found much greater in cultured *C. militaris* (79, 80).

Cordycepin is an adenosine analogue which has been known as an inhibitor of polyadenylation (86). The chemical structure of cordycepin (Figure 1.9) lacks a 3'-hydroxyl group that is necessary for RNA chain extension. Therefore, after incorporation into RNA, cordycepin might cause chain termination defects (87). It

has been shown to have biological activity *in vitro*, including anti-inflammatory (63, 64), inhibitor platelet aggregation (88, 89), anti-skin photo aging (90), immunomodulatory (91), prevention of hyperlipidaemia (92), anti-restenosis (93) and anticancer activity (88, 94-109). More attention has been given to cordycepin since it has been identified and proposed as anticancer agent. Many studies prove that combination of cordycepin and pentostatin, a deaminase inhibitor, have a significantly anti-proliferative activity in many kinds of malignant cells (94, 110).

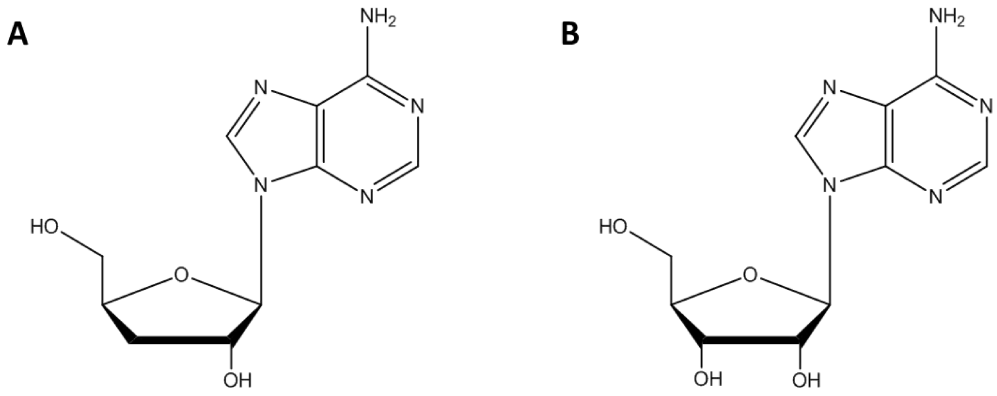

Figure 1.9. Chemical structure of cordycepin (A) and adenosine (B)

Intracellular drug-drug interactions at the nucleotide level can be explained by understanding the intracellular metabolism of nucleoside/nucleotide analogues as well as their plasma metabolism (111). Furthermore, there is a difference between the pharmacokinetic profile of the nucleotide analogues at an intracellular level and their nucleoside analogues in blood plasma (112); and their efficacy of therapy or toxicity does not associate with the plasma level of their nucleoside (113). Therefore, investigation of the metabolism of cordycepin as well as its pharmacokinetic profile at an intracellular level and in plasma is required for a full understanding of the action mechanism of cordycepin. For that reason, sensitive and

selective analytical techniques are required for quantitative analysis of cordycepin and the metabolites and its application to cell culture, *in vitro* and *in vivo* studies.

1.7. Nucleoside analogue 4-thiouridine

The nucleoside analogue 4-thiouridine (Figure 1.10A) was isolated in the first time from tRNA of *E. coli* as a rare nucleoside present only in position 8 (Figure 1.10B) (114). The presence of a sulphur atom instead of an oxygen at position 4 of the pyrimidine ring results in a near-UV light sensitivity (115). The sulphur atom produce a shifting in the UV/Vis spectrum absorption of 4-thiouridine to the red (λ_{max} = 330 nm) (116). A photochemical reaction occurs when bacteria is exposed to near-UV light, a carbon-carbon bond cross-linking is produced between 4-thiouridine at position 8 and cytidine at position 13 as a response to the exposure of the light. The cross-link significantly decreases the efficiency of tRNA as a substrate for amino acylation (117), and causes the bacteria to grow slowly (118).

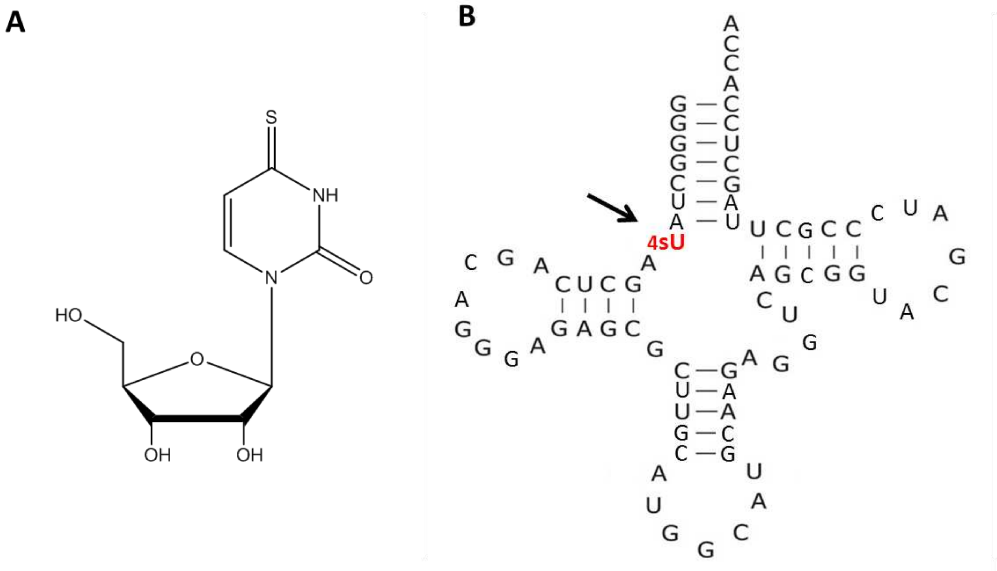

Figure 1.10. (A) Chemical structure of 4-thiouridine; (B) 4-thiouridine (4sU) was isolated in the first time from tRNA of *E. coli* as a rare nucleoside present only in position 8

Because of its characteristic spectral properties, 4-thiouridine is widely used in photochemical crosslinking as a cross-linking probe (119). The method has been applied for investigating protein translation and pre-mRNA splicing (120-122). This uridine analogue is phosphorylated into 4-thioUTP and is incorporated into RNA structures. Using 4-thiouridine as photoactivatable agent has a number of benefits. No bulky moiety is present and no base-pairing properties are changed since 4-thiouridine is a derivative of uridine with the oxygen atom at position 4 of the uracil ring replaced by a sulphur atom. It could be irradiated at wavelength above 300 nm, at which nonspecific UV cross-linking is at a minimum. Moreover, 4-thiouridine cross-linking can efficiently investigate both RNA-RNA and RNA-protein interactions (123).

The 4-thiouridine labelling method also has been applied for study of mRNA synthesis and polyadenylation. It has been applied to a broad range of cell types of human and murine origin including fibroblasts, endothelial cells, epithelial cells, macrophages and T-cells and the incorporation into RNA was found to be highly efficient (124). This method is also applicable for use in animals (125). Using this method, syntheses of RNA and protein are not significantly affected even after long incubation of high concentrations of 4-thiouridine (126). Nevertheless, Burger et al. (127) recognised that using a high concentration of 4-thiouridine on RNA metabolic labelling triggers a nucleolar stress response and Radle et al. (128) also suggest that the concentration of 4-thiouridine and the period of labelling should be minimized as high concentration of 4-thiouridine could be toxic to the cells. Therefore, the study of the intracellular metabolism of 4-thiouridine is crucial for understanding its

pharmacology or toxicity. A quantitative method, consequently, is needed for the determination of nucleoside analogue 4-thiouridine and its intracellular metabolites.

Nucleotide analogues are, however, often present in cells at very low levels, whereas their natural variants are present at very high levels. Sensitive and selective analytical techniques are therefore required to obtain quantitative and meaningful measurements of nucleotide analogues.

1.8. Methods of analysis for intracellular nucleotide analogues

The quantification of intracellular nucleotide analogues is challenging because of the presence of various endogenous interferences in complex matrices, the large difference in intracellular levels between nucleotide analogues and their natural compounds, and the high polarity of the compounds due to the phosphate groups. The extraction of the nucleotides is based on precipitation of unwanted protein using acid or organic solvent mixture and commonly done at low temperature. Various approaches have been used for determination of nucleotides such as capillary electrophoresis (CE) (129-131), thin layer chromatography (TLC) (132), ion exchange and ion-pair chromatography (133-135), whereas more recently, the methods have been coupled to mass spectrometry to increase sensitivity and specificity.

1.8.1. High-Performance Liquid Chromatography (HPLC)

HPLC has been generally used for quantification of nucleotides in many biological samples (136-140). HPLC has been shown to be one of the most suitable methods for measuring multiple nucleoside/nucleotide forms at the same time. Separation by

reversed-phase (RP) HPLC system is based on hydrophobic interaction between the analytes and the stationary phase and the separated analytes are typically quantified using ultraviolet absorption detection. This method has been used successfully to determine simultaneously ATP and its metabolites in human whole blood (140). The benefits of HPLC RP methods are the use of low concentration elution buffers and short analysis times compared with other methods such as ion-exchange HPLC. RP HPLC allows the simultaneous determination of ATP and its metabolites in a single short run time. However, the limit of detection is only in the µM range which is adequate for the quantification of ATP and its metabolites in whole blood since amount of ATP in whole blood are extremely high (1.5 – 1.9 mM) compared to plasma concentrations (141), but not sufficient for quantification of intracellular nucleotides.

Anion exchange and ion-pair liquid chromatography (IP-LC) are convenient methods for separation of nucleotides and nucleotide analogues since they are very polar compounds and contain a strong anion. Many methods using strong anion-exchange (SAX) and IP-LC have been developed for separation of intracellular or extracellular nucleotides followed by quantification with an enzymatic assay or radioactivity (142), fluorescence (136), or ultraviolet (138, 139) detection. These methods have been used for simultaneous separation and quantification of nucleotides due to their lack of retention on a RP column. Anion-exchange methods, however, in many instances need more extensive pre-treatment of samples and long running times (142-144). Slusher et al. (142) developed a method of anion-exchange HPLC combined with radioimmunoassay detection to analyse the metabolites of intracellular nucleotide analogue zidovudine (ZDV). The total analysis time was over than 90 min. Other

researchers also used a anion-exchange HPLC with radioactivity detection for determination of triphosphate metabolites of nucleoside analogues in cell lines (94, 110, 145); however, the methods were not be able to distinguish between the parent compound and the deaminated metabolite due to the same retention time (110). Moreover, columns of ion-exchange are generally poorly reproducible and not as strong as other LC columns as they have to be run with low pH mobile phase to elute ionic compounds (133); also the use of relatively in volatile salts, mean that anion-exchange chromatography is difficult to be applied using MS detection (49).

The use of anion-exchange cartridges combined with RIA detection to replace the HPLC-RIA method for quantification of the metabolites of zidovudine (ZDV) was demonstrated by Robbins et al. (146). ZDV phosphates were separated with anion-exchange cartridges into the mono, di, and triphosphate. After the separation, the metabolites went through enzymatic de-phosphorylation to the parent drug and then were determined their cellular concentration by a RIA. The use of cartridges instead of HPLC makes the quantification of metabolites of ZDV is more simple and less-time consuming than the HPLC-RIA method (142). This method, however, only analyse metabolites from a single drug.

Daxecker et al. (147) developed a method based on RP liquid chromatography using solvent generated ion-exchange as a mobile phase. Separation and quantification of 15 purine and pyrimidine nucleotides in human peripheral blood mononuclear cells (PBMCs) was achieved with solvent phosphoric acid containing triethylamine and phosphoric acid containing MgSO4 under gradient elution conditions. In acidic environment, the phosphate ion of nucleotides created ion pairs formation with

ammonium ions resulted from the protonation of triethylamine (TEA). The ion complexes were adsorbed and retained on the non-polar surface of a reversed-phase column; meanwhile ion complexes between Mg^{2+} ions and phosphate ions were poorly retained. Separation based on the adsorption and desorption of the ion complexes during elution using the mobile phase. However, this method is time consuming. They need almost one hour to elute one sample of cell extract using this method.

IP-LC has substituted the use of ion-exchange chromatography for nucleotide analysis since this method is more suitable to be combined with mass spectrometry. Several examples of the many applications of IP-LC for analysing of nucleotides using UV detection are measurement of purine nucleotide in erythrocyte of rats (138), simultaneous determination of 12 nucleotides and nucleosides in human urine and renal epithelium samples (139), and determination of adenine and guanine nucleotides of *Trypanosoma brucei* cells (148). The complete analysis of one sample using this method required 47 min to separate and quantify eight nucleotides in cell extracts of *Trypanosoma brucei*; and the LOD and LOQ values were in the range around 0.1 to 0.8 µM (148). Meanwhile, Bhatt et al. (136) used fluorescence detection to increase sensitivity of the IP-LC method to determine adenine nucleotides in primary astrocyte cells. However, to achieve a higher sensitivity of the method using a fluorescence detector, the nucleotides must be derivatized by mixing the nucleotides extract with chloroacetaldehyde at pH 4.5 and 60 °C for 60 min to form fluorescent, N6-ethenoderivatives of the nucleotides before being injected into HPLC system.

Other studies for simultaneous determination of intracellular nucleotides have been done by using IP-LC with UV detection in a number of types of cells, such as human mononuclear blood (PBMCs) and umbilical vein endothelial cells (HUVECs) (133), cerebellar granule cells (134), and in 16 normal or tumour cell lines (135). On those studies, however, only limited numbers of nucleotides were determined using the methods. Also, due to the low selectivity of UV detector, these methods do not provide sufficient selectivity and sensitivity for analysis intracellular nucleotide analogues where specificity and quantification in very low concentrations is compulsory.

1.8.2. Capillary Electrophoresis (CE)

Electrophoresis is a separation technique based on the ability of analytes to migrate through a conductive medium, usually a buffer solution, under influences of an electric field. Without other effects, anions move to the positively charged electric field anode and cations move to the negatively charged cathode, meanwhile neutral species, which do not respond to the electric field, remain stationary. Ions with a higher charge to size ratio, travel at a faster speed than larger ions, or lower charge ions. Differences in their degree of migration allows for the separation of complex mixtures of analytes (149). Then they are detected by UV, electrochemical, or fluorescence detector. CE is an alternative method of choice for analysing charged and polar compounds (150).

RP-HPLC separation is based on hydrophobic interaction between the analyte and the stationary phase, therefore charged and polar analytes are often not quite too well analysed. Particularly in these cases CE is an alternative method of choice (150).

CE columns contain considerably more theoretical plates than HPLC, result in better resolution and higher capacity; also efficient separations. The volume of sample injected into a CE column is significantly lower than that for HPLC and it requires only a few microliters of buffer solution for the separation compared with 20-30 mL of solvent for a typical HPLC separation. Nevertheless, detection limits for CE are much higher than those for HPLC (149).

Several researchers have developed a CE method with UV detection for determination of intracellular nucleotides. Feng et al. (131) have established the method for simultaneous quantification of intracellular nucleotides and sugar nucleotides in Chinese hamster ovary (CHO) cells. Nineteen nucleotides including seven nucleotide sugars were quantified by this method. However, the recoveries of the method for the nucleotides were around 69–83% and the detection limits were between 1.0 and 8.5 μM. Moreover, Friedecky et al. (130) also developed a CE-UV method and applied it for analysing nucleotides in CHO cells and human erythrocytes. Using the method 21 nucleotides and deoxynucleotides were separated in 15 min with high separation efficiency and the detection limits within the range of 0.3–1.2 μM.

CE combined with mass spectrometry (MS) detection has replaced the use of UV detector or fluorescence detector which is less universal and less informative. In the CE method, mass transfer limitations and Eddy diffusion which occur in HPLC are not applicable. Therefore the efficiency of separation and also mass sensitivity of CE-MS method are considerably better than with LC-MS (150).

Soga et al. (151) develop a method of pressure-assisted CE-MS for the detection of intracellular nucleotides and coenzyme A compounds of *E. coli* extracts. In this method, the Si-OH groups on the capillary wall were covered with phosphate groups, by using preconditioning buffer containing phosphate ions, to avoid adsorption of multi-phosphorylated species onto the fused-silica capillary. During preconditioning, the nebuliser gas was turned off in order to prevent the MS from contamination of phosphate ions. In this method, whereas nucleotides migrated to the anode, they were driven to the cathode by electroosmotic flow and also applied air pressure, and then detected by MS detector. The advantage of the using of air pressure during electrophoresis is reducing the analysis time. Using this method, 14 nucleotides including nicotinamide-adenine dinucleotides, purine nucleotides, and cytosine nucleotides, have been determined simultaneously within 20 min.

It appears that a CE-MS method is successful to quantify simultaneously intracellular nucleotides in biological samples. This approach, however, is not ideal. Particularly, significant fluctuations in time of migration of analytes, due to fluctuation of the current during electrophoresis, are frequently observed. Furthermore, the inlet of the capillary often blocked (151, 152).

1.8.3. Liquid Chromatography Mass Spectrometry (LC-MS)

Mass spectrometry detection offers excellent detection limits, typically 25 fg to 100 pg (149). There are three fundamental parts on a mass spectrometer i.e. the ionisation source, the analyser, and the detector. In the ionization compartment all molecules (solvent and analytes) are ionized, and the ions are separated by their mass to charge ratio (*m/z*). Because each analytes undertakes a specific

fragmentation into smaller ions, its mass spectrum of ion intensity as a function of *m/z* provides qualitative information that can be used to identify the analytes.

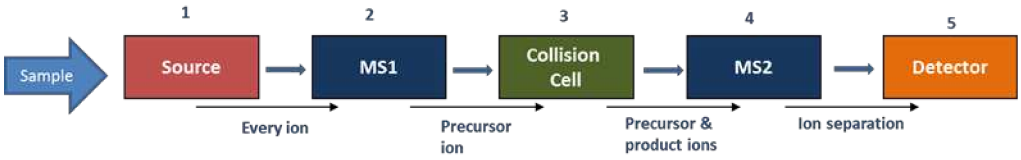

Figure 1.11. Schematic of tandem mass spectrometry

(1) Sample from LC are introduced into the ionisation source; (2) The ions are filtered according to their mass to charge ratio (m/z) in MS1; (3) The selected ion, the precursor ion, is fragmented in the collision cell into product ions; (4) The fragment ions are subsequently filtered according m/z in MS2; (5) The daughter ions are detected and the final spectrum shows the peaks of selected ion and all its products.

With a triple quadrupole instrument, the combination of two quadrupole mass filter (analysers) is separated by a collision cell into which an inert gas is admitted to collide with the selected sample ions. Liquid chromatography tandem mass spectrometry (LC-MS/MS) offers good benefits for selective and sensitive determination of analytes. The ionised samples pass through a first analyser (MS1) and are separated according to *m/z*. MS1 is used to select, from the primary ions, those of a particular *m/z* value which then pass into the fragmentation region (collision cell). The ion selected by the MS1, the precursor ion, is dissociated in the fragmentation region into product ions. The product ions are subsequently filtered according to *m/z* in the second analyser (MS2). In MS2, the product ions are detected and the final spectrum shows the peaks of selected ion and all its products. Different ions have characteristic fragmentation configurations determined by their structure. This allows the use of multiple reactions monitoring (MRM) where the mass spectrometer specifically detects the precursor ion and selected product ions

giving very specific detection of selected compounds. The illustrations of how a tandem mass spectrometry works is shown in in Figure 1.11.

High concentrations of IP agents or in volatile salts, as are often used in an HPLC system, however, obstruct the applicability of MS for detection. Nevertheless, currently, numerous LC-MS methods have been developed for the analysis of intracellular nucleotides using a weak anion-exchange (WAX) column, moderately volatile IP agents, or the use of IP agents at very low concentrations. Jansen et al. (49) review the development of MS methods for quantification of intracellular nucleotide analogues. They divided the methods into indirect and direct method based on the presence or absence of a fractionation process followed by de-phosphorylation and purified steps before being injected into the LC-MS system.

1.8.3.1 Indirect methods

Fractionation is achieved by elution with high salt levels on WAX (153) or SAX solid-phase extraction (SPE) columns (154-156). De-phosphorylation is mostly achieved enzymatically using alkaline or acid phosphatase. Dervieux and Boulieu (157), however, used hydrolysis (100°C, 60 min) to degrade the nucleotide analogues to their derivatives. After de-phosphorylation, a purification step using SPE is accomplished to eliminate enzymes and salts from the de-phosphorylated extracts. Lastly, the nucleosides have been separated on C18 columns using isocratic or gradient elution of acetonitrile or methanol containing acetic or formic acid combined with detection by MS (153-157).

Indirect methods require additional time due to fractionation, de-phosphorylation, and purification steps, although those procedures make the final analysis fast and relative simple. Furthermore, those sample pre-treatment processes also provide a potential source of errors. Additionally, those methods (153-157) are inadequate on a method validation and only for investigation of limited nucleotides.

1.8.3.2 Direct methods

A liquid chromatographic-tandem mass spectrometric (LC-MS/MS) method has been applied for the direct quantification of nucleoside and nucleotide analogues in various biological samples. Anion exchange columns with an alternate elution mechanism have been introduced by Shi et al. (158) to replace the use of non-volatile ions due to interfering of the ions on the detection with MS. The charge of the basic functional groups ($pK_a \approx 8$) of a WAX column was altered by applying a pH gradient (pH 6-10.5) to the column. As a result, the column capacity declined at a higher pH, thus the anionic nucleotides were eluted. Instead of requiring high concentrations of volatile opposite ions like conventional anion-exchange methods, this method only needs low amounts of the ions for the elution. Hence, it makes this anion exchange method directly applicable to MS detection. The method was validated to analyse the phosphorylated metabolites of antiviral dexelvucitabine in PBMCs (158).

Other anion exchange LC-MS methods using WAX columns have been developed and validated for simultaneous determination of the metabolites of nucleoside analogue anticancer drugs gemcitabine (2',2'-difluorodeoxycytidine: dFdC) in PBMCs (159) and cladribine in MDCKII cells and culture medium (160). Moreover, the method then

was modified to detect and quantify not only the phosphorylated metabolites of gemcitabine, but also the deaminated metabolites of dFdC, 2',2'-difluorodeoxyuridine (dFdU), and the phosphorylated metabolites of dFdU (161). Even though these methods are vigorous, very sensitive, and MS- favourable; the methods suffer from lack of retention of nucleosides.

Due to the polarity of phosphate groups, nucleotides are poorly retained on RP HPLC column. Ion pairing agents have been used to increase retention time of nucleotides on the column. The use of relatively volatile alkylamine or low amounts of in volatile tetraalkylammonium salts as IP agents for separation of nucleotide analogues make them more appropriate for a combination with MS detection. Kinai et al. (162) used tetrabutylammonium hydroxide (TBAH) as an ion pair for determination of the phosphorylated metabolites of antiretroviral drug zidovudine in PBMCs. Using very low concentrations of TBAH (0.01 mM) combined with ammonium hydrate as an alkalization agent; it allowed good separation and improved the sensitivity. Also, products can be simply washed from the lines and interfere less with the MS detection. Nevertheless, an exposure of a high pH of the mobile phase (pH 8.5), means a column is more vulnerable to degradation. Therefore, a highly stable HPLC column is more suitable to be used on this method instead of a conventional column.

An LC-ESI-MS/MS method using N,N-dimethylhexylamine (DMHA), a volatile ion-pairing agent, was fully described by Fung et al. (163) to determine intracellular concentrations of nucleoside analogue Ziagen and its metabolites. Their results showed that the use of 20 mM DMHA not only give an adequate separation, but also minimized the interference to mass spectrometry detection. Moreover, Tuytten et

al. (164) also used DMHA for analysis of the mixture of 12 nucleotides standards containing of mono-, di-, and triphosphates. They evaluated the influence of DMHA on the separation and MS detection of the nucleotides and recommended that gradient elution of methanol containing 5 mM DMHA resulted in good HPLC selectivity and MS detection. Moreover, using the smaller diameter column of 1.0 and 0.5 mm, Cai et al. (165) could decrease the amount of DMHA to 10 and 5 mM, respectively; and the MS signal improved 5 to 10-fold.

Furthermore, similar methods using alkylamine as ion pairing agent have been used to determine intracellular nucleoside analogues. Durand-Gasselin et al. (166) and Pruvost et al. (167) used IP-LC-MS/MS method with 1,5-DMHA as ion pairing agent for study of the intracellular metabolism of several nucleoside reverse transcriptase inhibitors (NTRI) in PBMCs and red blood cells (RBCs). Coulier et al. (168) developed a LC-MS/MS method using gradient elution of 5 mM hexylamine in water and 90% methanol/10% 10 mM ammonium acetate to determine nucleotides and polar metabolites in extracts of microorganism. Cordell et al. (169) quantified nucleotides and related phosphate-containing metabolites in Chinese hamster ovary (CHO) cells by LC-MS/MS using 5 mM DMHA as ion pair agent.

Despite the fact that DMHA has effectively been used by many researchers, several methods using DMHA were found difficult to apply because of source pollution, irreproducible runs and ion suppression (156, 170). Nonetheless, the IP-LC-MS/MS method with DMHA as ion pairing agent is one of the most suitable methods for separation and detection of low concentrations of endogenous nucleotides and has established its usefulness in various applications.

1.8.3.3 Mass Spectrometry Ionisation

There are various types of ionization methods are applied in mass spectrometry methods, such as electron impact (EI), Fast Atom Bombardment (FAB), atmospheric pressure chemical ionization (APCI), electrospray ionization (ESI), and matrix assisted laser desorption ionization (MALDI). The option of ionization method depends on nature of the analyte and the kind of data required from the analysis. The benefits of ESI are compatible with LC and capable of producing ions from polar analytes (171). It also works particularly well with weakly acidic or basic compounds and non-volatile molecules such as nucleotide and oligonucleotides (172). Meanwhile, APCI is regularly used for less polar or non-polar compounds (171).

Electrospray is produced by placing a charge of 3-5 kV on a flow of liquid at atmospheric pressure; the liquid is nebulised and small charged droplets are formed in the spray zone and are evaporated by a combination of heat, vacuum and acceleration into gas by voltages. Finally the ions are emitted from the droplets and accelerated into the mass analyser by voltages (Figure 1.12) (171).

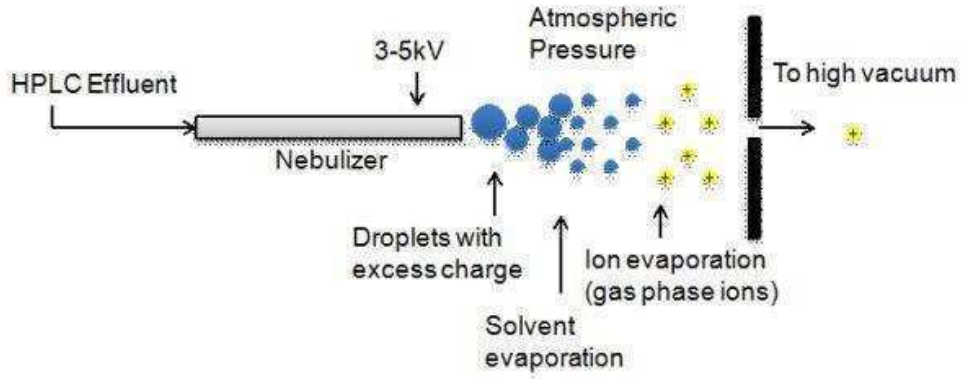

Figure 1.12. Illustration of an electrospray ionisation (171).

Naturally, nucleotides could be protonated as well as deprotonated. Nucleotides with basic amino groups (adenine, guanine, and cytosine) are protonated more efficiently than those that do not have this group (thymine and uracil) (167). Nevertheless, uridine and thymidine nucleosides and nucleotides could be detected in the negative ion mode with the deprotonated base as a common fragment. Therefore, most nucleotides are well ionized in a wide pH range using both the negative and the positive ionization mode.

Nucleoside analogues have been broadly used for medical treatment and research in cellular and molecular biology. These analogues are intracellularly metabolized into their pharmacologically active nucleotides and compete with the endogenous compounds. Observing intracellular nucleotide analogues, therefore, is more advantageous than observing the nucleoside analogues because the active metabolites are determined instead of their prodrug. Moreover, analysis of the intracellular level of nucleotide analogues along with the endogenous compound is important for a full understanding of their pharmacology activity.

Ion pairing LC-MS/MS with electrospray ionisation has been chosen for simultaneous determination of intracellular levels of nucleoside and nucleotide analogues due to very good selectivity and sensitivity of the method. Furthermore, DMHA has been used as ion pairing agent based on the previous studies (163-165, 169). It has been proven that DMHA is an appropriate ion-pairing agent, where the nucleotides are retained and well separated on a reversed-phase HPLC column and also it cause minimal interference in MS detection.

1.9. Aims of the PhD project

Cordycepin is an adenosine analogue found in *Cordyceps* and *Ophiocordyceps* which has been shown that the combination with pentostatin has potential action as anticancer treatment. Since their efficacy of therapy or toxicity of nucleoside drug does not associate with the plasma level of their nucleoside. Therefore, investigation of the metabolism of nucleoside analogues is required for a full understanding of their pharmacological activity and toxicity. For that reason, this study will aim to develop an ion pairing LC-MS/MS method for quantitative analysis of nucleoside analogue cordycepin and the metabolites and its application to cell culture, for *in vitro* and *in vivo* studies. As nucleotide analogues are often present in cells at very low levels, while their natural variants are present at very high levels, therefore ion pairing LC-MS/MS with electrospray ionisation has been chosen due to very good selectivity and sensitivity of the method.

The metabolism of cordycepin *in vitro* and *in vivo* will be investigated by studying the metabolism of cordycepin in cell lines and the culture medium, comparing the degradation of cordycepin and extract ethanol of *Cordyceps militaris* in non-heat-treated serum, and determination of the level of cordycepin and the metabolites in plasma and liver samples of rats. The effects of the treatment using cordycepin, pentostatin, or the combination of cordycepin and pentostatin on nucleotide metabolism in cancer lines will also be investigated. I will be comparing the intracellular metabolism of cordycepin to another nucleoside analogue by investigating intracellular metabolism of 4-thiouridine and the effect of its metabolite on the metabolic balance of adenine and uridine nucleotides.

CHAPTER 2
DEVELOPMENT OF AN LC-MS METHOD FOR THE INTRACELLULAR QUANTIFICATION OF CORDYCEPIN METABOLITES AND NUCLEOTIDES

DEVELOPMENT OF AN LC-MS/MS METHOD FOR THE INTRACELLULAR QUANTIFICATION OF CORDYCEPIN METABOLITES AND NUCLEOTIDES IN CELLS

2.1. Introduction

2.1.1. Mass Spectrometry for Quantitative Analysis of Intracellular Nucleotide Analogues

Intracellular nucleotide analogues usually present at very low concentrations, while their natural counterparts are present at relatively high concentrations. Therefore, sensitive and selective analytical methods are needed for determining their presence in biological samples. Many analytical methods have been developed for the quantitative determination of intracellular nucleotides. Previously, anion-exchange (173, 174) and ion-pair liquid chromatography (133-135) methods with ultraviolet detection have been used to identify and determine simultaneously nucleoside and nucleotides. Using these methods, however, only limited numbers of nucleotides were determined. Also, because of the low selectivity of UV detector, these methods do not provide adequate selectivity and sensitivity for analysis intracellular nucleotides where specificity and quantification in very low concentrations is required. LC coupled with the tandem mass spectrometry method has been applied to increase the selectivity and sensitivity compared with HPLC-UV methods. Nevertheless, the use of relatively non-volatile salts and ion pairing agents, interfere with the detection by MS.

An LC-ESI-MS/MS method using N,N-dimethylhexylamine (DMHA) as an ion-pairing agent was developed by Fung et al. (163) to determine phosphorylated metabolites. They found that DMHA, a volatile ion-pairing agent, not only gave an adequate

separation, but also minimized the interference with mass spectrometry detection. Moreover, Tuytten et al. (164) also used DMHA for analysis of a mixture of 12 nucleotide standards containing mono-, di-, and triphosphates. Based on their results, both positive and negative ESI modes were possible to generate spectra. This method provided good separation; however, it had not been applied to biological cells.

Later, other LC-MS methods using DMHA for analysis of nucleotides in biological cells have been published (175-177). The limitation of those methods, however, is for investigation of only a few nucleotides. Furthermore, the method which was developed by Cordell et al. (169) not only has shown a better sensitivity and selectivity, but also the number of analytes that can be analysed is greater than those that have been reported in many previous LC–MS methods. However, despite the development of the extraction method which was also examined by them, the optimization of cellular nucleotide extraction is still needed for specific applications, for example where other nucleotides or nucleosides and their metabolites are to be investigated.

2.1.2. Extraction of Nucleotide from Cells

Cell extraction procedures, including the selection of the extraction solvent, are essential for an accurate and precise quantification of analytes. For these purposes, enzymatic activity should be terminated quickly and the compounds of interest should be extracted with high and reproducible recovery (178) and in which the analytes are stable (179). As the cells are still intact during isolation, ongoing analyte

metabolism *ex vivo* must be prevented. Therefore, other factors to be considered are the simplicity of the method and the speed of the preparation. Moreover, the extraction solvent should also be compatible with the LC-MS analysis (180).

Perchloric acid (PCA) and trichloroacetic acid (TCA) have been widely used to precipitate cellular macromolecules and to extract cellular content. Although extraction with perchloric acid results in high recovery, the perchloric acid and low pH can deteriorate peak shapes and reduce retention times in ion-pair LC (181). Besides, non-volatile acid salts can cause major difficulties by pollution of the MS.

A preliminary study by Brown and Miech (180) showed that extraction using both PCA and TCA gave equivalent results. Research by Au et al. (181) compared PCA and acetonitrile (ACN):water (3:2 v/v) for the extraction of intracellular nucleosides and nucleotides. Based on their research, the PCA fraction contained more monophosphate nucleotides and ADP than in the ACN fraction, whereas the ACN fraction contained more triphosphate nucleotides and ATP than the PCA fraction. Moreover, ACN was more appropriate for extraction because it did not interfere with the HPLC analysis. On the other hand, Reijenga et al. (178) compared three extraction solvents for the extraction of nucleotides between PCA and methanol with and without EDTA. They found that the highest recovery of nucleotides was given by PCA. Furthermore, Yang and Gupta (182) observed that the direct extraction method with PCA gave more total adenosine nucleotide than the indirect method.

Research by Grob et al. (183) optimized cellular nucleotide extraction by investigation of several different concentrations of some organic solvents. Mixtures of organic solvents and water are hypotonic and disrupt cell membranes, thus effectively extracting nucleotides. For ATP, for example, recoveries of 80-104% were observed for several water-organic solvent combinations (183). Furthermore, the analytes are stable in methanol lysate during lysis (184). Finally, organic solvent can simply be concentrated by evaporation. Cordell et al. (169) also developed an extraction method of the intracellular nucleotides from biological samples. Based on their research, the addition of methanol precooled to -20°C followed by hexane extraction was found to be the best extraction technique. However, the nucleotide recovery was not high enough and therefore the optimization of the cellular nucleotide extraction is still needed. For this purpose, it is important to compare the range of extraction procedures which can be specifically applied to specific metabolite extraction for application to biological cells or tissue samples.

Finally, to express the determined concentration per cell, the number of cells isolated should be quantified. The most straightforward approach is to count the number of cells using a haemocytometer, microscope, or by flow cytometry.

2.1.3. Methods for Analysis of Cordycepin

Numerous methods have been reported for the qualitative and quantitative analysis of cordycepin. However, most of them are used for analysis of cordycepin in extract of *Cordyceps* (79, 80, 185-187); only a few methods have been applied to cell lines (94, 110). Furthermore, the drawback of current methods is in their scope of

analysis and the inadequacy of validation of the methods. An HPLC method demonstrated by Tsai et al.(188) was able to detect the metabolite of cordycepin in rat blood sample. However, because of the limitation of the UV detection, the metabolite was unidentified. Chen et al. (94) and Kodama et al. (110) used HPLC with flow-through radioactivity detection for quantification of triphosphate metabolites of cordycepin in cell lines; however, the methods were not be able to distinguish between cordycepin and the deaminated metabolite due to the same retention time. In addition, these methods also lacked validation which is important for producing quantitative data. Furthermore, the flow-through radioactivity detection is limited by insufficiency of sensitivity and often gives lower recovery (189).

Moreover, several methods using mass spectrometry detection have been developed for determination of cordycepin and other active components in *Cordyceps* (79, 80, 185). None of those methods, however, were used for application to biological cells. Therefore, the aim of this work is to develop a method for simultaneous quantification of metabolites of cordycepin and other intracellular nucleotides for application to biological cells or tissue samples. The initial point for the development of this method is based on the work by Cordell et al. (169). There are many important factors which need to be considered in the development of the method. These include not only the optimisation of the LC and the mass spectrometry method, but also the development and improvement of the method of sample extraction to obtain a maximum recovery of the compounds of interest and minimum interference from a matrix sample.

Even though the use of DMHA, the ion-pairing agent, has been previously reported by Cordell et al. (169), some of the important variables such as the gradient used, concentration of ion-pairing agent, and length of the column require optimisation to achieve an optimum separation.

2.1.4. Validation of Quantitative Analysis

A validation process is required to ensure that an analytical method is suitable for the intended purpose. Analytical characteristics used in method validation include determination of:

1. Specificity: the ability of the method to measure accurately and specifically the analyte of interest in the presence of other components that may be expected to be present in the sample matrix.
2. Linearity: the ability of the method to elicit test results that are directly, or by defined mathematical transformation, proportional to analyte concentration within a given range.
3. Limit of detection (LOD) and limit of quantification (LOQ). LOD is the lowest concentration of analyte in a sample that can be detected and LOQ is the lowest concentration of analyte in a sample that can be determined.
4. Accuracy: the closeness of test results to the true value. It is reported as the percent recovery of the known, added amount, or as the difference between the mean and true value with confidence intervals.

5. Precision: the degree of agreement among individual test results when an analytical method is used repeatedly to multiple samplings of homogenous sample.
6. Robustness: the capacity of a method to remain unaffected by small, deliberate variations in method parameters; as a measure of the reliability of a method.

2.2. Aim and Objectives

The aim of this chapter is to develop a quantitative LC-MS/MS method for nucleoside analogue cordycepin and its metabolites for application to cell culture, *in vitro* and *in vivo* studies.

The objectives of this chapter are as follows:

- To optimise a HPLC method for analysis of cordycepin and its metabolites in cell culture by the following investigation parameters:

  - Solvent gradient and mobile phase composition,

  - Ion-pairing concentration

  - Length of the column

- To optimise the extraction method
- To optimise the mass spectrometry method by examining fragmentation of nucleotides.
- To validate the method and apply it for analysis of intracellular nucleotides in cell lines.

2.3. Materials and Methods

2.3.1. Chemicals

All nucleoside (cordycepin, adenosine, 2'-deoxyinosine, inosine) and nucleotide standards (cordycepin 5'-triphosphate, 2'-deoxyadenosine-triphosphate, AMP, ADP, ATP, CMP, CDP, CTP, GMP, GDP, GTP, UMP, UDP, and UTP), internal standard (8-bromoadenosine 3',5'-cyclic monophosphate (8-Br-cAMP) and 8-bromoadenosine 3',5'-cyclic-triphosphate (8-Br-ATP)), ethylenediaminetetraacetic acid calcium disodium salt (Calcium Na_2-EDTA) were purchased from Sigma Aldrich (Poole, UK). Pentostatin was obtained from Tocris Bioscience (Bristol, UK). N, N-dimethylhexylamine (DMHA), perchloric acid (PCA) and acetic acid were purchased from Acros Organics (Geel, Belgium). Methanol, hexane, and acetonitrile (HPLC grade) were purchased from Fisher (Loughborough, UK). In all experiments, deionized water was used, and all mobile phases were filtered through a 0.47 µm nylon filter (Whatman, Maidstone, UK) before use.

2.3.2. Cell culture

2.3.2.1 Reagents and solutions for use in cell culture

Phosphate buffered saline (PBS) (4.3 mM Na2HPO4, 1.5 mM KH2PO4, 137 mM NaCl, 2.7 mM KCl, pH 7.4) was purchased from OXOID. Dulbecco's modified Eagles medium (DMEM) with 4.5 g/L of glucose and 4 mM glutamine, foetal bovine serum (FBS), foetal calf serum (FCS), and Trypsin/EDTA solutions (10x concentrated solutions of phosphate-buffered saline containing 0.5% trypsin and 0.2% EDTA) were purchased from PAA.

2.3.2.2 Cell lines

Cell culture was performed in a Class II biological safety cabinet under aseptic conditions. Cells are cultured at 37°C in a humidified atmosphere containing 5% CO_2. Mammalian cell lines used are described on Table 2.1.

Table 2.1. Description of cell lines

Cell Line	Origins	Description
MCF7	Human breast epithelia adenocarcinoma	Adherent cell line maintained in DMEM supplemented with 10 % FBS and 4 mM L-glutamine
HeLa	Human cervical epithelial carcinoma	Adherent cell line maintained in DMEM supplemented with 10% FBS and 4mM L-glutamine
NIH 3T3	Mouse embryonic fibroblast cells	Adherent cell line maintained in DMEM supplemented with 10 % FCS

2.3.2.3 Maintenance of cell lines

Cell lines used were purchased from the European Collection of Cell Cultures (ECACC) and were maintained in the medium as described on Table 2.1. For routine culture, cells grown to 75-80% confluent were washed with PBS (pre-warmed at 37°C) and treated with 1X Trypsin-0.5 mM EDTA for 2- 5 min at 37°C. Once cells had detached, fresh medium was added to neutralise the trypsin and 20-40% seeded into a new flask and passaged every couple of days as required. Cells were maintained for no more than 20 passages. Where a specific seeding density was required, a haemocytometer was used to count cell density from a neutralised sample. For each experiment cells, cells were seeded in a 6 well plate at a density of 0.35 million cells per well 24 hours before use or as indicated.

2.3.3. Ion-Pair Liquid Chromatography development

Samples were prepared at a final concentration of 100 µM dissolved in water. They were stored at -20°C before analysis.

Various mobile phase mixtures with different gradients were examined to achieve optimal separation, with mobile phase A containing of DMHA in water: methanol (95:5 v/v), and B containing DMHA in methanol: water (80:20 v/v). Mobile phase A was adjusted to pH 7 using acetic acid. The effect of the concentrations of DMHA (5 mM, 10 mM, or 20 mM) and the length of column (100 mm or 150 mm) were investigated to observe effects on separation and retentions.

Analyses of samples were carried out using an YL 9100 and HP 1050 HPLC system. A reversed-phase column 4.6 mm×100 mm (Hypersil ODS, 5 µm) (Thermo Fisher Scientific, Waltham, MA, USA) and 4.6 mmx150 mm (Polaris C-18, 5 µM) (Agilent, Santa Clara, CA, USA) were used. The column temperature was maintained at 60°C. The volume of sample injected on to the column was 5 µL. The flow rate was set at 1 mL/min. The peaks were detected with UV detector at 250 nm.

2.3.4. Optimization of intracellular nucleotide analysis using ion-pair LC

2.3.4.1 Sample preparation

Nucleotides in cells were extracted using six different methods which were distinguished by their extraction solvents. MCF7 cells were grown in six-well plates for 24 hours and then the medium was removed and replaced with 0.5 mL of

extraction solvent at −20°C and 10 µL 1 mM internal standards. An internal standard, 8-Br-cAMP was used in this experiment in order to calculate an accurate recovery. Extraction solvents evaluated were: methanol 100%, methanol 100% containing EDTA 1.25 mM, methanol: water (3:2 v/v), PCA 0.3 M containing EDTA 1 mM, PCA 0.5 M, and acetonitrile: water (3:2 v/v) (two replicates for each extraction solvent). Cells were scraped from the bottom of each well and centrifuged (12,000 RPM, 4°C for 5 min) and the supernatant removed. In the case of methanol extraction, methanol extract was added to 0.5 mL hexane and the methanol fraction being removed following the shaking. PCA was neutralised using KOH 1 M and the precipitate was removed using centrifugation. To prevent degradation of nucleoside triphosphates to diphosphate and monophosphate, extractions were carried out on ice and the centrifuge was maintained at 4°C. All samples were then evaporated to dryness in a Jouan Centrifugal evaporator at room temperature and re-dissolved in 50 µL water prior to analysis.

2.3.4.2 Ion-pair LC conditions

Analyses of samples were carried out using HP 1050 HPLC system (Agilent, Santa Clara, CA, USA). A 4.6 mm×150 mm (Polaris C-18, 5 µm) (Agilent, Santa Clara, CA, USA) column was used. The column temperature was maintained at 60°C. The standards and samples were separated using a gradient mobile phase containing of DMHA 5 mM in water: methanol (95:5 v/v) (A), and DMHA in methanol: water (80:20 v/v) (B). Mobile phase A was adjusted to pH 7 using acetic acid. The gradient condition is: 0–20 min, 0–40% B; 20–25 min, 40-0% B; 25–35 min, 0% B. The volume

of sample injected on to the column was 5 µL. The flow rate was set at 1 mL/min. The peaks were detected with UV detector at 250 nm.

2.3.5. Mass Spectrometry development

Before acquiring sample data, the instrument Waters Quattro Ultima triple quadrupole mass spectrometer (Waters, Milford, MA, USA), was tuned and calibrated using a suitable standard to obtain the maximum peak resolution and highest mass accuracy. For the initial tuning, each individual standard (10 µM in water) was infused into the mass spectrometer at a flow rate of 200 µL/min. Each of nucleotides was examined with full scan spectra of mass range of *m/z* 100-800. In negative ion electrospray the $[M-H]^-$ ion was examined at the cone voltage 40 V. Single ion recording (SIR) and multi reaction monitoring (MRM) was then carried out and further tuning was done to find the optimum cone voltage for each examination. The source temperature was set at 125°C and nitrogen was used as drying gas at 850 l/hour and nebulising gas for the electrospray at flow rate of 150 l/hour. Argon was used as the collision gas and initially set at 20 eV. These optimized conditions were used for measurement of a mixture of the nucleotides and nucleosides (10 µM).

2.3.6. Analyte and sample stability

The degradation of nucleotides during evaporation was investigated by evaporating them using centrifugal evaporator at room temperature for 2 h and repeated four times. Stability of cordycepin in cell culture medium was observed by incubating cordycepin in cell culture medium for 0.5 h, 1 h, 2, and 4 h. The effect of extraction solvent on the inhibition of degradation of cordycepin in cell culture medium was

analysed by the addition of 250 µL of the extraction solvent into 1 mL of 10 µM cordycepin in cell culture medium. In order to optimise extraction of cordycepin from cell culture medium, the extraction solvent was added in cell culture medium containing 50 µM cordycepin in different ratios. The recovery of cordycepin and the proportion of the amount of the degradation product formed were calculated by comparing the peak area of the extracted samples to the peak area from the 50 µM standard solution.

2.3.7. Method validation

Method validation was carried out using the extraction with cold methanol containing 1.25 mM EDTA and 0.5 µM internal standards. Accuracy and precision were evaluated by analysing of six replicates of standard solutions spiked into the cells. For this experiment, 10 µL of standards at concentration of 100 µM were spiked into the 6 wells after the addition of the extraction solvent. Similarly, 10 µL of water was added to six-well as extract of un-spiked cells. The analyte recovery was calculated by subtracting endogenous nucleotide levels from spiked samples and expressing as a percentage of the peak area of the standard solutions. Accuracy was reported as the per cent recovery. The precision was calculated from the relative standard deviation (RSD %) of the replicate analysis. Calibration curves were prepared by serial dilution of standards at concentrations of 100 µM, 50 µM, 25 µM, 10 µM, 5 µM, 2µM, and 1 µM. Each concentration of standards were spiked into the extraction solvent containing internal standard and carried out with the same procedure as the samples. R^2 values were calculated by linear regression analysis of the ratio of standard/internal standard peak areas versus the standard

concentrations in µM. Limit of detection (LOD) was estimated based on the standard deviation of y-intercepts of the regression line (SD) and the slope of calibration curve (S) at levels approximating the LOD according to the formula: LOD = 3.3(SD/S).

2.3.8. Application to the analysis of intracellular nucleotides in MCF7 cells

2.3.8.1 Cell extraction method

Cells were washed twice using PBS before 0.5 mL extraction solvent was added. Then, cells were scraped and centrifuged at 15,000 g, 4°C for 15 min. Supernatant was then evaporated to dryness in a Jouan Centrifugal evaporator at room temperature and re-dissolved in 50 µL water before being injected for LC-MS/MS analysis.

2.3.8.2 Calculation of total cell volume

The diameter of cells was determined using a Beckman Coulter LS230 Laser Diffraction Particle Size Analyzer and then the volume of a single cell was calculated using the following formula: $v= 4/3\ \pi r^3$. The number of cells was counted using a haemocytometer. The actual intracellular concentration subsequently was converted using the total cell volume.

2.3.8.3 LC-MS/MS conditions

Analyses of samples (Figure 2.1) were carried out on an Agilent 1100 HPLC system (Agilent, Santa Clara, CA, USA) with auto sampler maintained at 8°C. Separations were achieved on a Luna C-18, 3 µm (2 × 150 mm) column with Security Guard (4 x 2

mm) (Phenomenex, Macclesfield, UK) at 40°C. The standards and the samples were eluted using a gradient mobile phase containing of 5 mM DMHA in water: methanol (95:5 v/v) (A), and 5 mM DMHA in methanol: water (80:20 v/v) (B). Mobile phase A was adjusted to pH 7 using acetic acid. The gradient condition was: 0–5 min, 10–20 % B; 5–10 min, 20- 28 % B; 10-22, 28-40 % B; 22-25, 40-10 % B; 25–35 min, 10 % B. The volume of sample injected to the column was 5 µL. The flow rate was set at 200 µL/min.

MS data were acquired on Waters Quattro Ultima triple quadrupole mass spectrometer (Waters, Milford, MA, USA) in negative electrospray ionisation (ESI) mode. Source temperature was at 125°C, with nitrogen as drying and nebulising gas and argon as collision gas. Multiple reactions monitoring (MRM) scan was used with dwell time 0.1 s. The MS system and data were processed by Waters MassLynx™ Software.

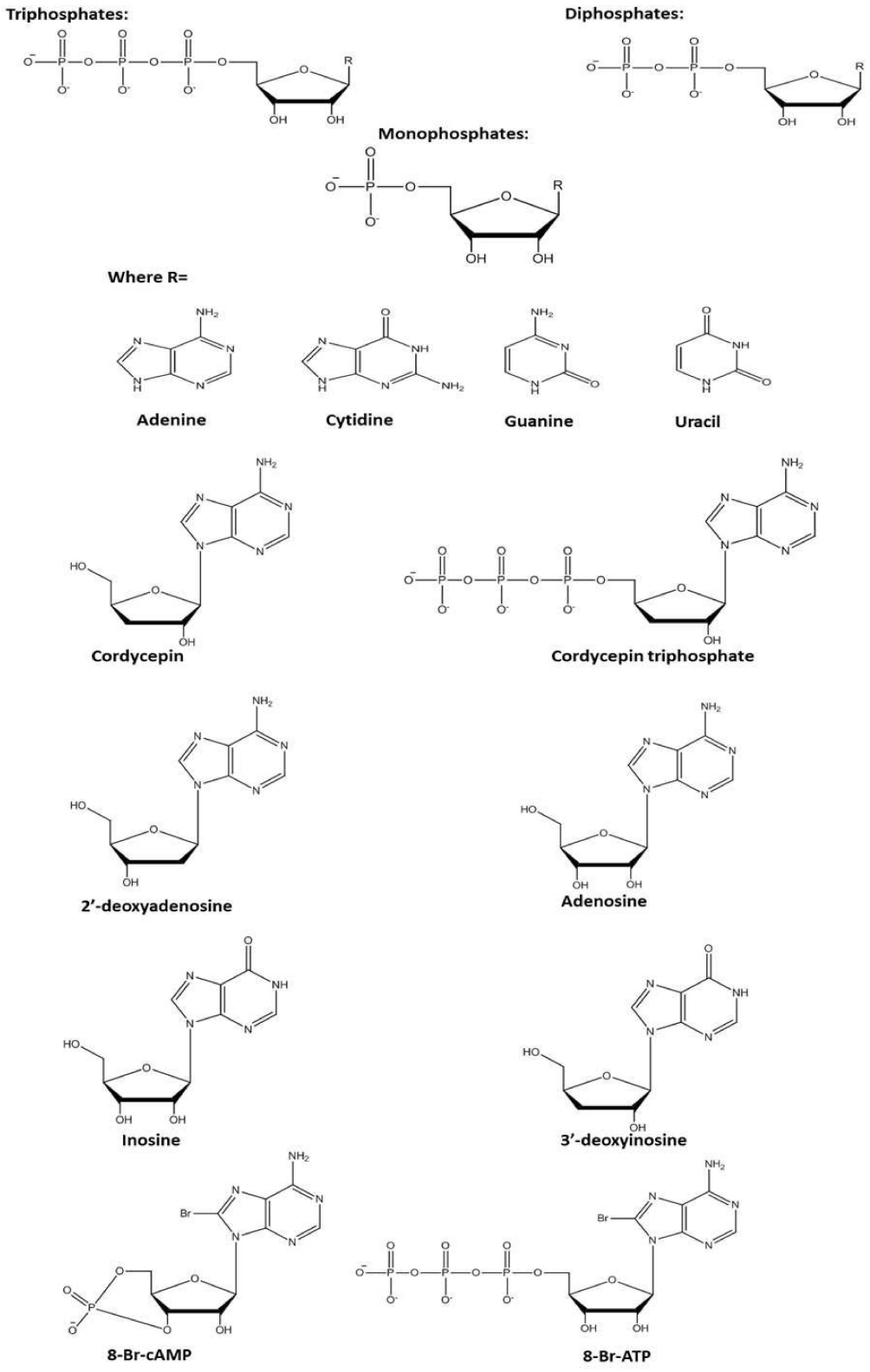

Figure 2.1. Structures of compounds detected

2.4. Results and Discussion

2.4.1. Ion-pair LC development for cordycepin and nucleotide analyses

2.4.1.1 Optimization of separation

An ion-pair HPLC method was developed for the simultaneous analysis of cordycepin, its metabolites and a full range of intracellular nucleotides in cell lines. DMHA was used as ion-pairing agent based on the previous research (164, 169, 176, 177) to retain and separate the nucleotides in a reversed-phase column with gradient elution.

Nucleotides are highly polar compounds due to the presence of phosphate group(s). Therefore they are not normally well-retained on a reversed-phase column. Longer retention time of the nucleotides can be produced by the formation of ion pairs between a positive charge of DMHA and a negative charge of the phosphate group of nucleotides (176). It can be seen from Figure 2.2 that, with the use of 5 mM DMHA ion-pairing agent in the mobile phase, nucleotides (AMP, ADP, and ATP) have longer retention time than cordycepin which has no phosphate group. The ion pairing-agent binds to the phosphate groups of the nucleotides to make them more hydrophobic, increasing their retention time in the column. The retention time of adenine nucleotide improved as the chain length of the phosphates increased from monophosphate to triphosphate. In addition, the ion-pairing agent might absorb to the C-18 stationary phase to effectively make an ion-exchange column. Thus, the analyte is retained in this column because of the ion-exchange mechanism. However, methanol used in the mobile phase could prevent the interaction between

the ion-pairing agent and C-18 stationary phase, thus reducing the capacity of the column. Figure 2.3 shows the interactions described above.

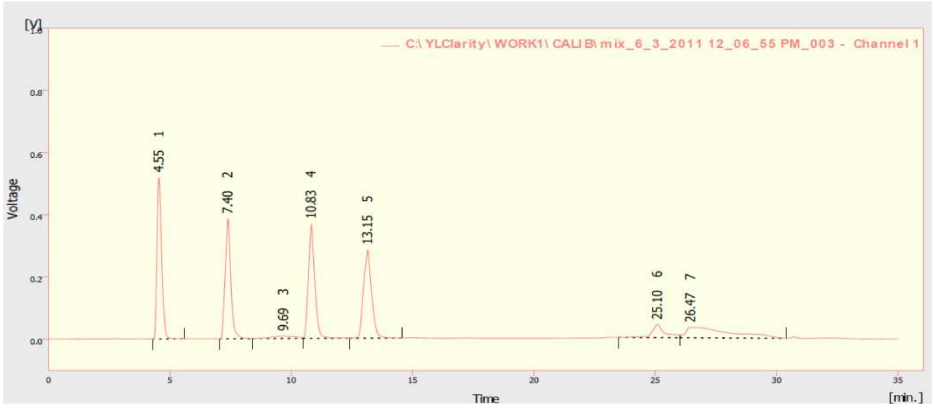

Figure 2.2. Ion-pair LC–UV Chromatogram of 1.Cordycepin, 2.AMP, 4.ADP and 5.ATP at 250 nm.

Chromatographic conditions: mobile phase A, 5 mM DMHA in water: methanol (95:5 v/v) pH 7; B, 5 mM DMHA in methanol: water (80:20 v/v). Gradient elution: 0–20min, 5–50% B; 20–25min, 50–100% B; 25–27min, 100% B; 27–30min, 100-5% B; 30-35min, 5% B.

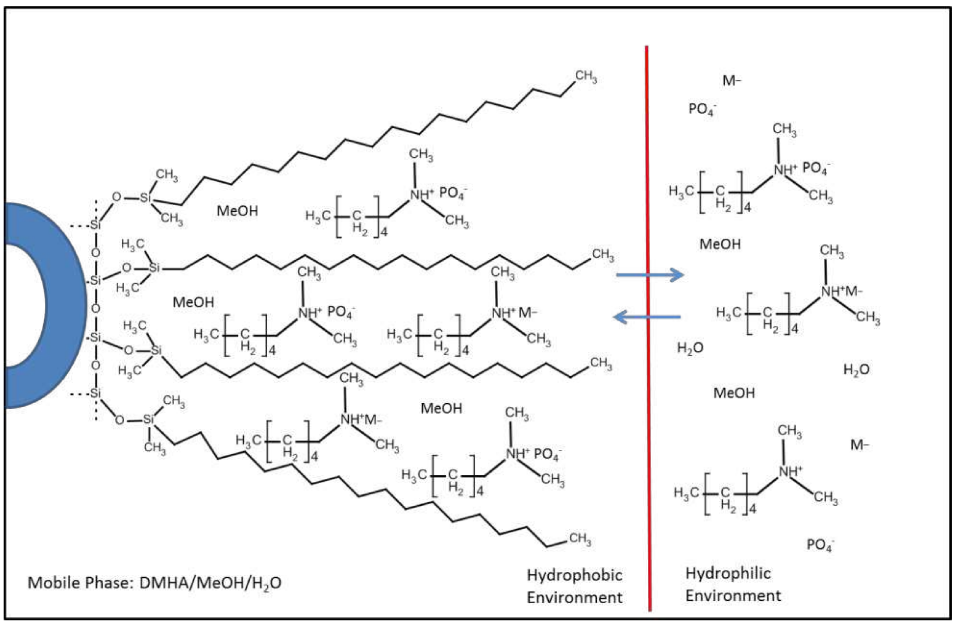

Figure 2.3. Nucleotide-DMHA interactions

The nucleotides are retained by a combination of their interaction with the DMHA that is adsorbed to the C-18 stationary phase (the hydrophobic environment) and by their interaction with DMHA ions in the mobile phase (the hydrophilic environment).

Firstly, the initial mobile phase was set at 95% of mobile phase A, 5 mM DMHA in water: methanol (95:5 v/v), (gradient 1, Figure 2.4) and then was changed to 100% (gradient2, Figure 2.4) because it was found that the more aqueous phase retains nucleotides for longer time in the column. It can be seen from Figure 2.5 that cordycepin, AMP, ADP, and ATP had longer retention time when they were eluted by mobile phase gradient 2 than that by mobile phase gradient 1 (Figure 2.2). However, mobile phase gradient 2 could not provide good resolution between some nucleotides (resolution < 1.5). Moreover, various gradients were investigated (gradient 3-7, Figure 2.4) to obtain a longer retention of some nucleotides and a better separation. Due to this observation, that the most retained analyte (ATP) was eluted by around 40% mobile phase B, the last gradient program was changed from 100% B to 40-53% B. Furthermore, the equilibration time at the end of the run was increased from 5 min to 10 min to reduce variability between runs (gradient 8-12, Figure 2.4).

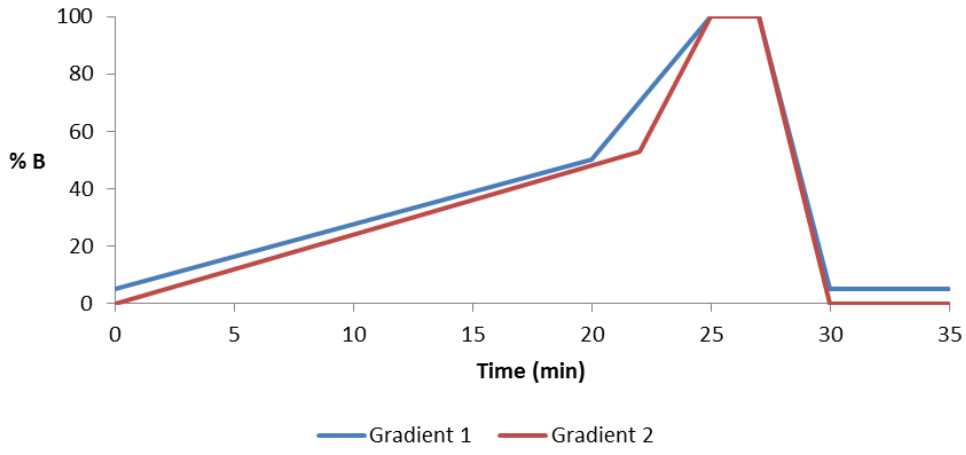

Figure 2.4. Different gradient used for separation of cordycepin and nucleotide mixtures using ion-pair LC with UV detection (gradient 1-2).

Gradients were shown: A, 5 mM DMHA in water: methanol (95:5 v/v); B, 5 mM DMHA in methanol/water: 80/20

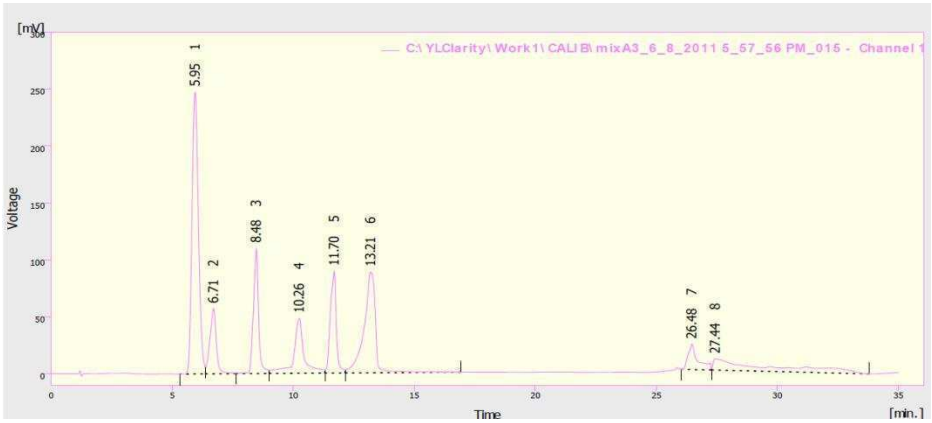

Figure 2.5. Ion-pair LC–UV Chromatogram of 1.Cordycepin & UMP, 2.GMP, 3.AMP, 4.UDP, 5.ADP and 6.ATP at 250 nm.

Chromatographic conditions: mobile phase A, 5 mM DMHA in water: methanol (95:5 v/v) pH 7; B, 5 mM DMHA in methanol: water (80:20 v/v). Gradient elution: 0–22min, 0–53% B; 22–25min, 53–100% B; 25–30min, 100% B; 27–30min, 100-5% B; 30-35min, 5% B.

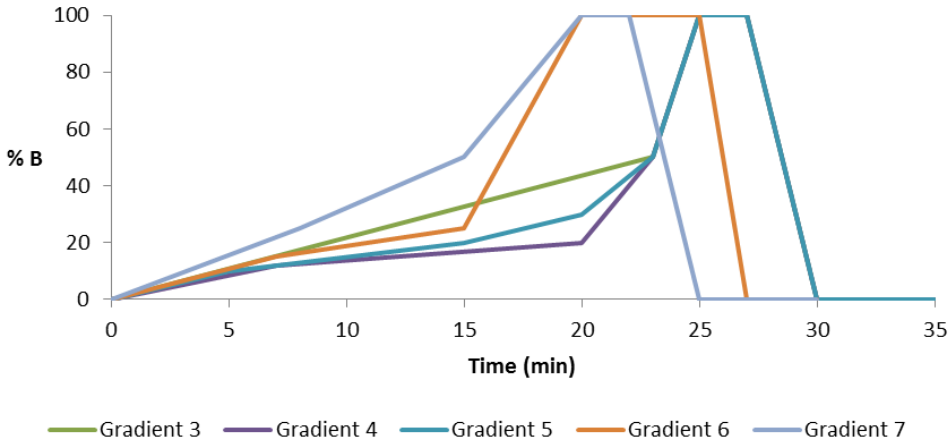

Figure 2.6. Different gradient used for separation of cordycepin and nucleotide mixtures using ion-pair LC with UV detection (gradient 3-7).

Gradients were shown: A, 5 mM DMHA in water: methanol (95:5 v/v); B, 5 mM DMHA in methanol/water: 80/20

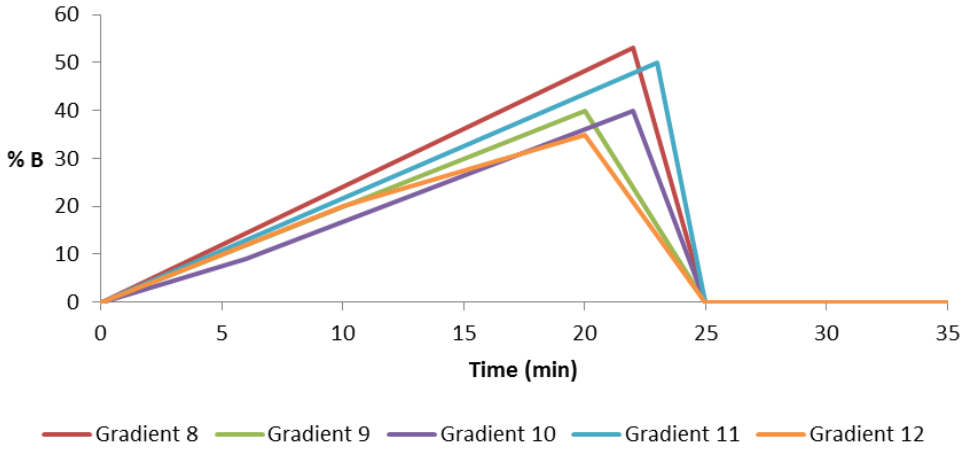

Figure 2.7. Different gradient used for separation of cordycepin and nucleotide mixtures using ion-pair LC with UV detection (gradient 8-12).

Gradients were shown: A, 5 mM DMHA in water: methanol (95:5 v/v); B, 5 mM DMHA in methanol/water: 80/20

2.4.1.2 The effect of DMHA concentration

The effect of concentrations of DMHA was investigated to observe effects on the retention and to find improvements in resolution. Usually, a higher concentration of ion pairing agent would increase the retention of nucleotides (177). Therefore, increasing DMHA concentration leads to longer retention of nucleotides (169). This experiment observed that increasing DMHA concentration from 5 (Figure 2.8A) to 10 mM (Figure 2.8B) could increase the retention of nucleotides but there was only a slight improvement in the resolution. On the contrary, application of 20 mM DMHA did not result in better resolution or even longer retention of nucleotides (Figure 2.8C). The finding of this experiment is consistent with those of other studies (164, 165, 169) and suggest that 5 mM to be optimum concentration.

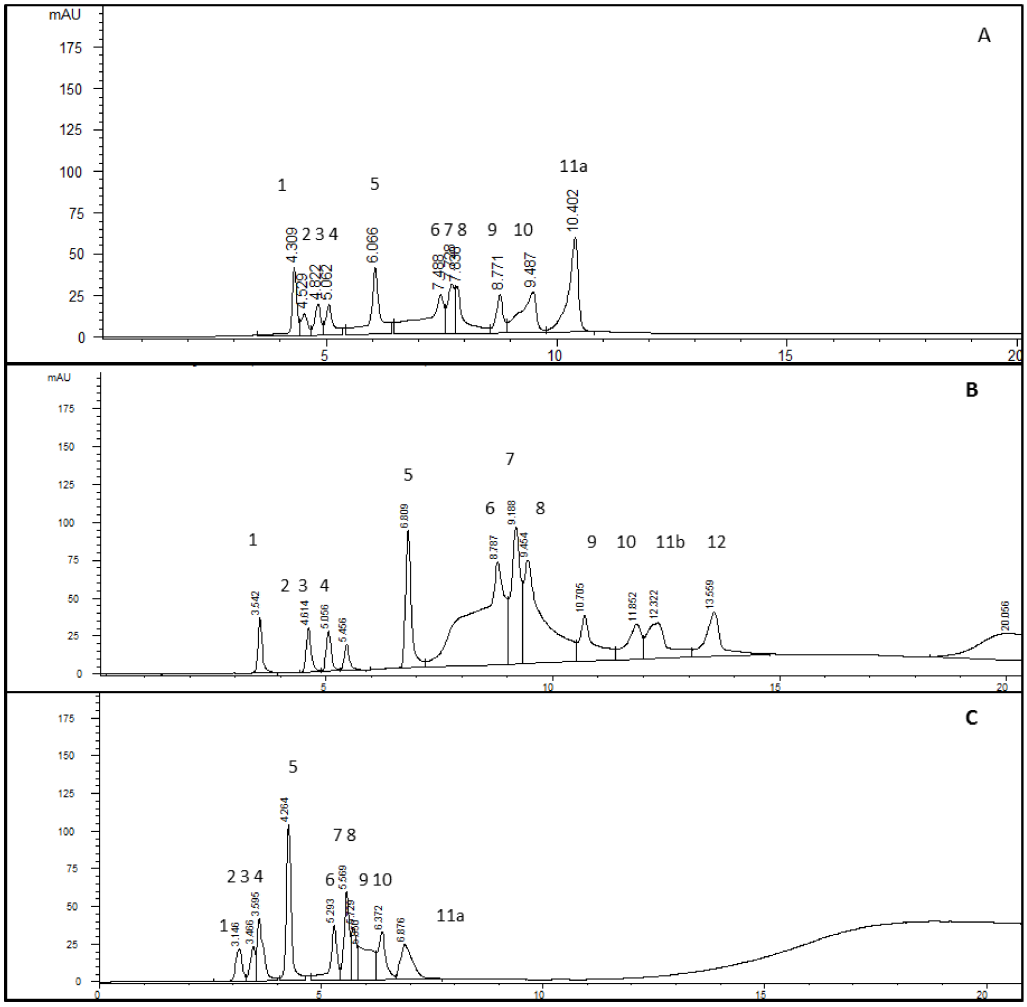

Figure 2.8. The effect of DMHA concentration on the ion-pair LC–UV analysis of 1.Cordycepin, 2.CMP, 3.UMP, 4.GMP, 5.AMP, 6.CDP, 7.UDP, 8.GDP, 9.ADP, 10.CTP & UTP, 11a.GTP, 11b.GTP & ATP, 12.ATP

Chromatographic conditions: mobile phase A, DMHA in water: methanol (95:5 v/v) pH 7 and B, DMHA in methanol: water (80:20 v/v); Gradient elution: 0–20min, 0–40% B; 20–25min, 40- 0% B; 25–35min, 0% B; Column temperature 40°C; Ion-pair LC-UV analysis at 250 nm; A. 5 mM, B. 10mM, C. 20mM

2.4.1.3 The effect of column length

In chromatography analysis, resolution can be increased by utilisation of a longer column. The chromatogram shown in Figure 2.9B was obtained when the 4.6 X 150 mm C-18 column was used. It can be seen that using a longer column results in a better resolution than that achieved using a shorter column (Figure 2.9A).

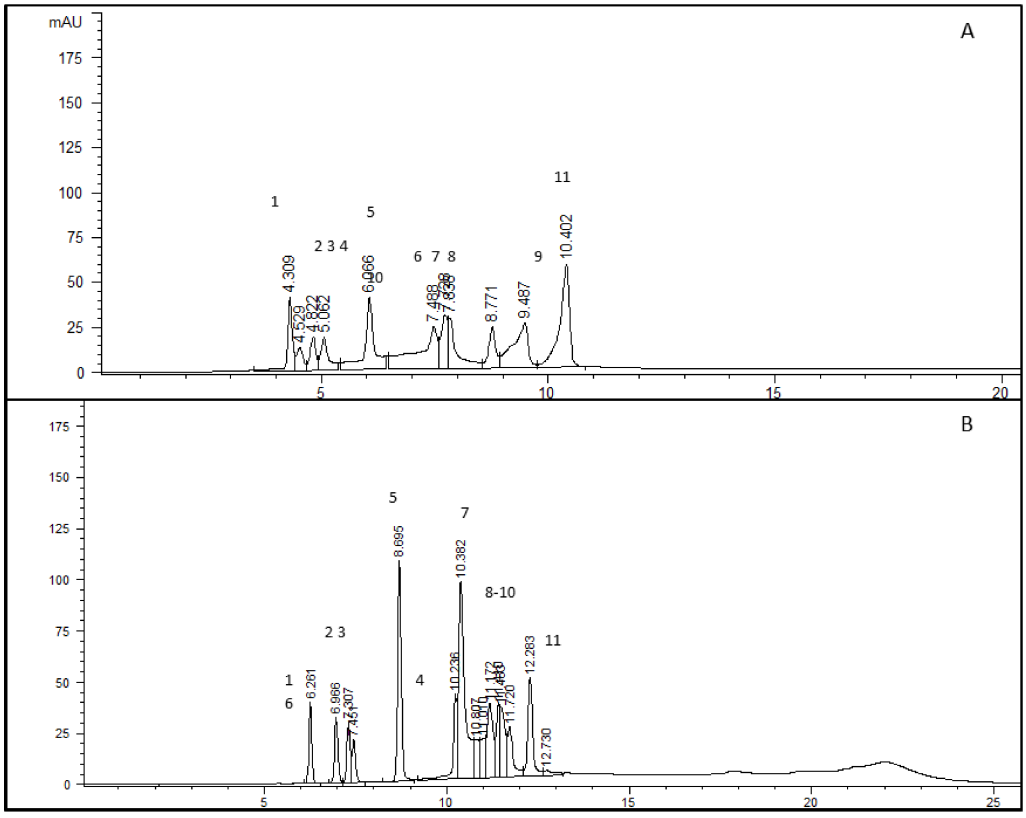

Figure 2.9. The effect of column length on the chromatogram of 1.Cordycepin, 2.CMP, 3.UMP, 4.GMP, 5.AMP, 6.CDP, 7.UDP, 8.GDP, 9.ADP, 10.CTP & UTP, 11.GTP & ATP

Chromatographic conditions: mobile phase A, 5 mM DMHA in water: methanol (95:5 v/v) pH 7; B, 5 mM DMHA in methanol: water (80:20 v/v); Gradient elution: 0–20min, 0–40% B; 20–25min,40- 0% B; 25–35min, 0% B; Column temperature 40°C; Ion-pair LC-UV analysis at 250 nm; A. Column 100 mm length, B. Column 150 mm length.

2.4.1.4 Final optimised HPLC mobile phase conditions

The final separation method determined was the use of 5 mM DMHA in the mobile phase A (water: methanol (95:5 v/v) pH 7) and B (methanol: water (80:20 v/v)) using RP column 4.6 mm×150 mm, with the gradient elution: 0–10 min, 0–20% B; 10–23 min, 20- 35% B; 23-25, 35-0% B; 25–35 min, 0% B. This produced better resolution of most of the components (Figure 2.10).

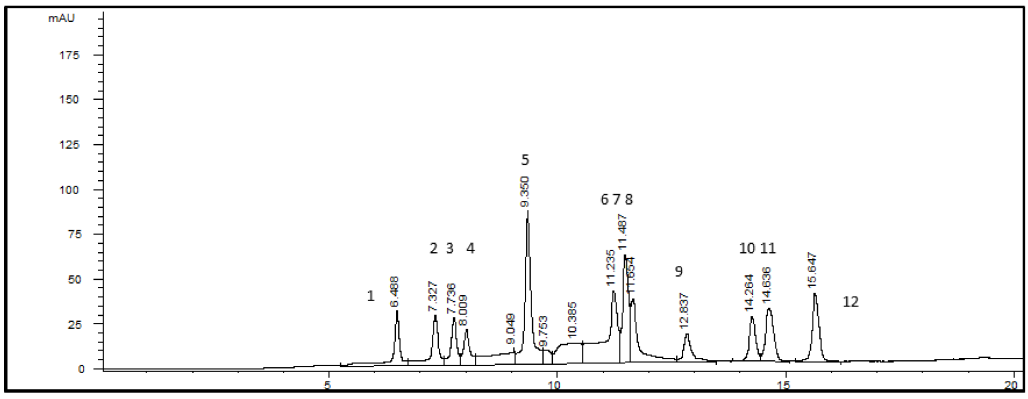

Figure 2.10. Ion-pair LC-UV Chromatogram of 1.Cordycepin, 2.CMP, 3.UMP, 4.GMP, 5.AMP, 6.CDP, 7.UDP, 8.GDP, 9.ADP, 10. CTP & UTP and 11.GTP, 12.ATP at 250 nm

Chromatographic conditions: mobile phase A, 5 mM DMHA in water: methanol (95:5 v/v) pH 7; B, 5 mM DMHA in methanol: water (80:20 v/v). Gradient elution: 0–10min, 0–20% B; 10–23min, 20- 35% B; 23-25min, 35-0% B; 25–35min, 0% B; Column temperature 40°C; Column: 4.6 mmx150 mm (Polaris C-18, 5 µM)

The current method provides equivalent separation to methods previously described (134, 135) but addressed the separation of more components than many HPLC methods detected with UV and also it is compatible with LC-MS.

2.4.2. Optimization of intracellular nucleotide analysis using ion-pair LC with UV detection

2.4.2.1 Internal standard

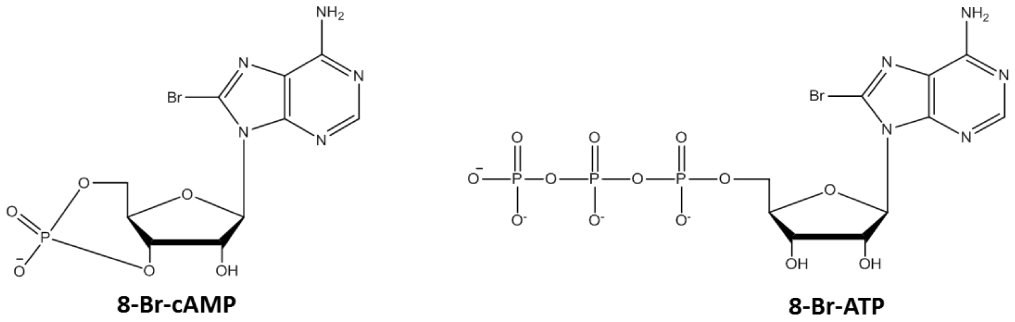

Figure 2.11. Structures of internal standards used

In this method 8-bromoadenosine 3',5'-cyclic monophosphate (8-Br-cAMP) and 8-bromoadenosine 5'-triphosphate (8-Br-ATP) (Figure 2.11) are used as internal standard to correct for the loss of analyte during sample preparation, sample inlet, or ionization. These compounds are not found endogenously; however, their structures are related to the nucleotides.

2.4.2.2 Extraction solvent

The six different extraction solvents evaluated were: methanol 100% followed by hexane extraction, methanol 100% containing EDTA 1.25 mM, methanol: water (3:2 v/v), PCA 0.3 M containing EDTA 1 mM, PCA 0.5 M, and acetonitrile: water (3:2 v/v). The selection of solvents used in this experiment was based on research by Au et al. (181), Reijenga (178), Grob et al. (183), and Cordell et al (169). In this experiment, the extraction solvent was added to the culture plate directly after medium was

removed and cells were washed twice by PBS. This method is based on the study by Yang and Gupta (67) where the total adenosine nucleotide which resulted from the direct extraction method was higher than the amount obtained from indirect method. In the direct extraction method, extraction solvent was added directly to the culture plate after the medium was removed, otherwise extraction solvent was added to the cells after the cells were treated using trypsin in the indirect extraction. Using the direct extraction method, enzyme activities that might degrade the nucleotides and reduce their concentrations in cells are terminated directly.

Figure 2.12 and Figure 2.13 show the effect of different extraction solvents on the chromatogram profile of the cellular extracts. It is clear from the chromatograms that the profiles of cellular extracts prepared with methanol as extraction solvent are almost similar (Figure 2.12). The largest peak which can be seen in these chromatograms is the peak of the internal standard. The other peaks which can be seen in these chromatograms might be the peaks of nucleoside monophosphates (t_R between 5 and 7 min) or nucleoside diphosphates (t_R between 8 and 10 min) (Table 2.2). The cellular extracts prepared using PCA with and without EDTA as the extraction solvent gave significantly different profiles (Figure 2.13 D and E). The peak of the internal standard in these extract were broad. This problem, which was also found by Au et al. (181), might be due to interference with the peak of the perchlorate ion. The cellular extract prepared using PCA with EDTA showed that the largest peak at the t_R was around 5 min, but this peak could not be identified using UV detection. Furthermore, research by Reijenga (178) concluded that the use of EDTA for PCA extraction was not required since the use of PCA alone was enough to

supress enzymatic activity. Moreover, the cellular extract prepared using acetonitrile: water (3:2 v/v) as the extraction solvent (Figure 2.13F) showed some peaks of nucleotide- mono and diphosphates. The peak of the internal standard in this extract, however, was as broad as the peak of the internal standard in PCA with EDTA extract, and hence not satisfactory.

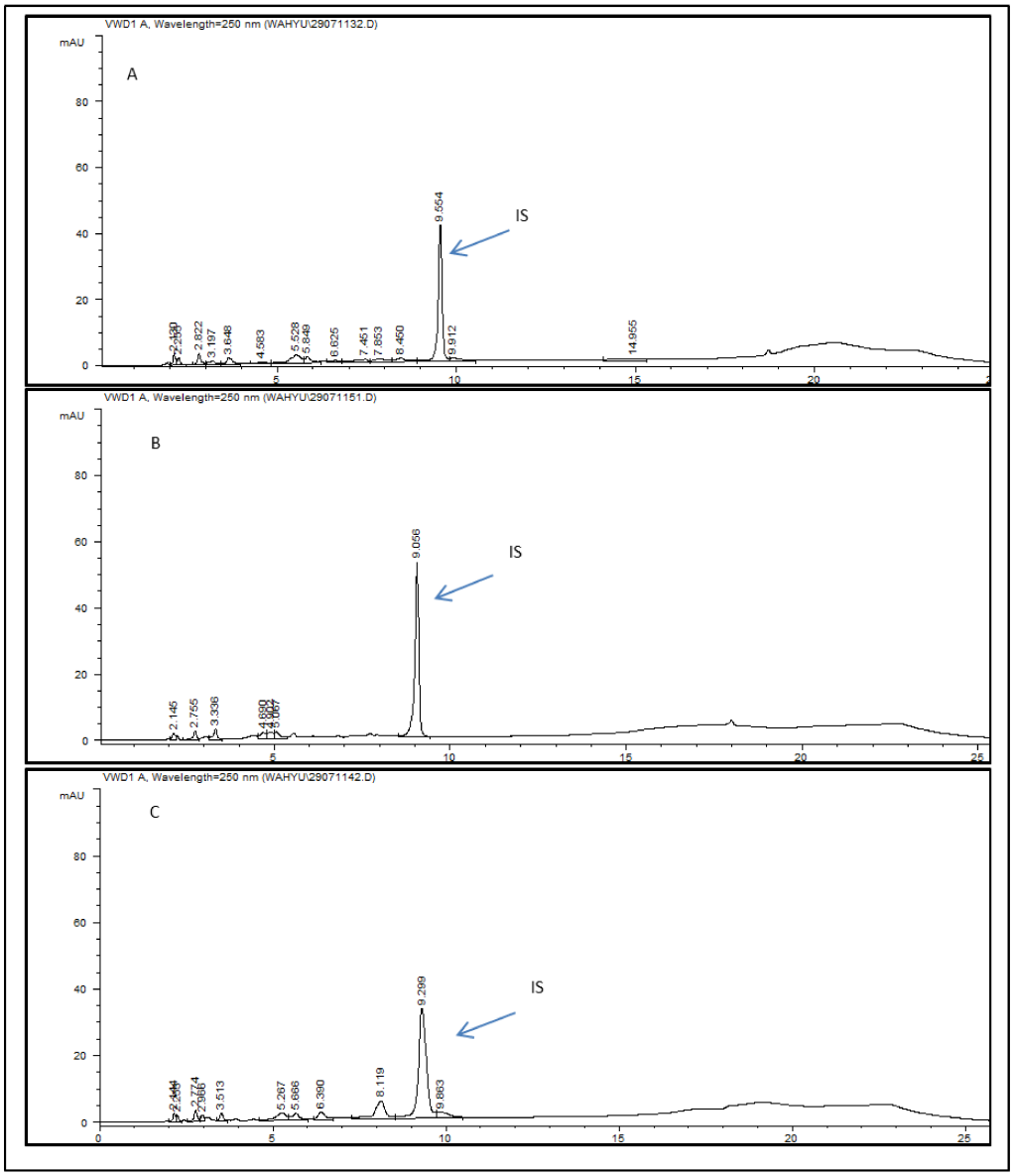

Figure 2.12. The effect of different extraction solvent on the chromatogram profile of intracellular nucleotides; A. methanol 100% was followed by hexane extraction, B. methanol 100% containing EDTA 1.25 mM, C. methanol: water (3:2 v/v).

Chromatographic conditions: mobile phase A, 5 mM DMHA in water: methanol (95:5 v/v) pH 7; B, 5 mM DMHA in methanol: water (80:20 v/v). Gradient elution: 0–10min, 0–20% B; 10–23min, 20- 35% B; 23-25min, 35-0% B; 25–35min, 0% B; Column temperature 40°C; Detection at 250 nm

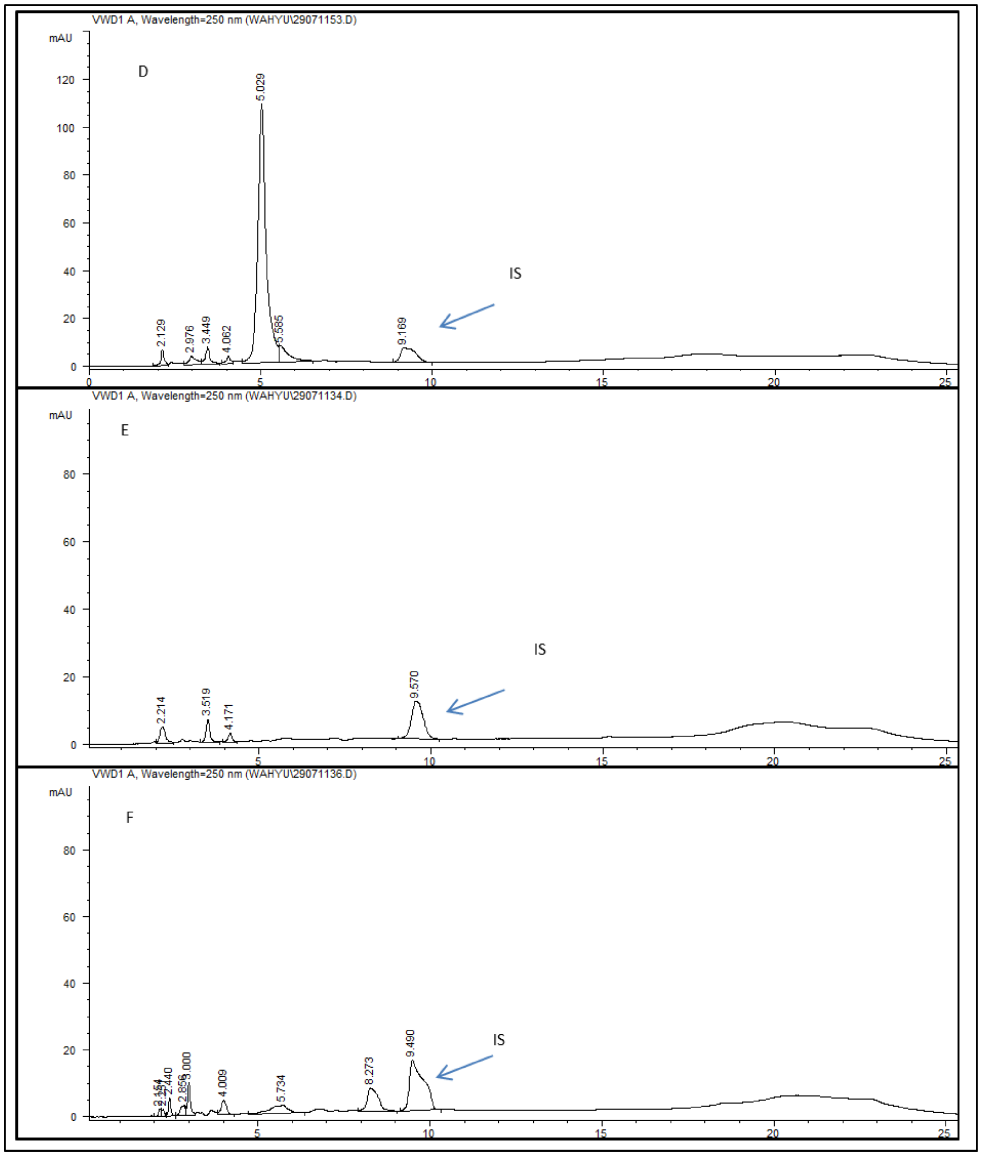

Figure 2.13. The effect of different extraction solvent on the chromatogram profile of intracellular nucleotides; D. PCA 0.3 M containing EDTA 1 mM, E. PCA 0.5 M, F. acetonitrile: water (3:2 v/v).

Chromatographic conditions: mobile phase A, 5 mM DMHA in water: methanol (95:5 v/v) pH 7; B, 5 mM DMHA in methanol: water (80:20 v/v). Gradient elution: 0–10min, 0–20% B; 10–23min, 20- 35% B; 23-25min, 35-0% B; 25–35min, 0% B; Column temperature 40°C; Detection at 250 nm

Table 2.2. The effect of different extraction solvent on the chromatogram profile of intracellular nucleotides

A. methanol 100% was followed by hexane extraction, B. methanol 100% containing EDTA 1.25 mM, C. methanol: water (3:2 v/v), D. PCA 0.3 M containing EDTA 1 mM, E. PCA 0.5 M, F. acetonitrile: water (3:2 v/v). Chromatographic conditions are identical to those described on Figure 2.12.

Extract A			Possible Compound	Extract B			Possible Compound	Extract C			Possible Compound
Peak	t_R (min)	Peak Area		Peak	t_R (min)	Peak Area		Peak	t_R (min)	Peak Area	
1.	2.13	12.42	-*	1.	2.15	12.72	-	1.	2.15	13.74	-
2.	2.25	7.50	-	2.	2.76	19.09	-	2.	2.75	21.59	-
3.	2.79	15.31	-	3.	3.40	24.77	-	3.	2.95	13.65	-
4.	3.55	17.85	-	4.	4.79	23.39	-	4.	3.50	12.69	-
5.	5.34	35.62	nucleoside	5.	5.09	62.91	nucleoside	5.	5.17	34.00	nucleoside
6.	5.72	14.63	monophosphate	6.	5.63	21.56	mono phosphate	6.	5.62	24.97	mono phosphate
7.	8.16	13.49	nucleoside diphosphate	7.	6.34	11.44		7.	6.31	26.10	
8.	9.36	312.54	IS**	8.	8.05	28.39	nucleoside diphosphate	8.	8.08	89.08	nucleoside diphosphate
9.	9.82	15.90	nucleoside diphosphate	9.	9.25	477.74	IS	9.	9.24	406.73	IS

Extract D			**Possible Compound**	**Extract E**			**Possible Compound**	**Extract F**			**Possible Compound**
Peak	t_R (min)	**Peak Area**		**Peak**	t_R (min)	**Peak Area**		**Peak**	t_R (min)	**Peak Area**	
1.	2.13	48.33	-	1.	2.14	42.93	-	1.	2.15	14.74	-
2.	3.00	44.47	-	2.	3.52	49.96	-	2.	2.43	23.67	-
3.	3.47	66.85	-	3.	4.15	19.71	-	3.	2.78	32.04	-
4.	4.09	32.13	-	4.	9.46	221.79	IS	4.	2.97	47.35	-
5.	5.03	1982.80	nucleoside monophosphate					5.	3.97	40.05	-
6.	9.21	208.04	IS					6.	5.65	53.98	nucleoside mono phosphate
								7.	8.19	146.15	nucleoside diphosphate
								8.	9.36	355.33	IS

*- = unknown; **= internal standard (8-bromoadenosine 3', 5'-cyclic monophosphate)

Further important criteria to compare the extraction procedures are recovery and reproducibility. Table 2.3 presents the effect of different extraction solvent on the recovery of internal standard. Recovery was calculated by the area of the internal

standard spiked in the cell and using an injection of internal standard as a 100% value. The cellular extract prepared using methanol containing EDTA 1.25 mM has given the best recovery. In addition, this extraction also provided the highest precision. The recovery of internal standard in the methanol: water (3:2 v/v) extract is almost the same as the recovery of internal standard in the methanol containing EDTA extract; however the former gave lower precision than that obtained using methanol containing EDTA extraction.

Table 2.3. The effect of different extraction solvent on the recovery of internal standard

A. methanol 100% was followed by hexane extraction, B. methanol 100% containing EDTA 1.25 mM, C. methanol: water (3:2 v/v), D. PCA 0.3 M containing EDTA 1 mM, E. PCA 0.5 M, F. acetonitrile: water (3:2 v/v). Chromatographic conditions are identical to those described on Figure 2.12.

The Extraction Solvent	Mean ± SD (%)
A	44.09 ± 6.19
B	67.42 ± 1.09
C	57.38 ± 13.45
D	29.35 ± 3.26
E	31.29 ± 5.06
F	50.13 ± 6.57

Considering the whole information, methanol containing EDTA 1.25 mM is the best extraction solvent. In addition, as methanol is a mild denaturing agent, the use of EDTA in methanol extraction is necessary (178).

IP-RP-HPLC with UV detection was successfully used for analysis of cordycepin and nucleotides. This method provides a simple and rapid separation and quantification. Further analysis of the peaks on the cellular extract using UV detection, however, remains unclear due to the limitation of UV detection on the selectivity. UV detection is less sensitive for quantification of nucleotides and their metabolites in biological cells because metabolites are generally present at low concentration in cells. Moreover, analysis of the metabolites in the biological cells is often difficult due to the complexity of the metabolites. Therefore, the method for determination of cordycepin and its metabolites should have highest sensitivity and selectivity in order to obtain an accurate and precise quantification. MS/MS provides a high selectivity detector, in which a selected ion can be used for quantification analysis. Due to the limitation of specificity and sensitivity of the UV detector, further studies moved to LC-MS/MS which is more suitable for the cell-based analysis. MS/MS provides good sensitivity and specificity which will be particularly important in the use of biological samples.

2.4.3. Development of an ion-pair-LC-MS/MS method for simultaneous analysis of cordycepin, metabolites and nucleotides

The LC-MS/MS method is more selective and provides higher sensitivity than HPLC/UV. Using LC-MS/MS, each analyte will be investigated by monitoring a specific fragmentation pattern, so maximum selectivity and sensitivity in analysis will be achieved using this method.

2.4.3.1 Mass spectrometry development

Several LC-MS/MS methods have been reported for quantitative profiling of intracellular nucleotides (164, 169, 175-177). However, they limit their methods to investigation of only a few nucleotides and the new developed method is needed for specific application to the nucleosides cordycepin and its metabolites as well as other major nucleotides. Negative ESI mode was chosen in this experiment based on research by Tuytten et al. (164) and Cordell et al. (169). Negative ESI mode resulted in a strong signal; compared with the complex spectra produced using positive mode because of the high background of the protonated DMHA ion. Using positive ESI mode, a positive amine group of DMHA produces a very strong signal that supresses other ions (169). For that reason, negative ESI mode was selected to use in this method.

Each analyte was measured by monitoring a specific fragmentation pattern using multi reaction monitoring (MRM) scan. It is essential to evaluate carefully the choice of product ions and optimise conditions for their production. This is achieved by a systematic optimisation of the MS conditions for each analyte. Using MRM scan some of the analytes for which one molecular weight unit apart, for example cordycepin (MW= 251) and the metabolites, 3'-deoxyinosine (MW= 252), could be distinguished by producing different fragmentation pattern when subjected to LC-MS/MS conditions. Cordycepin produces the product ion of *m/z* 134 which corresponds to adenine, while the metabolites produce the fragment of *m/z* 135 which corresponds to hypoxanthine (Figure 2.14).

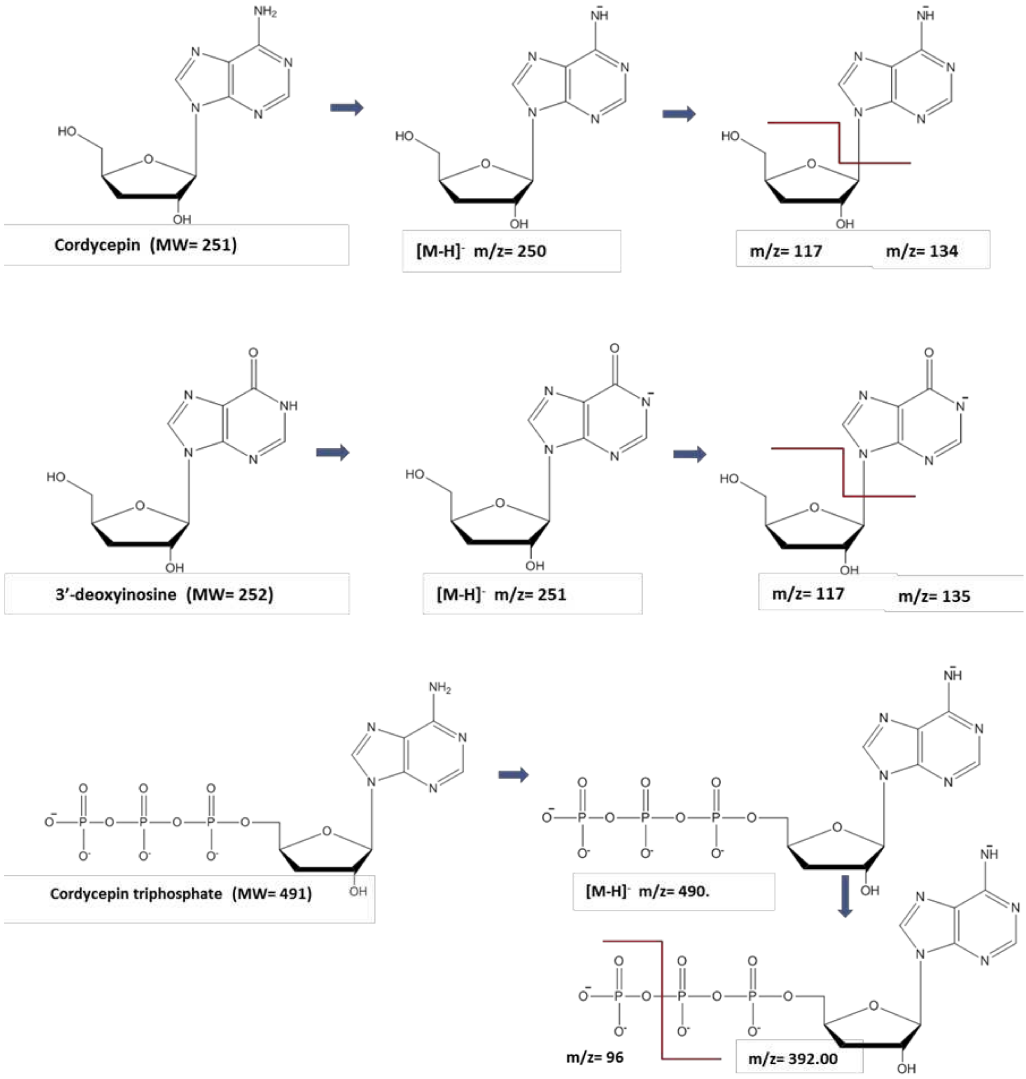

Figure 2.14. Fragmentation of cordycepin and the metabolites was examined in ESI⁻.

The cone voltages and collision energies are shown in Table 2.4. Source temperature was 125°C, with nitrogen as drying gas and nebulizing gas and argon as collision gas.

The prominent product ions produced from the nucleosides are produced by the cleavage of the glycosidic C-N bond to give the deprotonated bases. Cordycepin, deoxyinosine, adenosine, and inosine, lose the sugar moiety to produce their deprotonated bases. This finding corroborates the idea of Liu et al. (190), who suggested that the deprotonated bases were the base peaks for fragmentation of nucleoside in the negative ESI mode, even though cleavage of the glycosidic bonds

with charge retention on the sugar moiety eliminates the base moiety as a neutral molecules and product sugar ions can be found as well. Meanwhile, the nucleotides produce the product ions corresponding to the loss of PO_3^- group or PO_4^{2-} and also produce the fragments which correspond to the remaining structure after the loss of the bases. The optimised conditions for the production of the selected ion for each analyte are shown in Table 2.4.

Table 2.4. Parameters of MRM scan derived for nucleosides and nucleotides

Compound	t_R (min)	$[M-H]^-$ (*m/z*)	Selected Product Ion (*m/z*)	Cone Voltage (V)	Collision Energy (eV)
adenosine	4.70	266.02	133.99	36	20
2'-deoxyadenosine	4.90	250.10	134.00	40	24
cordycepin	5.44	250.10	134.00	40	24
deoxyinosine	3.75	251.08	135.00	40	21
cordycepin 5'-triphosphate	15.35	490.00	392.00	37	22
inosine	3.64	267.00	135.00	37	27
AMP	7.22	345.94	96.75	40	26
CMP	5.23	322.00	79.00	40	19
GMP	6.40	361.98	210.73	41	23
UMP	5.99	322.98	96.97	35	25
ADP	11.52	425.96	327.55	43	18
CDP	9.72	401.93	134.10	40	25
GDP	10.62	442.01	343.88	40	20
UDP	10.40	402.94	158.63	37	26
ATP	14.75	505.93	407.75	39	24
CTP	13.32	481.89	383.74	38	24
GTP	14.06	521.98	423.72	36	24
UTP	13.91	482.9	384.74	38	22
8-Br-cAMP	12.18	406.00	212.00	40	25

2.4.3.2 LC-MS/MS analysis of nucleotide standard mixture

The mixture containing 19 of standards at concentrations of 10 µM was analysed through this method, and Figure 2.15 shows the LC-MS chromatogram. All the compounds were detected simultaneously as (in order of elution): inosine, deoxyinosine, adenosine, 2'-deoxyadenosine, CMP, cordycepin, UMP, GMP, AMP, CDP, UDP, GDP, ADP, internal standard (8-Br-cAMP), CTP, UTP, GDP, ATP, and cordycepin 5'-triphosphate. It can be seen that the method worked well and all the metabolites of cordycepin and the nucleotides could be detected without interference.

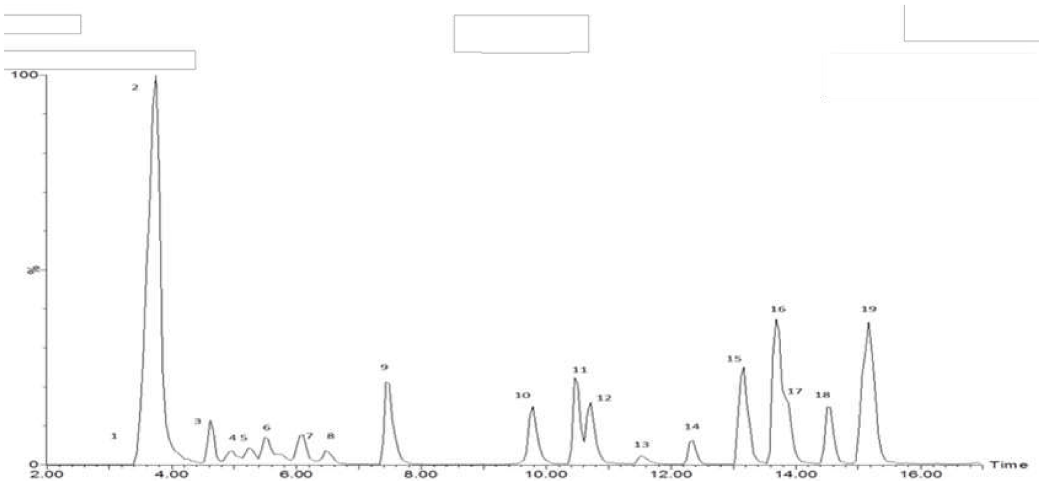

Figure 2.15. LC-MS/MS chromatogram of standard mixture of nucleotides and nucleosides

1.inosine, 2.deoxyinosine, 3.adenosine, 4.2'-deoxyadenosine, 5.CMP, 6.cordycepin, 7.UMP, 8.GMP, 9.AMP, 10.CDP, 11.UDP, 12.GDP, 13 ADP, 14.internal standard (8-Br-cAMP), 15.CTP, 16.UTP, 17.GDP, 18.ATP, 19.cordycepin 5'-triphosphate

Chromatographic conditions: mobile phase A, 5 mM DMHA in water: methanol (95:5 v/v) pH 7; B, 5 mM DMHA in methanol: water (80:20 v/v); Gradient elution: 0–10min, 0–20% B; 10–23min, 20- 35% B; 23-25min, 35-0% B; 25–35min, 0% B; Column temperature 40°C

2.4.4. Sample stability

The sample stability test was carried out to investigate the degradation of samples during preparation. This have to be ensured that the problem of degradation of the nucleotides is minimized as this could interference between analysis, by losing one or more phosphate groups (e.g. ATP to ADP or AMP). The stability analysis of ATP during evaporation showed that the compound was stable, no ADP or AMP was detected under any of the experimental conditions (Figure 2.16). This result provides information that no unexpected degradation of the nucleotides occurs during the evaporation process. The conversion of the triphosphate form to the diphosphate form and the diphosphate form to the monophosphate form because of the loss of phosphate group were not detected during evaporation.

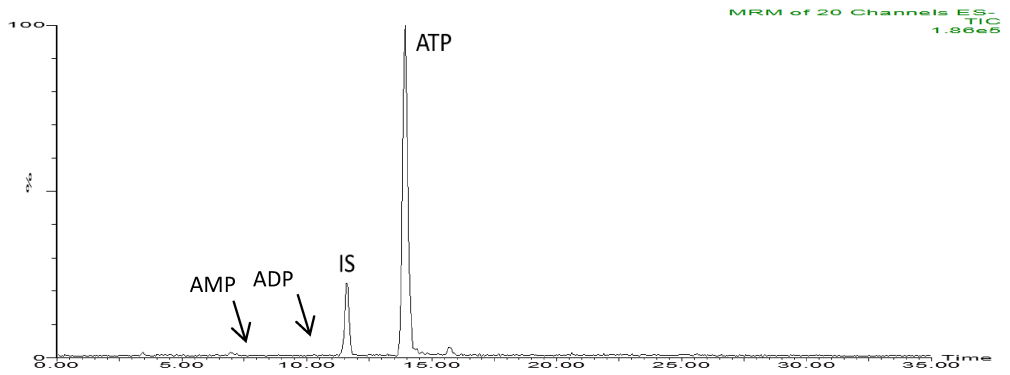

Figure 2.16. Degradation of ATP to ADP and AMP was not observed after processing of evaporation for 2 hours at room temperature (IS: internal standard = 8-Br-cAMP).

Chromatographic conditions: mobile phase A, 5 mM DMHA in water: methanol (95:5 v/v) pH 7; B, 5 mM DMHA in methanol: water (80:20 v/v). Gradient elution: 0–10min, 0–20% B; 10–23min, 20- 35% B; 23-25min, 35-0% B; 25–35min, 0% B; Column temperature 40°C; MRM scan as described on Table 2.4

In contrast, cordycepin in the cell culture medium was not stable, with declining amounts of cordycepin and increasing amounts of 3'-deoxyinosine seen after 0.5 h incubation. This experiment indicates that there is adenosine-deaminase (ADA) in

the cell culture medium and the activity of this enzyme could be inhibited by methanol-1.25 mM EDTA (Figure 2.17A). Therefore, to prevent the degradation of cordycepin during preparation sample, methanol-1.25 mM EDTA was added to the sample of media at the time points when the samples were collected. The ratio of methanol-EDTA to medium 1:1 was effective in inhibition of ADA.

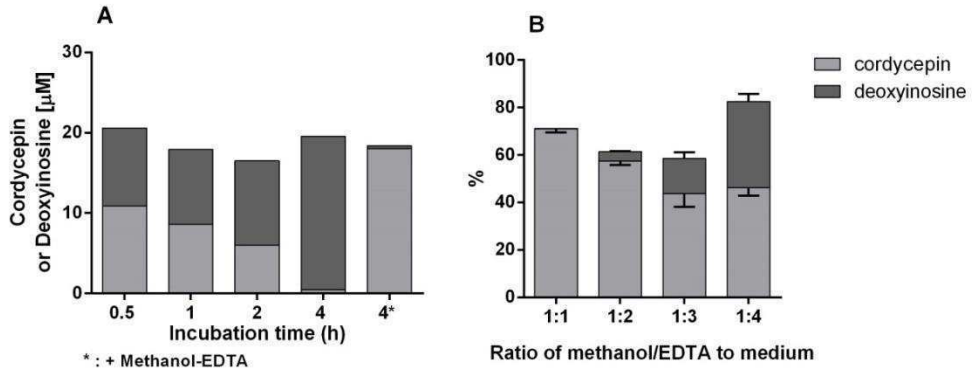

Figure 2.17. Result from LC-MS/MS analysis shows:

(A) The degradation of cordycepin in medium and the ability of methanol-EDTA to inhibit this degradation; (B) The effect of ratio of methanol-EDTA to medium 1:1 was effective to inhibit the degradation of cordycepin into 3'-deoxyinosine

2.4.5. Method validation

The method need to be validated to verify that the method is capable of producing quantitative data which is both reliable and reproducible. The result of validation data for the method is presented in Table 2.5. Compared to other methods applied to the measurement of intracellular nucleotides, the sensitivity of the method is much better than several HPLC-UV methods (133-135) and similar to other LC-MS/MS methods (165, 169, 176). Previous HPLC-UV methods have detection limits which are much higher than this method. Giannattasio et al. (134) obtained

detection limits of nucleotides and nucleosides in primary cultures cells in the range of 10m- 60 pmol, Cichna et al. (133) measured nucleosides and nucleotides in human blood cells with limits of detection of 3- 29 pmol and Huang et al.(135) found the detection limit of intracellular nucleoside triphosphate levels in normal and tumour cell lines between 1.39 and 14.6 pmol.

Table 2.5. Linearity, recovery and precision of the method for quantification of intracellular metabolites

Compound	LOD (pmol on column)	R^2	Recovery (%)	Precision (RSD %)
cordycepin	0.5	0.999	108.2	13.5
adenosine	2.5	0.995	77.3	28.5
deoxyinosine	2	0.999	91.0	15.9
inosine	2	0.988	58.1	15.1
cordycepin 5'-triphosphate	1	0.998	100.5	13.2
AMP	2.5	0.998	105.9	14.8
CMP	2.5	0.992	47.1	8.1
GMP	2.5	0.999	94.2	11.2
UMP	2.5	0.999	73.5	12.9
ADP	2.5	0.986	101.8	21.2
CDP	2.5	0.996	104.7	17.9
GDP	2.5	0.990	100.4	24.2
UDP	2.5	0.998	120.6	21.7
ATP	1.25	0.995	119.7	14.8
CTP	1.25	0.999	112.3	16.4
GTP	1.25	0.999	107.1	30.4
UTP	1.25	0.990	114.1	16.7

Compared with previous LC-MS methods applied to quantify intracellular nucleotides, sensitivities found in this method are essentially comparable. For example, Cordell et al. (169) measured nucleotides and related phosphate-containing metabolites in cultured mammalian cells by LC-ESI tandem mass spectrometry and the limit of detection were 0.25 – 10 pmol. Qian et al. (176) found that the limit detection of adenosine nucleotides in cultured cells were between 0.5 and 12 pmol. However, in terms of previous mass spectrometry methods applied for the quantification of the metabolites of cordycepin, the sensitivity of this method is better. Yang et al. (79) measured cordycepin in different species of *Cordyceps* by capillary electrophoresis-mass spectrometry and the limit detection was 0.12 μg/mL. Huang et al. (185) found the limit of detection of cordycepin determined in *Cordyceps* using LC/ESI-MS was 0.1 μg/mL. Yang et al. (80) obtained a better sensitivity of 0.01 μg/mL using ion-pair LC-MS, but the method was not applied in cell lines.

Furthermore, the number of compounds analysed in this method are larger than those analysed using previous other LC-MS method, including the metabolites of cordycepin. Moreover, other methods that have been applied to measure the metabolites of purine nucleoside analogues in cell samples lack validation procedures (94, 110, 191).

The calibration lines were shown to be linear within 0.25 μM and 100 μM concentration range. The coefficients of regression for all the compounds were above 0.99. Figure 2.18 shows the calibration curve of serial standard solution of

cordycepin. The recoveries of the method for some compounds were reduced and the precisions were just over 20%. However, recoveries are good enough to provide sufficient sensitivity to measure the majority of compounds examined. Overall, the data given indicates that the method exhibits sufficiently linear, sensitive, precise, and accurate for application to the measurement of the metabolites of cordycepin and the intracellular nucleotides in cancer cell lines.

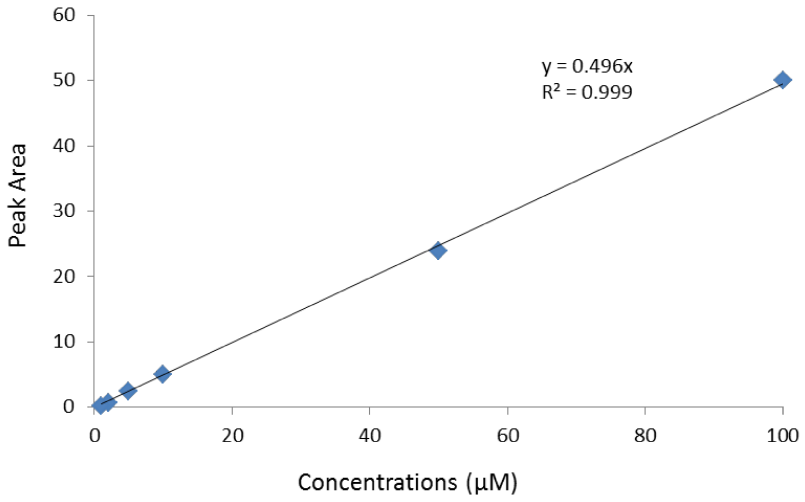

Figure 2.18. Calibration curve of serial standard solution of cordycepin (expressed in µM; peak area is corrected as a ratio to 8-Br-cAMP and 8-Br-ATP as the internal standard)

2.4.6. Application to the analysis of intracellular nucleotides in MCF7 cells

The LC-MS/MS method was initially applied to determine the levels of nucleotides in MCF7 cells (Figure 2.19). Most nucleotides could be detected from the cell extract. It can be seen that ATP gives the highest response while the lowest response is from CMP.

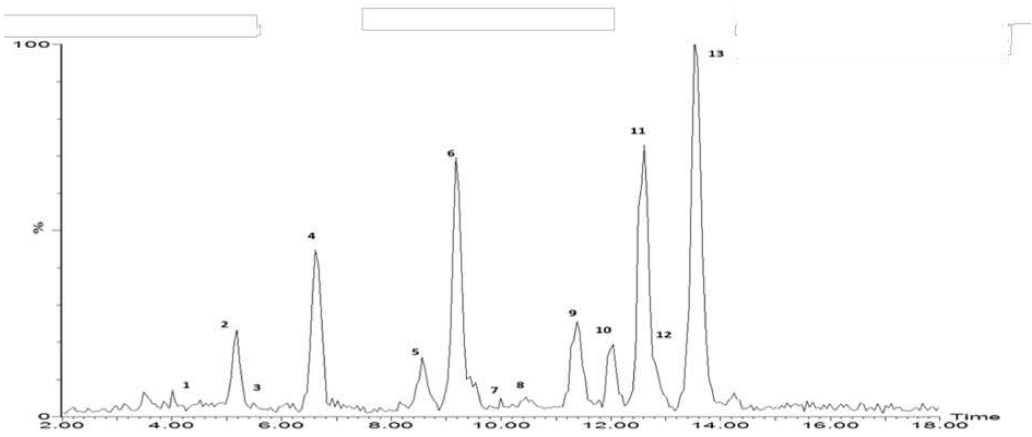

Figure 2.19. LC-MS chromatogram of MCF7 cell extract

1.CMP, 2.UMP, 3.GMP, 4.AMP, 5.CDP, 6.UDP, 7.GDP, 8.ADP, 9.internal standard (8-Br-cAMP), 10.CTP, 11.UTP, 12.GDP, 13.ATP

Chromatographic conditions: mobile phase A, 5 mM DMHA in water: methanol (95:5 v/v) pH 7; B, 5 mM DMHA in methanol: water (80:20 v/v). Gradient elution: 0–10min, 0–20% B; 10–23min, 20- 35% B; 23-25min, 35-0% B; 25–35min, 0% B ; Column temperature 40°C; MRM scan as described on Table 2.4

The intracellular levels of the nucleotides were estimated from the average cell volume and the total cell count. The average diameter of cells found by coulter counter was (20.26 ± 4.68) µm, therefore provided a mean volume of 4.3pL/cell. The average number of cells per well was obtained 0.71x 10^6. This gave a total volume of 3.09 µL/ well. Then, using a total volume of cells per well the measurement could be converted into cellular concentrations.

Table 2.6. The level of intracellular nucleotides (mM) in MCF7 untreated cells.

Compound	mM
ATP	2.51 ± 0.53
CTP	0.22 ± 0.04
GTP	0.58 ± 0.11
UTP	0.36 ± 0.09
ADP	0.42 ± 0.05
CDP	0.27 ± 0.06
GDP	0.16 ± 0.03
UDP	0.16 ± 0.07
AMP	0.29 ± 0.02
CMP	0.04 ± 0.01
GMP	0.17 ± 0.02
UMP	0.15 ± 0.04
ATP/ADP	6.0
ATP/TAN	0.76
EC	0.85

*Data represent the mean ± SD from 3 separate experiments (n=6-8)

The concentration of intracellular nucleotides measured in the MCF7 cell (Table 2.6) are in agreement with other data from previous studies (133, 135, 169, 192-194). The intracellular levels of ATP in HeLa cells and NHF cells were around 1 mM (194), about 2.5 mM in JeKo cells (193), and in other six cancer cell lines and three primary strains were in the range of 1.5 - 5.5 mM (192). The other nucleoside triphosphates (NTPs) were found to be lower from 0.01 to 1.3 mM or between 0.02 – 3.2 nmol/million cells (133, 135, 192). To compare with this method, as can be seen in Table 2.6, we also found ATP to be the nucleotide of highest concentration in MCF7 cells around 2.51 mM. The other triphosphates were present at levels of 0.22– 0.58 mM. The diphosphate levels are found around in the range of 0.10 – 102 µM or 0.28 – 1.53 nmol/million cells (133, 169). The levels of monophosphate are between 0.98 and 12.7 µM (169) and most of them often below detection in the investigation by Cichna et al. (133). The ATP/ADP ratios in some cancer cell under control condition found in these papers were in the range 3.0 – 8.0. Our results determined ATP/ADP

ratio around 6 and all nucleotides were detected by this method. Moreover, the energy charge (EC) of the cells of 0.8 and the intracellular levels of ATP was 76 percent of total adenine nucleotide (TAN) which indicated that the cells were healthy. The data above suggest that the results obtained here are valid and this method could be applied to analysis of intracellular metabolites and nucleotides in cell lines.

2.5. Conclusions

The LC-MS/MS method using the volatile ion pairing agent DMHA has demonstrated an ability to separate and detect mixtures of intracellular nucleotides. The extraction of nucleotides from cell lines has been well investigated and the optimised extraction has been developed. It has also been shown that the method can be successfully applied to MCF7 cells.

The ability of the method to measure the intracellular metabolites and nucleotides has been established with the validation results. The method has been shown to have sufficient sensitivity and selectivity to measure accurate intracellular concentrations.

The next step will use the method to investigate the intracellular metabolism of cordycepin in cell lines. The cells will be treated with either cordycepin, pentostatin, or the combination both of them in order to investigate its metabolism in the medium and the cell lines.

CHAPTER 3
STABILITY AND METABOLISM OF CORDYCEPIN *IN VITRO* AND *IN VIVO*

STABILITY AND METABOLISM OF CORDYCEPIN *IN VITRO* AND *IN VIVO*

3.1. Introduction

Cordycepin (3'-deoxyadenosine) is an inhibitor of polyadenylation, the process of addition of poly(A) tail at the 3'-end of mRNA molecule by poly(A) polymerase (PAP). Cordycepin reduced the efficiency of 3'-end formation at a step prior to poly(A) tail synthesis by PAP and affects mRNA synthesis (195). Wong et al. (196) confirmed that, at low doses of cordycepin, the poly(A) tail length of some mRNAs became shorter and Kondrashov et al. (86) showed that total poly(A) tail length is reduced in cordycepin treated cells. Moreover, the effect of cordycepin on the inhibition of the mRNAs was not observed on housekeeping mRNAs (86)

Cordycepin has been shown to inhibit the expression of inflammatory genes (63, 64) and the survival and proliferation of many cancer cells (94, 102, 103). Further investigation of the anti-inflammatory effect of other adenosine analogues showed that only the polyadenylation inhibitors have anti-inflammatory activity (86). These data strongly suggest that the mechanism of action of cordycepin as an anti-inflammatory agent is through its ability to inhibit polyadenylation (86).

The effect of cordycepin on cell proliferation by PAP modulation is exhibited in human epithelioid cervix, breast cancer, leukaemia, lymphoma, and in oral cancer cell lines (95, 97, 100). In human epithelioid cervix and breast cancer cell lines, PAP modulations by cordycepin affect the cell cycle rather than induce apoptosis (95). On the other hand, research by Chen et al. (94) exhibited that in combination with adenosine deaminase (ADA) inhibitors, cordycepin induced apoptosis in multiple

myeloma (MM) cells. Therefore, inhibition of polyadenylation by cordycepin resulted in either suppression of proliferation or induction of the apoptotic process, according to the cell type and cordycepin concentration (97, 100). Moreover, research by others in our laboratories has shown that treatment with 50 µM cordycepin reduces cell proliferation and survival on MCF7 cells after 72 hours and induces cell death by a non-apoptotic program (Khurshid, Singhania, Lin and De Moor, unpublished observation). Moreover, incubation with the combination of 50 µM cordycepin and 1 µM pentostatin showed that the majority of MCF7 cells enter apoptosis within four hours (Richa Singhania and Cornelia de Moor, unpublished observation).

Results from studies on the inhibition of tumour growth using B16-BL6, LLC, and HL60 cells have proposed that the inhibition by cordycepin occurs through the activation of adenosine A_3 receptors (A_3AR) (96, 98, 99). These receptors activate the Wnt signalling pathway, including GSK-3β activation and cyclin D1 inhibition, leading to reduced proliferation (99, 197). Moreover, higher levels of mRNA expression of A3 adenosine receptors were reported in colon and human breast cancer cells compared to non-malignant cells (198). The mechanism of action of cordycepin through activation of adenosine receptors expects that an inhibition of cordycepin transport or its phosphorylation should not prevent the activity of cordycepin. However, the inhibition of the transport and the phosphorylation was observed to lead to the prevention of the effect of cordycepin on inflammatory response and protein synthesis, suggesting that cordycepin acts intracellularly and needs to be phosphorylated for its biological activity (86, 196). In addition, research

by Lee et al. (199) observed that adenosine receptor did not facilitate the effects of cordycepin on the cell proliferation and apoptosis on oral squamous cell carcinoma. Therefore the biological effects of cordycepin in several other cell types appear not to be mediated by this receptor.

Another study by Kim et al. also suggested that cordycepin might act as a poly(ADP-ribose) polymerase (PARP) inhibitor (200). PARP is an enzyme that is involved in a number of cellular functions, including expression of inflammatory genes, DNA repair and programmed cell death (194, 201). Cordycepin has inhibited the expression of a number of inflammatory genes and reduced H_2O_2-induced PARP activation in A549 cells (200). Moreover, cordycepin demonstrated its ability to inhibit PARP-1 activity *in vitro* at very low concentrations (200). Furthermore, experiments using BRCA1-deficient MCF7 cells showed that cordycepin enhanced killing of cells in a similar manner to that achieved by the PARP inhibitor (200). Research by Lee et al. (202) observed that cordycepin induced DNA damage response, but this effect was apparently not facilitated by its deoxyribonucleotides. Further investigation showed inhibition of PARP activity by cordycepin and this inhibition was found to be more pronounced in highly undifferentiated breast cancer cells (202). However, the direct inhibition of PARP by cordycepin was not adequately demonstrated in this paper.

In spite of the promising results of cordycepin as an anticancer agent, the current limitation for cordycepin application in clinical practices is that it requires the co-administration of adenosine deaminase (ADA) inhibitors such as coformycin (CF) or deoxycoformycin (dCF), which is also known as pentostatin, (94) because cordycepin

is rapidly metabolized and quickly deaminated to an inactive metabolite by ADA (110, 188, 203). Tsai et al. (188) investigated biotransformation of cordycepin and adenosine in rat blood and liver. Their results showed an unidentified peak that had an HPLC retention time faster than cordycepin, indicating a more polar compound, probably a metabolite of cordycepin. When pre-treated with an ADA inhibitor, pentostatin, they found a smaller amount of the unidentified peak, indicating that it was the deaminated product, which they did not further identify. Furthermore, cordycepin goes through phosphorylation by adenosine kinase (AK) to become cordycepin monophosphate (110, 204-206) which is then further metabolized to cordycepin diphosphate and cordycepin triphosphate (Figure 3.1).

Moreover, in another study found that cordycepin was given in combination with pentostatin, a potential ADA inhibitor, resulted in an increasing toxicity compared to cordycepin alone (207). Clinical study to assess the combination of pentostatin and other agents have reported that toxicity of pentostatin in combination with interferon to be tolerable in patients, but combination with alkylating agents showed a significant immunosuppression in patients with chronic lymphocytic leukaemia (208). A clinical trial phase I and II to evaluate the combination of pentostatin and cordycepin in patients with acute lymphocytic leukaemia are undergoing and coordinated by Oncovista (website reference1-2).

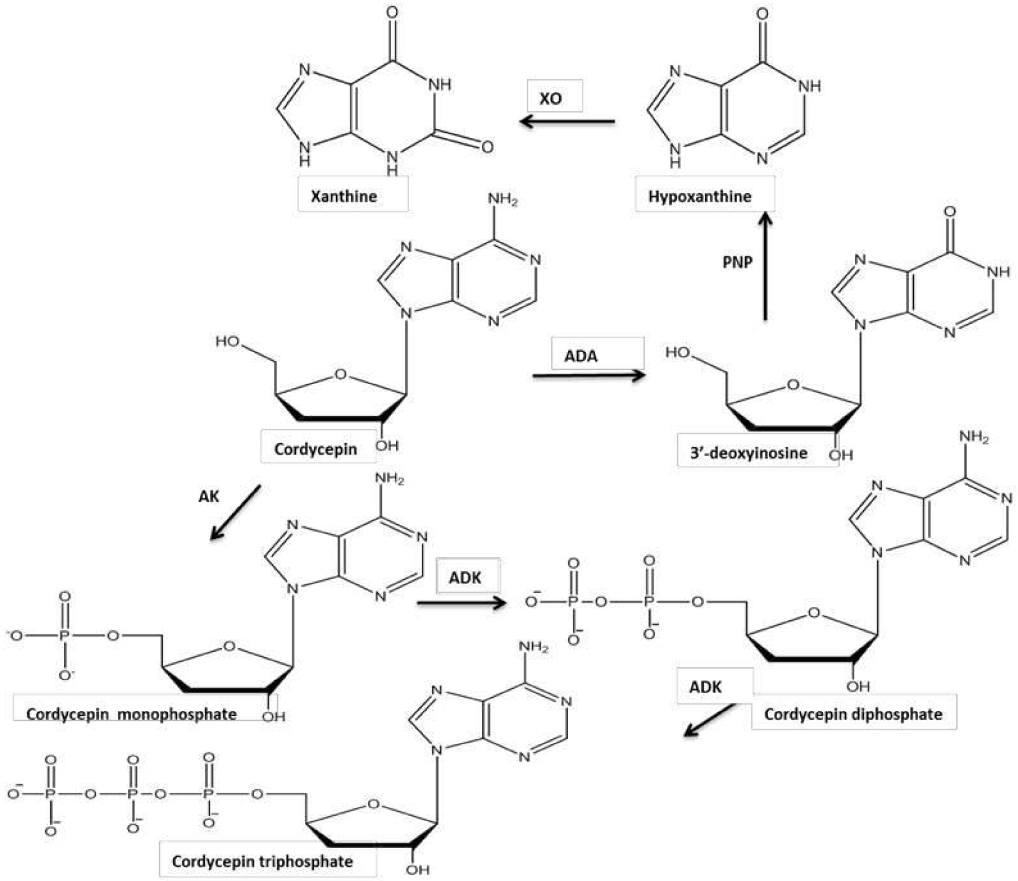

Figure 3.1. Metabolic Pathway of Cordycepin

AK= adenosine kinase; ADK= adenylate kinase; ADA= adenosine deaminase; PN= purine nucleoside phosphorylase; XO= xanthine oxidase

Although some research has been undertaken into the metabolism of cordycepin, more *in vivo* and *in vitro* metabolism studies, supported by bioanalytical research, are still needed for a full understanding of the action mechanism of cordycepin. Such studies will provide information relevant to the potential use of cordycepin as a drug for anti-cancer or anti-inflammatory applications. Therefore to investigate this, the metabolism of cordycepin in cancer cell lines and the medium, also in rat plasma and liver, were examined using the LC-MS/MS method.

3.2. Aim and Objectives

The aim of this chapter is to study metabolism of cordycepin *in vitro* and *in vivo*.

The objectives of this chapter are to apply the LC-MS/MS method for:

- Determination of cordycepin and its metabolites in the culture medium of MCF7 and HeLa cells treated with cordycepin in the presence or absence of pentostatin.
- Quantification of cordycepin and its metabolites in MCF7 and HeLa cells treated with cordycepin in the presence or absence of pentostatin.
- Comparison of the degradation of cordycepin in non-heat-treated serum between pure cordycepin and an ethanol extract of *Cordyceps militaris*.
- Measurement of the level of cordycepin and the metabolites in plasma and liver samples of MIA (monosodium iodoacetate)-treated rats.

3.3. Materials and Methods

3.3.1. Chemicals

The chemicals used are the same as described in Chapter 2 (Section 2.3.1).

3.3.2. Cell culture

MCF7 and HeLa cells were cultured using the same procedures as described in Chapter 2 (Section 2.3.2).

3.3.3. Drug treatment

Cells were seeded in a six-well plate and incubated for 24 hours. Cells then were treated with either vehicle (DMSO), 50 µM cordycepin, 1 µM pentostatin, or the combination of 50 µM cordycepin and 1 µM pentostatin (cordycepin/pentostatin) for 2, 8, and 24 hours. After the time points, media and cells were collected from the incubations and analysed for cordycepin and its metabolites by LC-MS/MS method. Quantification of metabolites and intracellular level of nucleotides were calculated from the regression of the calibration curve. Furthermore, the intracellular concentrations of the metabolites and nucleotides were estimated based on the measured total cell volume.

3.3.4. Samples extraction

3.3.4.1 Cell line culture medium samples

To the cell culture medium (200 µL) was added 200 µL extraction solvent (cold methanol-1.25 mM EDTA). Precipitated proteins were removed by centrifugation at 15,000 g, 4°C for 15 min. Subsequently supernatant was removed and analysed for the metabolites concentration using a liquid chromatography-tandem mass spectrometry (LC-MS/MS) method.

3.3.4.2 Cell line samples

Extraction of samples was done as described in Chapter 2 (Section 2.3.8.1).

3.3.5. Calculation of total cell volume

Calculation the total cell volume was done as described in Chapter 2 (Section 2.3.8.2).

3.3.6. Preparation of ethanol extract of *Cordyceps militaris*

The dried powder of *C. militaris* (100 mg) was extracted in an Eppendorf tube with 1 mL of ethanol. The Eppendorf tube was placed in a shaker for 30 min and then after the supernatant was removed, its pellet was re-extracted with a further 1 mL of ethanol. Then the supernatants were combined and centrifuged (15,000 g for 15 min). After that, the supernatant was collected and evaporated to dryness and the final extract was dissolved in 50 µL DMSO.

3.3.7. Degradation assay of cordycepin and extract of *C. militaris* in non-heat-treated serum

Cordycepin or extract ethanol of *C. militaris* was added into 50 µL non-heat-treated FBS and were incubated at 0, 15, 30, 45, and 60 min at room temperature. At the end of incubation, 500 µL of methanol was added to each of them and mixed by shaking and then was centrifuged at 15,000 g for 15 min. The supernatant then was injected into LC-MS/MS system.

3.3.8. Quantitative analysis of metabolites of cordycepin in plasma and liver samples of MIA (monosodium iodoacetate)-treated rats

3.3.8.1 Sample collection

Animals were grouped into three group of treatment: group 1 was MIA and given vehicle, group 2 was MIA injured and given cordycepin, and group 3 was saline injury and given vehicle. The rats in group 3 received 2 mg cordycepin (mixed in with a set amount of rat diet powder) every other day from day 0 to day 14 post MIA, i.e. day 0, 2, 4, 6, 8, 10, 12 and then on day 14, which was the day of euthanisation.

Blood samples were collected from tail vein into tubes containing heparin and 1 µM pentostatin at 45-50 min post ingestion, and then the plasma were transferred to tubes and frozen in liquid nitrogen immediately. The frozen samples were stored at −80 °C until analysis. The liver was rapidly removed and also frozen in liquid nitrogen immediately. The frozen samples were stored at -80 °C.

3.3.8.2 Sample extraction

Five hundred microliter of extraction solvent (1.25 mM EDTA in cold methanol) was added to 50 µL of plasma and then the extraction was managed by vortexing for 5 min. Protein was removed by centrifugation at 4 °C; 15,000 g for 15 min. The supernatant was evaporated under vacuum condition to dryness and re-dissolved in 50 µL of mobile phase then was injected into LC-MS/MS system.

Frozen liver samples (450.0-550.0 mg) were pulverized in a mortar with frequent additions of liquid nitrogen. The powder then was mixed with 5 mL of extraction solvent and carried out by vortexing for 5 min. Protein was removed by centrifugation at 4 °C; 15,000 g for 15 min. The supernatant was evaporated under vacuum condition to dryness and re-dissolved in 100 µL of mobile phase then was injected into LC-MS/MS system.

3.3.9. LC-MS/MS conditions

Analyses of samples were carried out by the method are described in Chapter 2 (Section 2.3.8.3). Multiple reactions monitoring (MRM) scan was used with dwell time 0.1 s as described in Table 2.4.

3.4. Results and Discussion

3.4.1. Calculation of cell volume

The intracellular levels of the nucleotides were estimated from the average cell volume and the total cell count. Using a total volume of cells per well the measurement could be converted into cellular concentrations. A laser light scattering technique was used to determine the average diameter of MCF7 and HeLa cells as shown in Figure 3.2. The average diameter of HeLa cells was estimated to be 20.70 µm which is consistent with result of 20 µm reported before (209, 210) but is slightly larger than the values of 15 and 18 µm reported by Schoeberl, et al. (211) and Luciani, et al. (212), respectively. The estimated volume of the cells was calculated assuming that they were sphere, therefore provided a mean volume cell of MCF7 and HeLa cells are 4.3 and 4.6 pL/cell, respectively.

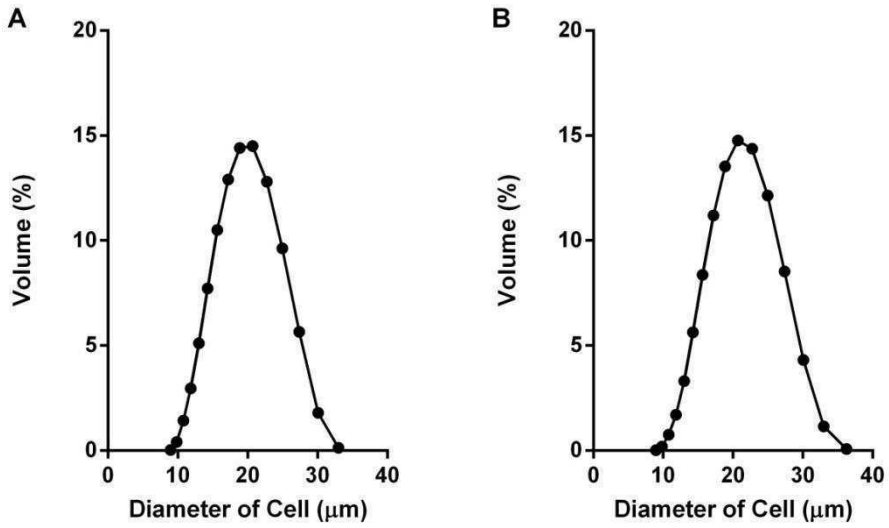

Figure 3.2. The average diameter of MCF7 (A) and HeLa (B) cells

The average diameter of MCF7 cells was found (20.26 ± 1.39) μm. This gave a mean volume of 4.3 pL/cell. The average diameter of HeLa cells was found (20.70± 4.86) μm. This gave a mean volume of 4.6 pL/cell (B).

3.4.2. Metabolism of cordycepin in the culture medium of MCF7 and HeLa cells

To examine the metabolism of cordycepin in the culture medium of MCF7 and HeLa cells, media containing 50 μM cordycepin with and without 1 μM pentostatin were analysed by the LC-MS/MS method after several time points of incubation. The concentrations of drugs used are based on the studies conducted by Wong et al (196) which have shown that there was a significant decrease on the protein synthesis rates in HeLa and NIH 3T3 cells treated with cordycepin of 50 μM for 2 hours, with lesser effects at 10 and 20 μM. Moreover, although the rate of protein synthesis in MCF-7 cells was insensitive to cordycepin, a notable effect was shown at 8 and 24 hours incubation using combination of 50 μM cordycepin with 1μM pentostatin as compared to the 2 hour time point (Asma Khurshid, unpublished

result). In addition, proliferation of MCF7 cells was gradually decreased with increased cordycepin concentration from 50 μM onwards after 24 hour of incubation (213).

Figure 3.3 shows the metabolism of cordycepin into the deaminated product, 3'-deoxyinosine, in the culture medium during incubation. The deamination of cordycepin was probably due to the presence of adenosine deaminase (ADA) in the medium since it contained 10% foetal bovine serum (FBS). Furthermore, in this study we observed that conversion of cordycepin to 3'-deoxyinosine in the medium in the absence of ADA inhibitor was very rapid. In MCF7 cells treated with cordycepin alone (Figure 3.4A), the level of cordycepin in the cell culture medium decreased sharply by 85% after 2 hours incubation and was not measureable in the cell culture medium after 8 hours. At 2 hours incubation, the level of 3'-deoxyinosine in the cell culture medium was almost twice that of the cordycepin level and remained at a similar level up to 24 hours.

The level of cordycepin in the cell culture medium of MCF7 cells treated with cordycepin and pentostatin (Figure 3.4B) declined by 24 % after 2 hours incubation and this level decreased significantly afterward to 55% (8 hours) and 21% (24 hours). Furthermore, treatment with cordycepin and pentostatin resulted in inhibition of the metabolism of cordycepin into 3'-deoxyinosine. It can be seen that no 3'-deoxyinosine was detected in the cell culture medium after 2 hours incubation and it was detected only at a low level after 8 hours, at less than 4% of the concentration of cordycepin.

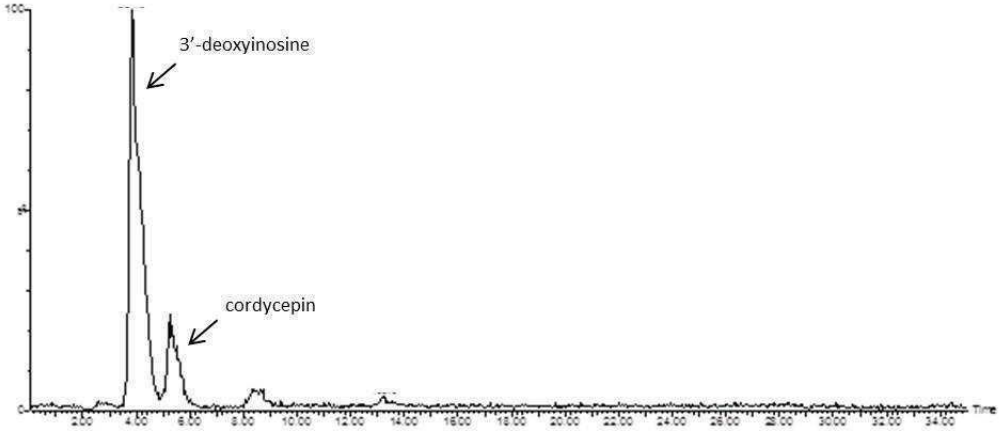

Figure 3.3. LC-MS chromatogram of extract culture medium after 2 hour incubation with 50 µM cordycepin

Chromatographic conditions: mobile phase A, 5mM DMHA in water: methanol (95:5 v/v) pH 7; B, 5mM DMHA in methanol: water (80:20 v/v). Gradient elution: 0–10min, 0–20% B; 10–23min, 20- 35% B; 23-25min, 35-0% B; 25–35min, 0% B. Column temperature: 40°C. MRM scan as described on Table 2.3 and Table 5.1.

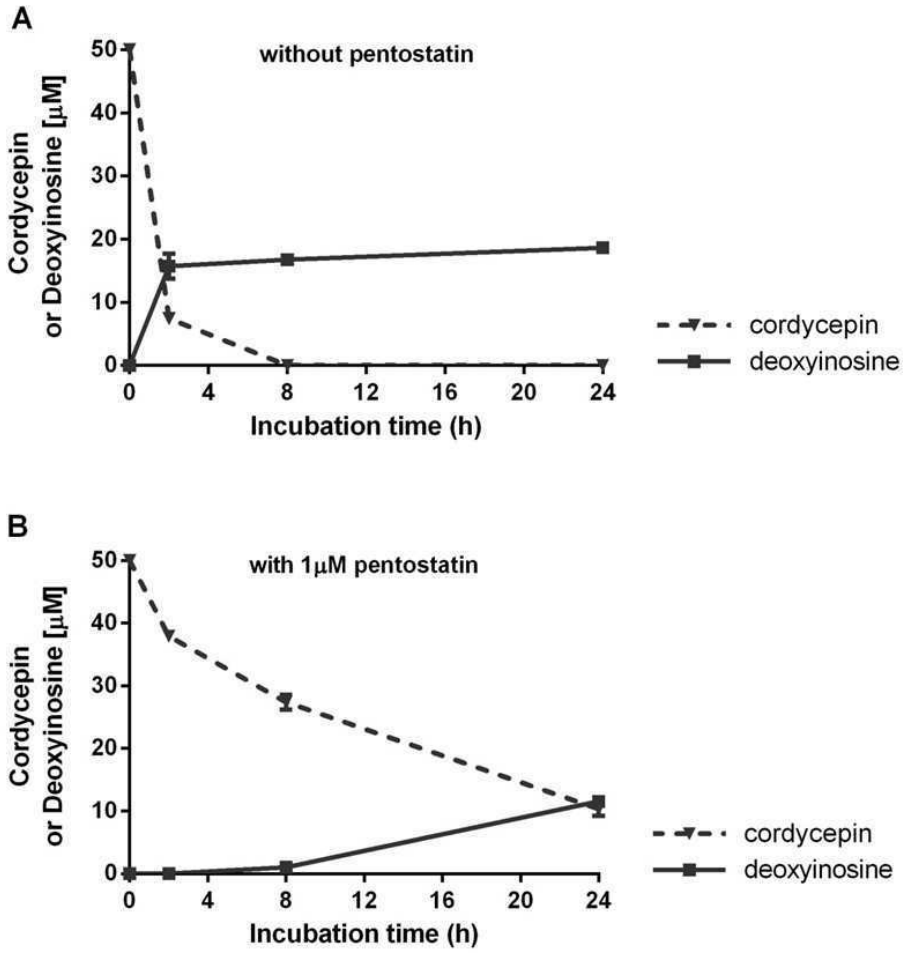

Figure 3.4. Decreasing the level of cordycepin and increasing the level of 3'-deoxyinosine in culture media of MCF7 cells were incubated with either 50 μM cordycepin (A) or the combination of 50 μM cordycepin and 1 μM pentostatin (B) for the indicated times.

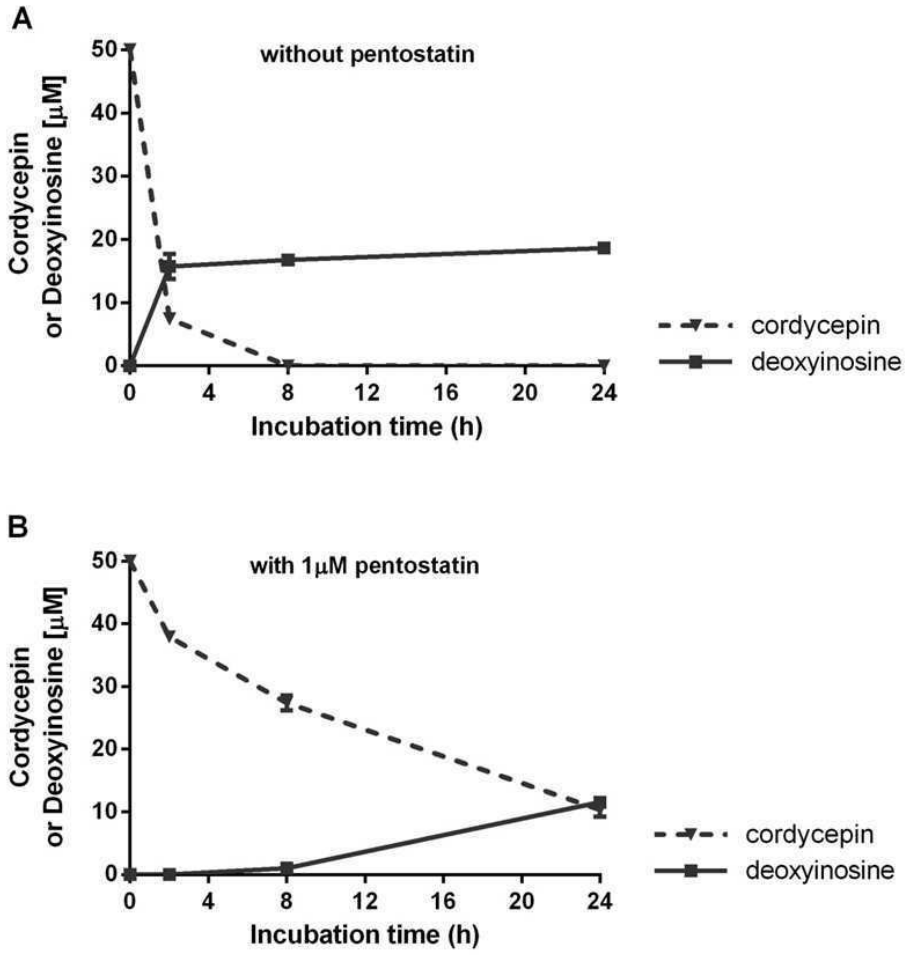

Figure 3.5. Decreasing the level of cordycepin and increasing the level of 3'-deoxyinosine in culture media of HeLa cells were incubated with either 50 μM cordycepin (A) or the combination of 50 μM cordycepin and 1 μM pentostatin (B) for the indicated times.

Similar results were obtained in the medium of HeLa cells treated with cordycepin alone (Figure 3.5A). The level of cordycepin was reduced by around 84% after 2 hours and it was not detected at all after 8 hours. In the presence of pentostatin, an ADA inhibitor, the level of cordycepin was only reduced by approximately 30 % after 2 hours incubation and this level decreased significantly afterward (Figure 3.5B). Also, as for the medium of MCF7 cells, no 3'-deoxyinosine was detected in the cell

culture medium after 2 hours incubation and it was observed only at a low level after 8 hours.

It is also apparent from both figures (Figure 3.4 and Figure 3.5) that some cordycepin seems to go missing in the medium. It is likely that cordycepin was metabolized into 3'-deoxyinosine which then rapidly converted to hypoxanthine and xanthine which were not measured in this study. However, in the presence of an ADA inhibitor, pentostatin, still some loss of cordycepin is observed in the medium. It is not possible that it is all inside the cells, because of their small volume, so probably an alternative degradation route for cordycepin exists. Research by Snyder and Henderson (214) have examined alternative pathway of adenosine and deoxyadenosine metabolism. Their results showed that glycosidic cleavage of deoxyadenosine to become adenine also occurs in Ehrlich ascites tumor cells; in addition to phosphorylation and deamination. Taken together, these results confirm that cordycepin (3'-deoxyadenosine) is rapidly degraded in cell culture medium, which is important for the interpretation of result obtained from long term cordycepin incubations with cells.

3.4.3. Intracellular metabolism of cordycepin in MCF7 and HeLa cells

To observe the intracellular metabolism of cordycepin, MCF7 and HeLa cells were incubated with 50 µM cordycepin with and without 1 µM pentostatin, the deaminase inhibitor, for several time points; and then cell extracts were analysed by the LC-MS/MS method.

From the Figure 3.6 and Figure 3.7 we can see that cordycepin, 3'-deoxyinosine, and cordycepin 5'-triphosphate accumulated in MCF7 cells both with and without pentostatin; and Table 3.1 summarizes the results. These results confirm that cordycepin is efficiently transferred across the cell membrane and is metabolized by phosphorylation to cordycepin 5'-triphosphate and by deamination into 3'-deoxyinosine.

The concentrations of cordycepin and its two metabolites in cordycepin treated cells were at a maximum at 2 hours incubation with levels of 13, 40, and 494 µM for cordycepin, 3'-deoxyinosine, and cordycepin triphosphate, respectively (Figure 3.6). After 8 hours of incubation, no cordycepin was detected that indicates that all cordycepin has been metabolized. The concentrations of cordycepin 5'-triphosphate decreased gradually with only 73 µM left at 24 hours incubation and the level of 3'-deoxyinosine remained constant over 24 hours of incubation. These results indicate that 3'-deoxyinosine is quite stable inside the cell, while the phosphorylated metabolite is eliminated faster, but persists longer than unmodified cordycepin.

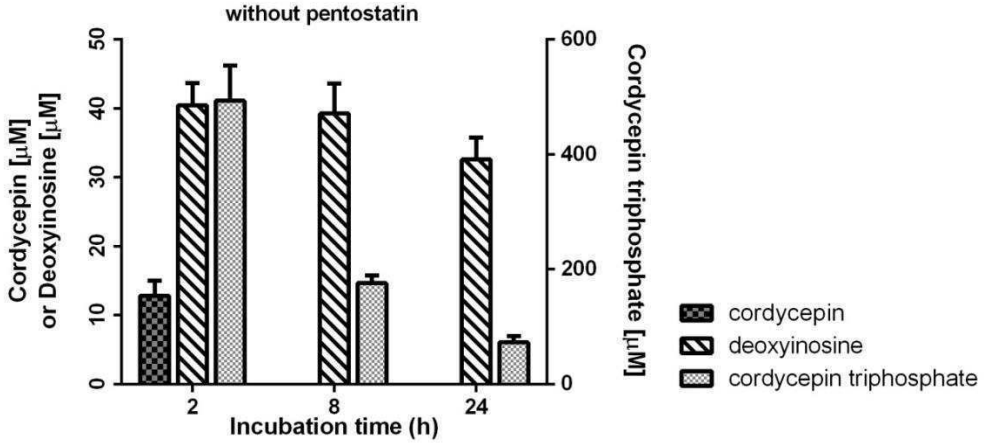

Figure 3.6. Accumulation of cordycepin, 3'-deoxyinosine, and cordycepin 5'-triphosphate in MCF7 cells were incubated with 50 µM cordycepin for the indicated times.

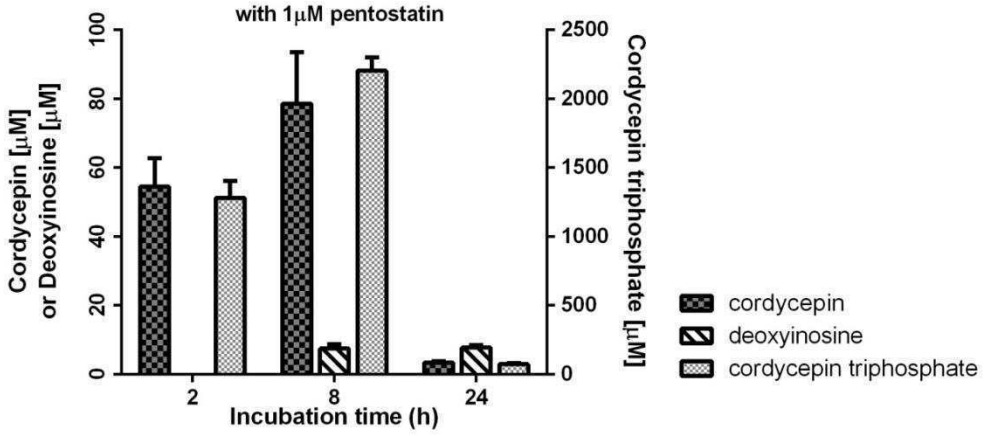

Figure 3.7. Accumulation of cordycepin, 3'-deoxyinosine, and cordycepin 5'-triphosphate in MCF7 cells were incubated with 50 µM cordycepin and 1 µM pentostatin for the indicated times.

Results from incubation with the combination of cordycepin and pentostatin found that 1 μM pentostatin was adequate to prevent the intracellular degradation of cordycepin into 3'-deoxyinosine. No 3'-deoxyinosine was detected at 2 hours incubation and only a very low level (7 μM) was found at 8 hours, which remained steady over 24 hours incubation. At 2 hours incubation the level of cordycepin and the triphosphate metabolite in cordycepin/pentostatin treated cells were around four and 2.5-fold higher than in cordycepin treated cells (without pentostatin). In addition, maximum concentrations of cordycepin and cordycepin 5'-triphosphate in cordycepin/pentostatin treated cells reached maximum at 8 hours incubation (79 and 2203 μM), were about six and 4.5-fold higher than the maximum concentrations in cordycepin treated cells (13 and 494 μM). This result is in agreement with a previous study in leukemic cells (110) in which cordycepin 5'-triphosphate was detected in some leukemic cells at significantly lower concentrations when incubated with cordycepin without pentostatin.

Table 3.1. Summary of concentrations of metabolites of cordycepin in the MCF7 cells incubated with 50 µM cordycepin either in the absence or presence of 1 µM pentostatin

	Treatment					
	50 µM cordycepin			50 µM cordycepin + 1 µM pentostatin		
	2 h	8 h	24 h	2 h	8 h	24 h
Cordycepin (µM)	13 ± 6	N.d.	N.d.	55 ± 27	79 ± 50	3 ± 1
Deoxyinosine (µM)	40 ± 11	39 ± 14	33 ± 9	N.d.	7 ± 4	8 ± 2
Cordycepin triphosphate (µM)	494 ± 182	176 ± 41	73 ± 31	1281 ± 388	2203 ± 312	73 ± 19

*Data represent the mean ± SD from 3 separate experiments (n=8-12). N.d. = not detectable

Table 3.2. Summary of concentrations of metabolites of cordycepin in the HeLa cells incubated with 50 µM cordycepin either in the absence or presence of 1 µM pentostatin

	Treatment					
	50 µM cordycepin			50 µM cordycepin + 1 µM pentostatin		
	2 h	8 h	24 h	2 h	8 h	24 h
Cordycepin (µM)	6 ± 2	N.d.	N.d.	26 ± 11	29 ± 14	14 ± 4
Deoxyinosine (µM)	48 ± 13	51 ± 23	39 ± 4	N.d.	11 ± 7	13 ± 9
Cordycepin triphosphate (µM)	251 ± 134	27 ± 13	4 ± 2	1089 ± 645	1277 ± 374	560 ± 363

*Data represent the mean ± SD from 3 separate experiments (n=8-12). N.d. = not detectable

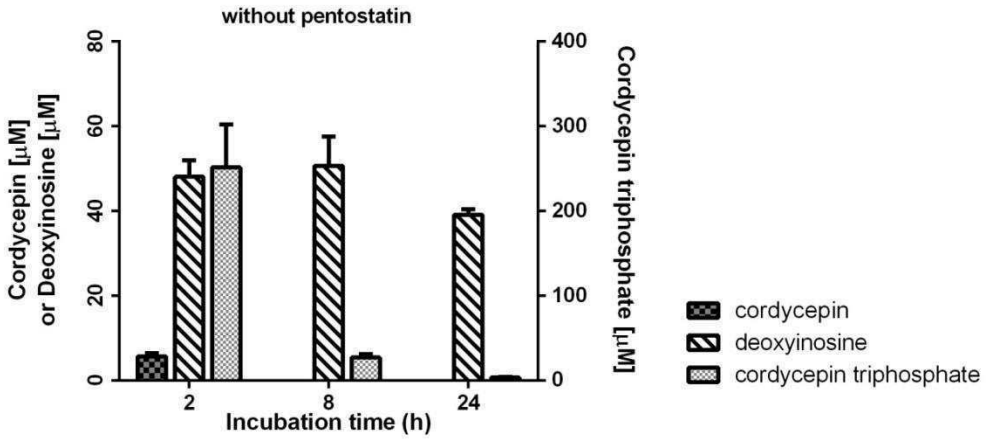

Figure 3.8. Accumulation of cordycepin, 3'-deoxyinosine, and cordycepin 5'-triphosphate in HeLa cells were incubated with 50 µM cordycepin for the indicated times.

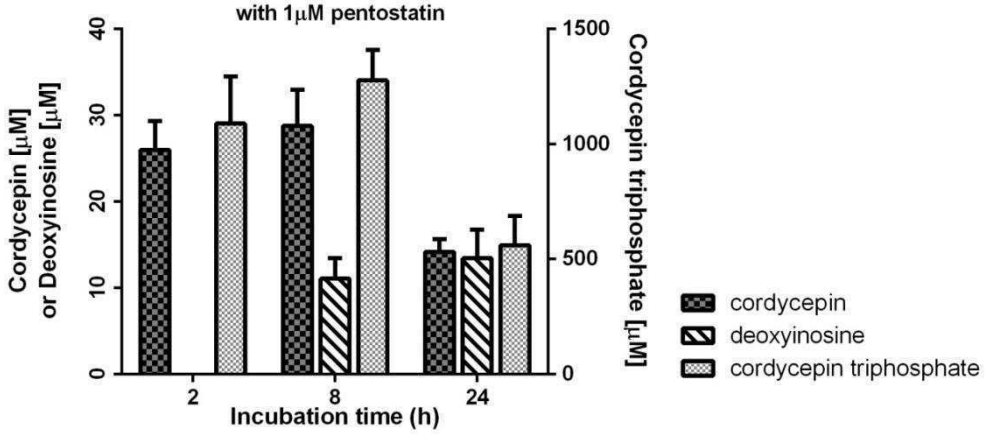

Figure 3.9. Accumulation of cordycepin, 3'-deoxyinosine, and cordycepin 5'-triphosphate in HeLa cells were incubated with 50 µM cordycepin and 1 µM pentostatin for the indicated times.

It can be seen that the intracellular metabolism of cordycepin in HeLa cells was similar with that in MCF7 cells. Cordycepin and its active metabolite, cordycepin triphosphate, were at an intracellular maximum level at 2 hours incubation with 50 µM cordycepin, while the level of deaminated metabolite was found in high

concentrations, 8 times higher than the level of cordycepin, and remained steady over 24 h (Figure 3.8). Treatment using combination with 1 µM pentostatin resulted in an increase of the level of cordycepin and the active metabolite around four times higher at 2 hours incubation whereas there was no 3'-deoxyinosine detected at that time point (Figure 3.9). At 8 hours incubation, the maximum concentrations of cordycepin and cordycepin 5'-triphosphate in cordycepin/pentostatin treated cells reached maximum (29 and 1277 µM), were around five-fold higher than the maximum concentrations in cordycepin treated cells (6 and 251 µM) (Table 3.2).

3.4.4. Degradation of cordycepin in non-heat-treated serum

The results obtained from the previous experiments (Section 3.4.2 and Section 3.4.3) showed that cordycepin was rapidly metabolized into the inactive metabolite, 3'-deoxyinosine both in the medium and in the cells. These results are consistent with the previous studies that the use of cordycepin as therapeutic agent required an addition of deaminase inhibitor to inhibit deactivation of cordycepin (94, 110, 204) and to extend the half-life of cordycepin since the half-life of cordycepin is short, at 1.6 minutes *in vivo* (188). However, other studies found that cordycepin in a crude extract of *Cordyceps* exhibited significant pharmacological activity without the presence of deaminase inhibitor (215-220). Questions have therefore been raised about the possible presence of a natural deaminase inhibitor in the extract of *Cordyceps*. Therefore, a set of experiments was conducted in order to assess this possibility.

Cordycepin or extract ethanol of *C. militaris* in non-heat-treated FBS were analysed by the LC-MS/MS method after several time points of incubation. Figure 3.10 presents the results obtained from the degradation assay of cordycepin and extract ethanol of *C. militaris* in non-heat-treated serum. The current experiment found that there was a gradual degradation of cordycepin into 3'-deoxyinosine in non-heat-treated serum. Over 60 min incubation, around 25% of cordycepin had been changed into 3'-deoxyinosine. Moreover, there were significant correlation between the declining of the level of cordycepin in non-heat-treated serum and the length of incubation ($r = -0.92$; $p<0.05$), also between the developing of the level of 3'-deoxyinosine in non-heat-treated serum and the length of incubation ($r = 0.99$; $p<0.05$).

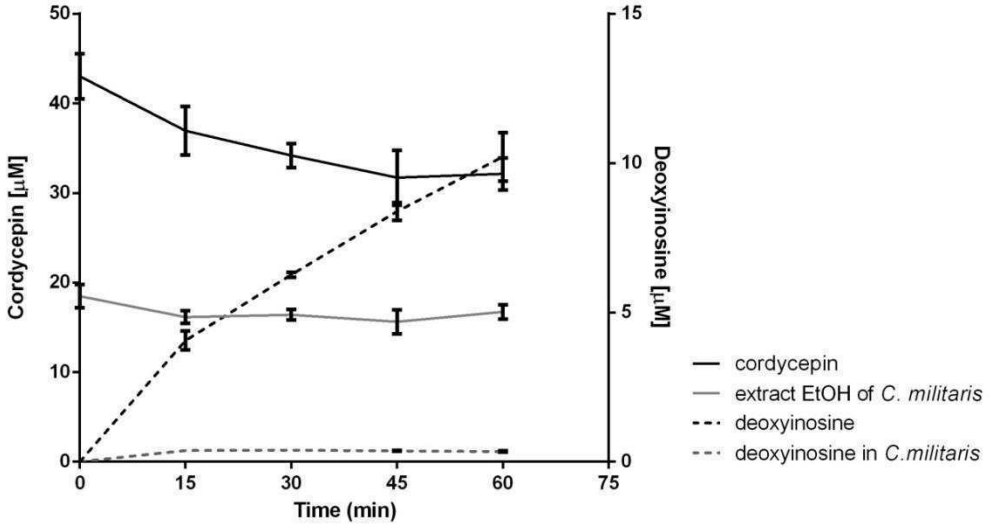

Figure 3.10. Degradation of cordycepin into 3'-deoxyinosine in non-heat-treated serum over 60 minutes of incubation

The most interesting finding in this experiment was that the degradation of cordycepin in the extract of *C. militaris* was very low, less than 0.1% of cordycepin had been changed into 3'-deoxyinosine after 15 min incubation in non-heat-treated serum and both the level of cordycepin and 3'-deoxyinosine remain steady over 60 min incubation. This experiment indicates strong evidence for the presence of a deaminase inhibitor in extract of *Cordyceps*.

3.4.5. Quantitative analysis of metabolites of cordycepin in plasma and liver samples of MIA-treated rats

Monosodium iodoacetate (MIA) induced osteoarthritis (OA) is commonly used to study the pathophysiology and development of joint injury with characterisation of the related pain. Weight bearing asymmetry and allodynia are observed in this MIA-induced OA model (221). The MIA experiments showed that cordycepin significantly reduced MIA induced weight bearing asymmetry and significantly reversed MIA induced allodynia at day 10 and 14 (Burston, De Moor and Chapman, unpublished results). Therefore, the objective of this study was to determine the level of cordycepin and the metabolites in plasma and liver samples of MIA-treated rats. Before the measurement of concentration of the active metabolites of cordycepin, validation of the method was performed.

The result of validation data of the method for quantification of cordycepin and its metabolites in plasma and liver sample is presented in Table 3.3 and Table 3.4. The results show that recoveries of the deaminated and phosphorylated metabolites were around or less than 50% which could be caused by precipitation of these

metabolites with proteins during the centrifugation step of the extraction of the samples. These low recoveries indicate a need for further improvement on the extraction of the samples. To compare with the results of Tsai et al. (188), their method showed the average of recovery of cordycepin in blood and liver were 37.7 and 48.3%, respectively; however, the concentration of cordycepin in the liver was undetectable using their method and also the method could not identify the metabolites of cordycepin.

Table 3.3. Linearity, recovery and precision of the method for quantification of metabolites in rat plasma

Compound	R^2	Recovery (%)	Precision (RSD %)
cordycepin	0.999	96.2	10.4
deoxyinosine	0.999	56.2	4.4
cordycepin 5'-triphosphate	0.998	49.2	2.5

Table 3.4. Linearity, recovery and precision of the method for quantification of metabolites in rat liver

Compound	R^2	Recovery (%)	Precision (RSD %)
cordycepin	0.999	100.2	18.4
deoxyinosine	0.999	49.9	5.7
cordycepin 5'-triphosphate	0.998	36.5	12.5

In this experiment rats were dosed with 2 mg of cordycepin every other day for 2 weeks. The last dose was administered 45-50 minutes before blood and liver samples were collected. Result from analysis of plasma samples shows that neither cordycepin nor its metabolites were detected in the plasma samples. The result indicates that degradation of cordycepin and the metabolites were rapid in the plasma. Since the samples were collected after 45-50 minutes last ingestion of

cordycepin, cordycepin may already be degraded to hypoxanthine and xanthine which was not measured in this study. Tsai et al. (188) reported that the half-life time of cordycepin and its metabolites are very short in the rat plasma. The half-life time of cordycepin was 1.6 min; while when pre-treated with pentostatin 30 min before administration of cordycepin, the elimination half-life of cordycepin was increased up to 23.3 min. Moreover, their study also observed that the elimination half-life of inosine and its further conversion, hypoxanthine, are also short in the plasma (188) since inosine and hypoxanthine are rapidly metabolized in human plasma (222).

Table 3.5. Levels of cordycepin and its metabolites in liver samples of rats dosed with cordycepin

Sample	Cordycepin (μmol/g sample)	3'-deoxyinosine (μmol/g sample)	Cordycepin triphosphate (μmol/g sample)
Liver 1	0.26	1.49	-
Liver 2	0.33	1.55	0.03
Liver 3	0.34	1.63	0.03
Liver 4	0.38	1.22	0.04
Liver 5	0.37	1.59	0.03
Liver 6	0.28	1.64	0.04
Liver 7	0.86	1.19	-
Liver 8	0.30	1.50	-
Average ± SD	0.39 ± 0.19	1.47 ± 0.18	0.03 ± 0.01

However, the concentration of cordycepin, the deaminated metabolites, 3'-deoxyinosine, and cordycepin triphosphates were determined in the liver samples. The levels of cordycepin and the metabolites in rat liver samples are shown in Table 3.5. The actual concentrations of cordycepin and the metabolites in the rat liver were corrected by their respective recoveries. From the table we can see that cordycepin and the both metabolites were accumulated in the liver. Concentration

of the deaminated metabolite was the highest at around 4 times of the concentration of the precursor, cordycepin, whereas the phosphorylated metabolite was only accumulated less than 10% of cordycepin.

3.4.6. Discussion

In this study we demonstrated that the major intracellular metabolite of cordycepin was cordycepin triphosphate, which was developed rapidly and accumulated intracellularly in high concentration in both of the cell lines, MCF7 and HeLa cells. Since this metabolite, cordycepin triphosphate, has been proven as the active metabolite which is responsible for the pharmacological activity of cordycepin (86, 110, 223), these findings support the previous observation that both MCF7 and HeLa cells were found to be sensitive to cordycepin (95). The maximum intracellular level of cordycepin triphosphate in MCF7 cells was approximately two-fold higher than that in HeLa cells when incubated either with cordycepin alone or in the presence of pentostatin. The lower level of cordycepin triphosphate in HeLa cells compared with in MCF7 cells is probably because MCF7 cells express a higher adenosine kinase (AK) activity than HeLa cells.

The phosphorylated metabolite of cordycepin was accumulated to a much higher level than the deaminated metabolites in MCF7 and HeLa cells, indicating that phosphorylation of cordycepin is much more efficient than deamination. Previous study found that in most tissue investigated, the K_m values of AK for adenosine are lower than those of the deaminase, between one and two orders of magnitude lower (15). Since the bonding between purine base of adenosine and AK (224) is

quite similar to the bonding between purine base of cordycepin and AK, it is likely that K_m values of AK for cordycepin also quite similar with that for adenosine. In addition, a study on the comparison of ADA and AK activities in Ehrlich ascites tumour cells observed that at low concentrations of adenosine, less than 150 µM, phosphorylation of adenosine was greater than that of deamination (214). Moreover, Agarwal et al. (225) reported that the K_m values of ADA from human erythrocytes for adenosine and cordycepin were 25 and 41 µM, respectively; whereas K_m values of AK for adenosine was 1.8 µM (226) and efficiency of phosphorylation of cordycepin is 12.5 % of adenosine phosphorylation (226). Therefore, the efficiency of phosphorylation of cordycepin is much more efficient than the deamination of cordycepin.

Investigation of the activity of enzymes in cancer tissues observed higher activities of enzymes which are responsible for purine metabolism as a compensatory mechanism for enhanced purine metabolism in tumour tissue (227). The study discovered that in tumour tissues, the activities of ADA, AK, 5'-nucleotidase (5'-NT), and purine nucleoside phosphorylase (PNP) are much higher than in non-neoplastic mucosa. Giglioni et al. (228) also detected a significant increase in gene expression of AK and higher of AK activities (227) in colorectal tumour samples compare to non-tumour mucosa. Consequently, phosphorylation of adenosine and adenosine analogues are much higher as a result of high activity of AK in malignant tissue.

Deamination of cordycepin to the inactive metabolite deoxyinosine has been shown extensively in cells incubated without pentostatin; most of cordycepin was readily

deaminated by ADA and converted to 3'-deoxyinosine. Furthermore, the combination of 50 µM cordycepin and 1 µM pentostatin found that concentration of 1 µM of inhibitor was adequate to prevent the intracellular degradation of cordycepin into 3'-deoxyinosine. Agarwal et al. (225) reported that K_i of ADA for pentostatin is 2.5 nM while the K_m for cordycepin is 41 µM. This large discrepancy indicates that affinity of ADA for pentostatin is much higher than that for cordycepin, thus pentostatin effectively inhibit the deamination of cordycepin by ADA even at the highest intracellular level of cordycepin. After MCF7 and HeLa cells were treated with cordycepin in the presence of pentostatin, the level of cordycepin triphosphate in MCF7 and HeLa cells rose by approximately 4.5 and five-fold, respectively. These results indicate that both MCF7 and HeLa cells express considerable amounts of ADA.

Other published studies in breast tissues reported increased ADA activity in malignant tissues compared with non-malignant tissue (229, 230). It was proposed that increased activity of ADA has a significant part in the salvage pathway activity of malignant tissues and cells (230). Moreover, the high activity of ADA is likely play a role in the mechanism against toxic accumulation of adenosine and deoxyadenosine substrates produced from accelerated purine metabolism in the malignant tissues (229). Moreover, there were significant differences in activity of ADA in different clinical phases of breast cancer (231). Therefore, it can be concluded that an ADA inhibitor should be used in combination with cordycepin as anticancer agent, or cordycepin requires chemical modification to make it less sensitive to ADA metabolism while retaining its anti-cancer cell activity.

In this study, the deaminated metabolite of cordycepin, 3'-deoxyinosine was found highly accumulated in both types of cells which were incubated with cordycepin in the absence of pentostatin, an ADA inhibitor. The intracellular accumulation of 3'-deoxyinosine might be not only from intracellular deamination of cordycepin but could be also from the uptake of 3-deoxyinosine from the medium since there were high concentrations of 3'-deoxyinosine in the media of both cells which was possibly because of the deamination of cordycepin by ADA from the serum in the medium. A previous study revealed that the transport of gemcitabine, an nucleoside analogue, into the cells was inhibited by its deaminated metabolite since the metabolite and the parent compound competed to be transported into the cells using the same nucleoside transporter (232); however, in the longer term the deaminated metabolite increased the intracellular level of gemcitabine triphosphate by a mechanism which remains unclear (233). Therefore, further research is needed to investigate the transport of 3'-deoxyinosine and cordycepin into the cells. Furthermore, if both 3'-deoxyinosine and cordycepin are transported via the same nucleoside transporters, more research is required to determine the effect of 3'-deoxyinosine on the uptake of cordycepin into the cells and also in the intracellular phosphorylation of cordycepin.

The level of the deaminated metabolite, 3'deoxyinosine, was quite constant inside the cell, whereas the phosphorylated metabolite was degraded rapidly. It might be possible that cordycepin triphosphate degraded through de-phosphorylation and further converted to 3'-deoxyinosine and hypoxanthine. As a result, the level of 3'-deoxyinosine was not only from deamination of cordycepin but also from

degradation of cordycepin triphosphate. This finding corroborates the ideas of Klenow (234) who suggested that degradation of deoxyadenosine triphosphate mainly to deoxyinosine and hypoxanthine.

Since there is a high amount of the deaminated metabolite of cordycepin, 3'-deoxyinosine, therefore it will be interesting to investigate whether 3'-deoxyinosine have an effect on the cells viability. Kodama et al. (110) have investigated that possibility and found that there was no cytotoxic effect of 3'-deoxyinosine. It may be due to the low level of 3-deoxyinosine triphosphate in the cells since the phosphorylation of 3'-deoxyinosine was detected extremely low in the cells as compared with that of cordycepin (110). The low phosphorylation efficiency of 3'-deoxyinosine could be predicted since the presence of guanosine/inosine kinase, the enzyme which is responsible for phosphorylation of inosine and deoxyinosine, are limited in most tissue investigated (235).

The results of this study will now be compared to the findings of previous work. Chen et al. (94) reported that there was approximately 75 µM cordycepin triphosphate accumulated in multiple myeloma cells after 24 hours of incubation with 10 µM cordycepin. In addition, research on the intracellular metabolism of cordycepin by Kodama et al. (110) also detected a high level of cordycepin triphosphate accumulated in NALM-6 cells (67 pmol/10^6 cells), K562 cells (49 pmol/10^6 cells), and HUT-102 cells (27 pmol/10^6 cells) when incubated with 1 µM cordycepin in the presence of 2.5 mM pentostatin, even though it was low in MOLT-4 cells (0.3 pmol/10^6 cells). However, the deaminated metabolite could not be

identified using their HPLC method since its retention time as similar with the parent compound, cordycepin. Meanwhile, the study in this chapter found a higher level of cordycepin triphosphate accumulated in the cells, 2203 and 1277 µM or 9.5 and 5.9 nmol/10^6 cells in MCF7 and HeLa cells, respectively. Since in this current study we used a concentration of cordycepin of 50 µM, fifty times higher than the previous study, therefore the amount of cordycepin triphosphate accumulated in cells was much higher than the previous study (110). Furthermore, using the LC-MS/MS method we could identify and quantify the deaminated metabolites simultaneously with other metabolites.

On the other hand, in this study we found a very low level of deamination of cordycepin in an extract of *C. militaris* during incubation in non-heat-treated serum. This result indicates a strong evidence for the presence of a deaminase inhibitor in extract of *Cordyceps*. As mentioned in the introduction, nucleosides are found in relatively high concentrations in *Cordyceps* with cordycepin as a major compound (79, 80). However, flavonoids and polyphenolics are also present in extract of *Cordyceps* (236). The content of polyphenolic compounds in an extract of *C. militaris* is higher than in extract of *C. sinensis*. Moreover, Jiang et al. (237) have isolated a flavonoid compound from the extract of *C. militaris* which has significant antioxidant activity and inhibition activity of HIV-1 protease. Research to examine inhibitory effects of natural compounds on the enzyme adenosine deaminase (ADA) demonstrated that some prominent flavonoids have an ability to inhibit the ADA activity (238, 239). In addition, the flavonoid naringin was found to significantly inhibit the deamination of cordycepin and the combination with cordycepin showed

an increase in the cytotoxic effect of cordycepin to Jurkat cells (239). All of those results from the previous studies support the possibility of ADA inhibitor in extract of *C. militaris*. Overall, this result from this chapter demonstrates for the first time that there is a natural deaminase inhibitor in extract of *C. militaris*. Further experimental investigations are needed to examine the inhibition of the extract of *Cordyceps* on the activity of enzyme adenosine deaminase.

Result from experiments using rat samples shows that cordycepin and its metabolites are not stable in rat plasma. Not only cordycepin but also the metabolites are rapidly degraded in the plasma. These results are consistent with the previous study (188) and suggest that administration of cordycepin combine with an ADA inhibitor is required to overcome the problem of rapid elimination. On the other hand, cordycepin and the deaminated and phosphorylated metabolites are accumulated in the liver sample. It suggests that although cordycepin is unstable, it can accumulate in tissues with repeated dosing. Therefore, it can conclude that pharmacokinetic and bio-distribution studies are required to elucidate this, and that the LC-MS/MS method is ideal for this purpose.

In its triphosphate form, cordycepin is incorporated into mRNA as a chain terminator for polyadenylation by PAP and affects mRNA synthesis (86, 195, 196). The study discovered that inactivation of PAP triggered higher cellular ATP levels in the mutant strains which is defective in cleavage and polyadenylation of pre-mRNA which suggest a possibility that the efficiency of polyadenylation is in some way functionally related to the energy status of the cell (195). Moreover, the study also confirmed

that cordycepin needs to be phosphorylated into the active metabolite by AK (86, 196). Therefore, due to this phosphorylation of cordycepin, it could have effects on the cellular energy balance and the endogenous nucleotide concentrations. Since the energy status of the cells is related to the intracellular level of adenine nucleotide, therefore effect of the phosphorylated cordycepin in relation to intracellular nucleotide levels (including ATP) is of potential importance and will be further investigated in the next chapter 4 of the thesis.

3.5. Conclusions

The LC-MS/MS method has demonstrated an ability to measure the metabolites of cordycepin in medium and cell lines. Using this method, the metabolism of cordycepin has been observed in MCF7 and HeLa cells as well as in the cell culture medium. Cordycepin and its active metabolite reached maximum accumulation in both cells at 2 hours incubation with cordycepin and at 8 hours incubation with combination of cordycepin and pentostatin. The study of the intracellular metabolism of cordycepin shows that cordycepin was rapidly metabolized into the deaminated form by ADA; all cordycepin had been metabolized at 8 hours incubation with cordycepin alone. However, in the presence of ADA inhibitor the phosphorylated metabolite was highly accumulated in the cells.

On the other hand, our result indicates that there is a natural ADA inhibitor found in *Cordyceps* extracts which may need to be further investigated. Moreover, determination of concentrations of cordycepin and the metabolites in the plasma and liver of rats dosed with cordycepin suggests that the half-life of cordycepin and

its metabolites are very short in the plasma; however they are accumulated in the liver with repeated administration. It is recommended that further research be undertaken in the in the pharmacokinetic and bio-distribution of cordycepin.

CHAPTER 4
THE EFFECT OF CORDYCEPIN ON NUCLEOTIDE METABOLISM AND SURVIVAL OF CANCER CELLS

THE EFFECT OF CORDYCEPIN ON NUCLEOTIDE METABOLISM AND SURVIVAL OF CANCER CELLS

4.1. Introduction

Eukaryotic cells demand energy through ATP production to carry out normal metabolic functions for maintaining cell growth and proliferative homeostasis. Although glucose is the primary carbon source for energy production, amino acids and lipids can also be as a source of ATP synthesis. ATP production occurs in the mitochondria by aerobic respiration or in the cytoplasm through glycolysis. Although both aerobic respiration and glycolysis are used simultaneously to produce the energy necessary for eukaryotic cell function, the balance between the two processes is tightly regulated and adaptable to varying metabolic conditions. The glycolysis process may become the preferred method of ATP production where there is a high demand for energy or during conditions of mitochondrial dysfunction (240).

Several studies have observed that metabolism in tumour cells are different with in the normal cells. Tumour cells show a changed energetic metabolism. For production of energy, most cancer cells primarily rely not on aerobic respiration but on glycolysis, even in the presence of oxygen. This phenomenon is called as Warburg effect (241). The glycolysis process is vital for the cells survival since the process prevented cell death induced by accumulation of hydrogen peroxide and ATP depletion (5). Moreover, a metabolic alteration in intracellular nucleotide levels happens throughout the development of cancer.

Determination of intracellular nucleotide concentrations is necessary for studying the mechanism action of nucleoside drugs in mammalian cells. Nucleotides are involved in the regulation of cellular energy metabolism. The possible toxic effects of most nucleoside analogues in the cells include the depletion of precursor compounds for syntheses of RNA/DNA, inhibition of nucleoside triphosphates and/or deoxynucleoside triphosphates synthesis, or antagonism with endogenous nucleotides for incorporation into RNA or DNA strands (46). All of these effects could cause disturbance in endogenous nucleotides pools. Hence, the quantification of intracellular nucleotides concentrations is essential for fully understanding the mechanisms of the nucleoside analogues and monitoring the outcome of the treatment.

Previous research shows that adenosine analogues, 8−NH_2-adenosine and 8−Cl-adenosine reduced synthesis of RNA and stimulated cytotoxicity in multiple myeloma (MM) cells by declining the intracellular level of ATP (51, 54). Experiments confirmed that metabolism of cordycepin into the active metabolite relied on the activity of adenosine kinase (86, 196). Therefore, due to this phosphorylation of cordycepin, it could have effects on the cellular energy balance and the endogenous nucleotide concentrations. This study aimed to investigate the effect of the cordycepin treatment on nucleotide metabolism in cancer cell lines.

4.2. Aim and Objectives

The aim of this chapter is to investigate the effect of the treatment using cordycepin, pentostatin or the combination of cordycepin and pentostatin on nucleotide metabolism in cancer cell lines.

The objectives of this chapter are to apply the LC-MS/MS method for:

- Determination of intracellular level of endogenous nucleotides in MCF7 and HeLa cells treated with cordycepin.
- Determination of intracellular level of endogenous nucleotides in MCF7 and HeLa cells treated with pentostatin.
- Determination of intracellular level of endogenous nucleotides in MCF7 and HeLa cells treated with combination of cordycepin and pentostatin.

4.3. Materials and Methods

4.3.1. Chemicals

The chemicals used are the same as described in Chapter 2 (Section 2.3.1).

4.3.2. Cell culture

MCF7 and HeLa cells were cultured using the same procedures as described in Chapter 2 (Section 2.3.2).

4.3.3. Drug treatment

MCF7 and HeLa cells were treated with cordycepin and/or pentostatin as described in Chapter 3 (Section 3.3.3).

4.3.4. Samples extraction

Extraction of samples was done as described in Chapter 2 (Section 2.3.8.1).

4.3.5. Calculation of total cell volume

Calculation the total cell volume was done as described in Chapter 2 (Section 2.3.8.2).

4.3.6. LC-MS/MS conditions

Analyses of samples were carried out by the method are described in Chapter 2 (Section 2.3.8.3). Multiple reactions monitoring (MRM) scan was used with dwell time 0.1 s as described in Table 2.4.

4.4. Results and Discussion

Nucleoside analogues used as anti-tumour agents work in a variety of mechanism such as causing DNA-strand damage, integration into nucleic acids, inhibition of RNA synthesis, and perturbation of intracellular nucleotide pools. The present study was designed to determine the effect of either cordycepin, pentostatin, or their combination on intracellular nucleotide pools. In order to investigate, MCF7 and HeLa cells were incubated with 50 µM cordycepin with and without 1 µM pentostatin for 2, 8, and 24 hours. At the three time points, cells were collected, extracted, and analysed by LC-MS/MS method. The nucleotides level was quantified using the regression of the calibration curve. In this study, the intracellular concentrations of the nucleotides were calculated from the average cell volume and the total cell count according to the method described.

4.4.1. Intracellular nucleotides level in cell lines

The intracellular levels of each nucleotide in control untreated cells for three time points are shown in Table 4.1. Cells extracts were collected and analysed at three time points: 2, 8, and 24 hours after 24 hours of seeding, when control cells were in

exponential growth. The time points are same as the duration of drug incubation. As shown in Table 4.1. an increase in nucleotide concentrations was observed during the three time points which is consistent with other research which found that the level of nucleotides remains low during the lag phase (0-24 hours after seeding), significantly increases during log phase (24-72 hours after seeding), and then reaches a maximum before declines at the onset of the plateau phase (242). Considerable differences were detected between MCF7 and HeLa cells, with obviously higher nucleotide pools in MCF7 cells.

Table 4.1. The level of intracellular nucleotides (μM) in MCF7 and HeLa cells untreated at the indicated times.

	Time (h)					
	MCF7			HeLa		
	2	8	24	2	8	24
ATP	1440 ± 427	1657 ± 536	2518 ± 1399	809 ± 62	930 ± 87	1067 ± 125
ADP	263 ± 147	263± 140	420 ± 134	219 ± 21	236 ± 99	378 ± 52
AMP	114 ± 40	148 ± 88	288 ± 67	94 ± 22	117 ± 20	163 ± 14
UTP	237 ± 92	263 ± 112	426 ± 231	179 ± 21	322 ± 4	379 ± 33
UDP	299 ± 127	422 ± 229	495 ± 343	115 ± 45	197 ± 55	168 ± 56
UMP	62 ± 42	154 ± 126	275 ± 125	47 ± 4	78 ± 9	74 ± 8
GTP	217 ± 124	422 ± 125	626 ± 278	147 ± 10	223 ± 37	336 ± 68
GDP	119 ± 74	132 ± 73	162 ± 75	83 ± 19	161 ± 21	176 ± 28
GMP	59 ± 19	46 ± 15	151 ± 48	37 ± 16	49 ± 16	54 ± 10
CTP	163 ± 56	190 ± 52	194 ± 67	84 ± 19	110 ± 19	138 ± 16
CDP	183 ± 112	162 ± 72	327 ± 137	75 ± 5	75 ± 8	75 ± 3
CMP	37 ± 25	25 ± 15	41 ± 16	34 ± 4	50 ± 11	59 ± 5
EC	0.86	0.86	0.85	0.82	0.82	0.80

*Data represent the mean ± SD from 3 separate experiments (n=6-8)

Energy charge (EC) is considered a quantitative parameter of energy status of cell and as an assessment of the balance between adenine nucleotides. In the present study, we found that the EC of MCF7 and HeLa cells at all the time points was between 0.8 and 0.9, indicating that about 70-80% of the adenine nucleotides are in the form of ATP. This result matched that observed in an earlier study that found that MCF7 cells have an EC value of 0.89 and its value is higher than that of HeLa cells (5). Generally, the EC value of cells in culture is about 0.8-0.9 (243, 244); and investigation by Zhang et al. (5) found that the level of adenosine and uridine triphosphate were significantly higher in malignant cells compared with normal cells since malignant cells are metabolically active, therefore large quantities of energy need be produced and spent in the process of growth, causing a significant accumulation of ATP.

4.4.2. Effects of cordycepin on the nucleotides levels in cancer cells

Effects of cordycepin on the adenosine nucleotides levels in MCF7 and HeLa cells are shown in Figure 4.1. In MCF7 cells, it has been observed that there was an increase of 130% in the intracellular ATP level compared to control after 2 hours incubation with cordycepin alone. However, this phenomenon was not observed at 8 and 24 hours of incubation. At 8 hours, the level of intracellular ATP returned to the same as control untreated cells and then dropped to 19% of control over 24 hours of incubation. Surprisingly, the increase in intracellular ATP level at 2 hours was not accompanied with a parallel decline in the intracellular level of ADP or AMP. Also, the decrease in intracellular ATP level at 24 hours was not followed with a parallel incline in the level of intracellular ADP or AMP. The intracellular level of ADP and

AMP were relatively steady during incubation with cordycepin up to 8 hours and then significantly decreased at 24 hours. The EC values as an indicator of the energy status of the cells initially increased to 0.94 relate to an increase of the ATP level at the beginning of incubation, then returned at a value of 0.86 at 8 and 24 hours incubation.

In contrast, in HeLa cells, the levels of adenine nucleotides remained same as control over 8 hours. At 24 hours, the level of ATP was still constant, but the level of ADP and AMP declined to 50% of control. In addition, the EC of the both cells were also not affected by these changes; during period of incubation, the values remained in the range of 0.8 to 0.9. The results from HeLa cells accords the findings of other study in multiple myeloma cells, which described that ATP intracellular levels remain unaffected after 24 hour incubation with 10 μM cordycepin (94).

Furthermore, determination of uridine nucleotides in MCF7 cells (Figure 4.2A) detected that the amount of UTP rose by 185 % at 2 hours and later returned to the control level after 8 hours incubation; while the amounts of UDP and UMP were not significantly different with the control at those times. In HeLa cells, the amount of UTP was about 118% of control at 2 hours and became same as the control level at 8 hours. Furthermore, at 24 hours, the amounts of uridine nucleotides in MCF7 and HeLa cells decreased to the range of 15-20% and 25-70% of control, respectively.

From the data in Figure 4.3, it is apparent that at 2 hours incubation, the intracellular concentration of GTP increased to about 3.5 and 2.5 times the initial level in MCF7 and HeLa cells, respectively. In contrast, its level decreased to about 50% at 8 and 24 hours in MCF7 cells; however, the concentration in HeLa cells was still higher than that of control at 8 hours before returned to the original level at 24 hours. In addition, GDP and GMP concentration in both cells were around 20-85% of control at 24 hours incubation.

The same effects were observed in cytidine nucleotides content in both cells as are shown in Figure 4.4. At 2 hours incubation, the content of CTP went up about two and 1.5 times of control in both MCF7 and HeLa cells; and this growth was followed by a decline of CDP and CMP content. At 8 hours of incubation, cytidine nucleotides returned to the original level and decreased (55-65%) later at the last time point of the study.

In summary, these results show that cordycepin has an effect on nucleotide metabolism. The intracellular contents of nucleotide triphosphates (NTPs) in MCF7 and HeLa cells mostly increased at 2 hours incubation with 50 μM cordycepin. It induced a highest increase in GTP in both cells. These increases, however, were not always followed by declining of the nucleotide di- or monophosphates. Their levels then decreased to the same as or lower than the initial levels over 8 hours of incubation. The effect of cordycepin on the intracellular concentration of NTPs is similar with that of other adenosine analogues. Investigation on the influences of

pentostatin, cladribine, and fludarabine on nucleotides metabolism observed that NTPs levels in Raji cells increased after 4 to 8 hours incubation with these nucleoside analogues before going down at later times (191).

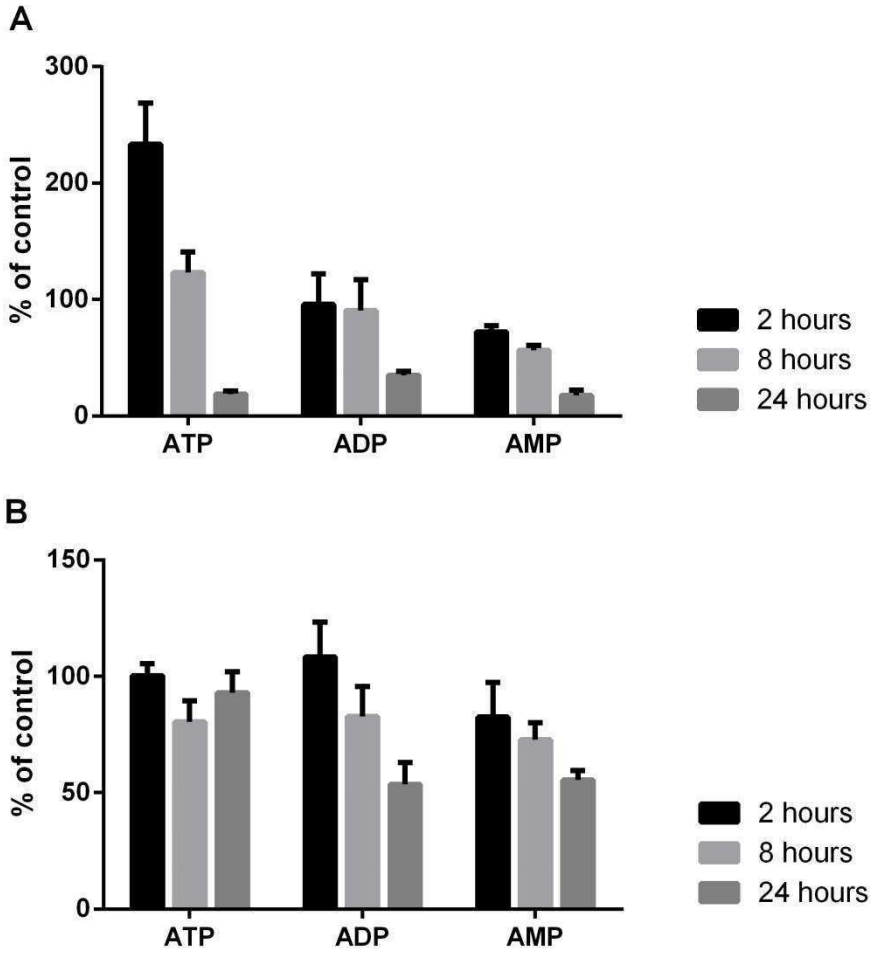

Figure 4.1. Effect of treatment with 50 µM cordycepin on the intracellular level of adenine nucleotides in MCF7 cells (A) and HeLa cells (B) at the indicated times.

The level of nucleotides was determined in treated and untreated control cells at each time point. Each bar represents the mean ± SEM (n = 6-8).

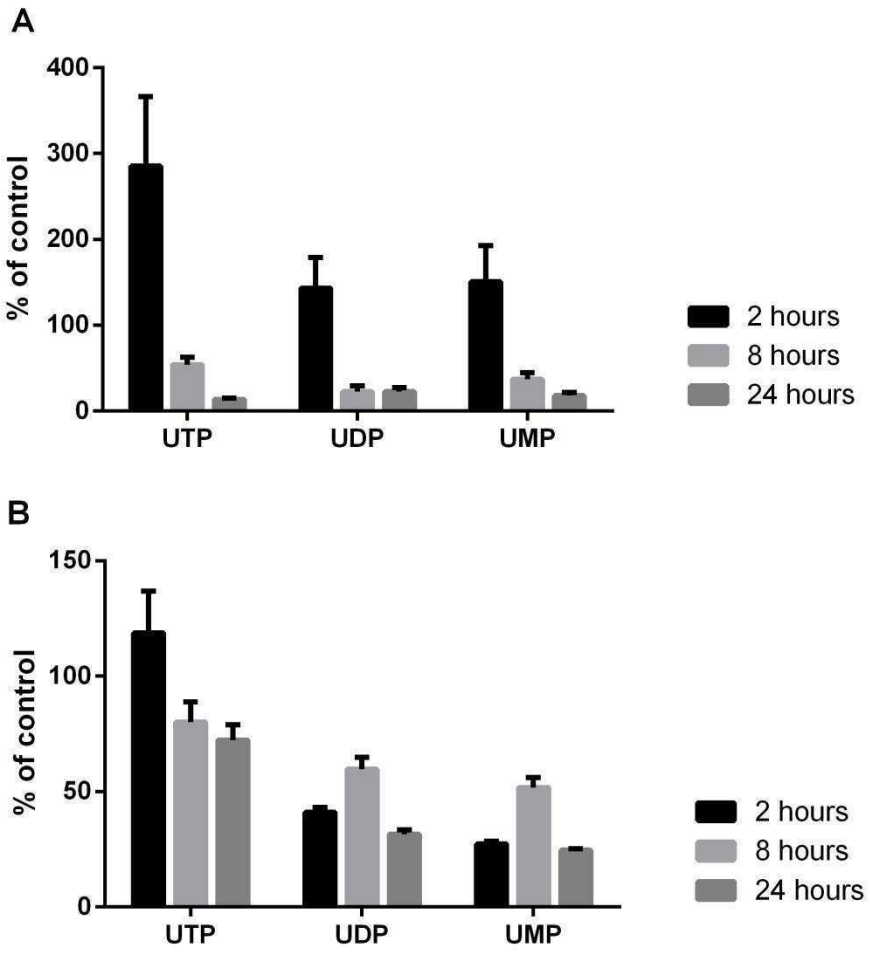

Figure 4.2. Effect of treatment with 50 µM cordycepin on the intracellular level of uridine nucleotides in MCF7 cells (A) and HeLa cells (B) at the indicated times.

The level of nucleotides was determined in treated and untreated control cells at each time point. Each bar represents the mean ± SEM (n = 6-8).

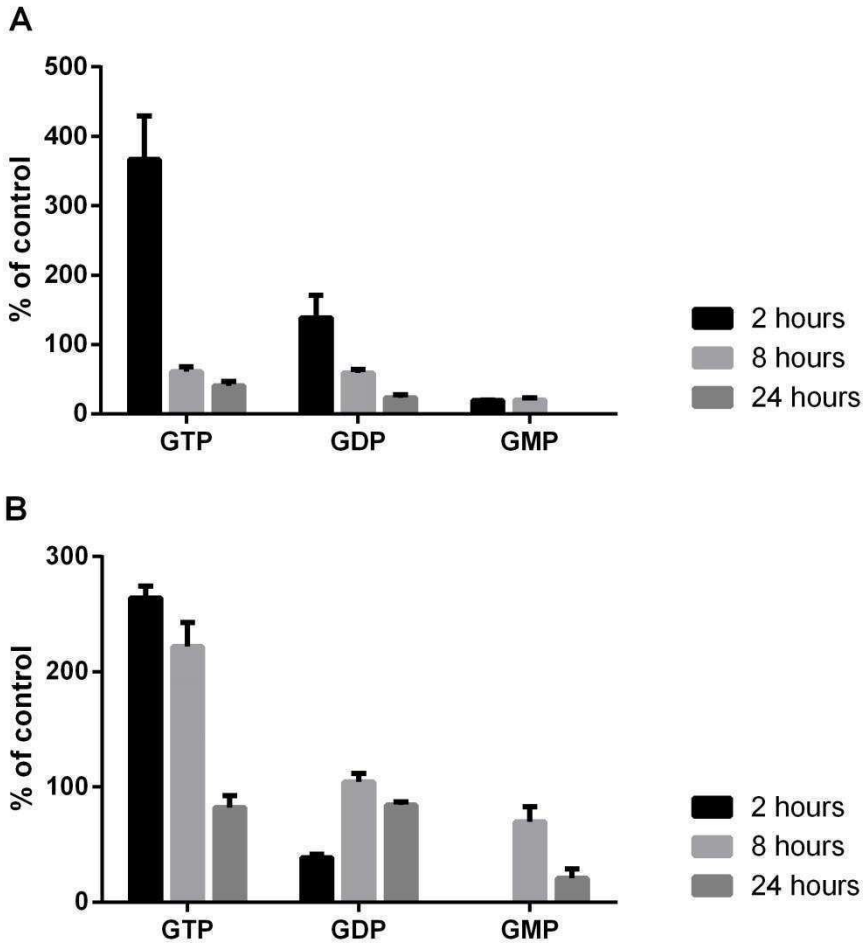

Figure 4.3. Effect of treatment with 50 µM cordycepin on the intracellular level of guanine nucleotides in MCF7 cells (A) and HeLa cells (B) at the indicated times.

The level of nucleotides was determined in treated and untreated control cells at each time point. Each bar represents the mean ± SEM (n = 6-8).

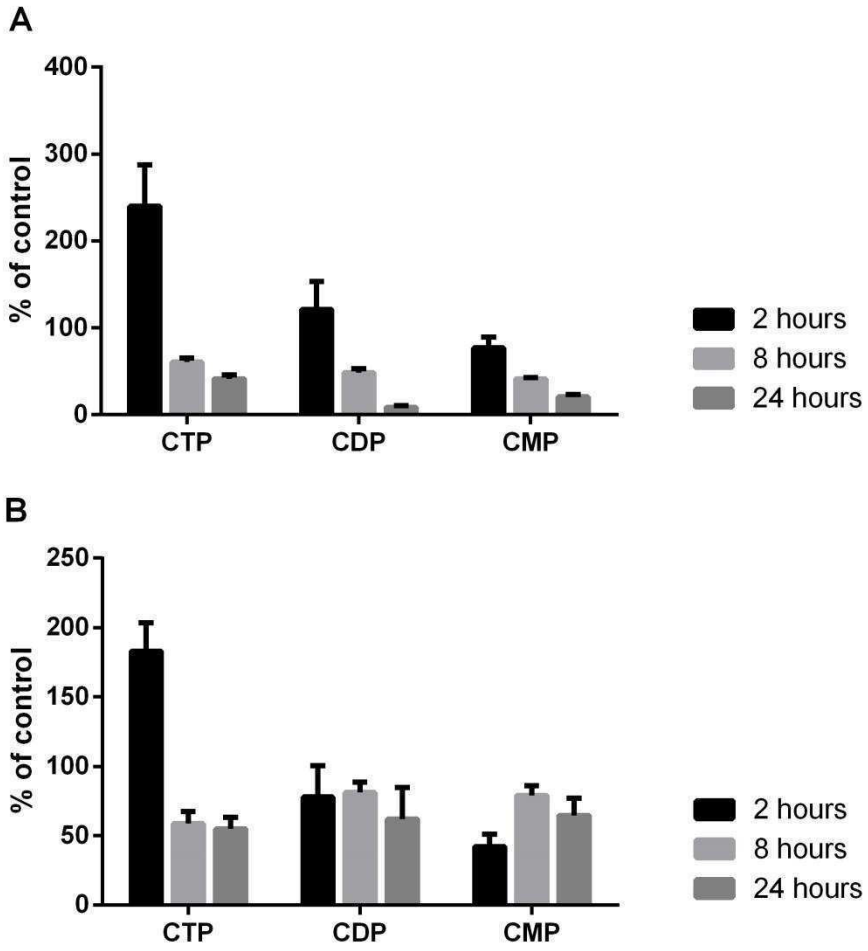

Figure 4.4. Effect of treatment with 50 µM cordycepin on the intracellular level of cytidine nucleotides in MCF7 cells (A) and HeLa cells (B) at the indicated times.

The level of nucleotides was determined in treated and untreated control cells at each time point. Each bar represents the mean ± SEM (n = 6-8).

4.4.3. Effects of pentostatin on the nucleotides levels in cancer cells

Pentostatin is a deoxyadenosine analogue which is used in the treatment with cordycepin due to its ability to inhibit deactivation of cordycepin by adenosine deaminase (ADA). Therefore, in this experiment we also investigated the effects of pentostatin alone on intracellular nucleotide levels.

In the pentostatin treated cells (Figure 4.5), the cellular concentration of ATP in MCF7 cells remained constant until 8 hours incubation and decreased in the long term. In contrast, the levels of diphosphate and monophosphate declined significantly after 2 hours. At 24 hours, the concentrations of adenine nucleotides were between 20 and 56% of initial concentration. On the other hand, the cellular concentrations of adenine nucleotides (ATP, ADP, and AMP) in HeLa cells were not significantly different from the untreated cells during 24 hours of incubation with pentostatin.

The same phenomenon was observed for other nucleotides in MCF7 and HeLa cells treated with pentostatin. The amount of UTP and UDP in MCF7 cells stayed the same as in untreated cells during 8 hour while UMP rose by 100%; and then their concentrations went down at 24 hours (Figure 4.6). Meanwhile, GTP and CTP level stayed constant at 2 hours and dropped later to 20-54% (GTP) and 52-60% (CTP) after 8 hour (Figure 4.7 and Figure 4.8). Their di- and monophosphates levels were around 20-90% during time of incubation, except CMP level which increased 1.5 times of initial level at 8 hours. Similar with the content of adenine nucleotides,

generally, there were no significant differences on the concentrations of UTP, GTP, and CTP in HeLa cells between treated and untreated cells during 24 hours incubation.

Overall, no significant reductions in the levels of NTPs were found in either MCF7 or HeLa cells treated with 1 μM pentostatin for 2 and 8 hours compared with untreated cells, but there were falls in the levels of NTPs in MCF7 cells at 24 hours. The effect of pentostatin on these cells is slightly different when compared to the effect on Raji cells and CCRF-CEM cells. The levels of NTPs in those cells remained steady over 3 h, then inclined with maximum concentrations reached after 4 – 8 h before declining in the long term (191).

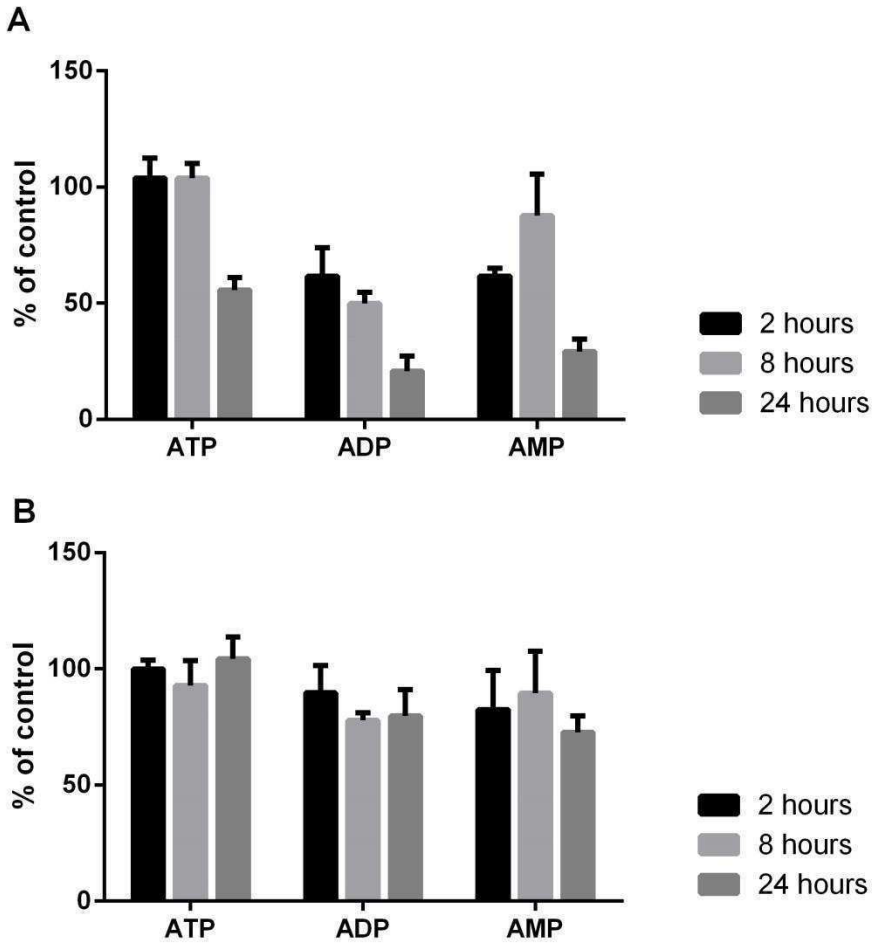

Figure 4.5. Effect of treatment with 1 µM pentostatin on the intracellular level of adenine nucleotides in MCF7 cells (A) and HeLa cells (B) at the indicated times.

The level of nucleotides was determined in treated and untreated control cells at each time point. Each bar represents the mean ± SEM (n = 6-8).

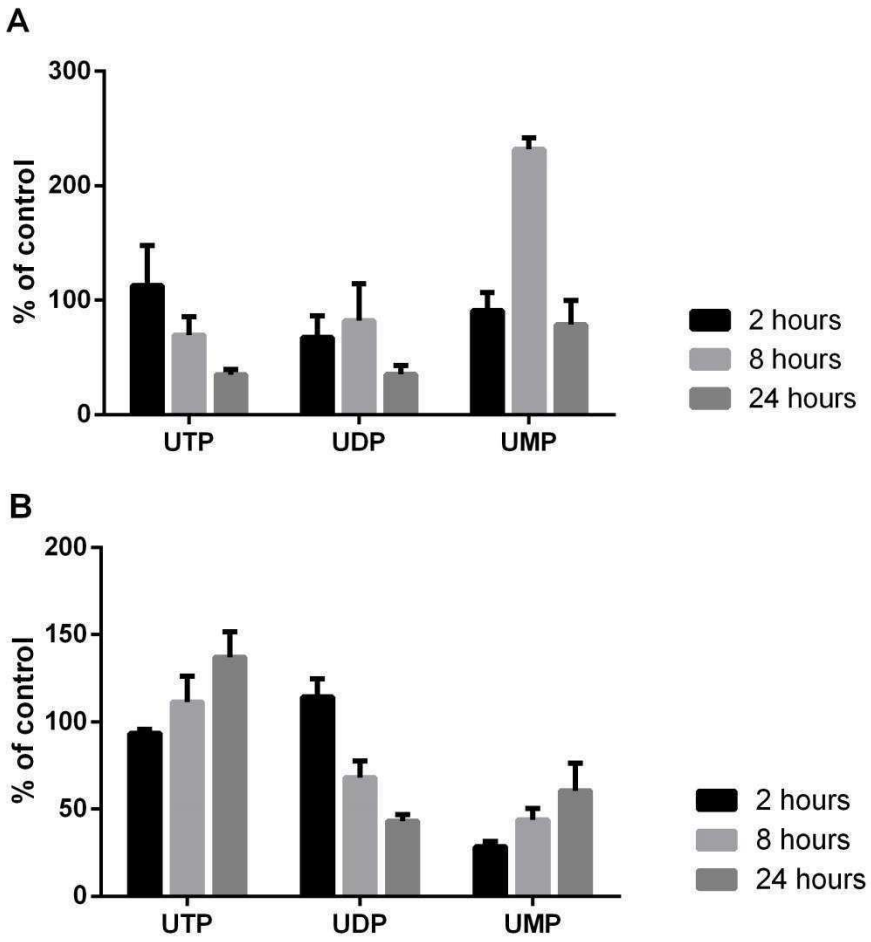

Figure 4.6. Effect of treatment with 1 µM pentostatin on the intracellular level of uridine nucleotides in MCF7 cells (A) and HeLa cells (B) at the indicated times.

The level of nucleotides was determined in treated and untreated control cells at each time point. Each bar represents the mean ± SEM (n = 6-8).

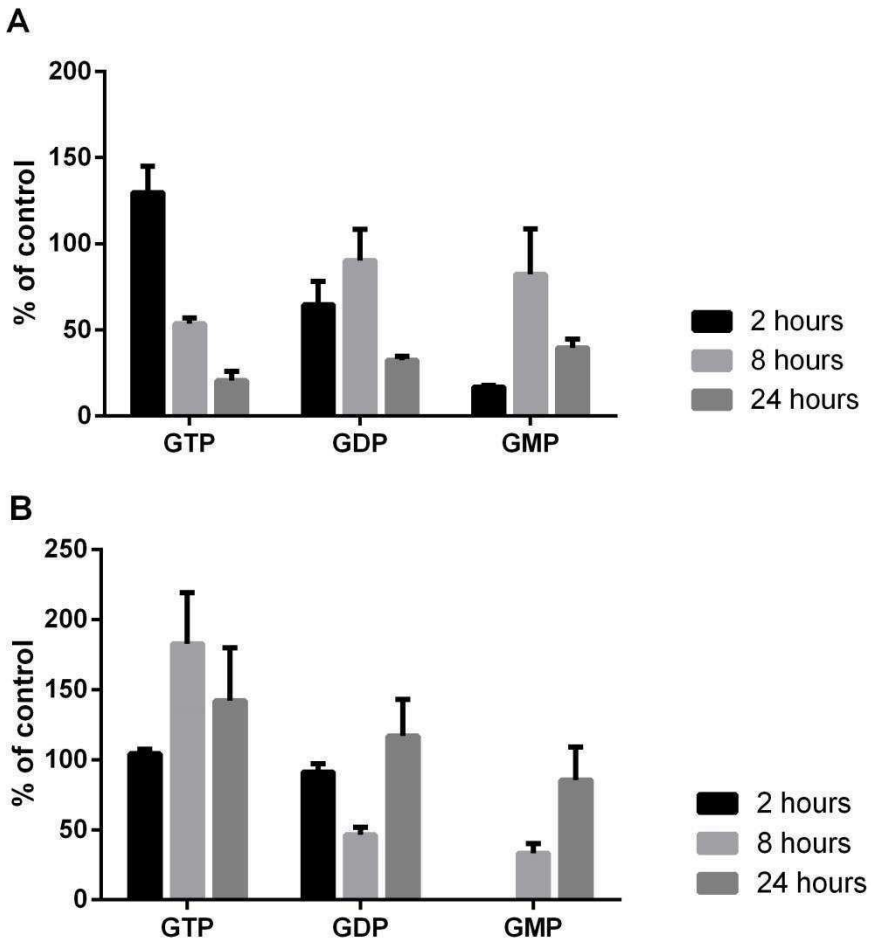

Figure 4.7. Effect of treatment with 1 µM pentostatin on the intracellular level of guanidine nucleotides in MCF7 cells (A) and HeLa cells (B) at the indicated times.

The level of nucleotides was determined in treated and untreated control cells at each time point. Each bar represents the mean ± SEM (n = 6-8).

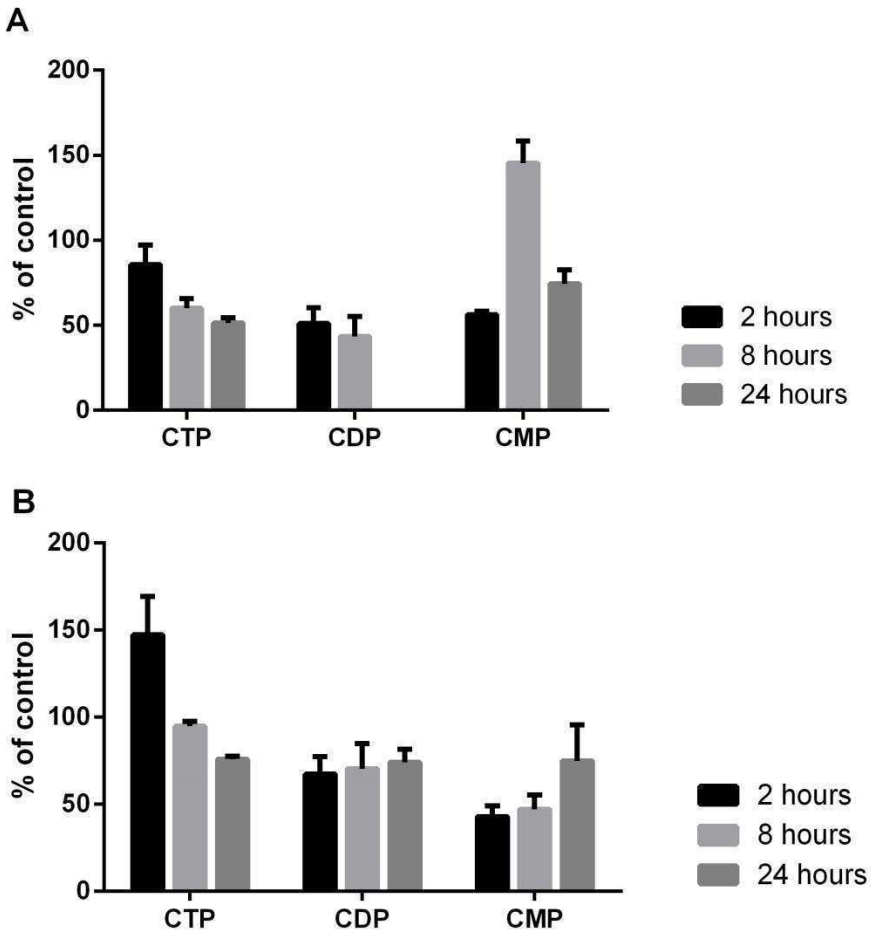

Figure 4.8. Effect of treatment with 1 µM pentostatin on the intracellular level of cytidine nucleotides in MCF7 cells (A) and HeLa cells (B) at the indicated times.

The level of nucleotides was determined in treated and untreated control cells at each time point. Each bar represents the mean ± SEM (n = 6-8).

4.4.4. Effects of combination of cordycepin and pentostatin on the nucleotides levels in cancer cells

Figure 4.9 shows a progressive decrease of adenine nucleotide concentration in both MCF7 and HeLa cells treated for 2, 8, and 24 hours with combination of 50 µM cordycepin and 1 µM pentostatin. We observed a decrease in ATP levels which reached up to 53% of control in MCF7 cells and 18% of control in HeLa cells at 2

hours, which became 95% after 8 hours. Moreover the level of ADP and AMP were dramatically decreased as well during the treatment. At 24 hours, the levels of adenine nucleotides were around 0-14% of control in MCF7 cells and 5-30% in HeLa cells, therefore the total adenine nucleotides was very low and the energy charge of MCF7 and HeLa cells was 0.50 and 0.67, respectively. The decrease of the energy charge reflects depletion of the ratio of ATP/ADP.

The same effects were also observed for the concentration of UTP and CTP (Figure 4.10 and Figure 4.12), their levels reduced to 56% and 58%, respectively at 2 hours of incubation in MCF7 cells; while GTP level remained steady (Figure 4.11). Later, the concentrations of the nucleotides were between 13 and 47% at 8 hours and undetected on the last time point of study. In contrast, UTP, GTP, and CTP levels in HeLa cells were not significantly different with untreated cells at 2 hours, then significantly decreased and reached about 5-75% at 24 hours. The result exhibits that in the presence of pentostatin, cordycepin metabolites disturbed cellular energy metabolism and has a massive impact on the nucleotide metabolism, which is unlikely to be compatible with cell survival.

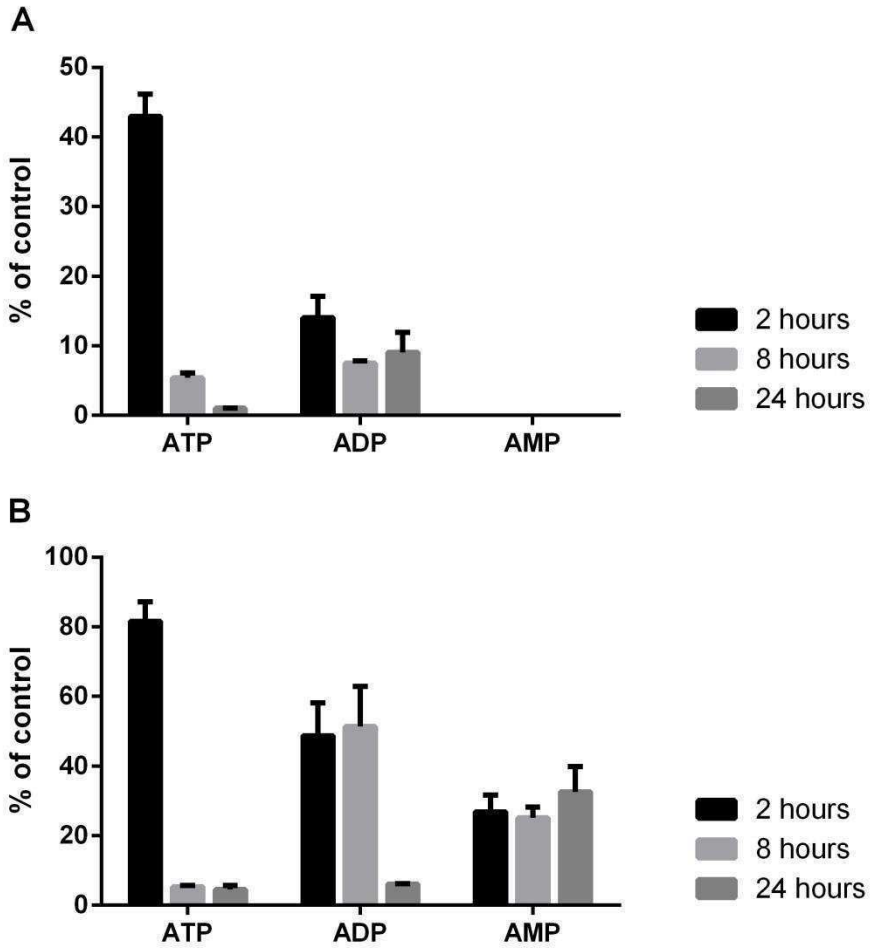

Figure 4.9. Effect of treatment with 50 µM cordycepin and 1 µM pentostatin on the intracellular level of adenine nucleotides in MCF7 cells (A) and HeLa cells (B) at the indicated times.

The level of nucleotides was determined in treated and untreated control cells at each time point. Each bar represents the mean ± SEM (n = 6-8).

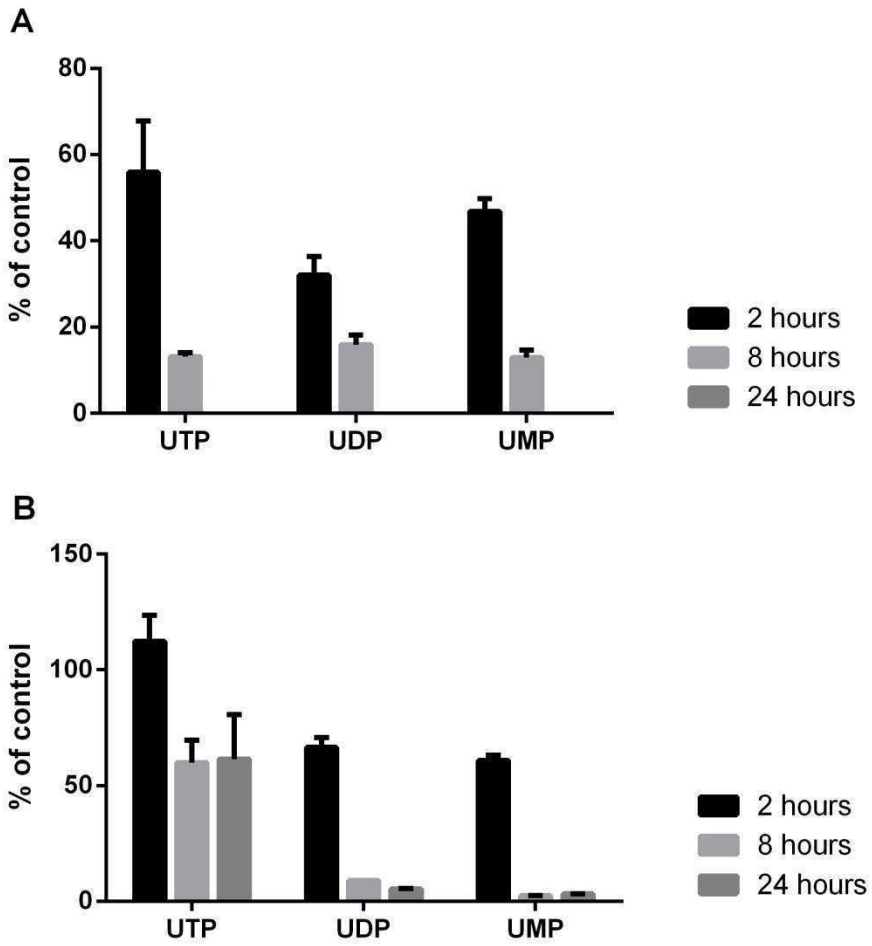

Figure 4.10. Effect of treatment with 50 µM cordycepin and 1 µM pentostatin on the intracellular level of uridine nucleotides in MCF7 cells (A) and HeLa cells (B) at the indicated times.

The level of nucleotides was determined in treated and untreated control cells at each time point. Each bar represents the mean ± SEM (n = 6-8).

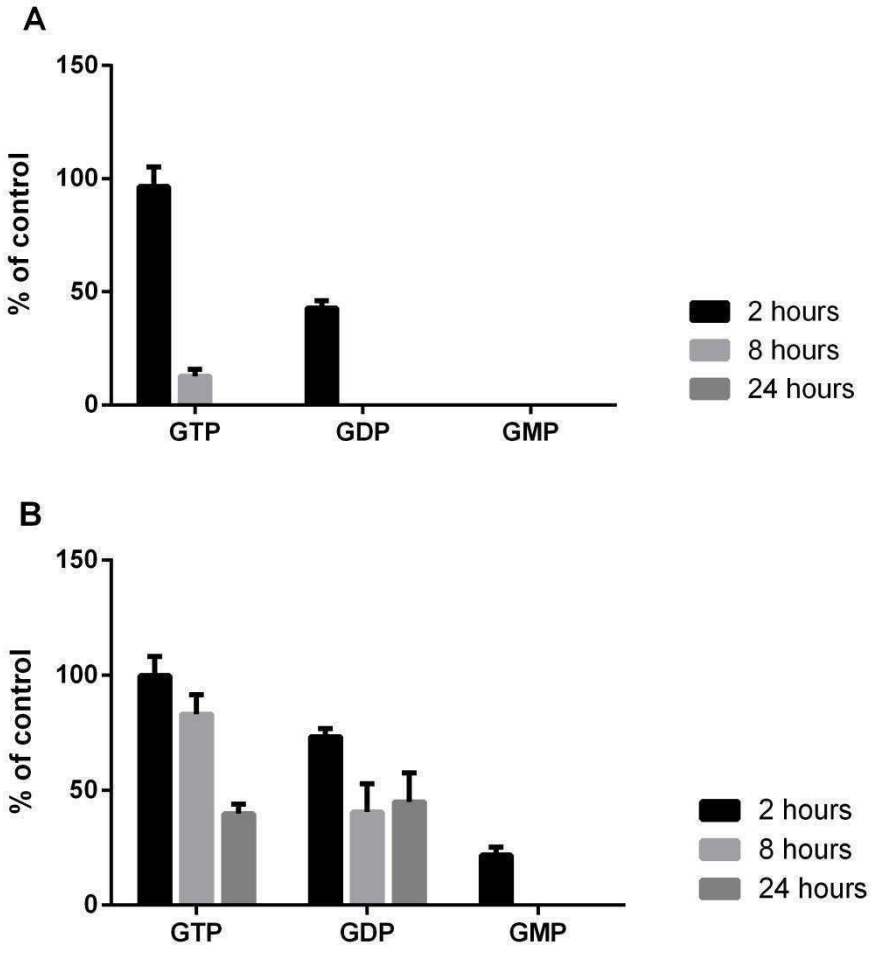

Figure 4.11. Effect of treatment with 50 µM cordycepin and 1 µM pentostatin on the intracellular level of guanidine nucleotides in MCF7 cells (A) and HeLa cells (B) at the indicated times.

The level of nucleotides was determined in treated and untreated control cells at each time point. Each bar represents the mean ± SEM (n = 6-8).

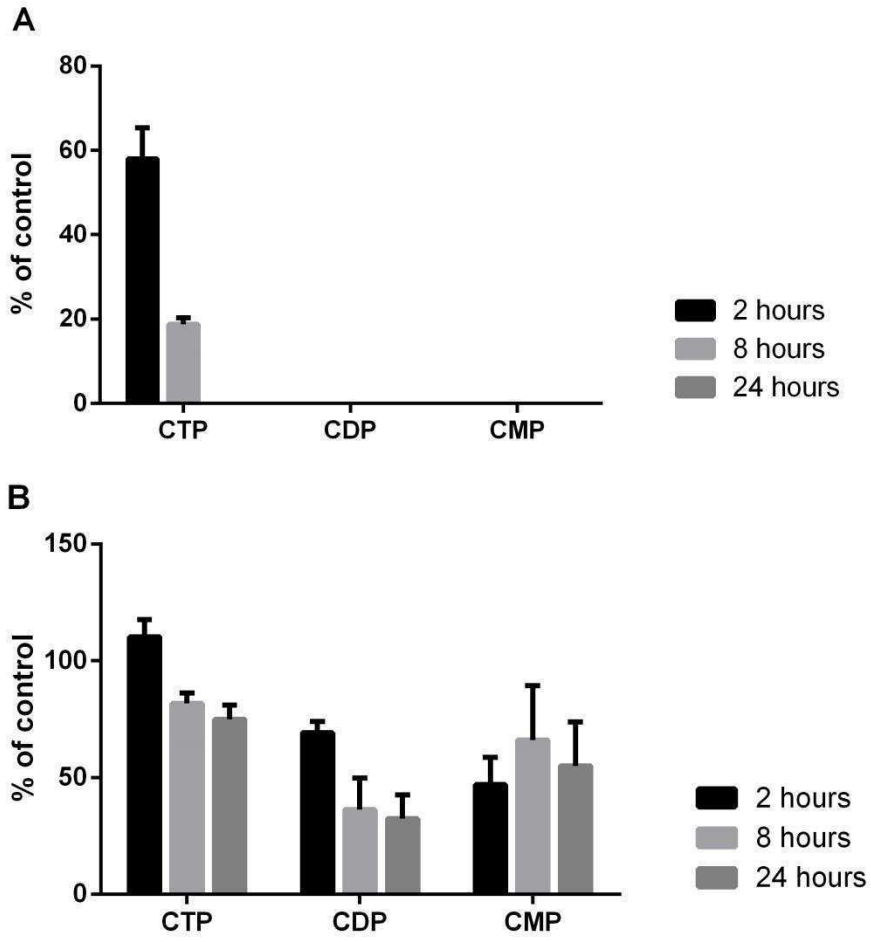

Figure 4.12. Effect of treatment with 50 µM cordycepin and 1 µM pentostatin on the intracellular level of cytidine nucleotides in MCF7 cells (A) and HeLa cells (B) at the indicated times.

The level of nucleotides was determined in treated and untreated control cells at each time point. Each bar represents the mean ± SEM (n = 6-8).

4.4.5. Discussion

In this study we have shown that in MCF7 and HeLa cells, cordycepin initially brought an increase in NTPs level, whereas GTP was the highest induced by cordycepin. Those increases are probably due to effects on RNA synthesis by the active metabolite of cordycepin. In its triphosphate form, cordycepin is incorporated into mRNA as a chain terminator for polyadenylation by PAP and affects mRNA synthesis (86, 195, 196). It has been presented on the chapter 3 that cordycepin triphosphate, the active metabolite of cordycepin, was highly accumulated at 2 hours in MCF7 and HeLa cells, but the accumulation in HeLa cells (251 μM) was approximately 50% lower than that in MCF7 cells (494 μM). This lower accumulation in HeLa cells could explain why the increasing of NTPs levels in cordycepin-treated HeLa cells was not as high as that in MCF7 cells.

The high levels of NTPs then returned to the same as or lower than in untreated cells over 8 hours of incubation. In addition, 40-80% decreases in nucleotides levels were still observed at 24 hours, even though there appears no cordycepin precursor left at 8 hours. This indicates that the drop in the nucleotides levels is not a direct effect of cordycepin triphosphate, but caused by long term changes induced by cordycepin triphosphate in the cells, such as the induction of cell death programs. Indeed, treatment with 50 μM cordycepin reduces cell proliferation and survival after 72 hours and induces cell death by a non-apoptotic program, possibly autophagy (Khurshid, Singhania, Lin and De Moor, unpublished observation).

The results of the investigation on the effect of pentostatin observed that pentostatin had no influence on the nucleotide metabolism until 8 hours of incubation. At 2 and 8 hours, mostly, there were no significant differences on the level of NTPs in both pentostatin treated cells compared with untreated cells, but there was a decrease in NTPs level in MCF7 cells at 24 hours. In contrast to earlier findings, however, the levels of NTPs on Raji cells and CCRF-CEM cells treated with pentostatin remained steady up to three hours, then inclined between four and 8 hours by unknown mechanism before declined on the long term (191).

Furthermore, the current study found that combination of cordycepin and pentostatin in tumour cells causes a severe depletion in several intracellular NTPs. At 2 hours, the combination of drugs reduced the amount of ATP, UTP, and CTP in MCF7 cells by 40-60% and the content of ATP in HeLa cells by 18%, while the level of cordycepin triphosphate in MCF7 and HeLa cells were 1281 and 1089 µM, respectively. These decreases were followed by an extreme reduction of NTPs levels in both cells in the longer incubation times. These effects are likely dependent on the accumulation of cordycepin triphosphate as it can be seen from data on the previous chapter that the highest accumulation of cordycepin triphosphate was achieved after 8 hours incubation with cordycepin and pentostatin (2203 and 1277 µM in MCF7 and HeLa cells, respectively). This finding corroborates the ideas of Hansen, who suggested that cordycepin triphosphate inhibits ribose phosphate phosphokinase which catalyses the formation of PRPP from ribose-5-P and ATP (245). This enzyme is contributed in the synthesis of endogenous purines; hence, it is

possible that the metabolite active of cordycepin might cause an inhibition of the synthesis of nucleotides.

There are, however, other possible explanations. Cellular nucleotide pool reduction has been related with drug-induced cytotoxicity (246). Moreover, intracellular ATP concentration plays a critical role in the determination of cell death fate by apoptosis or necrosis (247, 248). It has previously been demonstrated that depletion of ATP (≈ 10-65 % of control) induces apoptosis, as evidenced by internucleosomal DNA cleavage, changes in cellular morphology, and alterations in the plasma membrane; and complete ATP depletion (< 5% of control) results in necrosis (249). Moreover, investigation by Chandra et al. (192) observed that there was a decline in the level of intracellular nucleotides during apoptotic stimulation. The levels of NTPs decreased by 40-80 % and the total of ATP and ADP levels declined up to 48 % as percentage of control (192). Research by others in our laboratories has revealed that the majority of MCF7 cells enter apoptosis within four hours of treatment with the combination of cordycepin and pentostatin (Richa Singhania and Cornelia de Moor, unpublished observation). In addition, results in this study showed that after 8 hours incubation, most of the nucleotides levels were around 3-80% of control. It is likely that cordycepin triphosphate may cause a reduction in nucleotide levels indirectly by inducing apoptosis through changes in gene expression caused by its effects on polyadenylation (86). In the long term, high levels of the accumulated cordycepin triphosphate may interfere with a number of ATP-dependent cellular reactions, either directly or indirectly resulting in a decrease in energy charge and then in NTPs.

In addition, cordycepin had greater effects on nucleotide levels in MCF7 cells than HeLa cells resulting in permanent suppression of NTPs.

A previous study suggested that the ratio of the metabolite triphosphate to ATP were more highly related with cell death than percent loss of ATP alone (193). In this present study found that the ratio between cordycepin triphosphate to ATP in MCF7 and HeLa cells at 8 hours incubation on the presence of pentostatin were 24.7 and 27.5, respectively. The effect of cordycepin on the depletion of ATP can be attributed to its ability to induce cell death by independent pathways, or could be itself a cause of the cell death. It is also possible that the effects of cordycepin on nucleotides in the both cells are caused by the different metabolism of cancer cells, which rely more on glycolysis and less on oxidative phosphorylation.

Compared to other adenosine analogues, the intracellular level of ATP in MM cells declined to around 25% of control by incubation with 8-amino-adenosine of 30 μM for 4 hours while its triphosphate metabolite reached 5800 μM; and decreased to undetectable levels by 12 hours (51). Moreover, after 3 hours incubation with 30 μM 8-chloro-adenosine, the cellular concentration of ATP was decreased by 25% of the control value while its triphosphate metabolite reached about 150 μM; and at 12 h incubation with 10 μM of it in the presence of dCF, the ATP level was 40% of the control level (54). However, whereas the 8-Cl-ATP pool declined due to elimination, the ATP pool was recovered. By 18 h after drug removal, the ATP pool size reached around 75% of that of the control. After 3 days, 90% of ATP was recovered, and the

ATP pool size was similar to that in the untreated control cells. The findings of the current study are consistent with those of Gandhi et al. (54) who suggested that there is a relationship between the accumulation of nucleotide adenosine analogue and the decline in the ATP pool. In addition, their results also observed that a decrease in ATP levels was recovered when the active metabolite was eliminated from the cells (54).

4.5. Conclusions

Cordycepin has an effect on the inhibition of nucleotide metabolism and the intracellular nucleotide depletion could account for the anti-proliferative effect of cordycepin. The results show that cordycepin induce the following progressive effects. In the beginning, low concentrations of the cordycepin triphosphate resulting in an increase in the levels of NTPs probably due to its effects on RNA synthesis. However, it caused a severe drop in the long term probably due to long term change induced by cordycepin triphosphate in the cell.

Pentostatin on its own reduced nucleoside triphosphates levels in the long term and the effect of cordycepin on nucleotide levels was increased by pentostatin. At high levels, cordycepin triphosphate caused a reduction in nucleotide levels likely by inhibition of the synthesis of nucleotides caused by its inhibition on ribose phosphate phosphokinase or by inducing apoptosis through changes in gene expression caused by its effects on polyadenylation. Further depletion on the long term could be contributed from long term alteration induced by the metabolite through interfering

ATP-dependent cellular reactions. In addition, cordycepin had greater effects on nucleotide levels in MCF7 cells than HeLa cells resulting in permanent suppression of NTPs.

It is possible that the effect of cordycepin on nucleotides in MCF7 and HeLa cells is caused by the different metabolism of cancer cells, which rely less on oxidative phosphorylation and more on glycolysis. If the treatment is not cancer cell specific then the combination of cordycepin and pentostatin could be very toxic, so further studies should be conducted using normal cells to compare the effect of cordycepin and pentostatin treatment on the metabolism of intracellular nucleotides in non-malignant cells.

CHAPTER 5
INTRACELLULAR METABOLISM OF THIOURIDINE

INTRACELLULAR METABOLISM OF THIOURIDINE

5.1. Introduction

Gene regulation in eukaryotic cells is the outcome of a series of complex mechanisms that are started by transcription in the nucleus and completed by translation in the cytoplasm. Several points of control, such as transcription, pre-mRNA processing, mRNA transport, translation efficiency, and mRNA degradation, undertake the regulation of gene expression. The cellular mRNA levels represent a balance between the rates of nuclear RNA synthesis, processing and transport, and the rates of cellular mRNA degradation. The rate of mRNA decay is important, not only to determine its abundance, but also in quality control of RNA (250, 251). Previous studies have reported that altering the abundance of transcripts is a critical step in the control of many biological pathways (252). It has been estimated that the mRNA abundance of 5–10% of human genes is controlled through the regulation of RNA stability (253). Furthermore, changes in RNA stability play a critical role in determining the kinetics of gene induction in mammalian cells (254), particularly the induction kinetics of genes encoding inflammatory proteins (255). Therefore, the regulation of mRNA stability is considered a major control point in the regulation of gene expression.

Recently, 4-thiouridine labelling has been developed as a method for determining RNA stabilities in mammalian cells and has been applied to the study of mRNA synthesis and polyadenylation. Using this method, the rates of mRNA synthesis and decay can be measured with minimal interference of the cellular system (124, 125, 256).

In this method, endogenous RNAs are pulse labelled using uridine analogue such as 4-thiouridine (Figure 5.1). The nucleoside analogue 4-thiouridine is taken up by cells, phosphorylated, and incorporated into mRNA through transcription. The modified base is incorporated into the growing RNA chain in place of uridine and serves as an attachment point for a biotin tag for easy separation of newly transcribed RNA from the total RNA population. The thiol-labelled newly transcribed RNA can then be isolated by affinity chromatography (125, 126) or using biotinylation and purification using streptavidin-coated magnetic beads (124, 256) since eukaryotic mRNAs generally do not contain thiol-groups.

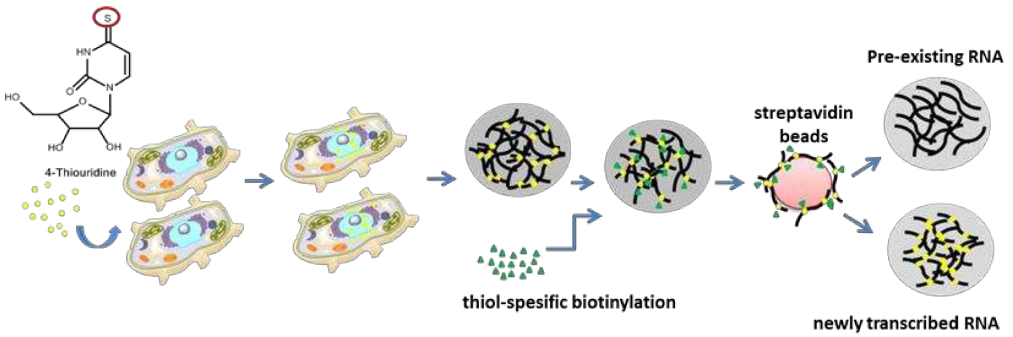

Figure 5.1. Schematic principle of 4-thiouridine labelling

Cells are incubated with 4-thiouridine for the required time followed by preparation of total cellular RNA. Following thiol-specific biotinylation, total cellular RNA is separated into newly transcribed RNA (4-thiouridine-labelled) and pre-existing RNA (unlabelled) using streptavidin-coated magnetic beads. Using a reducing agent newly transcribed RNA is detached from the beads by cleaving the disulphide bonds between biotin residue and the thiol group (128).

Intracellular 4-thiouridine is phosphorylated to 4-thio-UMP by uridine cytidine kinase (UCK), the enzyme which is also responsible for catalysing the phosphorylation of uridine and cytidine to UMP and CMP (257, 258). UCK catalyses the transfer reaction of phosphoryl group from ATP to pyrimidine ribonucleoside

through the mechanism similar to those of other kinases in the NMP kinase family (259). The enzymatic reaction with UCK is the rate-limiting step in the phosphorylation of 4-thiouridine into 4-thio-UTP. A thio substitution at the 4-position on uridine is well tolerated; therefore it can be phosphorylated by both UCK1 and UCK2. Subsequently, 4-thio-UMP is further phosphorylated by UMP-CMP kinase (260) and nucleoside diphosphate kinases with ATP as the phosphate donor in this reaction (261). In addition, other studies also confirmed that GTP could be used as efficient phosphate donors, whereas no activity was detected with either CTP or UTP (258, 262).

The 4-thiouridine labelling has been applied to a broad range of cell types of human and murine origin including fibroblasts, endothelial cells, epithelial cells, macrophages and T-cells and the incorporation into RNA was found to be highly efficient (124). This method is also applicable for use in animals (125). This labelling method allows the determination of the contribution of synthesis and decay to mRNA levels. Nevertheless, large fluctuations in the 4-thio-UTP/UTP ratio or a slow build-up of 4-thio-UTP could affect the quality of the data obtained, hence it might require corrections.

Furthermore, Burger et al. (127) identified that using a high concentration of 4-thiouridine on RNA metabolic labelling triggers a nucleolar stress response, which might affect the gene expression and make it impossible to determine mRNA stability because transcription rates may no longer be constant over the labelling period. Radle et al. (128) also suggest that the concentration of 4-thiouridine and

the period of labelling should be minimized as high concentrations of 4-thiouridine could be toxic to cells.

HPLC with UV detection has been used for separation and qualitative analysis of 4-thiouridine from the digestion product of tRNA of *E. coli* mutant (115, 118). To our knowledge, however, no method has been developed to measure simultaneously thiouridine, the metabolite thio-UTP, and other nucleotides in cells. The aim of this research is, therefore, to apply the LC-MS/MS method for studying the intracellular metabolism of 4-thiouridine and the effect on the intracellular levels of nucleotides.

5.2. Aim and Objectives

The aim of this chapter is to investigate intracellular metabolism of 4-thiouridine and the effect of its metabolite on the metabolic balance of adenine and uridine nucleotides.

The objectives of this chapter are to apply the LC-MS/MS method for:

- Determination of 4-thiouridine and 4-thio-UTP in serum-starved and serum-stimulated NIH 3T3 cells treated with 4-thiouridine.
- Quantification of intracellular levels of adenine and uridine nucleotides in serum-starved and serum-stimulated NIH 3T3 cells treated with 4-thiouridine.

5.3. Materials and Methods

5.3.1. Chemicals

4-thiouridine was purchased from Sigma Aldrich (Poole, UK). 4-thio-UTP was purchased from Jena Bioscience (Jena, Germany). Other chemicals are the same as described in Chapter 2 (Section 2.3.1).

5.3.2. Cell culture

NIH 3T3 cells were cultured using the same procedures as described in Chapter 2 (Section 2.3.2).

5.3.3. 4-Thiouridine Labelling

Cells were seeded in a six-well plate and incubated for 24 hours and then were serum starved, medium were replaced with medium containing 0.5% calf serum, for another 24 hours. Cells then were incubated with vehicle (DMSO), 250 µM or 500 µM 4-thiouridine for the required times. For the experiment in serum-stimulated cells, after cells were incubated on serum-starved cells for 24 hours, medium were replaced with medium containing 10% calf serum and 250 µM 4-thiouridine then cells were incubated for the indicated times. After the time points, medium was removed and cells were collected from the incubations and analysed for 4-thiouridine, its metabolites, and the nucleotides by LC-MS/MS method. Then, the intracellular concentrations of the metabolites and nucleotides were estimated based on the measured total cell volume.

5.3.4. Samples Extraction

Extraction of samples was done as described in Chapter 2 (Section 2.3.8.1).

5.3.5. Calculation of total cell volume

Calculation the total cell volume was conducted as described in Chapter 2 (Section 2.3.8.2).

5.3.6. LC-MS/MS conditions

Method validation and analyses of samples (Figure 5.2) were carried out using the methods which are described in Chapter 2 (Section 2.3.7 and Section 2.3.8.3). Multiple reactions monitoring (MRM) scan was used with dwell time of 0.1 s as described in Table 2.4 and Table 5.1.

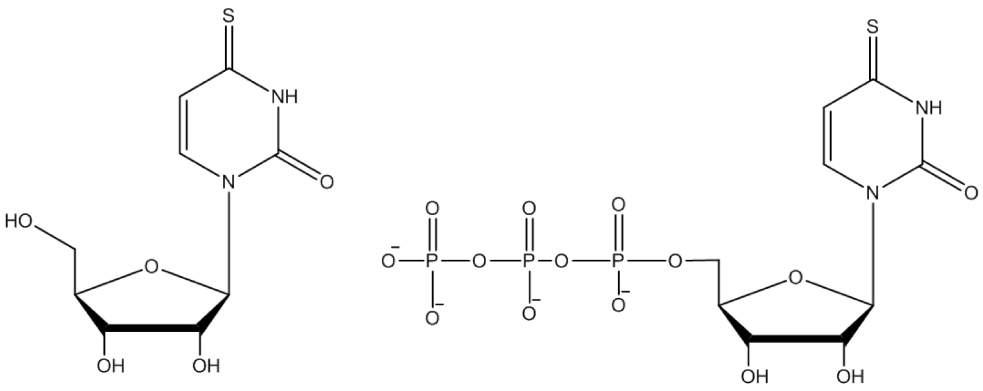

Figure 5.2. Structures of compounds detected

Table 5.1. Parameters of MRM scan derived for metabolites of thiouridine

Compound	$[M-H]^-$ (*m/z*)	Selected Product Ion (*m/z*)	Cone Voltage (V)	Collision Energy (eV)
4-thiouridine	258.92	126.20	43	20
4-thio-UTP	498.90	401.10	43	20

5.4. Results and Discussion

5.4.1. Calculation of cell volume

A study to determine the intracellular metabolism of 4-thiouridine was conducted in NIH 3T3 cells. The intracellular concentration of metabolites contained in the extract was calculated from a given number of cells of a determined mean volume. The calculation assumed that the metabolites were uniformly distributed in a total cell volume.

Figure 5.3 presents the average diameter of NIH 3T3 cells which was measured using a laser light scattering technique. The estimated volume of the cells was calculated based on the assumption that the cells were spherical in shape. The average diameter of cells determined using coulter counter was (22.45 ± 1.24) µm. This gave a mean volume of 4.7 pL/cell. Subsequently, using a total volume of cells per well the quantity could be converted into cellular levels.

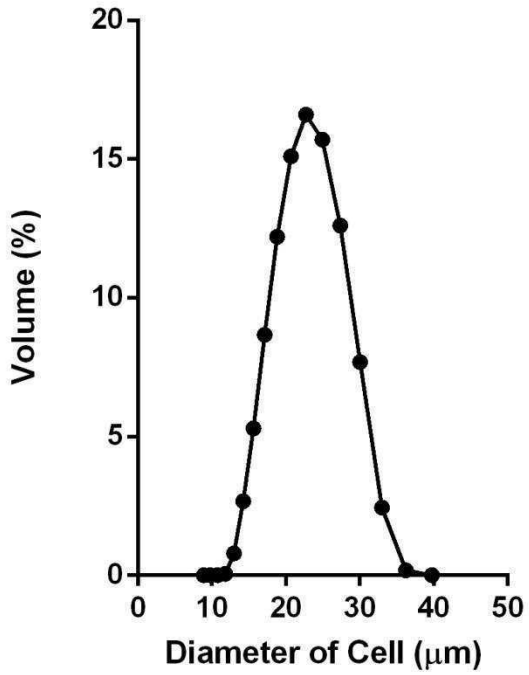

Figure 5.3. The average diameter of NIH 3T3 cells was found (22.45 ± 1.24) μm. This gave a mean volume of 4.7 pL/cell.

5.4.2. Method Validation

The method needs to be validated to prove that it could produce quantitative data which are both reliable and reproducible. A serial dilution of nine concentrations of each compound, between 0.25 and 100 μM was prepared in order to construct the calibration curves. Each concentration was analysed in duplicate and the concentration of internal standard was 5 μM. The limits of detection of 4-thiouridine and 4-thio-UTP were 2.5 and 0.5 pmol on column, respectively, which were determined from signal to noise ratios of 3.3. The lower limits of the range of the calibration curves can be considered as the limits of quantification of the method. The interday precision and accuracy were determined using samples that were

analysed between different days. The result of validation data for the method is presented in Table 5.2.

Table 5.2. Result of validation data of the method for quantification of thiouridine metabolites.

Compound	Linearity (R^2)	LOD (pmol on column)	Interday Precision (RSD %)	Interday Accuracy (%)
4-thiouridine	0.998	2.5	14.4	103.3
4-thio-UTP	0.999	0.5	11.0	101.3

The developed method was used to determine the concentration of thiouridine metabolites in the cell extracts. Representative LC/MS-MS chromatograms of NIH 3T3 cell extract before and after 2 min labelling of 500 µM 4-thiouridine is shown in Figure 5.4. The results showed that there were differences between the chromatogram before and after 2 min labelling with 4-thiouridine. It is apparent from the figure that the selected method was able to detect the metabolite of 4-thiouridine even after only 2 min labelling. Also, it is possible to measure simultaneously the metabolites of 4-thiouridine and other intracellular nucleotides using this method.

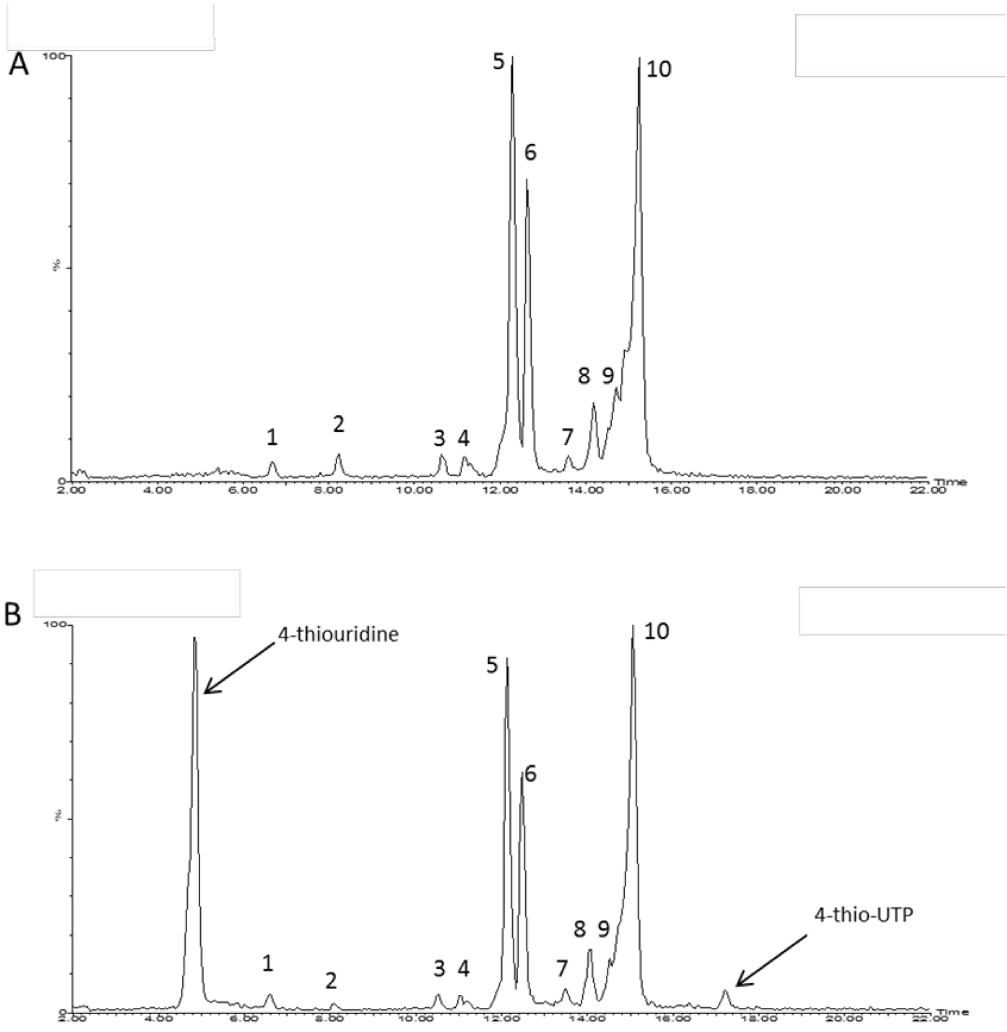

Figure 5.4. LC-MS chromatogram of NIH 3T3 cell extract before (A) and after 2 min labelling of 500 µM 4-thiouridine (B)

1.UMP, 2.AMP, 3.UDP, 4.GDP, 5.ADP, 6.internal standard, 7.CTP, 8.UTP, 9.GTP, 10.ATP

Chromatographic conditions: mobile phase A, 5mM_DMHA in water: methanol (95:5 v/v) pH 7; B, 5mM DMHA in methanol: water (80:20 v/v); Gradient elution: 0–10min, 0–20% B; 10–23min, 20- 35% B; 23-25min, 35-0% B; 25–35min, 0% B; Column temperature: 40°C; MRM scan as described on Table 2.3 and Table 5.1

5.4.3. Accumulation of 4-thiouridine and 4-thio-UTP in cells

There are two phases for the uptake of nucleosides by mammalian cells, first the nucleosides are quickly transported through the plasma membrane by a mechanism of facilitated diffusion (263) and secondly, the intracellular nucleosides are phosphorylated by specific nucleoside kinases and the nucleotides formed are

accumulated intracellularly (264). Figure 5.5 illustrates the accumulation of intracellular 4-thiouridine and 4-thio-UTP in NIH 3T3 cells during 60 min labelling of 500 µM 4-thiouridine. It is apparent from this chart that intracellular levels of 4-thiouridines were relatively constant after 5 min labelling. The results of this experiment indicate that exposure of cells to 4-thiouridine is followed by rapid uptake.

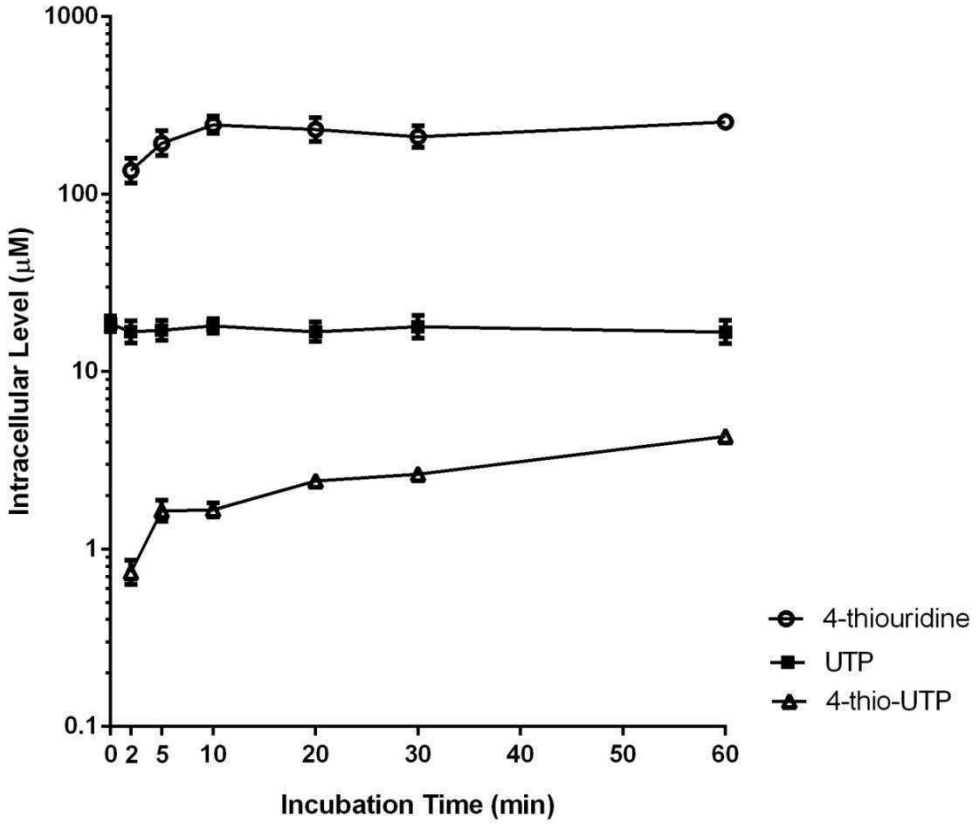

Figure 5.5. Accumulation of 4-thiouridine and 4-thio-UTP and the intracellular level of UTP in NIH 3T3 cells were incubated with 500 µM 4-thiouridine for the indicated times. Each bar represents the mean ± SEM (n =6- 12).

Furthermore, the phosphorylated metabolite, intracellular 4-thio-UTP was also readily detected in cell extracts by LC-MS/MS after 2 min of labelling. Table 5.3 summarises the levels of 4-thiouridine and its metabolite. What is interesting in this data is that the phosphorylated metabolite was rapidly formed even at 2 min labelling. Thus, it is evident that a new nucleotide is synthesized in as early as 2 min. Also, this finding further support the idea by Dolken et al. (124) that there is sufficient labelled RNA to couple to biotin for subsequent separation on beads after only 10 min labelling.

Table 5.3. The concentrations of 4-thiouridine and its metabolite in NIH 3T3 cells during several times labelling of 500 µM 4-thiouridine

Labelling time (min)	Concentration			4-thio-UTP/UTP	4-thio-UTP/ 4-thiouridine
	4-thiouridine (µM)	4-thio-UTP (µM)	UTP (µM)		
0	-	-	17 ± 7	-	-
2	136 ± 72	0.7 ± 0.3	18 ± 10	0.05 ± 0.01	0.005
5	194 ± 83	1.6 ± 0.7	17 ± 7	0.11 ± 0.02	0.008
10	246 ± 76	1.7 ± 0.5	18 ± 6	0.12 ± 0.05	0.008
20	232 ± 110	2.4 ± 0.5	17 ± 7	0.23 ± 0.07	0.010
30	211 ± 76	2.6 ± 0.7	17 ± 8	0.21 ± 0.07	0.012
60	255 ± 17	4.3 ± 0.78	19 ± 8	0.33 ± 0.06	0.017

*Data represent the mean ± SD from 3 separate experiments (n=6-12).

From Figure 5.5 we can also see that the concentration of 4-thio-UTP was stable between 5 and 10 min then increases after 10 min, although the concentration of 4-

thiouridine in cells was relatively constant after 5 min labelling. The increase in the level of 4-thio-UTP after 10 min might be as a result of recycling of 4-thio-UTP in RNA which cannot be detected using this method. Moreover, there was a significant positive correlation between the intracellular 4-thio-UTP level and the time of labelling (r=0.95; p=0.001). Hence, labelling efficiency can be adjusted according to the preferred duration of labelling.

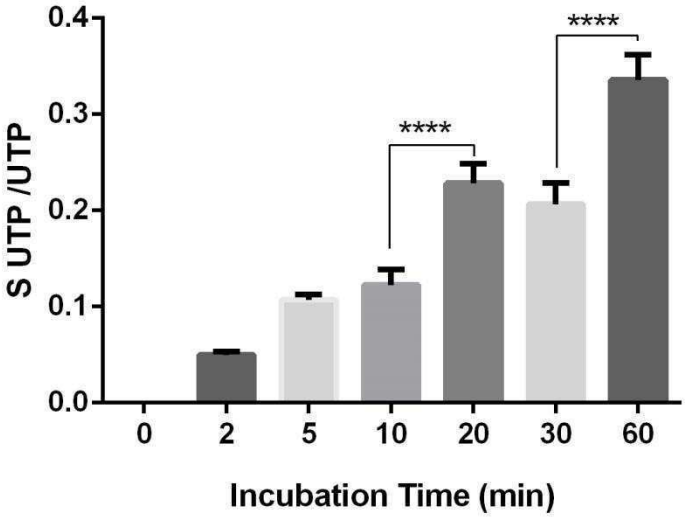

Figure 5.6. Ratio of 4-thio-UTP/UTP in NIH 3T3 cells that were incubated with 500 µM 4-thiouridine for the indicated times.

Each bar represents the mean ± SEM from 3 separate experiments. ****= p < 0.0001; ***=p < 0.001; **= p < 0.01; *= p <0.05

It is of interest to determine whether the 4-thiouridine conversion into 4-thio-UTP influences the intracellular level of UTP. The results show that there was no significant difference in the level of UTP between the periods of times of labelling (Figure 5.5). It is almost certain that the production of 4-thio-UTP did not cause effect on the synthesis of intracellular UTP. In addition, it can be seen from Figure

5.6 that no large fluctuations on the 4-thio-UTP/UTP ratio and the ratio was only around 20% even at 30 min labelling. It is very clear that the 4-thiouridine conversion into 4-thio-UTP is not very efficient. These results indicate that the side effects of 4-thiouridine treatment may be due to 4-thiouridine instead of 4-thio-UTP.

The next part of this study is to compare between two different conditions of labelling, i.e. 500 μM and 250 μM 4-thiouridine. Comparing the two results as shown in Figure 5.7, interestingly, there was only a slight difference in the levels of the 4-thio-UTP under labelling at different 4-thiouridine concentrations (Figure 5.7B), even though the concentration of 4-thiouridine was taken up to the cells on the condition 500 μM 4-thiouridine labelling was higher than in 250 μM (Figure 5.7A). These results further support the hypothesis that 4-thiouridine conversion into 4-thio-UTP is not very efficient. Although the substrate was available at higher level; still, the phosphorylation product was not significantly increased. This finding indicates that the availability of the enzyme is limited in the cell. Moreover, these data suggest that labelling with 250 μM of 4-thiouridine provides sufficient 4-thio-UTP for 4-thiouridine labelling. In addition, using a lower concentration of 4-thiouridine has an advantage since a high concentration of 4-thiouridine on RNA metabolic labelling RNA initiates a nucleolar stress response (127). Therefore, in the following experiments, the concentration of 4-thiouridine of 250 μM has been used.

.

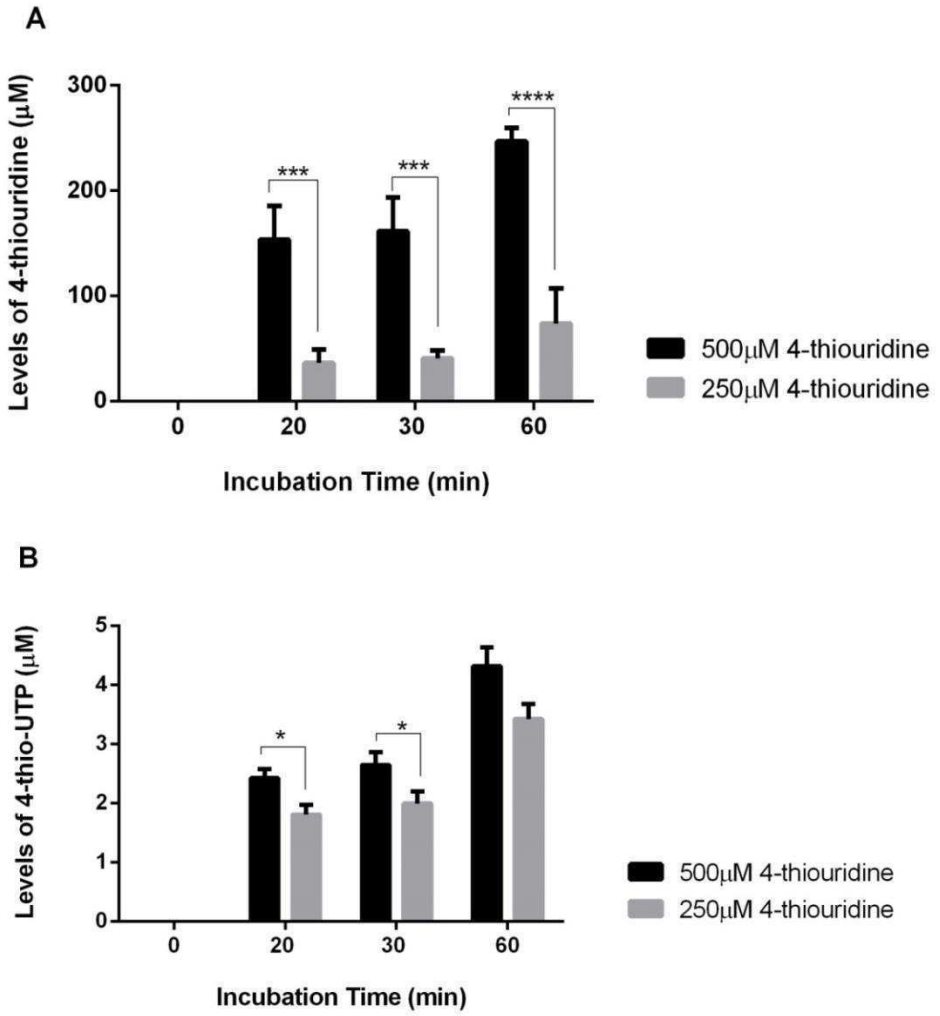

Figure 5.7. Accumulation of 4-thiouridine (A) and 4-thio-UTP (B) in NIH 3T3 cells were incubated with either 500 μM or 250 μM 4-thiouridine for the indicated times.

Each bar represents the mean ± SEM from 3 separate experiments. ****= p < 0.0001; ***=p < 0.001; **= p < 0.01; *= p <0.05

Furthermore, as expected, there were no significant differences between the two conditions of labelling in the level of intracellular UTP (Figure 5.8A) and ratio of 4-thio-UTP/UTP in cells (Figure 5.8B). It is apparent from the figure that none of these differences were statistically significant.

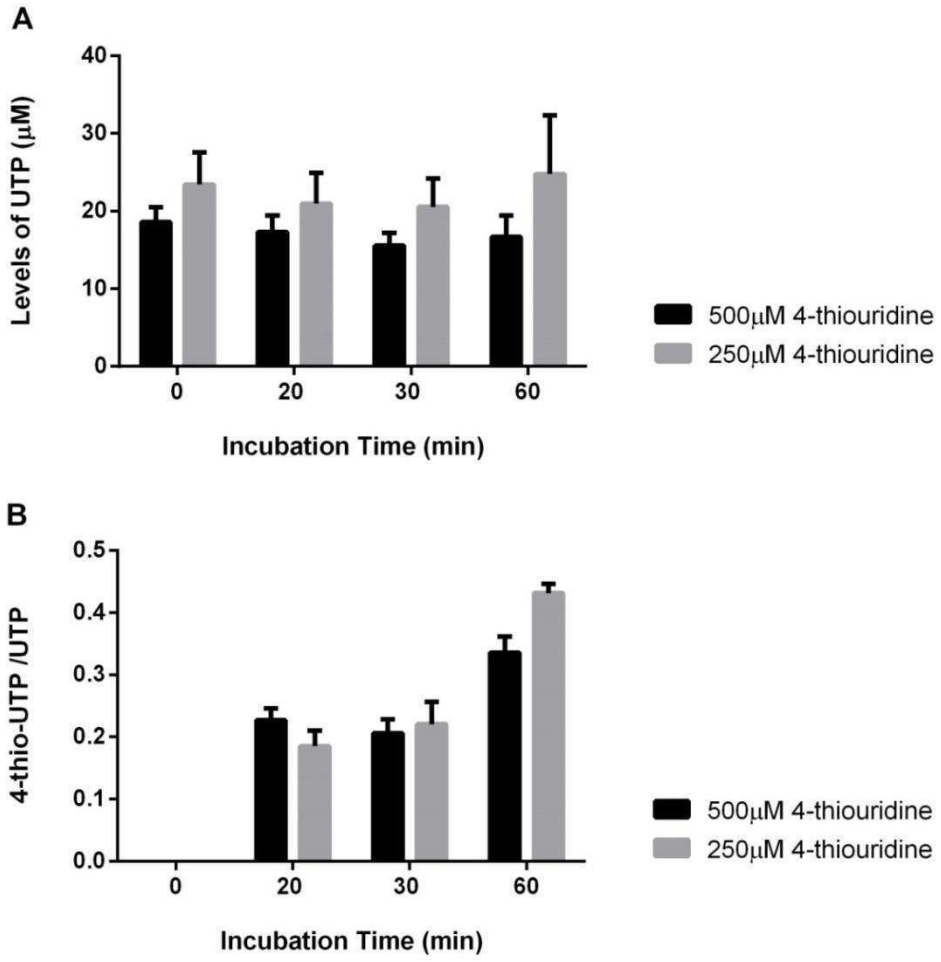

Figure 5.8. Levels of UTP (A) and 4-thio-UTP/UTP ratio (B) in NIH 3T3 cells were incubated with either 500 μM or 250 μM 4-thiouridine for the indicated times (B).

Each bar represents the mean ± SEM from 3 separate experiments. ****= p < 0.0001; ***=p < 0.001; **= p < 0.01; *= p <0.05

5.4.4. Intracellular levels of adenine nucleotide

The accurate determination of adenine nucleotide concentrations provides information on the metabolic state of the cells. From the graph in Figure 5.9A we can see that overall intracellular ATP concentrations in the cells were low. This result may be explained by the fact that these are serum-starved cells, therefore they are not growing. Moreover, mTORC1 activity is low and metabolic flux through de novo

pyrimidine synthesis pathway is blocked, so synthesis of new pyrimidine nucleotides is inhibited. The findings of the current study are consistent with those of Ben-Sahra et al. (265) who recently showed that cellular growth signals stimulate anabolic processes through mTROC1. Activation of mTORC1 regulates the metabolic pathway which directly phosphorylates the enzyme that catalyses the de novo pyrimidine synthesis thus stimulates the production of new nucleotides.

Furthermore, as expected, an alteration in the level of ATP was not observed during labelling as well as the ATP/ADP ratio (Figure 5.9B). ATP/ADP ratio fluctuations have been recognised to distinguish modes of cell death and viability. Reduced levels of ATP and increased levels of ADP signify apoptotic or necrotic cells where the decrease in ATP and increase in ADP are much more pronounced in necrosis versus apoptosis. In contrast, increased levels of ATP and decreased levels of ADP indicate proliferating cells. Overall, these results indicate that the 4-thiouridine labelling does not have an effect on the metabolic state of the cells over the 1 hour labelling period.

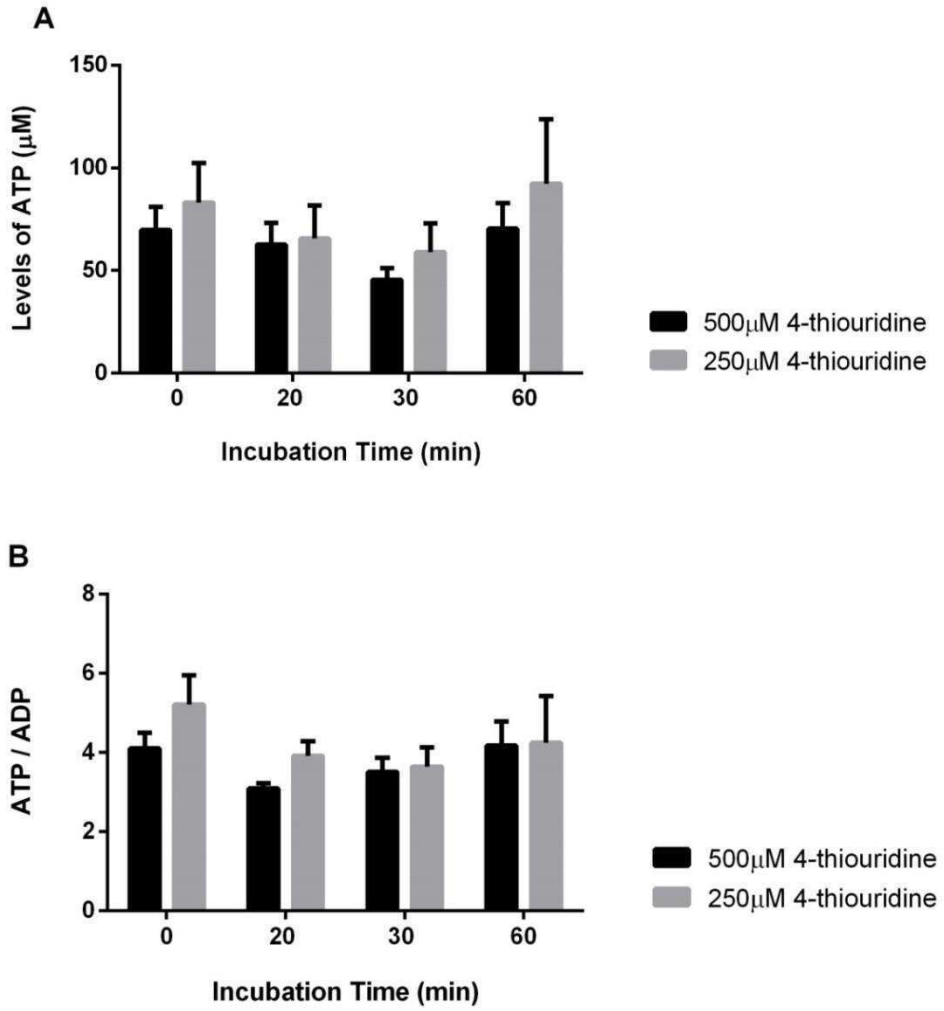

Figure 5.9. Levels of ATP (A) and Ratio of ATP/ADP in NIH 3T3 cells were incubated with either 500 μM or 250 μM 4-thiouridine for the indicated times (B).

Each bar represents the mean ± SEM from 3 separate experiments. ****= p < 0.0001; ***=p < 0.001; **= p < 0.01; *= p <0.05

5.4.5. Accumulation of 4-thiouridine metabolites in serum-stimulated cells

A study by Rozengurt et al. (266) found that intracellular phosphorylation is the rate limiting stage in the uptake of nucleoside. Moreover, the addition of serum enhances the rate of phosphorylation but does not have any effect on the transport of nucleoside. To determine the effects of serum, particularly growth factor, on the metabolism of 4-thiouridine, we investigated the metabolism of 4-thiouridine in serum-stimulated cells compared to that in serum-starved cells.

Figure 5.10A shows that there was no difference in the amount of 4-thiouridine taken up over the 1 hr labelling in the serum-starved and stimulated cells. From the data in this figure, it is apparent that the addition of the serum does not stimulate the rate of transport of 4-thiouridine. However, as can be seen in Figure 5.10B the accumulation of the phosphorylated metabolite in serum-stimulated cells was greater than in serum-starved cells. There was a significant difference between the two conditions at each time of labelling. At only 20 min serum stimulation a significant increase in the level of 4-thio-UTP was observed compared with serum-starved cells. It seems possible that UCK, the enzyme for phosphorylation of 4-thiouridine, is up regulated by exposure to growth factors, thus the phosphorylation of 4-thiouridine in serum-stimulated cells is much higher than in serum-starved cells. This suggests that serum rapidly stimulates the rate of 4-thiouridine phosphorylation but not that of transport.

.

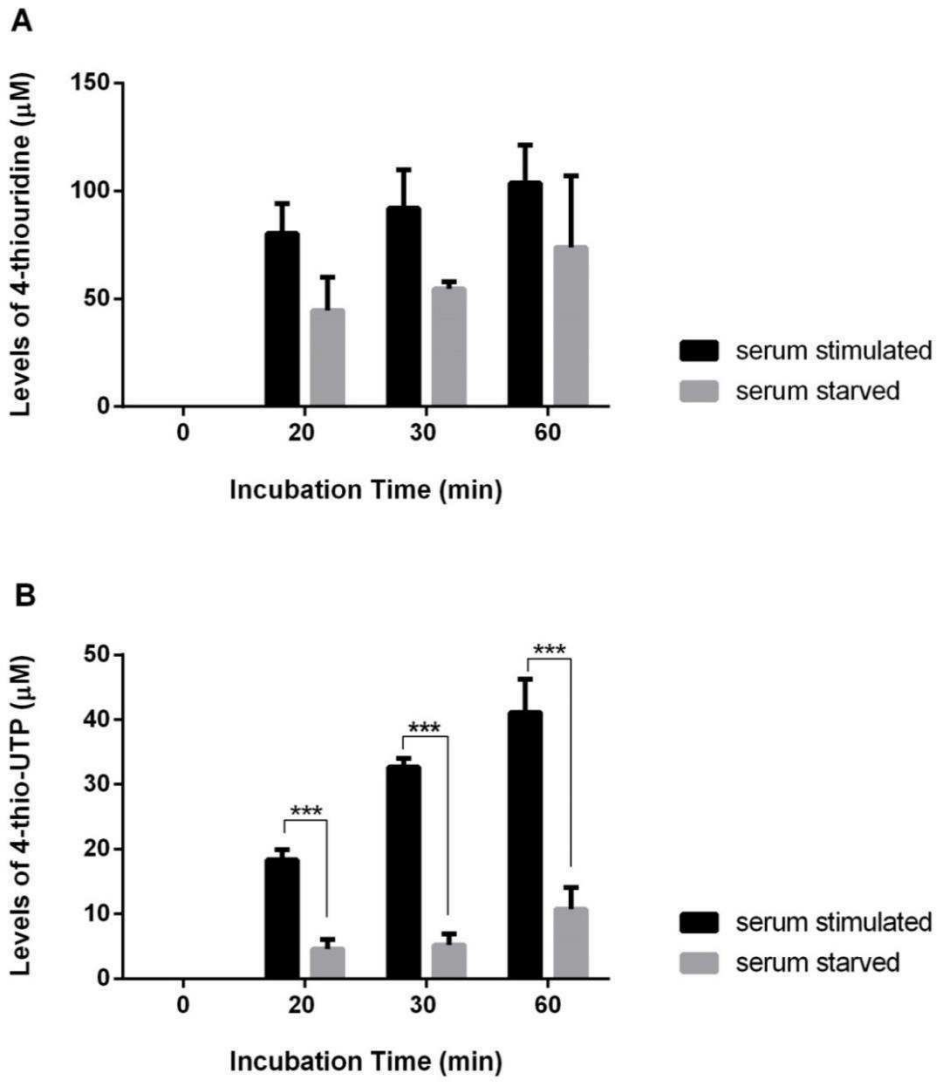

Figure 5.10. Accumulation of 4-thiouridine (A) and 4-thio-UTP (B) in NIH 3T3 cells were incubated with 250 µM 4-thiouridine for the indicated times.

Each bar represents the mean ± SEM from 3 separate experiments. ****= p < 0.0001; ***=p < 0.001; **= p < 0.01; *= p <0.05

5.4.6. Intracellular levels of UTP and ATP in serum-stimulated cells

The intracellular level of UTP and ATP before and after 4-thiouridine labelling either in serum-starved cells or in serum-stimulated cells was also compared in this study.

The level of UTP did not change during labelling of 4-thiouridine over 60 min both for serum starved cell or serum-stimulated cells (Figure 5.11A). Moreover, consistent with the previous result that the ratio of 4-thioUTP/UTP was stable after 30 min and slightly increased at 60 min in serum-starved cells; however, this increase was much higher in serum-stimulated cells (Figure 5.11B). The high increase of the ratio in serum-stimulated cells is caused by the increase of phosphorylated metabolites in the cell which is stimulated by the growth factors.

Contrary to expectations, this study did not find a significant difference between the intracellular level of ATP in serum-starved cells and in serum-stimulated cells even after 1 hour serum stimulation. Also, no significant difference in the level of UTP was detected between serum-starved cells and serum-stimulated cells. The present findings seem to be inconsistent with other research which found that growth factors induce activation of mTOR which directly phosphorylates the enzyme that catalyses the de novo pyrimidine synthesis thus a production of new nucleotides is stimulated (265, 267). It is difficult to explain this result, but it might be related to the low level of intracellular ATP at the start point of serum stimulation since the cells was starved over 24 hours before receiving a serum stimulation. Research by Dennis et al. (268) revealed that dropping the ATP level could lead to a steady alteration in mTOR activity. They demonstrated that high ATP level is required for mTOR activity.

Furthermore, no significant differences in the intracellular concentrations of ATP and the ratio of ATP to ADP were found during several times of 4-thiouridine labelling

either in serum-starved cells or in serum-stimulated cells (Figure 5.12). Overall, these results indicate that 4-thiouridine labelling has no adverse effect on the metabolic balance of adenine nucleotides in the cell not only in the serum-starved cells but also in the serum-stimulated cells.

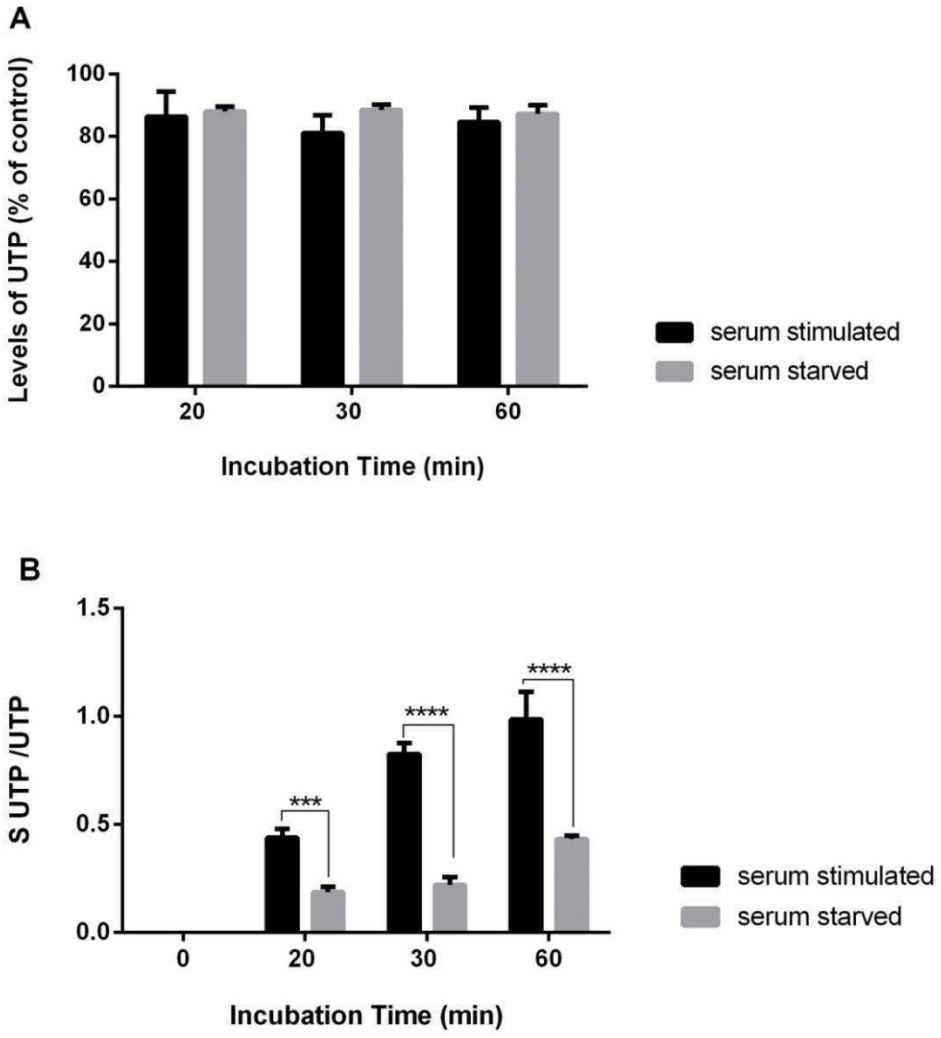

Figure 5.11. Intracellular concentrations of UTP (A) and Ratio of 4-thio-UTP/UTP in NIH 3T3 cells were incubated with 250 µM 4-thiouridine for the indicated times (B).

Each bar represents the mean ± SEM from 3 separate experiments. ****= p < 0.0001; ***=p < 0.001; **= p < 0.01; *= p <0.05

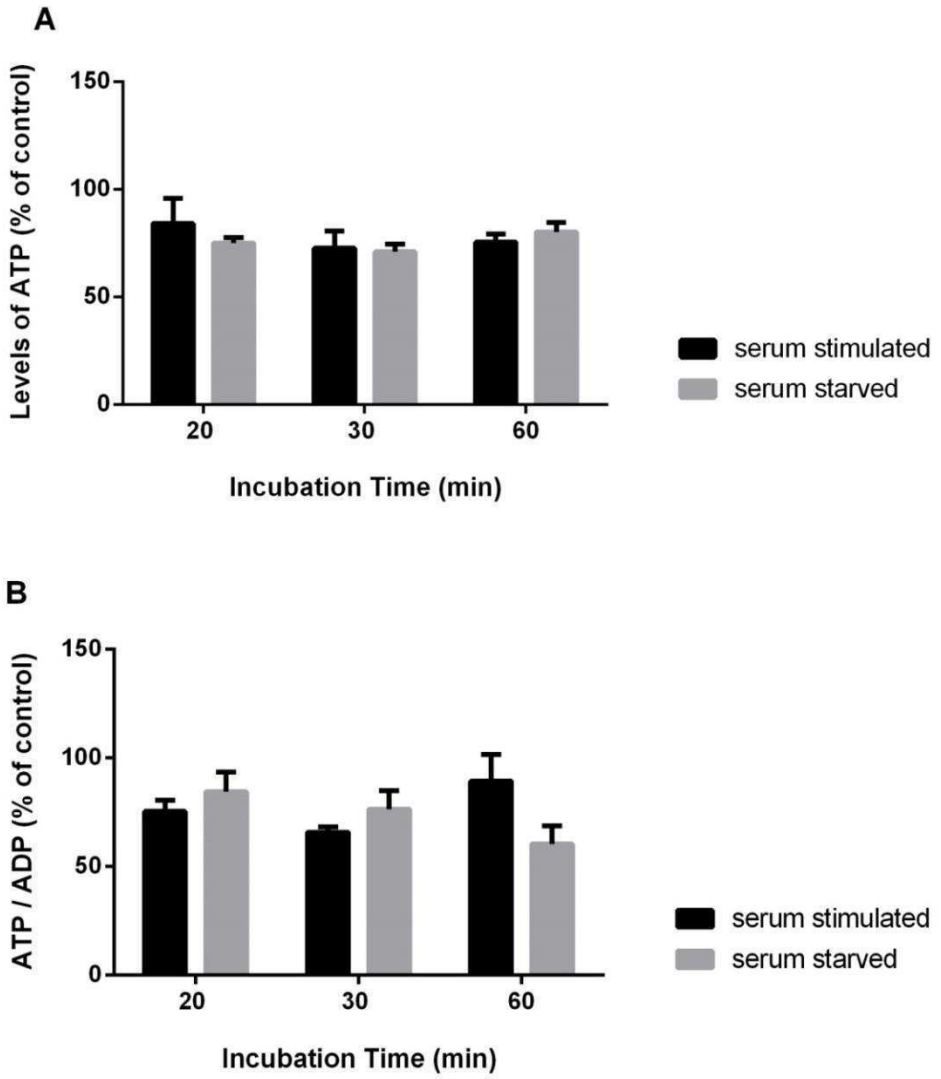

Figure 5.12. Intracellular concentrations of ATP (A) and ratio of ATP/ADP in NIH 3T3 cells were incubated with 250 µM 4-thiouridine for the indicated times (B).

Each bar represents the mean ± SEM from 3 separate experiments.

5.4.7. Discussion

The objective of this study was to investigate the intracellular development of 4-thiouridine metabolite and its effect on the intracellular levels of nucleotides in serum-starved and serum-stimulated cells using the developed LC-MS/MS method. The most interesting finding was that conversion of 4-thiouridine into 4-thio-UTP in

the NIH 3T3 cells is not very efficient. There are several possible explanations for the low efficiency of the phosphorylation of 4-thiouridine. It was observed that the levels of ATP in the cells were low and were less than 0.1 mM. Because a high level of ATP, generally in mM order, is required for optimal activity of UCK, the enzyme responsible for the phosphorylation of 4-thiouridine (258, 269); it is possible, therefore, that the low level of intracellular ATP has contributed to the low activity of the UCK. Hence, the conversion of 4-thiouridine into 4-thio-UTP was very low.

Moreover, data from UCK purified from several sources have indicated that UCK protein has a very low abundance in most normal mammalian tissues. Payne et al. (262) needed a 60,000-fold purification to isolate uridine kinase from tumour cells which have the highest enzyme activity, while the activity of this enzyme in neoplastic tissue at least 10-fold greater than in non-neoplastic tissues (270). Therefore the level of this protein in normal tissue could be only about 10^{-6} of the total intracellular protein (271). Moreover, the phosphorylation efficiency of 4-thiouridine related to the efficiency of uridine phosphorylation catalysed by UCK1 and UCK2 are 13 and 81% respectively (258). It indicates that even though 4-thiouridine is a substrate for both UCK1 and UCK2, it is more efficiently phosphorylated by UCK2 than by UCK1. Furthermore, previous studies have reported that even though the activity of UCK has been identified in most examined tissues (270, 272, 273); the UCK2 mRNA could only be detected in a few tissues such as placenta (258), rat brain (274) and testis (275) while the UCK1 mRNA was detected in almost all investigated tissues. It is likely therefore that because of the low level of UCK2 in NIH 3T3 cells, the phosphorylation of 4-thiouridine in this study was not very

efficient. In addition, results from comparing the two different concentrations of labelling, 250 µM and 500 µM are further support for the indication that the enzyme was limited in the cells since that the phosphorylation product was found not significantly increased even though the substrate was available at higher level.

One possible implication of the finding is that the development of 4-thio-UTP highly relies on the level of UCK2 on the investigating tissue. Thus, the effectiveness of the RNA labelling would depend on the activity of UCK2 in the tissue, and overexpression of this enzyme could enhance the labelling of RNA with 4-thiouridine.

There are, however, other possible explanations. The activity of the enzyme depends on the binding affinity of the substrate to the enzyme (K_m) and the catalytic activity of the enzyme (K_{cat}). The low catalytic efficiency is generally caused by both poor substrate binding and slow catalysis. The bonding between 4-thiouridine and UCK likely is the same as the bonding between uridine and the enzyme, although the oxygen atom of the second carboxyl group of uracil is replaced by a sulphur atom for 4-thiouridine.

The base of uridine develops three hydrogen bonds with UCK; the second carboxyl group of uracil bonds with the Oη atom of Tyr-112 and the Nδ1 atom of His-117, and the first carboxyl group of uracil bonds with the Nη1 atom of Arg-176 (Figure 5.13). On the other hand, cytosine base develops four hydrogen bonds with UCK which three of the four hydrogen bonds are formed in the same way as uracil. The N4

atom of cytosine bonds with the Oη atom of Tyr-112 and the Nδ1 atom of His-117 as proton donor, the carboxyl group of cytosine bonds with the Nη1 atom of Arg-176, and the fourth bond between N3 atom of cytosine with the Nη2 atom of Arg-176 (257). The fourth hydrogen bond cannot be developed between uracil and the enzyme because both the N3 atom of uracil and the Nη2 atom of Arg-176 are functioned as proton donor. Although the enzyme efficiently phosphorylated uridine and cytidine; compared with cytidine, the affinity of uridine was lower than that of cytidine (276, 277) therefore efficiency of the catalytic activity of uridine was nearly half of cytidine for both UCK1 and UCK2 (258). Also, the result of the previous study (262, 278, 279) found that CTP is more effective as an UCK inhibitor than UTP. It is likely that the missing hydrogen bonding between the nucleotide bases is critical for substrate recognition and efficient catalysis by the enzyme. The absence of this bonding might cause the decrease of reactivity, thus catalytic efficiency of uridine for UCK is lower than that of cytidine.

The factors mentioned above may also explain why 4-thiouridine in NIH 3T3 cells in this study was not efficiently phosphorylated since the bonding between 4-thiouridine and UCK is likely the same as the bonding between uridine and the enzyme. In addition, a previous study by Ropp and Traut (280) has revealed that a single amino acid substitution of UCK near the uridine binding site brings on a 160-fold decline in affinity for uridine, therefore leading to a dramatic decrease on the activity of the enzyme.

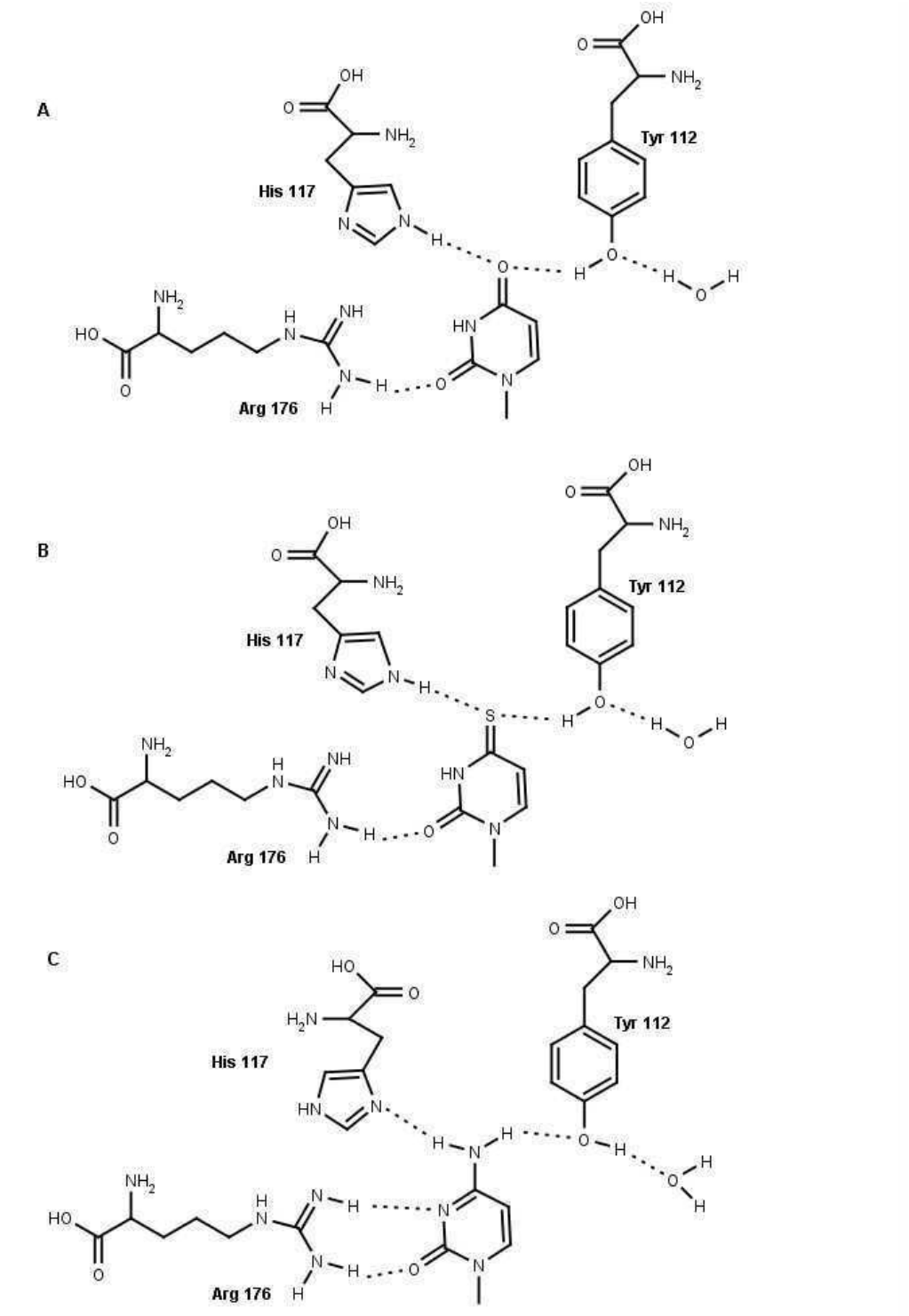

Figure 5.13. Hydrogen bonding between the binding site of UCK and (A) uridine, (B) 4-thiouridine and (C) cytidine

Hydrogen bond pairs are connected with dotted lines.

A number of studies have found that UTP and CTP can function to produce a feedback inhibition of UCK activity (262, 278-280). Furthermore, the inhibition of UCK activity by UTP or CTP could be reversed by either ATP or GTP (278, 279). Cheng et al. (279) proposed that the inhibitors bind the enzyme on the different site than ATP. They bind at the catalytic site as bisubstrate analogue (280) providing dissociation of the active tetramer to the inactive monomers (269, 279) while ATP stabilises the tetrameric form of the enzyme (279).

As the inhibition of UCK activity was also demonstrated by the analogues of UTP, i.e. aza-UTP and F-UTP (278), it might be possible that 4-thio-UTP could be as effective inhibitor of the activity of the enzyme. Based on the previous study, UTP and the analogues exhibit considerate inhibition of uridine phosphorylation at a ratio of the inhibitor and substrate as low as 10% in mouse tumour cells and two percent in human epidermoid carcinoma, while CTP was significantly much more effective than UTP as a feedback inhibitor (278). The results of this study are presented in Table 5.3 show that the ratio of 4-thio-UTP to 4-thiouridine was less than two percent over the 60 min labelling period. Although the inhibition on 4-thiouridine phosphorylation by 4-thio-UTP through feedback mechanism was not detected on this result; it might be another possible explanation for the low level of the phosphorylated metabolite of 4-thiouridine in cells.

Furthermore, the results of this study indicate that serum rapidly stimulates the rate of 4-thiouridine phosphorylation but not that of transport. The findings of the current study are consistent with those of Rozengurt et al. (281) who found that

serum enhances nucleoside phosphorylation. They found that after the addition of serum, the phosphorylated uridine increased two to six-fold in several cell lines. They also observed that within several minutes, insulin, FDGF and epidermal growth factor (EGF), raised the phosphorylation of uridine.

The indication that increase of phosphorylated metabolite was due to upregulation of the UCK in serum-stimulated cells is also supported by the previous study (282, 283). They found that either serum or the combination of purified platelet-derived growth factor (PDGF) and platelet-poor plasma (PPP), components in serum, did produce a stimulation of UCK activity in BALB/c-3T3 cells. It was observed that there was a dramatic increase in enzyme activity in the cells between three and six hours after stimulation with each concentration of bovine calf serum (2.5 – 10%) and it remained elevated through 12 h after stimulation. However, in this current study we observed that even at 20 min after stimulation with 10% of serum the phosphorylation product of the enzyme was increased. Evidently, this finding corroborates the ideas of Wharton and Pledger (282), who suggested that there were factors present in plasma capable of the early induction of UCK activity.

Research on the investigation of resistance to nucleoside analogues, interestingly, found that UCK activity appears associated with the sensitivity of cells to cytotoxic nucleoside analogues. This enzyme is over expressed in cancer cells compared with normal tissues (270, 272, 284, 285), suggesting that UCK might contribute to the tumour-selective cytotoxicity of the nucleoside analogues. A study by Tabata et al. (286) provides evidence that the tumour cells resistant to ethynylnucleosides have

lower UCK activity than that of the parent cells. These results proposed that the decline in UCK activity is one of the key mechanisms of nucleoside analogues resistance. The fact that UCK activity is indeed regulated by growth factor signalling would explain the effectiveness of nucleoside analogues as cancer drugs, because growth factor signalling is up regulated in cancer.

Data from this chapter can be compared with the data in Chapter 3 (Section 3.4.3) to compare between the phosphorylation of two nucleoside analogues, 4-thiouridine and cordycepin. The data shows that even in serum-stimulated cells, the development of phosphorylated metabolite of 4-thiouridine was not very effective compared with the formation of the phosphorylated metabolite of cordycepin or other nucleoside analogues (287, 288). After one hour labelling of 250 µM 4-thiouridine, 4-thio-UTP accumulated in NIH 3T3 cells was 41 µM, while cordycepin triphosphates reached in MCF7 and HeLa cells 494 and 251 µM, respectively after 2 hr incubation with 50 µM cordycepin; also 1281 and 1089 µM after 2 hr incubation with 50 µM cordycepin and 1 µM pentostatin. It was also shown that the ratio of 4-thio-UTP/UTP (0.9) was much lower than the ratio of cordycepin triphosphate/ATP (24.7 and 27.5 in MCF7 and HeLa cells, respectively). It is apparent that the phosphorylation reaction of cordycepin by adenosine kinase (AK) is much more efficient than that of 4-thiouridine by UCK.

There are several possible explanations for the large difference in the phosphorylation efficiency between cordycepin by AK and 4-thiouridine by UCK. It might be that the concentration of UCK protein or its activity is much lower than the

enzyme which is responsible for the phosphorylation of cordycepin. AK is an abundant and universal enzyme which controls extracellular and intracellular adenosine nucleotide concentrations and is responsible for the phosphorylation of several pharmacologically relevant adenosine analogues (15, 235, 289). Meanwhile, UCK is an enzyme which is present at a low level in most eukaryotic tissues (262, 270).

In addition, data from several studies indicate that affinity of the substrates to AK is much higher than the affinity of the substrates to UCK. AK has a K_m for adenosine of 0.2-0.4 µM (12, 15, 290-292) and the phosphorylation efficiency of cordycepin is 12.5 % of adenosine phosphorylation (226), while UCK has K_m for uridine of 40-50 µM and the phosphorylation efficiency of 4-thiouridine is 13-81 % of phosphorylation of uridine (258, 262).

Moreover, the reactivity of these two enzymatic activities is also extremely influenced by the availability of appropriate substrates, nucleoside triphosphate activators, other small molecular effectors, and the environment pH (293). In both cells the intracellular level of ATP, which is important for activity of both enzymes, were much different. The level of ATP in NIH 3T3 cells was less than 0.1 mM while in HeLa and MCF7 cells were more than 1 mM. Therefore, the phosphorylation of 4-thiouridine in NIH 3T3 cells was much less efficient than the phosphorylation of cordycepin in HeLa and MCF7 cells.

5.5. Conclusions

The purpose of the current study is to apply the developed LC-MS/MS method for study the intracellular metabolism of 4-thiouridine. This study has shown that the method has been established and validated for simultaneous separation and determination of the metabolite of 4-thiouridine in cell extracts. This study has found that generally the uptake of 4-thiouridine into NIH 3T3 cells was fast and the phosphorylated metabolite rapidly was developed after only 2 min labelling. However, it was also shown that the phosphorylation process catalysed by UCK in NIH 3T3 is not very efficient. The further investigation has shown that there was just a slight difference in the intracellular level of 4-thio-UTP between 250 µM 4-thiouridine labelling and that of 500 µM. The results indicate that therefore 250 µM of 4-thiouridine provides enough of 4-thio-UTP for 4-thiouridine labelling.

One of the more significant findings to emerge from this study is that the level of the phosphorylated metabolite increased in serum-stimulated cells likely because the enzyme was upregulated in the presence of growth factor. The ratio of S UTP/UTP was stable until 30 min and increased after that 30 min, either in serum-starved cells or in serum-stimulated cells. The second major finding was that there are no significant differences in the intracellular concentrations of UTP and ATP during 4-thiouridine labelling, also on the ratio of ATP/ADP either in serum-starved cells or in serum-stimulated cells. Therefore, the present study provides additional evidence that 4-thiouridine labelling process has no adverse effect on the metabolic balance of adenine and uridine nucleotides.

Since 4-thiouridine phosphorylation depends on the activity of UCK and since the enzyme has low abundance in most non-malignant tissue, this study suggests that further research might be required to explore other agents for labelling RNA which do not need activation by UCK.

CHAPTER 6
GENERAL CONCLUSIONS AND FUTURE WORK

GENERAL CONCLUSIONS AND FUTURE WORK

Through the work described in this thesis, an ion pairing LC-MS/MS method using DMHA has been developed for quantitative determination of nucleoside and nucleotide analogues for *in vitro* and *in vivo* study. The method has successfully separated and detected mixtures of intracellular nucleotides. The extraction of nucleotides from cell lines has been well investigated and optimised. The LC-MS/MS method has also been successfully applied to MCF7 cells and has been established with the results of the validation for determination of intracellular metabolites and nucleotides. It has been demonstrated to have adequate sensitivity and selectivity to measure accurate intracellular concentrations. The LC-MS/MS method has potential applications for analysis of nucleoside drugs in the biomedical area and can be applied to measure other nucleoside drug metabolites due to their similar chemical characteristics.

The metabolism of cordycepin *in vitro* and *in vivo* has been successfully investigated by using the developed method. Cordycepin and its active metabolite reached maximum accumulation in MCF7 and HeLa cells at 2 hours incubation with cordycepin and at 8 hours incubation with a combination of cordycepin and pentostatin. The study of the intracellular metabolism of cordycepin shows that cordycepin was rapidly metabolized in the cells as well as in the cell culture medium into the deaminated form by adenosine deaminase (ADA); at 8 hours incubation with cordycepin alone, all cordycepin had been intracellularly metabolized. Nevertheless, the phosphorylated metabolite was highly accumulated in the cells in the presence of pentostatin, an ADA inhibitor. In contrast, cordycepin in *C. militaris* extracts

showed much lower degradation in non-heat-treated serum compared with pure cordycepin. It indicates a strong evidence for the presence of a deaminase inhibitor in the extract of *Cordyceps* which may need to be further investigated. Hence, further experimental investigations are needed to examine the inhibition of the extract of *Cordyceps* on the activity of enzyme adenosine deaminase.

Moreover, results from the quantification of cordycepin and the metabolites in the plasma and liver of rats dosed with cordycepin proves that the half-life of cordycepin and its metabolites are very short in the plasma; nonetheless they are accumulated in the liver with repeated administration. It is recommended that further research be undertaken in the pharmacokinetic and bio-distribution of cordycepin.

Investigation on the effects of cordycepin treatment on the intracellular nucleotide metabolism shows that cordycepin initially caused an increase in the intracellular levels of nucleoside triphosphates probably due to effects on RNA synthesis by the active metabolite of cordycepin. At longer incubation times, however, cordycepin caused an intense reduction in the amount of intracellular nucleotides, when most of the cordycepin and its active metabolite were gone. These results indicate that cordycepin triphosphate induced long term change in the cell, which resulted in a drop in nucleotides level. In the long term, treatment using pentostatin alone resulted in a reduction of the amount of nucleoside triphosphates (NTPs) and it synergistically increased the effect of cordycepin on nucleotide levels. High levels of the accumulated cordycepin triphosphate led to a massive decline in nucleotide levels. It seems possible that these results are due to inhibition of the synthesis of

nucleotides caused by its inhibition on ribose phosphate phosphokinase or by inducing apoptosis through changes in gene expression caused by its effects on polyadenylation. A possible consequence of high accumulations of cordycepin triphosphate in the long term is it interferes with a number of ATP-dependent cellular reactions, either directly or indirectly, leading to a decline in energy charge and then in NTPs level. Furthermore, effects of cordycepin on nucleotide levels in MCF7 cells were greater than in HeLa cells causing of permanent suppression of NTPs level.

It is possible that the effect of cordycepin on nucleotides in MCF7 and HeLa cells is caused by the different metabolism of cancer cells; therefore, further studies need to be conducted using normal cells to compare the effect of cordycepin and pentostatin treatment on the metabolism of intracellular nucleotides in non-malignant cells.

Moreover, the developed LC-MS/MS method has been successfully applied for study of the intracellular metabolism of 4-thiouridine. The results of this investigation show that generally the uptake of 4-thiouridine into NIH 3T3 cells was fast and the phosphorylated metabolite rapidly was developed only after two min labelling. The most obvious finding to emerge from this study is that the phosphorylation process catalysed by uridine cytidine kinase (UCK) in NIH 3T3 was not very efficient. Compare with the phosphorylation of cordycepin, the ratio of the phosphorylated metabolites to its related endogenous nucleotide (sUTP/UTP) was much lower than the ratio of cordycepin triphosphate to ATP; it was less than 4% of that of

cordycepin. It indicates that the phosphorylation of 4-thiouridine is much less efficient than that of cordycepin.

Furthermore, the level of the phosphorylated metabolite increased in serum-stimulated cells likely because the enzyme was upregulated in the presence of growth factor. In addition, there are no significant differences in the intracellular concentrations of UTP and ATP during 4-thiouridine labelling, also on the ratio of ATP/ADP either in serum-starved cells or in serum-stimulated cells. Hence, the current study confirms that 4-thiouridine and its metabolite have no adverse effect on the metabolic balance of adenine and uridine nucleotides. Since 4-thiouridine phosphorylation depends on the activity of UCK and since the enzyme is low abundance in most non-malignant tissue, this study suggests that further research might be required to explore other agents for labelling RNA which do not need activation by UCK.

Taken together, these results suggest that pharmacological activity of nucleoside analogues and their cytotoxicity highly rely on the accumulation of their phosphorylated metabolites. Consequently, the activity and the level of the enzymes involved in their metabolism highly influence on their pharmacological activity as well as their toxicity. Therefore, data on their intracellular metabolism as well as a better understanding of enzymes involved in their metabolism provide valuable information for drug design and clinical therapy.

REFERENCES

1. Henderson JF, Paterson ARP. Nucleotide metabolism: an introduction: Academic Press; 2014.

2. Ataullakhanov FI, Vitvitsky VM. What determines the intracellular ATP concentration. Bioscience Reports. 2002 Dec;22(5-6):501-11.

3. Berg JM, Tymoczko JL, Stryer L. Disruptions in nucleotide metabolism can cause pathological conditions. 2002.

4. Atkinson DE. Cellular energy metabolism and its regulation: Elsevier; 2012.

5. Zhang C, Liu Z, Liu X, Wei L, Liu Y, Yu J, et al. Targeted metabolic analysis of nucleotides and identification of biomarkers associated with cancer in cultured cell models. Acta Pharmaceutica Sinica B. 2013;3(4):254-62.

6. Van Rompay AR, Johansson M, Karlsson A. Substrate specificity and phosphorylation of antiviral and anticancer nucleoside analogues by human deoxyribonucleoside kinases and ribonucleoside kinases. Pharmacology & therapeutics. 2003;100(2):119-39.

7. Reichard P. Interactions between deoxyribonucleotide and DNA synthesis. Annual review of biochemistry. 1988;57(1):349-74.

8. Wright JA, Chan AK, Choy BK, Hurta RA, McClarty GA, Tagger AY. Regulation and drug resistance mechanisms of mammalian ribonucleotide reductase, and the significance to DNA synthesis. Biochemistry and Cell Biology. 1990;68(12):1364-71.

9. Xu Y-Z, Huang P, Plunkett W. Functional Compartmentation of dCTP Pools preferential utilization of salvaged deoxycytidine for DNA repair in human lymphoblasts. Journal of Biological Chemistry. 1995;270(2):631-7.

10. Cano-Soldado P, Pastor-Anglada M. Transporters that translocate nucleosides and structural similar drugs: structural requirements for substrate recognition. Medicinal research reviews. 2012;32(2):428-57.

11. Moriwaki Y, Yamamoto T, Higashino K. Enzymes involved in purine metabolism-a review of histochemical localization and functional implications. Histology and histopathology. 1999;14(4):1321-40.

12. Yamada Y, Goto H, Ogasawara N. Purification and properties of adenosine kinase from rat brain. Biochimica et Biophysica Acta (BBA)-Enzymology. 1980;616(2):199-207.

13. Bianchi V, Spychala J. Mammalian 5'-nucleotidases. Journal of Biological Chemistry. 2003;278(47):46195-8.

14. LEHTO M, Sharom F. Release of the glycosylphosphatidylinositol-anchored enzyme ecto-5'-nucleotidase by phospholipase C: catalytic activation and modulation by the lipid bilayer. Biochem J. 1998;332:101-9.

15. Arch J, Newsholme EA. Activities and some properties of 5'-nucleotidase, adenosine kinase and adenosine deaminase in tissues from vertebrates and invertebrates in relation to the control of the concentration and the physiological role of adenosine. Biochem J. 1978;174:965-77.

16. Rubio R, Berne RM. Localization of purine and pyrimidine nucleoside phosphorylases in heart, kidney, and liver. American Journal of Physiology-Heart and Circulatory Physiology. 1980;239(6):H721-H30.

17. Zeleznikar R, Heyman R, Graeff R, Walseth T, Dawis S, Butz E, et al. Evidence for compartmentalized adenylate kinase catalysis serving a high energy phosphoryl transfer function in rat skeletal muscle. Journal of Biological Chemistry. 1990;265(1):300-11.

18. Eltzschig HK, Sitkovsky MV, Robson SC. Purinergic signaling during inflammation. New England Journal of Medicine. 2012;367(24):2322-33.

19. Bours M, Swennen E, Di Virgilio F, Cronstein B, Dagnelie P. Adenosine 5′-triphosphate and adenosine as endogenous signaling molecules in immunity and inflammation. Pharmacology & therapeutics. 2006;112(2):358-404.

20. Lazarowski ER. Vesicular and conductive mechanisms of nucleotide release. Purinergic Signalling. 2012;8(3):359-73.

21. Di Virgilio F, Chiozzi P, Ferrari D, Falzoni S, Sanz JM, Morelli A, et al. Nucleotide receptors: an emerging family of regulatory molecules in blood cells. Blood. 2001;97(3):587-600.

22. Idzko M, Ferrari D, Eltzschig HK. Nucleotide signalling during inflammation. Nature. 2014;509(7500):310-7.

23. Burnstock G, Brouns I, Adriaensen D, Timmermans J-P. Purinergic signaling in the airways. Pharmacological reviews. 2012;64(4):834-68.

24. Elliott MR, Chekeni FB, Trampont PC, Lazarowski ER, Kadl A, Walk SF, et al. Nucleotides released by apoptotic cells act as a find-me signal to promote phagocytic clearance. Nature. 2009;461(7261):282-6.

25. Chen Y, Yao Y, Sumi Y, Li A, To UK, Elkhal A, et al. Purinergic signaling: a fundamental mechanism in neutrophil activation. Science signaling. 2010;3(125):ra45.

26. Zhang Z, Wang Z, Ren H, Yue M, Huang K, Gu H, et al. P2Y6 agonist uridine 5′-diphosphate promotes host defense against bacterial infection via monocyte chemoattractant protein-1–mediated monocytes/macrophages recruitment. The Journal of Immunology. 2011;186(9):5376-87.

27. Idzko M, Panther E, Sorichter S, Herouy Y, Berod L, Geissler M, et al. Characterization of the biological activities of uridine diphosphate in human dendritic cells: Influence on chemotaxis and CXCL8 release. Journal of Cellular Physiology. 2004;201(2):286-93.

28. Ferrari D, Idzko M, Dichmann S, Purlis D, Virchow C, Norgauer J, et al. P2 purinergic receptors of human eosinophils: characterization and coupling to oxygen radical production. FEBS letters. 2000;486(3):217-24.

29. Riegel A-K, Faigle M, Zug S, Rosenberger P, Robaye B, Boeynaems J-M, et al. Selective induction of endothelial P2Y6 nucleotide receptor promotes vascular inflammation. Blood. 2011;117(8):2548-55.

30. Grbic DM, Degagné É, Langlois C, Dupuis A-A, Gendron F-P. Intestinal inflammation increases the expression of the P2Y6 receptor on epithelial cells and the release of CXC chemokine ligand 8 by UDP. The Journal of Immunology. 2008;180(4):2659-68.

31. Semple JW, Italiano JE, Freedman J. Platelets and the immune continuum. Nature Reviews Immunology. 2011;11(4):264-74.

32. Surprenant A, North RA. Signaling at purinergic P2X receptors. Annual Review of Physiology. 2009;71:333-59.

33. Khakh BS, North RA. P2X receptors as cell-surface ATP sensors in health and disease. Nature. 2006;442(7102):527-32.

34. Köhler D, Eckle T, Faigle M, Grenz A, Mittelbronn M, Laucher S, et al. CD39/ectonucleoside triphosphate diphosphohydrolase 1 provides myocardial protection during cardiac ischemia/reperfusion injury. Circulation. 2007;116(16):1784-94.

35. Pinsky DJ, Broekman MJ, Peschon JJ, Stocking KL, Fujita T, Ramasamy R, et al. Elucidation of the thromboregulatory role of CD39/ectoapyrase in the ischemic brain. The Journal of clinical investigation. 2002;109(109 (8)):1031-40.

36. Zimmermann H, Zebisch M, Sträter N. Cellular function and molecular structure of ecto-nucleotidases. Purinergic Signalling. 2012;8(3):437-502.

37. Ohta A, Sitkovsky M. Role of G-protein-coupled adenosine receptors in downregulation of inflammation and protection from tissue damage. Nature. 2001;414(6866):916-20.

38. Colgan SP, Eltzschig HK. Adenosine and hypoxia-inducible factor signaling in intestinal injury and recovery. Annual Review of Physiology. 2012;74.

39. Antonioli L, Haskó G, Fornai M, Colucci R, Blandizzi C. Adenosine pathway and cancer: where do we go from here? Expert opinion on therapeutic targets. 2014;18(9):973-7.

40. Antonioli L, Blandizzi C, Pacher P, Haskó G. Immunity, inflammation and cancer: a leading role for adenosine. Nature Reviews Cancer. 2013;13(12):842-57.

41. Virtanen SS, Kukkonen-Macchi A, Vainio M, Elima K, Härkönen PL, Jalkanen S, et al. Adenosine inhibits tumor cell invasion via receptor-independent mechanisms. Molecular Cancer Research. 2014;12(12):1863-74.

42. Eltzschig HK, Faigle M, Knapp S, Karhausen J, Ibla J, Rosenberger P, et al. Endothelial catabolism of extracellular adenosine during hypoxia: the role of surface adenosine deaminase and CD26. Blood. 2006;108(5):1602-10.

43. Morote-Garcia JC, Rosenberger P, Kuhlicke J, Eltzschig HK. HIF-1–dependent repression of adenosine kinase attenuates hypoxia-induced vascular leak. Blood. 2008;111(12):5571-80.

44. Nishiyama T, Yamamoto H, Uchiumi T, Nakashima N. Eukaryotic ribosomal protein RPS25 interacts with the conserved loop region in a dicistroviral intergenic internal ribosome entry site. Nucleic Acids Research. 2007 2007;35(5):1514-21.

45. Davidsson J, Andersson A, Paulsson K, Heidenblad M, Isaksson M, Borg Å, et al. Tiling resolution array comparative genomic hybridization, expression and methylation analyses of dup (1q) in Burkitt lymphomas and pediatric high hyperdiploid acute lymphoblastic leukemias reveal clustered near-centromeric breakpoints and overexpression of genes in 1q22-32.3. Human molecular genetics. 2007;16(18):2215-25.

46. Jordheim LP, Durantel D, Zoulim F, Dumontet C. Advances in the development of nucleoside and nucleotide analogues for cancer and viral diseases. Nat Rev Drug Discov. [Review]. 2013 Jun;12(6):447-64.

47. Galmarini CM, Mackey JR, Dumontet C. Nucleoside analogues and nucleobases in cancer treatment. The lancet oncology. 2002;3(7):415-24.

48. Jordheim LP, Dumontet C. Review of recent studies on resistance to cytotoxic deoxynucleoside analogues. Biochimica et Biophysica Acta (BBA)-Reviews on Cancer. 2007;1776(2):138-59.

49. Jansen RS, Rosing H, Schellens JHM, Beijnen JH. Mass spectrometry in the quantitative analysis of therapeutic intracellular nucleotide analogs. Mass Spectrometry Reviews. 2011 Mar-Apr;30(2):321-43.

50. Minuesa G, Huber-Ruano I, Pastor-Anglada M, Koepsell H, Clotet B, Martinez-Picado J. Drug uptake transporters in antiretroviral therapy. Pharmacology & therapeutics. 2011;132(3):268-79.

51. Krett NL, Davies KM, Ayres M, Ma C, Nabhan C, Gandhi V, et al. 8-Amino-adenosine is a potential therapeutic agent for multiple myeloma. Molecular cancer therapeutics. 2004;3(11):1411-20.

52. Yamamoto S, Yamauchi T, Kawai Y, Takemura H, Kishi S, Yoshida A, et al. Fludarabine-mediated circumvention of cytarabine resistance is associated with fludarabine triphosphate accumulation in cytarabine-resistant leukemic cells. International journal of hematology. 2007;85(2):108-15.

53. Månsson E, Flordal E, Liliemark J, Spasokoukotskaja T, Elford H, Lagercrantz S, et al. Down-regulation of deoxycytidine kinase in human leukemic cell lines resistant to cladribine and clofarabine and increased ribonucleotide reductase activity contributes to fludarabine resistance. Biochemical Pharmacology. 2003;65(2):237-47.

54. Gandhi V, Ayres M, Halgren RG, Krett NL, Newman RA, Rosen ST. 8-chloro-cAMP and 8-chloro-adenosine act by the same mechanism in multiple myeloma cells. Cancer Res. 2001;61(14):5474-9.

55. Cohen S, Jordheim LP, Megherbi M, Dumontet C, Guitton J. Liquid chromatographic methods for the determination of endogenous nucleotides and nucleotide analogs used in cancer therapy: a review. Journal of Chromatography B. 2010;878(22):1912-28.

56. Agarwal RP. Inhibitors of adenosine deaminase. Pharmacology & therapeutics. 1982;17(3):399-429.

57. Agarwal RP, Spector T, Parks RE. Tight-binding inhibitors—IV. Inhibition of adenosine deaminases by various inhibitors. Biochemical Pharmacology. 1977;26(5):359-67.

58. Carson DA, Wasson DB, Kaye J, Ullman B, Martin DW, Robins RK, et al. Deoxycytidine kinase-mediated toxicity of deoxyadenosine analogs toward malignant human lymphoblasts in vitro and toward murine L1210 leukemia in vivo. Proceedings of the National Academy of Sciences. 1980;77(11):6865-9.

59. Eriksson S, Thelander L, Akerman M. Allosteric regulation of calf thymus ribonucleoside diphosphate reductase. Biochemistry. 1979;18(14):2948-52.

60. Cunningham KG, Manson W, Spring FS, Hutchinson SA. CORDYCEPIN, A METABOLIC PRODUCT ISOLATED FROM CULTURES OF CORDYCEPS-MILITARIS (LINN) LINK. Nature. 1950;166(4231):949-.

61. Kaczka EA, Trenner NR, Arison B, Walker RW, Folkers K. Identification of cordycepin, a metabolite of Cordycepsmilitaris, as 3′-deoxyadenosine. Biochemical and Biophysical Research Communications. 1964;14(5):456-7.

62. Ng TB, Wang HX. Pharmacological actions of Cordyceps, a prized folk medicine. Journal of Pharmacy and Pharmacology. 2005 Dec;57(12):1509-19.

63. Kim HG, Shrestha B, Lim SY, Yoon DH, Chang WC, Shin D-J, et al. Cordycepin inhibits lipopolysaccharide-induced inflammation by the suppression of NF-[kappa]B through Akt and p38 inhibition in RAW 264.7 macrophage cells. European Journal of Pharmacology. 2006;545(2-3):192-9.

64. Jeong J-W, Jin C-Y, Kim G-Y, Lee J-D, Park C, Kim G-D, et al. Anti-inflammatory effects of cordycepin via suppression of inflammatory mediators in BV2 microglial cells. International Immunopharmacology. 2010;10(12):1580-6.

65. Paterson RRM. Cordyceps - A traditional Chinese medicine and another fungal therapeutic biofactory? Phytochemistry. 2008;69(7):1469-95.

66. Dong CH, Yao YJ. In vitro evaluation of antioxidant activities of aqueous extracts from natural and cultured mycelia of Cordyceps sinensis. LWT - Food Science and Technology. 2008;41(4):669-77.

67. Liu ZQ, Li PT, Zhao D, Tang HL, Guo JY. Protective effect of extract of Cordyceps sinensis in middle cerebral artery occlusion-induced focal cerebral ischemia in rats. Behavioral and Brain Functions. 2010 Oct;6.

68. Kawanishi T, Ikeda-Dantsuji Y, Nagayama A. Effects of two basidiomycete species on interleukin 1 and interleukin 2 production by macrophage and T cell lines. Immunobiology. 2010;215(7):516-20.

69. Kuo C-F, Chen C-C, Lin C-F, Jan M-S, Huang RY, Luo Y-H, et al. Abrogation of streptococcal pyrogenic exotoxin B-mediated suppression of phagocytosis in U937 cells by Cordyceps sinensis mycelium via production of cytokines. Food and Chemical Toxicology. 2007;45(2):278-85.

70. Siu KM, Mak DHF, Chiu PY, Poon MKT, Du Y, Ko KM. Pharmacological basis of 'Yin-nourishing' and 'Yang-invigorating' actions of Cordyceps, a Chinese tonifying herb. Life Sciences. 2004 Dec;76(4):385-95.

71. Wang ZM, Peng X, Lee KLD, Tang JCO, Cheung PCK, Wu JY. Structural characterisation and immunomodulatory property of an acidic polysaccharide from mycelial culture of Cordyceps sinensis fungus Cs-HK1. Food Chemistry. 2011;125(2):637-43.

72. Jia J-MM. Cordycedipeptide A, a new cyclodipeptide from the culture liquid of Cordyceps sinensis (Berk.) Sacc. Chemical & pharmaceutical bulletin. 2005;53(5):582-3.

73. Wang Y, Yin H, Lv X, Gao H, Wang M. Protection of chronic renal failure by a polysaccharide from Cordyceps sinensis. Fitoterapia. 2010;81(5):397-402.

74. Han ES, Oh JY, Park H-J. Cordyceps militaris extract suppresses dextran sodium sulfate-induced acute colitis in mice and production of inflammatory mediators from macrophages and mast cells. Journal of Ethnopharmacology.In Press, Corrected Proof.

75. Rao YK, Fang S-H, Wu W-S, Tzeng Y-M. Constituents isolated from Cordyceps militaris suppress enhanced inflammatory mediator's production and human cancer cell proliferation. Journal of Ethnopharmacology. 2010;131(2):363-7.

76. Han JY, Im J, Choi JN, Lee CH, Park HJ, Park DK, et al. Induction of IL-8 expression by Cordyceps militaris grown on germinated soybeans through lipid rafts formation and signaling pathways via ERK and JNK in A549 cells. Journal of Ethnopharmacology. 2010;127(1):55-61.

77. Oh JY, Choi W-S, Lee CH, Park H-J. The Ethyl acetate extract of Cordyceps militaris inhibits IgE-mediated allergic responses in mast cells and passive cutaneous anaphylaxis reaction in mice. Journal of Ethnopharmacology.In Press, Accepted Manuscript.

78. Kim HG, Song H, Yoon DH, Song B-W, Park SM, Sung GH, et al. Cordyceps pruinosa extracts induce apoptosis of HeLa cells by a caspase dependent pathway. Journal of Ethnopharmacology. 2010;128(2):342-51.

79. Yang FQ, Ge L, Yong JWH, Tan SN, Li SP. Determination of nucleosides and nucleobases in different species of Cordyceps by capillary electrophoresis-mass spectrometry. Journal of Pharmaceutical and Biomedical Analysis. 2009;50(3):307-14.

80. Yang FQ, Li DQ, Feng K, Hu DJ, Li SP. Determination of nucleotides, nucleosides and their transformation products in Cordyceps by ion-pairing reversed-phase liquid chromatography-mass spectrometry. Journal of Chromatography A. 2010;1217(34):5501-10.

81. Guan J, Li SP. Discrimination of polysaccharides from traditional Chinese medicines using saccharide mapping--Enzymatic digestion followed by chromatographic analysis. Journal of Pharmaceutical and Biomedical Analysis. 2010;51(3):590-8.

82. Guan J, Yang FQ, Li SP. Evaluation of Carbohydrates in Natural and Cultured Cordyceps by Pressurized Liquid Extraction and Gas Chromatography Coupled with Mass Spectrometry. Molecules. 2010 Jun;15(6):4227-41.

83. Nie SP, Cui SW, Phillips AO, Xie MY, Phillips GO, Al-Assaf S, et al. Elucidation of the structure of a bioactive hydrophilic polysaccharide from Cordyceps sinensis by methylation analysis and NMR spectroscopy. Carbohydrate Polymers. 2011 Mar;84(3):894-9.

84. Yang FQ, Feng K, Zhao J, Li SP. Analysis of sterols and fatty acids in natural and cultured Cordyceps by one-step derivatization followed with gas chromatography-mass spectrometry. Journal of Pharmaceutical and Biomedical Analysis. 2009;49(5):1172-8.

85. Zhou XW, Gong ZH, Su Y, Lin J, Tang KX. Cordyceps fungi: natural products, pharmacological functions and developmental products. Journal of Pharmacy and Pharmacology. 2009 Mar;61(3):279-91.

86. Kondrashov A, Meijer HA, Barthet-Barateig A, Parker HN, Khurshid A, Tessier S, et al. Inhibition of polyadenylation reduces inflammatory gene induction. RNA. 2012.

87. Penman S, Rosbash M, Penman M. Messenger and heterogeneous nuclear RNA in HeLa cells: differential inhibition by cordycepin. Proceedings of the National Academy of Sciences. 1970;67(4):1878-85.

88. Cho H-J, Cho JY, Rhee MH, Park H-J. Cordycepin (3'-deoxyadenosine) inhibits human platelet aggregation in a cyclic AMP- and cyclic GMP-dependent manner. European Journal of Pharmacology. 2007;558(1-3):43-51.

89. Nishiuchi A, Yoshikawa N, Takahashi Y, Kimoto Y, Sato A, Kunitomo M, et al. Inhibitory effect of cordycepin on platelet aggregation activity in rats. Journal of Pharmacological Sciences. 2010;112:84P-P.

90. Lee YR, Noh EM, Jeong EY, Yun SK, Jeong YJ, Kim JH, et al. Cordycepin inhibits UVB-induced matrix metalloproteinase expression by suppressing the NF-kappa B pathway in human dermal fibroblasts. Experimental and Molecular Medicine. 2009 Aug;41(8):548-54.

91. Zhou X, Meyer CU, Schmidtke P, Zepp F. Effect of cordycepin on interleukin-10 production of human peripheral blood mononuclear cells. European Journal of Pharmacology. 2002;453(2-3):309-17.

92. Guo P, Kai Q, Gao JA, Lian ZQ, Wu CM, Wu CA, et al. Cordycepin Prevents Hyperlipidemia in Hamsters Fed a High-Fat Diet via Activation of AMP-Activated Protein Kinase. Journal of Pharmacological Sciences. 2010 Aug;113(4):395-403.

93. Chang W, Lim S, Song H, Song B-W, Kim H-J, Cha M-J, et al. Cordycepin inhibits vascular smooth muscle cell proliferation. European Journal of Pharmacology. 2008;597(1-3):64-9.

94. Chen LS, Stellrecht CM, Gandhi V. RNA-directed agent, cordycepin, induces cell death in multiple myeloma cells. British Journal of Haematology. 2008 Mar;140(6):682-91.

95. Thomadaki H, Tsiapalis CM, Scorilas A. Polyadenylate polymerase modulations in human epithelioid cervix and breast cancer cell lines, treated with etoposide or cordycepin, follow cell cycle rather than apoptosis induction. Biological Chemistry. 2005;386(5):471-80.

96. Nakamura K, Yoshikawa N, Yamaguchi Y, Kagota S, Shinozuka K, Kunitomo M. Antitumor effect of cordycepin (3 '-deoxyadenosine) on mouse melanoma and lung carcinoma cells involves adenosine A(3) receptor stimulation. Anticancer Research. 2006;26(1A):43-7.

97. Wu WC, Hsiao JR, Lian YY, Lin CY, Huang BM. The apoptotic effect of cordycepin on human OEC-M1 oral cancer cell line. Cancer Chemotherapy and Pharmacology. 2007;60(1):103-11.

98. Yoshikawa N, Nakamura K, Yamaguchi Y, Kagota S, Shinozuka K, Kunitomo M. Cordycepin and Cordyceps sinensis reduce the growth of human promyelocytic leukaemia cells through the Wnt signalling pathway. Clinical and Experimental Pharmacology and Physiology. 2007;34:S61-S3.

99. Yoshikawa N, Yamada S, Takeuchi C, Kagota S, Shinozuka K, Kunitomo M, et al. Cordycepin (3 '-deoxyadenosine) inhibits the growth of B16-BL6 mouse melanoma cells through the stimulation of adenosine A(3) receptor followed by glycogen synthase kinase-3 beta activation and cyclin D-1 suppression. Naunyn-Schmiedebergs Archives of Pharmacology. 2008;377(4-6):591-5.

100. Thomadaki H, Scorilas A, Tsiapalis CM, Havredaki M. The role of cordycepin in cancer treatment via induction or inhibition of apoptosis: implication of polyadenylation in a cell type specific manner. Cancer Chemotherapy and Pharmacology. 2008;61(2):251-65.

101. Lee S-J, Kim S-K, Choi W-S, Kim W-J, Moon S-K. Cordycepin causes p21WAF1-mediated G2/M cell-cycle arrest by regulating c-Jun N-terminal kinase activation in human bladder cancer cells. Archives of Biochemistry and Biophysics. 2009;490(2):103-9.

102. Chen Y, Chen YC, Lin YT, Huang SH, Wang SM. Cordycepin Induces Apoptosis of CGTH W-2 Thyroid Carcinoma Cells through the Calcium-Calpain-Caspase 7-PARP Pathway. Journal of Agricultural and Food Chemistry. 2010 Nov;58(22):11645-52.

103. He W, Zhang MF, Ye J, Jiang TT, Fang X, Song Y. Cordycepin induces apoptosis by enhancing JNK and p38 kinase activity and increasing the protein expression of Bcl-2 pro-apoptotic molecules. Journal of Zhejiang University-Science B. 2010 Sep;11(9):654-60.

104. Lee EJ, Kim WJ, Moon SK. Cordycepin Suppresses TNF-alpha-induced Invasion, Migration and Matrix Metalloproteinase-9 Expression in Human Bladder Cancer Cells. Phytotherapy Research. 2010 Dec;24(12):1755-61.

105. Lee S-J, Moon G-S, Jung K-H, Kim W-J, Moon S-K. c-Jun N-terminal kinase 1 is required for cordycepin-mediated induction of G2/M cell-cycle arrest via p21WAF1 expression in human colon cancer cells. Food and Chemical Toxicology. 2010;48(1):277-83.

106. Noh EM, Youn HJ, Jung SH, Han JH, Jeong YJ, Chung EY, et al. Cordycepin inhibits TPA-induced matrix metalloproteinase-9 expression by suppressing the MAPK/AP-1 pathway in MCF-7 human breast cancer cells. International Journal of Molecular Medicine. 2010 Feb;25(2):255-60.

107. Nakamura K, Konoha K, Yoshikawa N, Yamaguchi Y, Kagota S, Shinozuka K, et al. Effect of cordycepin (3 '-deoxyadenosine) on hematogenic lung metastatic model mice. In Vivo. 2005;19(1):137-41.

108. Yoshikawa N, Kunitomo M, Kagota S, Shinozuka K, Nakamura K. Inhibitory Effect of Cordycepin on Hematogenic Metastasis of B16-F1 Mouse Melanoma Cells Accelerated by Adenosine-5 '-diphosphate. Anticancer Research. 2009 Oct;29(10):3857-60.

109. Yoshikawa N, Nakamura K, Yamaguchi Y, Kagota S, Shinozuka K, Kunitomo M. Antitumour activity of cordycepin in mice. Clin Exp Pharmacol Physiol. 2004;31 Suppl 2:S51-3.

110. Kodama EN, McCaffrey RP, Yusa K, Mitsuya H. Antileukemic activity and mechanism of action of cordycepin against terminal deoxynucleotidyl transferase-positive (TdT(+)) leukemic cells. Biochemical Pharmacology. 2000 Feb 1;59(3):273-81.

111. Barreiro P, García-Benayas T, Rendón A, Rodríguez-Novoa S, Soriano V. Combinations of nucleoside/nucleotide analogues for HIV therapy. AIDS Rev. 2004;6(4):234-43.

112. Wang LH, Begley J, St. Claire III RL, Harris J, Wakeford C, Rousseau FS. Pharmacokinetic and pharmacodynamic characteristics of emtricitabine support its once daily dosing for the treatment of HIV infection. AIDS Research & Human Retroviruses. 2004;20(11):1173-82.

113. Rodríguez-Orengo JF, Santana J, Febo I, Díaz C, Rodríguez JL, García R, et al. Intracellular studies of the nucleoside reverse transcriptase inhibitor active metabolites: a review. Puerto Rico health sciences journal. 2014;19(1).

114. Lipsett MN. Isolation of 4-thiouridylic acid from soluble ribonucleic acid of *Escherichia coli*. Journal of Biological Chemistry. 1965;240(10):3975-&.

115. Mueller EG, Buck CJ, Palenchar PM, Barnhart LE, Paulson JL. Identification of a gene involved in the generation of 4-thiouridine in tRNA. Nucleic Acids Research. 1998 Jun;26(11):2606-10.

116. Favre A, Michelson A, Yaniv M. Photochemistry of 4-thiouridine in Escherichia coli transfer RNA 1 Val. Journal of molecular biology. 1971;58(1):367-79.

117. Carre D, Thomas G, Favre A. Conformation and functioning of tRNAs: cross-linked tRNAs as substrate for tRNA nucleotidyl-transferase and aminoacyl synthetases. Biochimie. 1974;56(8):1089-101.

118. Kambampati R, Lauhon CT. IscS is a sulfurtransferase for the in vitro biosynthesis of 4-thiouridine in Escherichia coli tRNA. Biochemistry. 1999 Dec 14;38(50):16561-8.

119. Ninio J, Favre A, Yaniv M. Molecular model for transfer RNA. Nature. 1969;223(5213):1333-5.

120. Stade K, Rinke-Appel J, Brimacombe R. Site-directed cross-linking of mRNA analogues to the Escherichia coli ribosome; Identification of 30S rlbosomal components that can be cross-linked to the mRNA at various points 5’ withrespect to the decoding site. Nucleic Acids Research. 1989;17(23):9889-908.

121. Tate W, Greuer B, Brimacombe R. Codon recognition in polypeptide chain termination: site directed crosslinking of termination codon to Escherichia coli release factor 2. Nucleic Acids Research. 1990;18(22):6537-44.

122. Rinke-Appel J, Jünke N, Stade K, Brimacombe R. The path of mRNA through the Escherichia coli ribosome; site-directed cross-linking of mRNA analogues carrying a photo-reactive label at various points 3'to the decoding site. The EMBO journal. 1991;10(8):2195.

123. Yu Y-T. [6] Site-specific 4-thiouridine incorporation into RNA molecules. Methods in enzymology. 2000;318:71-88.

124. Dölken L, Ruzsics Z, Rädle B, Friedel CC, Zimmer R, Mages J, et al. High-resolution gene expression profiling for simultaneous kinetic parameter analysis of RNA synthesis and decay. RNA. 2008;14(9):1959-72.

125. Kenzelmann M, Maertens S, Hergenhahn M, Kueffer S, Hotz-Wagenblatt A, Li L, et al. Microarray analysis of newly synthesized RNA in cells and animals. Proceedings of the National Academy of Sciences. 2007;104(15):6164-9.

126. Melvin WT, Milne HB, Slater AA, Allen HJ, Keir HM. Incorporation of 6-Thioguanosine and 4-Thiouridine into RNA. European Journal of Biochemistry. 1978;92(2):373-9.

127. Burger K, Muehl B, Kellner M, Rohrmoser M, Gruber-Eber A, Windhager L, et al. 4-thiouridine inhibits rRNA synthesis and causes a nucleolar stress response. Rna Biology. 2013 Oct 1;10(10):1623-30.

128. Radle B, Rutkowski AJ, Ruzsics Z, Friedel CC, Koszinowski UH, Dolken L. Metabolic labeling of newly transcribed RNA for high resolution gene expression profiling of RNA synthesis, processing and decay in cell culture. Journal of visualized experiments : JoVE. 2013 2013 Aug(78).

129. Geldart SE, Brown PR. Analysis of nucleotides by capillary electrophoresis. Journal of Chromatography A. 1998 Dec 18;828(1-2):317-36.

130. Friedecky D, Tomkova J, Maier V, Janost'akova A, Prochazka M, Adam T. Capillary electrophoretic method for nucleotide analysis in cells: Application on inherited metabolic disorders. Electrophoresis. 2007 Feb;28(3):373-80.

131. Feng H-T, Wong N, Wee S, Lee MM. Simultaneous determination of 19 intracellular nucleotides and nucleotide sugars in Chinese Hamster ovary cells by capillary electrophoresis. Journal of Chromatography B-Analytical Technologies in the Biomedical and Life Sciences. 2008 Jul 1;870(1):131-4.

132. Jendresen CB, Kilstrup M, Martinussen J. A simplified method for rapid quantification of intracellular nucleoside triphosphates by one-dimensional thin-layer chromatography. Analytical Biochemistry. 2011;409(2):249-59.

133. Cichna M, Raab A, Daxecker H, Griesmacher A, Muller MM, Markl R. Determination of fifteen nucleotides in cultured human mononuclear blood and umbilical vein endothelial cells by solvent generated ion-pair chromatography. Journal of Chromatography B-Analytical Technologies in the Biomedical and Life Sciences. 2003 Apr 25;787(2):381-91.

134. Giannattasio S, Gagliardi S, Samaja M, Marra E. Simultaneous determination of purine nucleotides, their metabolites and beta-nicotinamide adenine dinucleotide in cerebellar granule cells by ion-pair high performance liquid chromatography. Brain Research Protocols. 2003;10(3):168-74.

135. Huang D, Zhang YH, Chen XG. Analysis of intracellular nucleoside triphosphate levels in normal and tumor cell lines by high-performance liquid chromatography. Journal of Chromatography B-Analytical Technologies in the Biomedical and Life Sciences. 2003;784(1):101-9.

136. Bhatt DP, Chen X, Geiger JD, Rosenberger TA. A sensitive HPLC-based method to quantify adenine nucleotides in primary astrocyte cell cultures. Journal of Chromatography B. 2012;889:110-5.

137. Zur Nedden S, Eason R, Doney AS, Frenguelli BG. An ion-pair reversed-phase HPLC method for determination of fresh tissue adenine nucleotides avoiding freeze–thaw degradation of ATP. Analytical Biochemistry. 2009;388(1):108-14.

138. Yeung P, Ding L, Casley WL. HPLC assay with UV detection for determination of RBC purine nucleotide concentrations and application for biomarker study in vivo. Journal of Pharmaceutical and Biomedical Analysis. 2008;47(2):377-82.

139. Contreras-Sanz A, Scott-Ward TS, Gill HS, Jacoby JC, Birch RE, Malone-Lee J, et al. Simultaneous quantification of 12 different nucleotides and nucleosides released from renal epithelium and in human urine samples using ion-pair reversed-phase HPLC. Purinergic Signalling. 2012;8(4):741-51.

140. Coolen EJ, Arts IC, Swennen EL, Bast A, Stuart MAC, Dagnelie PC. Simultaneous determination of adenosine triphosphate and its metabolites in human whole blood by RP-HPLC and UV-detection. Journal of Chromatography B. 2008;864(1):43-51.

141. Leij-Halfwerk S, Agteresch HJ, Sijens PE, Dagnelie PC. Adenosine triphosphate infusion increases liver energy status in advanced lung cancer patients: An in vivo31P magnetic resonance spectroscopy study. Hepatology. 2002;35(2):421-4.

142. Slusher J, Kuwahara S, Hamzeh F, Lewis L, Kornhauser D, Lietman P. Intracellular zidovudine (ZDV) and ZDV phosphates as measured by a validated combined high-pressure liquid chromatography-radioimmunoassay procedure. Antimicrobial Agents and Chemotherapy. 1992;36(11):2473-7.

143. de Korte D, Haverkort WA, van Gennip AH, Roos D. Nucleotide profiles of normal human blood cells determined by high-performance liquid chromatography. Analytical Biochemistry. 1985;147(1):197-209.

144. Brown EG, Newton RP, Shaw NM. Analysis of the free nucleotide pools of mammalian tissues by high-pressure liquid chromatography. Analytical Biochemistry. 1982;123(2):378-88.

145. Balakrishnan K, Wierda WG, Keating MJ, Gandhi V. Mechanisms of cell death of chronic lymphocytic leukemia lymphocytes by RNA-directed agent, 8-NH2-adenosine. Clin Cancer Res. [Article]. 2005 Sep;11(18):6745-52.

146. Robbins BL, Waibel BH, Fridland A. Quantitation of intracellular zidovudine phosphates by use of combined cartridge-radioimmunoassay methodology. Antimicrobial Agents and Chemotherapy. 1996;40(11):2651-4.

147. Daxecker H, Raab M, Cichna M, Markl P, Müller MM. Determination of the effects of mycophenolic acid on the nucleotide pool of human peripheral blood mononuclear cells in vitro by high-performance liquid chromatography. Clinica chimica acta. 2001;310(1):81-7.

148. Graven P, Tambalo M, Scapozza L, Perozzo R. Purine metabolite and energy charge analysis of Trypanosoma brucei cells in different growth phases using an optimized ion-pair RP-HPLC/UV for the quantification of adenine and guanine pools. Exp Parasitol. [Article]. 2014 Jun;141:28-38.

149. Harvey D. Modern analytical chemistry: McGraw-Hill New York; 2000.

150. von Brocke A, Nicholson G, Bayer E. Recent advances in capillary electrophoresis/electrospray-mass spectrometry. Electrophoresis. 2001 Apr;22(7):1251-66.

151. Soga T, Ishikawa T, Igarashi S, Sugawara K, Kakazu Y, Tomita M. Analysis of nucleotides by pressure-assisted capillary electrophoresis–mass spectrometry using silanol mask technique. Journal of Chromatography A. 2007;1159(1):125-33.

152. Soga T, Igarashi K, Ito C, Mizobuchi K, Zimmermann H-P, Tomita M. Metabolomic profiling of anionic metabolites by capillary electrophoresis mass spectrometry. Analytical Chemistry. 2009;81(15):6165-74.

153. Williams LD, Von Tungeln LS, Beland FA, Doerge DR. Liquid chromatographic–mass spectrometric determination of the metabolism and disposition of the anti-retroviral nucleoside analogs zidovudine and lamivudine in C57BL/6N and B6C3F1 mice. Journal of Chromatography B. 2003;798(1):55-62.

154. Cahours X, Tran TT, Mesplet N, Kieda C, Morin P, Agrofoglio LA. Analysis of intracellular didanosine triphosphate at sub-ppb level using LC-MS/MS. Journal of Pharmaceutical and Biomedical Analysis. 2001;26(5):819-27.

155. King T, Bushman L, Kiser J, Anderson PL, Ray M, Delahunty T, et al. Liquid chromatography–tandem mass spectrometric determination of tenofovir-diphosphate in human peripheral blood mononuclear cells. Journal of Chromatography B. 2006;843(2):147-56.

156. Meléndez M, Blanco R, Delgado W, García R, Santana J, García H, et al. Lack of evidence for in vivo transformation of zidovudine triphosphate to stavudine triphosphate in human immunodeficiency virus-infected patients. Antimicrobial Agents and Chemotherapy. 2006;50(3):835-40.

157. Dervieux T, Boulieu R. Identification of 6-methylmercaptopurine derivative formed during acid hydrolysis of thiopurine nucleotides in erythrocytes, using liquid chromatography–mass spectrometry, infrared spectroscopy, and nuclear magnetic resonance assay. Clinical Chemistry. 1998;44(12):2511-5.

158. Shi G, Wu Jt, Li Y, Geleziunas R, Gallagher K, Emm T, et al. Novel direct detection method for quantitative determination of intracellular nucleoside

triphosphates using weak anion exchange liquid chromatography/tandem mass spectrometry. Rapid Communications in Mass Spectrometry. 2002;16(11):1092-9.

159. Veltkamp S, Hillebrand M, Rosing H, Jansen R, Wickremsinhe E, Perkins E, et al. Quantitative analysis of gemcitabine triphosphate in human peripheral blood mononuclear cells using weak anion-exchange liquid chromatography coupled with tandem mass spectrometry. Journal of Mass Spectrometry. 2006;41(12):1633-42.

160. Jansen RS, Rosing H, de Wolf CJ, Beijnen JH. Development and validation of an assay for the quantitative determination of cladribine nucleotides in MDCKII cells and culture medium using weak anion-exchange liquid chromatography coupled with tandem mass spectrometry. Rapid Communications in Mass Spectrometry. 2007;21(24):4049-59.

161. Veltkamp SA, Jansen RS, Callies S, Pluim D, Visseren-Grul CM, Rosing H, et al. Oral administration of gemcitabine in patients with refractory tumors: a clinical and pharmacologic study. Clin Cancer Res. 2008;14(11):3477-86.

162. Kinai E, Gatanaga H, Kikuchi Y, Oka S, Kato S. Ultrasensitive method to quantify intracellular zidovudine mono-, di-and triphosphate concentrations in peripheral blood mononuclear cells by liquid chromatography–tandem mass spectrometry. Journal of Mass Spectrometry. 2015;50(6):783-91.

163. Fung EN, Cai ZW, Burnette TC, Sinhababu AK. Simultaneous determination of Ziagen and its phosphorylated metabolites by ion-pairing high-performance liquid chromatography-tandem mass spectrometry. Journal of Chromatography B. 2001 Apr 25;754(2):285-95.

164. Tuytten R, Lemiere F, Van Dongen W, Esmans EL, Slegers H. Short capillary ion-pair high-performance liquid chromatography coupled to electrospray (tandem) mass spectrometry for the simultaneous analysis of nucleoside mono-, di- and triphosphates. Rapid Communications in Mass Spectrometry. 2002;16(12):1205-15.

165. Cai ZW, Song FR, Yang MS. Capillary liquid chromatographic-high-resolution mass spectrometric analysis of ribonucleotides. Journal of Chromatography A. 2002 Nov 8;976(1-2):135-43.

166. Durand-Gasselin L, Da Silva D, Benech H, Pruvost A, Grassi J. Evidence and possible consequences of the phosphorylation of nucleoside reverse transcriptase inhibitors in human red blood cells. Antimicrobial Agents and Chemotherapy. 2007;51(6):2105-11.

167. Pruvost A, Théodoro F, Agrofoglio L, Negredo E, Bénech H. Specificity enhancement with LC-positive ESI-MS/MS for the measurement of nucleotides: application to the quantitative determination of carbovir triphosphate, lamivudine triphosphate and tenofovir diphosphate in human peripheral blood mononuclear cells. Journal of Mass Spectrometry. 2008;43(2):224-33.

168. Coulier L, Bas R, Jespersen S, Verheij E, van der Werf MJ, Hankemeier T. Simultaneous quantitative analysis of metabolites using ion-pair liquid chromatography-electrospray ionization mass spectrometry. Analytical Chemistry. 2006;78(18):6573-82.

169. Cordell RL, Hill SJ, Ortori CA, Barrett DA. Quantitative profiling of nucleotides and related phosphate-containing metabolites in cultured mammalian cells by liquid

chromatography tandem electrospray mass spectrometry. Journal of Chromatography B-Analytical Technologies in the Biomedical and Life Sciences. 2008 Aug;871(1):115-24.

170. King T, Bushman L, Anderson PL, Delahunty T, Ray M, Fletcher CV. Quantitation of zidovudine triphosphate concentrations from human peripheral blood mononuclear cells by anion exchange solid phase extraction and liquid chromatography–tandem mass spectroscopy; an indirect quantitation methodology. Journal of Chromatography B. 2006;831(1):248-57.

171. Ni J, Rowe J. Microdosing Assessment to Evaluate Pharmacokinetics and Drug Metabolism Using Liquid Chromatography-Tandem Mass Spectrometry Technology. Topics on Drug Metabolism. 2012.

172. Apffel A, Chakel JA, Fischer S, Lichtenwalter K, Hancock WS. New procedure for the use of high-performance liquid chromatography–electrospray ionization mass spectrometry for the analysis of nucleotides and oligonucleotides. Journal of Chromatography A. 1997;777(1):3-21.

173. Tomiya N, Ailor E, Lawrence SM, Betenbaugh MJ, Lee YC. Determination of nucleotides and sugar nucleotides involved in protein glycosylation by high-performance anion-exchange chromatography: Sugar nucleotide contents in cultured insect cells and mammalian cells. Analytical Biochemistry. 2001 Jun 1;293(1):129-37.

174. Blokhin DY, Poteshnykh AV. Separation and analysis of ribo nucleotide mixtures by anion exchange high performance liquid chromatography. Bioorganicheskaya Khimiya. 1983 1983;9(5):673-7.

175. Hennere G, Becher F, Pruvost A, Goujard C, Grassi J, Benech H. Liquid chromatography-tandem mass spectrometry assays for intracellular deoxyribonucleotide triphosphate competitors of nucleoside antiretrovirals. Journal of Chromatography B-Analytical Technologies in the Biomedical and Life Sciences. 2003;789(2):273-81.

176. Qian TX, Cai ZW, Yang MS. Determination of adenosine nucleotides in cultured cells by ion-pairing liquid chromatography-electrospray ionization mass spectrometry. Analytical Biochemistry. 2004;325(1):77-84.

177. Auriola S, Frith J, Rogers MJ, Koivuniemi A, Monkkonen J. Identification of adenine nucleotide-containing metabolites of bisphosphonate drugs using ion-pair liquid chromatography-electrospray mass spectrometry. Journal of Chromatography B. 1997 Dec 19;704(1-2):187-95.

178. Reijenga JC, Wes JH, Vandongen CAM. Comparison of methanol and perchloric-acid extraction procedures for analysis of nucleotides by isotachophoresis. Journal of Chromatography. 1986;374(1):162-9.

179. Becher F, Pruvost A, Goujard C, Guerreiro C, Delfraissy JF, Grassi J, et al. Improved method for the simultaneous determination of d4T, 3TC and ddI intracellular phosphorylated anabolites in human peripheral-blood mononuclear cells using high-performance liquid chromatography/tandem mass spectrometry. Rapid Communications in Mass Spectrometry. 2002 2002;16(6):555-65.

180. Brown PR, Miech RP. Comparison of cell extraction procedures for use with high-pressure liquid chromatography. Analytical Chemistry. 1972;44(6):1072-&.

181. Au JLS, Su MH, Wientjes MG. Extraction of intracellular nucleosides and nucleotides with acetonitrile. Clinical Chemistry. 1989;35(1):48-51.

182. Yang MS, Gupta RC. Determination of energy charge potential in the C6 glioma and the HepG-2 cell culture. Toxicology Mechanisms and Methods. 2003;13(2):97-101.

183. Grob MK, O'Brien K, Chu JJ, Chen DDY. Optimization of cellular nucleotide extraction and sample preparation for nucleotide pool analyses using capillary electrophoresis. Journal of Chromatography B-Analytical Technologies in the Biomedical and Life Sciences. 2003;788(1):103-11.

184. Kimball E, Rabinowitz JD. Identifying decomposition products in extracts of cellular metabolites. Analytical Biochemistry. 2006 Nov 15;358(2):273-80.

185. Huang LF, Liang YZ, Guo FQ, Zhou ZF, Cheng BM. Simultaneous separation and determination of active components in Cordyceps sinensis and Cordyceps militarris by LC/ESI-MS. Journal of Pharmaceutical and Biomedical Analysis. 2003 Dec;33(5):1155-62.

186. Harsahay M, Mohsin M, Pandey HK, Negi PS, Ahmed Z. Estimation of cordycepin by improved HPLC method in the natural and cultured mycelia of high medicinal value Himalayan entomogenous fungus Cordyceps sinensis. EJEAFChe, Electronic Journal of Environmental, Agricultural and Food Chemistry. 2010;9(10):1598-603.

187. Li SP, Li P, Dong TTX, Tsim KWK. Determination of nucleosides in natural Cordyceps sinensis and cultured Cordyceps mycelia by capillary electrophoresis. Electrophoresis. 2001 Jan;22(1):144-50.

188. Tsai YJ, Lin LC, Tsai TH. Pharmacokinetics of Adenosine and Cordycepin, a Bioactive Constituent of Cordyceps sinensis in Rat. Journal of Agricultural and Food Chemistry. 2010 Apr;58(8):4638-43.

189. Nassar A-E, Parmentier Y, Martinet M, Lee D. Liquid chromatography-accurate radioisotope counting and microplate scintillation counter technologies in drug metabolism studies. Journal of chromatographic science. 2004;42(7):348-53.

190. Liu R, Ye Y, Qiang L, Liao X, Zhao Y. The fragmentation pathway of the nucleosides under the electrospray ionization multi-stage mass spectrometry. Life Science Journal-Acta Zhengzhou University Overseas Edition. 2008 2008;5(2):37-40.

191. Wilson PK, Szabados E, Mulligan SP, Christopherson RI. Comparative effects of cladribine, fludarabine and pentostatin on nucleotide metabolism in T- and B-cell lines. International Journal of Biochemistry & Cell Biology. 1998 Jul;30(7):833-42.

192. Chandra D, Bratton SB, Person MD, Tian Y, Martin AG, Ayres M, et al. Intracellular nucleotides act as critical prosurvival factors by binding to cyctochrome c and inhibiting apoptosome. Cell. 2006 Jun 30;125(7):1333-46.

193. Dennison JB, Ayres ML, Kaluarachchi K, Plunkett W, Gandhi V. Intracellular Succinylation of 8-Chloroadenosine and Its Effect on Fumarate Levels. Journal of Biological Chemistry. 2010 Mar 12;285(11):8022-30.

194. Liu X, Luo X, Shi YY, Zhu G, Penning T, Giranda VL, et al. Poly (ADP-ribose) polymerase activity regulates apoptosis in HeLa cells after alkylating DNA damage. Cancer biology & therapy. 2008;7(6):934-41.

195. Holbein S, Wengi A, Decourty L, Freimoser FM, Jacquier A, Dichtl B. Cordycepin interferes with 3' end formation in yeast independently of its potential to terminate RNA chain elongation. RNA. 2009;15(5):837-49.

196. Wong YY, Moon A, Duffin R, Barthet-Barateig A, Meijer HA, Clemens MJ, et al. Cordycepin inhibits protein synthesis and cell adhesion through effects on signal transduction. Journal of Biological Chemistry. 2010;285(4):2610.

197. Fishman P, Bar-Yehuda S, Madi L, Cohn I. A3 adenosine receptor as a target for cancer therapy. Anti-Cancer Drugs. [Review]. 2002 Jun;13(5):437-43.

198. Madi L, Ochaion A, Rath-Wolfson L, Bar-Yehuda S, Erlanger A, Ohana G, et al. The A3 adenosine receptor is highly expressed in tumor versus normal cells potential target for tumor growth inhibition. Clin Cancer Res. 2004;10(13):4472-9.

199. Lee JH, Yoon JY, Myoung H, Hong SM, Kim SM, Kim MJ. Anti-cancer effects of cordycepin on oral squamous cell carcinoma proliferation and apoptosis in vitro. Oral Oncology. 2011 Jul;47:S75-S.

200. Kim H, Naura AS, Errami Y, Ju J, Boulares AH. Cordycepin Blocks Lung Injury-Associated Inflammation and Promotes BRCA1-Deficient Breast Cancer Cell Killing by Effectively Inhibiting PARP. Molecular Medicine. 2011 Sep-Oct;17(9-10):893-900.

201. Strosznajder R, Jesko H, Zambrzycka A. Poly(ADP-ribose) polymerase. Mol Neurobiol. 2005 2005/02/01;31(1-3):149-67.

202. Lee HJ, Burger P, Vogel M, Friese K, Bruening A. The nucleoside antagonist cordycepin causes DNA double strand breaks in breast cancer cells. Investigational new drugs. 2012 Oct;30(5):1917-25.

203. Adamson RH, Zaharevitz DW, Johns DG. Enhancement of biological-activity of adenosine-analogs by adenosine-deaminase inhibitor 2'-deoxycoformycin. Pharmacology. 1977;15(1):84-9.

204. Rodman LE, Farnell DR, Coyne JM, Allan PW, Hill DL, Duncan KLK, et al. Toxicity of Cordycepin in Combination with the Adenosine Deaminase Inhibitor 2'-Deoxycoformycin in Beagle Dogs* 1. Toxicology and applied pharmacology. 1997;147(1):39-45.

205. Klenow H. Formation of mono-, di- and triphosphate of cordycepin in ehrlich ascites-tumor cells *in vitro*. Biochimica Et Biophysica Acta. 1963 1963;76(3):347-&.

206. Iwashima A, Ogata M, Nosaka K, Nishimura H, Hasegawa T. Adenosine kinase-deficient mutant of Saccharomyces cerevisiae. FEMS microbiology letters. 1995;127(1-2):23-8.

207. Rodman LE, Farnell DR, Coyne JM, Allan PW, Hill DL, Duncan KLK, et al. Toxicity of cordycepin in combination with the adenosine deaminase inhibitor 2'-deoxycoformycin in beagle dogs. Toxicology and applied pharmacology. [Article]. 1997 Nov;147(1):39-45.

208. Foss F. Combination therapy with purine nucleoside analogs. Oncology (Williston Park, NY). 2000;14(6 Suppl 2):31-5.

209. Zhao L, Kroenke CD, Song J, Piwnica-Worms D, Ackerman JJH, Neil JJ. Intracellular water-specific MR of microbead-adherent cells: the HeLa cell intracellular water exchange lifetime. Nmr in Biomedicine. 2008 Feb;21(2):159-64.

210. Shi Y, Ryu DDY, Ballica R. Rheological properties of mammalian cell culture suspensions: Hybridoma and HeLa cell lines. Biotechnology and Bioengineering. 1993;41(7):745-54.

211. Schoeberl B, Eichler-Jonsson C, Gilles ED, Müller G. Computational modeling of the dynamics of the MAP kinase cascade activated by surface and internalized EGF receptors. Nature Biotechnology. 2002;20(4):370-5.

212. Luciani AM, Rosi A, Matarrese P, Arancia G, Guidoni L, Viti V. Changes in cell volume and internal sodium concentration in HeLa cells during exponential growth and following lonidamine treatment. European Journal of Cell Biology. 2001;80(2):187-95.

213. Choi S, Lim MH, Kim KM, Jeon BH, Song WO, Kim TW. Cordycepin-induced apoptosis and autophagy in breast cancer cells are independent of the estrogen receptor. Toxicology and applied pharmacology. 2011 Dec;257(2):165-73.

214. Snyder FF, Henderson JF. Alternative pathways of deoxyadenosine and adenosine metabolism. Journal of Biological Chemistry. 1973;248(16):5899-904.

215. Chen Y, Guo H, Du Z, Liu XZ, Che Y, Ye X. Ecology-based screen identifies new metabolites from a Cordyceps-colonizing fungus as cancer cell proliferation inhibitors and apoptosis inducers. Cell proliferation. 2009;42(6):838-47.

216. Sun Y, Zhao Z, Feng Q, Xu Q, Lü L, Liu JK, et al. Unusual spirodecane sesquiterpenes and a fumagillol analogue from Cordyceps ophioglossoides. Helvetica Chimica Acta. 2013;96(1):76-84.

217. Park SE, Yoo HS, Jin C-Y, Hong SH, Lee Y-W, Kim BW, et al. Induction of apoptosis and inhibition of telomerase activity in human lung carcinoma cells by the water extract of Cordyceps militaris. Food and Chemical Toxicology. 2009;47(7):1667-75.

218. Yang C, Kao Y, Huang K, Wang C, Lin L. Cordyceps militaris and mycelial fermentation induced apoptosis and autophagy of human glioblastoma cells. Cell death & disease. 2012;3(11):e431.

219. Park C, Hong SH, Lee J-Y, Kim G-Y, Choi BT, Lee YT, et al. Growth inhibition of U937 leukemia cells by aqueous extract of Cordyceps militaris through induction of apoptosis. Oncology reports. 2005;13(6):1211-6.

220. Jin C-Y, Kim G-Y, Choi YH. Induction of apoptosis by aqueous extract of Cordyceps militaris through activation of caspases and inactivation of Akt in human breast cancer MDA-MB-231 Cells. Journal of Microbiology and Biotechnology. 2008;18(12):1997-2003.

221. Combe R, Bramwell S, Field MJ. The monosodium iodoacetate model of osteoarthritis: a model of chronic nociceptive pain in rats? Neuroscience letters. 2004;370(2):236-40.

222. Farthing D, Sica D, Gehr T, Wilson B, Fakhry I, Larus T, et al. An HPLC method for determination of inosine and hypoxanthine in human plasma from healthy volunteers and patients presenting with potential acute cardiac ischemia. Journal of Chromatography B. 2007;854(1):158-64.

223. Klenow H, Frederiksen S. Effect of 3 -deoxyATP (cordycepin triphosphate) + 2 -deoxyATP on DNA-dependent RNA nucleotidyltransferase from Ehrlich ascites tumor cells. Biochimica Et Biophysica Acta. 1964 1964;87(3):495-&.

224. Mathews II, Erion MD, Ealick SE. Structure of human adenosine kinase at 1.5 Å resolution. Biochemistry. 1998;37(45):15607-20.

225. Agarwal RP, Sagar SM, Parks RE. Adenosine deaminase from human erythrocytes: purification and effects of adenosine analogs. Biochemical Pharmacology. 1975;24(6):693-701.

226. Schnebli HP, Hill DL, Bennett LL. Purification and properties of adenosine kinase from human tumor cells of type H. Ep. No. 2. Journal of Biological Chemistry. 1967;242(9):1997-2004.

227. Vannoni D, Bernini A, Carlucci F, Civitelli S, Di Pietro M, Leoncini R, et al. Enzyme activities controlling adenosine levels in normal and neoplastic tissues. Medical Oncology. 2004;21(2):187-95.

228. Giglioni S, Leoncini R, Aceto E, Chessa A, Civitelli S, Bernini A, et al. Adenosine kinase gene expression in human colorectal cancer. Nucleosides, Nucleotides, and Nucleic Acids. 2008;27(6-7):750-4.

229. Canbolat O, Durak I, Çetin R, Kavutcu M, Demirci S, Öztürk S. Activities of adenosine deaminase, 5′-nucleotidase, guanase, and cytidine deaminase enzymes in cancerous and non-cancerous human breast tissues. Breast cancer research and treatment. 1996;37(2):189-93.

230. Aghaei M, Karami-Tehrani F, Salami S, Atri M. Adenosine deaminase activity in the serum and malignant tumors of breast cancer: the assessment of isoenzyme ADA1 and ADA2 activities. Clinical biochemistry. 2005;38(10):887-91.

231. Mahajan M, Tiwari N, Sharma R, Kaur S, Singh N. Oxidative Stress and Its Relationship With Adenosine Deaminase Activity in Various Stages of Breast Cancer. Indian Journal of Clinical Biochemistry. 2013;28(1):51-4.

232. Hodge L, Taub M, Tracy T. Effect of its deaminated metabolite, 2′, 2′-difluorodeoxyuridine, on the transport and toxicity of gemcitabine in HeLa cells. Biochemical Pharmacology. 2011;81(7):950-6.

233. Hodge LS, Taub ME, Tracy TS. The Deaminated Metabolite of Gemcitabine, 2′, 2′-Difluorodeoxyuridine, Modulates the Rate of Gemcitabine Transport and Intracellular Phosphorylation via Deoxycytidine Kinase. Drug Metabolism and Disposition. 2011;39(11):2013-6.

234. Klenow H. Further studies on the effect of deoxyadenosine on the accumulation of deoxyadenosine triphosphate and inhibition of deoxyribonucleic acid synthesis in Ehrlich ascites tumor cells in vitro. Biochimica et Biophysica Acta (BBA)-Specialized Section on Nucleic Acids and Related Subjects. 1962;61(6):885-96.

235. Carson DA, Kaye J, Seegmiller J. Lymphospecific toxicity in adenosine deaminase deficiency and purine nucleoside phosphorylase deficiency: possible role of nucleoside kinase (s). Proceedings of the National Academy of Sciences. 1977;74(12):5677-81.

236. Yu HM, Wang B-S, Huang SC, Duh P-D. Comparison of protective effects between cultured Cordyceps militaris and natural Cordyceps sinensis against oxidative damage. Journal of Agricultural and Food Chemistry. 2006;54(8):3132-8.

237. Jiang Y, Wong J, Fu M, Ng T, Liu Z, Wang C, et al. Isolation of adenosine, iso-sinensetin and dimethylguanosine with antioxidant and HIV-1 protease inhibiting activities from fruiting bodies of Cordyceps militaris. Phytomedicine. 2011;18(2):189-93.

238. Koch H, Jäger W, Groh U, Plank G. In vitro inhibition of adenosine deaminase by flavonoids and related compounds. New insight into the mechanism of action of plant phenolics. Methods and findings in experimental and clinical pharmacology. 1991;14(6):413-7.

239. Li G, Nakagome I, Hirono S, Itoh T, Fujiwara R. Inhibition of adenosine deaminase (ADA)-mediated metabolism of cordycepin by natural substances. Pharmacology Research & Perspectives. 2015;3(2).

240. Deisenroth C, Zhang Y. The Ribosomal Protein-Mdm2-p53 Pathway and Energy Metabolism: Bridging the Gap between Feast and Famine. Genes & cancer. 2011 2011-Apr;2(4):392-403.

241. Hanahan D, Weinberg RA. The hallmarks of cancer. Cell. 2000 Jan 7;100(1):57-70.

242. Karu T, Pyatibrat L, Kalendo G. Irradiation with He□ Ne laser increases ATP level in cells cultivated in vitro. Journal of Photochemistry and photobiology B: Biology. 1995;27(3):219-23.

243. Brown GC. Control of respiration and ATP synthesis in mammalian mitochondria and cells. Biochem J. 1992;284:1-13.

244. Yang M, Yu L, Gupta R. Analysis of changes in energy and redox states in HepG2 hepatoma and C6 glioma cells upon exposure to cadmium. Toxicology. 2004;201(1):105-13.

245. Overgaardhansen K. Inhibition of 5-phosphoribosyl-1-pyrophosphate formation by cordycepin triphosphate in extracts of Ehrlich ascites tumor cells. Biochimica Et Biophysica Acta. 1964 1964;80(3):504-&.

246. Lu X, Errington J, Chen VJ, Curtin NJ, Boddy AV, Newell DR. Cellular ATP depletion by LY309887 as a predictor of growth inhibition in human tumor cell lines. Clin Cancer Res. 2000;6(1):271-7.

247. Eguchi Y, Shimizu S, Tsujimoto Y. Intracellular ATP levels determine cell death fate by apoptosis or necrosis. Cancer Res. 1997 May;57(10):1835-40.

248. Verrax J, Dejeans N, Sid B, Glorieux C, Calderon PB. Intracellular ATP levels determine cell death fate of cancer cells exposed to both standard and redox chemotherapeutic agents. Biochemical Pharmacology. [Article]. 2011 Dec;82(11):1540-8.

249. Feldenberg LR, Thevananther S, Del Rio M, De Leon M, Devarajan P. Partial ATP depletion induces Fas- and caspase-mediated apoptosis in MDCK cells. American Journal of Physiology-Renal Physiology. 1999 Jun;276(6):F837-F46.

250. Tani H, Akimitsu N. Genome-wide technology for determining RNA stability in mammalian cells. Rna Biology. 2012;9(10):1233-8.

251. Tani H, Mizutani R, Salam KA, Tano K, Ijiri K, Wakamatsu A, et al. Genome-wide determination of RNA stability reveals hundreds of short-lived noncoding transcripts in mammals. Genome research. 2012;22(5):947-56.

252. Keene JD. Minireview: global regulation and dynamics of ribonucleic Acid. Endocrinology. 2010;151(4):1391-7.

253. Bolognani F, Perrone-Bizzozero NI. RNA–protein interactions and control of mRNA stability in neurons. Journal of neuroscience research. 2008;86(3):481-9.

254. Rabani M, Levin JZ, Fan L, Adiconis X, Raychowdhury R, Garber M, et al. Metabolic labeling of RNA uncovers principles of RNA production and degradation dynamics in mammalian cells. Nature Biotechnology. 2011;29(5):436-42.

255. Hao S, Baltimore D. The stability of mRNA influences the temporal order of the induction of genes encoding inflammatory molecules. Nature immunology. 2009;10(3):281-8.

256. Cleary MD, Meiering CD, Jan E, Guymon R, Boothroyd JC. Biosynthetic labeling of RNA with uracil phosphoribosyltransferase allows cell-specific microarray analysis of mRNA synthesis and decay. Nat Biotech. [10.1038/nbt1061]. 2005;23(2):232-7.

257. Suzuki NN, Koizumi K, Fukushima M, Matsuda A, Inagaki F. Structural basis for the specificity, catalysis, and regulation of human uridine-cytidine kinase. Structure. 2004;12(5):751-64.

258. Van Rompay AR, Norda A, Linden K, Johansson M, Karlsson A. Phosphorylation of uridine and cytidine nucleoside analogs by two human uridine-cytidine kinases. Molecular Pharmacology. 2001 May;59(5):1181-6.

259. Yan H, Tsai MD. Nucleoside monophosphate kinases: structure, mechanism, and substrate specificity. Adv Enzymol Relat Areas Mol Biol. 1999;73:103-34.

260. Van Rompay AR, Johansson M, Karlsson A. Phosphorylation of deoxycytidine analog monophosphates by UMP-CMP kinase: Molecular characterization of the human enzyme. Molecular Pharmacology. 1999 Sep;56(3):562-9.

261. Ratliff RL, Weaver RH, Kuby SA, Lardy HA. Nucleoside triphosphate-nucleoside diphosphate transphosphorylase (nucleoside diphosphokinase). I. Isolation of crystalline enzyme from brewers yeast. Journal of Biological Chemistry. 1964 1964;239(1):301-&.

262. Payne R, Cheng N, Traut T. Uridine kinase from Ehrlich ascites carcinoma. Purification and properties of homogeneous enzyme. Journal of Biological Chemistry. 1985;260(18):10242-7.

263. Wohlhueter RM, Marz R, Graff JC, Plagemann PG. The application of rapid kinetic techniques to the transport of thymidine and 3-O-methylglucose into

mammalian cells in suspension culture. Journal of Cellular Physiology. 1976;89(4):605-12.

264. Plagemann PG, Richey DP. Transport of nucleosides, nucleic acid bases, choline and glucose by animal cells in culture. Biochimica et Biophysica Acta (BBA)-Reviews on Biomembranes. 1974;344(3):263-305.

265. Ben-Sahra I, Howell JJ, Asara JM, Manning BD. Stimulation of de Novo Pyrimidine Synthesis by Growth Signaling Through mTOR and S6K1. Science. 2013 Mar 15;339(6125):1323-8.

266. Rozengurt E, Stein WD, Wigglesworth NM. Uptake of nucleosides in density-inhibited cultures of 3T3 cells. 1977.

267. Hay N, Sonenberg N. Upstream and downstream of mTOR. Genes & development. 2004;18(16):1926-45.

268. Dennis PB, Jaeschke A, Saitoh M, Fowler B, Kozma SC, Thomas G. Mammalian TOR: A homeostatic ATP sensor. Science. 2001 Nov 2;294(5544):1102-5.

269. Payne RC, Traut TW. Regulation of uridine kinase quaternary structure - dissociation by the inhibitor CTP. Journal of Biological Chemistry. 1982 1982;257(21):2485-8.

270. Herzfeld A, Raper SM. Uridine kinase activities in developing, adult and neoplastic rat tissues. Biochem J. 1979;182:771-8.

271. Ropp PA, Traut TW. Cloning and expression of a cDNA encoding uridine kinase from mouse brain. Archives of Biochemistry and Biophysics. 1996;336(1):105-12.

272. Shen F, Look KY, Yeh YA, Weber G. Increased uridine kinase (ATP: uridine 5'-phosphotransferase; EC 2.7.1.48) activity in human and rat tumors. Cancer biochemistry biophysics. 1998 1998-Jun;16(1-2):1-15.

273. Absil J, Tuilie M, Roux J-M. Electrophoretically distinct forms of uridine kinase in the rat. Tissue distribution and age-dependence. Biochem J. 1980;185:273-6.

274. Yuh I, Yaoi T, Watanabe S, Okajima S, Hirasawa Y, Fushiki S. Up-regulated uridine kinase gene identified by RLCS in the ventral horn after crush injury to rat sciatic nerves. Biochemical and Biophysical Research Communications. 1999;266(1):104-9.

275. Ozaki K, Kuroki T, Hayashi S, Nakamura Y. Isolation of three testis-specific genes (TSA303, TSA806, TSA903) by a differential mRNA display method. Genomics. 1996;36(2):316-9.

276. Liacouras A, Anderson E. Uridine-Cytidine Kinase IV. Kinetics of the Competition Between 5-Azacytidine and the Two Natural Substrates. Molecular Pharmacology. 1979;15(2):331-40.

277. Lortet S, Aussedat J, Rossi A. Synthesis of pyrimidine nucleotides in the heart: uridine and cytidine kinase activity. Archives internationales de physiologie et de biochimie. 1987;95(4):289-98.

278. Anderson EP, Brockman RW. Feedback inhibition of uridine kinase by cytidine triphosphate + uridine triphosphate. Biochimica Et Biophysica Acta. 1964 1964;91(3):380-&.

279. Cheng N, Payne RC, Traut TW. Regulation of uridine kinase - evidence for a regulatory site. Journal of Biological Chemistry. 1986 Oct 5;261(28):3006-12.

280. Ropp PA, Traut TW. Uridine kinase: Altered enzyme with decreased affinities for uridine and CTP. Archives of Biochemistry and Biophysics. 1998 Nov 1;359(1):63-8.

281. Rozengurt E, Mierzejewski K, Wigglesworth N. Uridine transport and phosphorylation in mouse cells in culture - effect of growth-promoting factors, cell-cycle transit and oncogenic transformation. Journal of Cellular Physiology. 1978 1978;97(2):241-51.

282. Wharton W, Pledger WJ. Regulation of uridine kinase-activity in balb-c-3t3 cells by serum components. In Vitro-Journal of the Tissue Culture Association. 1981 1981;17(8):706-12.

283. Cheng N, Traut TW. Uridine kinase: Altered subunit size or enzyme expression as a function of cell type, growth stimulation, or mutagenesis. Journal of Cellular Biochemistry. 1987;35(3):217-29.

284. Zlatopolskiy BD, Morgenroth A, Kunkel FHG, Urusova EA, Dinger C, Kull T, et al. Synthesis and Biologic Study of IV-14, a New Ribonucleoside Radiotracer for Tumor Visualization. Journal of Nuclear Medicine. 2009 Nov;50(11):1895-903.

285. Krystal G, Webb TE. Multiple forms of uridine kinase in normal and neoplastic rat liver. Biochem J. 1971;124:943-7.

286. Tabata S, Tanaka M, Endo Y, Obata T, Matsuda A, Sasaki T. Anti-tumor mechanisms of 3'-ethynyluridine and 3'-ethynylcytidine as RNA synthesis inhibitors: Development and characterization of 3'-ethynyluridine-resistant cells. Cancer Letters. 1997 Jun 24;116(2):225-31.

287. Adema AD, Smid K, Losekoot N, Honeywell RJ, Verheul HM, Myhren F, et al. Metabolism and accumulation of the lipophilic deoxynucleoside analogs elacytarabine and CP-4126. Investigational new drugs. [Article]. 2012 Oct;30(5):1908-16.

288. Van Haperen VWR, Veerman G, Boven E, Noordhuis P, Vermorken JB, Peters GJ. Schedule dependence of sensitivity to 2', 2'-difluorodeoxycytidine (Gemcitabine) in relation to accumulation and retention of its triphosphate in solid tumour cell lines and solid tumours. Biochemical Pharmacology. 1994;48(7):1327-39.

289. Spychala J, Datta NS, Takabayashi K, Datta M, Fox IH, Gribbin T, et al. Cloning of human adenosine kinase cDNA: sequence similarity to microbial ribokinases and fructokinases. Proceedings of the National Academy of Sciences of the United States of America. 1996;93(3):1232-7.

290. Yamada Y, Goto H, Ogasawara N. Differences of adenosine kinases from various mammalian tissues. Comparative Biochemistry and Physiology Part B: Comparative Biochemistry. 1982;71(3):367-72.

291. Yamada Y, Goto H, Ogasawara N. Adenosine kinase from human liver. Biochimica et Biophysica Acta (BBA)-Enzymology. 1981;660(1):36-43.

292. Boison D. Adenosine kinase: exploitation for therapeutic gain. Pharmacological reviews. 2013;65(3):906-43.

293. Wu JZ, Larson G, Walker H, Shim JH, Hong Z. Phosphorylation of ribavirin and viramidine by adenosine kinase and cytosolic 5'-nucleotidase II: implications for ribavirin metabolism in erythrocytes. Antimicrobial Agents and Chemotherapy. 2005;49(6):2164-71.

Website Reference

1. http://www.oncovista.com/our-products/
2. https://clinicaltrials.gov/ct2/show/study/NCT00709215